

Investigation of enzymes catalyzing the production of acetaldehyde from pyruvate in hyperthermophiles

by

Seyed Mohammad Eram

A thesis
presented to the University of Waterloo
in fulfillment of the
thesis requirement for the degree of
Doctor of Philosophy
in
Biology

Waterloo, Ontario, Canada, 2012

©Seyed Mohammad Eram 2012

AUTHOR'S DECLARATION

I hereby declare that I am the sole author of this thesis. This is a true copy of the thesis, including any required final revisions, as accepted by my examiners.

I understand that my thesis may be made electronically available to the public.

Abstract

Extreme thermophiles and hyperthermophiles are microorganisms with the ability to grow optimally at 65-79°C and 80°C plus, respectively. Many of the enzymes isolated from these microorganisms are thermostable, which makes them a potential resource for research and industrial applications. An increasing number of hyper/thermophiles is shown to be able to produce ethanol as an end-metabolite. Despite characterization of many alcohol dehydrogenases (ADHs) with a potential role in the production of ethanol, to date there has been no significant progress in identifying the enzymes responsible for the production of acetaldehyde, which is an intermediate in production of ethanol from pyruvate.

Pyruvate decarboxylase (PDC encoded by *pdh*) is a thiamine pyrophosphate (TPP)-containing enzyme responsible for conversion of pyruvate to acetaldehyde in many mesophilic organisms. However, no *pdh*/PDC homolog has yet been found in fully sequenced genomes and proteomes of hyper/thermophiles. The only PDC activity reported in hyperthermophiles was a bifunctional, TPP- and CoA-dependent pyruvate ferredoxin oxidoreductase (POR)/PDC enzyme from the hyperthermophilic archaeon *Pyrococcus furiosus*. No further investigation of such bifunctionality in other hyper/thermophilic PORs has been conducted.

The bifunctional and TPP-containing POR/PDC enzyme was isolated and characterized from the ethanol-producing hyperthermophilic archaeon *Thermococcus guaymasensis* ($T_{opt}=88^{\circ}\text{C}$), as well as the bacteria *Thermotoga hypogea* ($T_{opt}=70^{\circ}\text{C}$) and *Thermotoga maritima* ($T_{opt}=80^{\circ}\text{C}$). The *T. guaymasensis* enzyme was purified anaerobically to homogeneity as judged by SDS-PAGE analysis. POR and PDC activities were co-eluted from each of the chromatographic columns, and the ratio of POR to PDC activities remained constant throughout the purification steps. Similar to other POR counterparts, the enzyme was extremely oxygen sensitive, with a half-life of about 30 min upon exposure to air. The purified enzyme showed POR/PDC bifunctionality with specific activities of 20.2 and $3.8\pm 0.22 \text{ U mg}^{-1}$ for oxidative and non-oxidative decarboxylation of pyruvate, respectively. Both of the enzyme activities were CoA- and TPP- dependent. The apparent kinetic parameters were determined for the main substrates, including pyruvate and CoA for both activities. Since the genome sequence of *T. guaymasensis* was not available, sequence of the genes encoding POR and the closely related enzyme 2-ketoisovalerate ferredoxin oxidoreductase (VOR) were determined *via* primer walking and inverse PCR.

T. hypogea and *T. maritima* bifunctional POR/PDC enzymes were heterotetramers with estimated native molecular weights of 260 kDa. Although the POR of *T. maritima* was characterized previously, its PDC activity was not reported. Since the *T. hypogea* genome sequence is not available, the primary structure of the genes encoding each of the POR four subunits were determined using inverse PCR and the primer-walking approaches. The deduced amino acid sequences of both PORs were compared with available sequences from other organisms. Both activities of POR and PDC were highly sensitive toward exposure to air, with half-lives of less than 15 min for *T. maritima* POR/PDC and less than 5 min for *T. hypogea* POR/PDC. The optimal pHs were determined to be pH 8.4 for both POR and PDC activities, and their optimal temperatures were determined to be 85°C. The *T. hypogea* enzyme had a specific activity of 96.7 ± 15.1 and 1.82 ± 0.44 Umg^{-1} for POR and PDC, respectively, while the *T. maritima* enzyme had a specific activity of 90.8 ± 11 and 1.4 ± 0.15 Umg^{-1} for POR and PDC, respectively.

A novel enzyme capable of catalyzing the production of acetaldehyde from pyruvate in hyperthermophiles was also characterized. This enzyme is a TPP- and flavin-containing acetohydroxyacid synthase (AHAS), which is found to be involved in the biosynthesis of branched-chain amino acids. AHAS activities were detected in the cell-free extracts of *T. maritima*, *T. hypogea*, *Thermotoga neapolitana*, *P. furiosus*, *T. guaymasensis* and *Thermococcus kodakaraensis*. Among these, the ones that harbor a complete *ilv* (isoleucine-leucine valine) operon (including *T. maritima*, *T. neapolitana*, and *P. furiosus*) had the highest AHAS activity at nearly neutral pH, but the ones without *ilv* operon still had some residual AHAS activity mostly at a higher pH value (pH 10.5). It was shown that the cell-free extracts of *T. maritima* can catalyze the non-oxidative decarboxylation of the pyruvate to produce acetaldehyde.

The genes encoding each of the catalytic and regulatory subunits of AHAS from *T. maritima* were over-expressed in the mesophilic host, *E. coli*. The recombinant proteins were purified to homogeneity by heat-treatment and fast performance liquid chromatography (FPLC). The highly active catalytic (large) subunit was responsible for both synthase and decarboxylase activities, which were 134 ± 30 and 16.7 ± 3.4 Umg^{-1} , respectively. The activity had an optimal pH of 7.0 and an optimal temperature of 85°C for both activities, and was stable at 80°C ($t_{1/2} \geq 24$ hours). The enzyme contained flavin and TPP and remained partially active without addition of these cofactors to the assay mixture. The enzyme can also use 2-ketoisovalerate instead of pyruvate as a substrate. The catalytic and regulatory (small) subunits had native molecular weights of 156 kDa and 38 kDa, which

was suggestive of a dimeric structure for each subunit. Reconstitution of the holoenzyme *via* mixing individually purified catalytic and regulatory subunits led to a substantial increase in both synthase and decarboxylase activities. This is the first report on characterization of a thermostable AHAS and also represents the highest specific activity of AHAS activity found to date.

Another enzyme known to be involved in catalysis of acetaldehyde production from pyruvate is CoA-acetylating acetaldehyde dehydrogenase (AcDH encoded by *mhpF* and *adhE*). Pyruvate is oxidized into acetyl-CoA by either POR or pyruvate formate lyase (PFL), and AcDH catalyzes the reduction of acetyl-CoA to acetaldehyde. AcDH is present in some mesophilic (such as clostridia) and thermophilic bacteria (*e.g.* *Geobacillus* and *Thermoanaerobacter*). However, no AcDH gene or protein homologs could be found in the released genomes and proteomes of hyperthermophiles. Moreover, no such activity was detectable from the cell-free extracts of different hyperthermophiles under different assay conditions.

In conclusion, no commonly-known PDCs was found in hyperthermophiles, but two types of acetaldehyde-producing enzymes were present in various bacterial and archaeal hyperthermophiles. These enzymes were the bifunctional POR/PDC and AHAS/PDC. Although the deduced amino acid sequences from different hyperthermophiles are quite similar, the levels of POR and PDC activities appeared to differ significantly between the archaeal and bacterial enzymes, which most likely reflects the different physiological implications of each activity. The PDC to POR ratios for the archaeal enzyme from *T. guaymasensis* and *P. furiosus* were about 0.19 and 0.2, respectively. In the case of bacterial enzymes, the PDC to POR ratios were 0.016 and 0.018 for *T. maritima* and *T. hypogea*, respectively. Remarkably, the archaeal bifunctional enzymes showed different pH optima for POR (pH 8.4) and PDC (pH 9.5-10.2), while the bacterial POR/PDC had the same pH optima of 8.4. The recombinant AHAS enzyme from *T. maritima* is the first one characterized in hyperthermophiles, and it is also capable of catalyzing the production of acetaldehyde from pyruvate with a PDC to AHAS activity ratio of 0.13. Besides the physiological implications of the AHAS *per se*, the characterized PDC activity of this enzyme is of great importance in determination of the ethanol production pathways in hyperthermophiles. Instead of the commonly-known PDC, it appears that various multifunctional enzymes are responsible for catalyzing the non-oxidative decarboxylation of pyruvate to acetaldehyde in hyperthermophiles.

Acknowledgements

I would foremost like to thank my advisor, Dr. Kesen Ma, for his assistance and support through this study. I am grateful to the other advisory committee members Dr. Owen P. Ward and Dr. Trevor Charles for their guidance and activities in the completion of this dissertation.

I deeply appreciate the help and support of Dr. Cheryl Duxbury. Her constructive guidance, optimistic support, and helpful insights have nourished my intellectual maturity, from which I will continue to benefit. I thank helps of Yong Li for his helps with inverse PCR and sequencing of *T. hypogea*.

So many incredible people I have worked with at University of Waterloo. I would like to express my profound gratitude to my colleagues and friends at the Department of Biology, I learned a lot from Dr. Xiangxian Ying and Dr. Xianqin Yang. I would like to specially thank all of the undergraduate students who I had the pleasure of working with during these years, Alton Wong, Benozir Sarafuddin, Frank Gong, Hanieh Park, Annie Hsu, Mikhail Sadhu, and the others. Many thanks to Kate Wood for editing the manuscripts and constructive comments.

I would also like to extend my appreciation to my friends Dr. Sheva Naahidi and Dr. Hamed Majedi. Their experience and advices in this endeavor was indispensable for my success. I am grateful for their friendship, advice, kindness, and the good moments.

Finally I would like to thank my beloved wife Nafiseh for being beside me through this long journey. Without her continuous love, support, and encouragement, this success would have been very difficult to achieve. I would like to thank my dear son Omid for his love.

Dedication

To Nafiseh and Omid

My loving family

Table of Contents

AUTHOR'S DECLARATION	ii
Abstract	iii
Acknowledgements	vi
Dedication	vii
Table of Contents	viii
List of Figures	xii
List of Tables	xiv
List of Abbreviations	xv
Chapter 1 General introduction	1
1.1 Hyperthermophiles	2
1.1.1 The order Thermotogales	5
1.1.2 The order Thermococcales	8
1.2 Microbial production of ethanol	9
1.2.1 Ethanol production by thermophiles.....	13
1.2.2 Ethanol production by hyperthermophiles	14
1.3 Acetaldehyde production pathways.....	16
1.3.1 TPP-dependent enzymes	16
1.3.2 Pyruvate decarboxylase (PDC).....	21
1.3.3 Pyruvate ferredoxin oxidoreductase (POR).....	23
1.3.4 POR/PDC bifunctional enzyme.....	32
1.3.5 Acetaldehyde dehydrogenase (CoA acetylating)	32
1.3.6 Acetohydroxy acid synthase (AHAS)	33
1.3.7 Objectives of the present study.....	33
Chapter 2 Characterization of a bifunctional POR/PDC from the hyperthermophilic archaeon <i>Thermococcus guaymasensis</i>	35
2.1 Overview	36
2.2 Introduction	37
2.3 Materials and Methods	40
2.3.1 Reagents and chemicals.....	40
2.3.2 Microorganisms and growth conditions	40
2.3.3 Sequencing of <i>por/vor</i> operon	43

2.3.4 Anaerobic techniques	45
2.3.5 Preparation of cell-free extracts.....	45
2.3.6 Enzyme purification	46
2.3.7 Protein concentration determination.....	48
2.3.8 SDS-PAGE.....	48
2.3.9 Estimation of native molecular mass.....	48
2.3.10 AcDH assay	48
2.3.11 POR activity assay.....	49
2.3.12 PDC activity assay.....	50
2.3.13 Determination of PDC of pyruvate dehydrogenase (PDH)	52
2.3.14 Biochemical and biophysical characterization	52
2.4 Results	54
2.4.1 Growth of <i>T. guaymasensis</i>	54
2.4.2 Sequencing of the <i>por/vor</i> gene cluster in <i>T. guaymasensis</i>	54
2.4.3 Searching for AcDH (CoA acetylating) activity in hyperthermophiles	56
2.4.4 Purification	61
2.4.5 Estimation of native molecular mass.....	67
2.4.1 Catalytic properties of the enzymes.....	67
2.5 Discussion	73
Chapter 3 POR/PDC bifunctional enzyme from <i>Thermotoga maritima</i> and <i>Thermotoga hypogea</i>	85
3.1 Overview	86
3.2 Introduction	87
3.3 Materials and Methods	90
3.3.1 Reagents and chemicals.....	90
3.3.2 Microorganisms and growth conditions	90
3.3.3 Sequencing of <i>por</i> genes of <i>T. hypogea</i>	91
3.3.4 Anaerobic techniques	93
3.3.5 Preparation of cell-free extracts.....	93
3.3.6 Enzyme purification	93
3.3.7 Protein concentration determination.....	95
3.3.8 SDS-PAGE.....	95
3.3.9 Estimation of native molecular masses	95

3.3.10 POR assay.....	95
3.3.11 PDC activity assay.....	96
3.3.12 Biochemical and biophysical characterization	99
3.4 Results	101
3.4.1 Sequence analysis of <i>por</i> genes.....	101
3.4.2 Purification of POR/PDC from <i>T. maritima</i> and <i>T. hypogea</i>	106
3.4.3 Molecular mass determination	110
3.4.4 Catalytic properties of the enzymes.....	110
3.5 Discussion	122
Chapter 4 AHAS/PDC activities of recombinant AHAS from <i>Thermotoga maritima</i>	128
4.1 Overview	129
4.2 Introduction	130
4.3 Materials and Methods	139
4.3.1 Reagents and chemicals.....	139
4.3.2 Microorganisms and plasmids.....	139
4.3.3 CFE preparation from hyperthermophiles.....	141
4.3.4 Genomic DNA isolation from <i>T. maritima</i> and <i>P. furiosus</i>	141
4.3.5 Genome searches	142
4.3.6 Construction of expression plasmids.....	142
4.3.7 Purification of recombinant proteins	142
4.3.8 Protein determination	148
4.3.9 SDS-PAGE.....	148
4.3.10 AHAS activity assay.....	148
4.3.11 PDC activity assay (of AHAS).....	150
4.3.12 Anaerobic techniques	152
4.3.13 Native molecular mass estimation.....	152
4.3.14 Biochemical and biophysical characterization	153
4.3.15 Reconstitution of TmAHAS	154
4.4 Results	154
4.4.1 The <i>ilv</i> operon in hyperthermophiles: genome sequence analysis (<i>in silico</i> study).....	154
4.4.2 FAD- and TPP-binding motif in hyperthermophilic AHASs.....	159
4.4.3 AHAS activity in cell-free extracts of hyperthermophiles	161

4.4.4 Oxygen sensitivity of native AHAS activity	161
4.4.5 Expression of recombinant AHAS	166
4.4.6 Purification of recombinant TmAHAS subunits	173
4.4.7 Molecular weights of the recombinant proteins	178
4.4.8 PDC activity of recombinant AHAS	182
4.4.9 Catalytic properties of synthase and decarboxylase reactions.....	182
4.4.10 Oxygen sensitivity of TmAHAS	186
4.4.11 Thermal stability of TmAHAS	187
4.4.12 Reconstitution of holoenzyme	187
4.5 Discussion	195
Chapter 5 General conclusions.....	205
5.1 Commonly-known PDC and AcDH are not present in hyperthermophiles.....	206
5.2 POR/PDC and AHAS/PDC are novel enzymes catalyzing the production of acetaldehyde from pyruvate in hyperthermophiles	206
5.3 Outlook.....	209
Copyright Permissions	211
Bibliography	216

List of Figures

Figure 1-1. Universal phylogenetic tree based on small-subunit rRNA sequence.....	4
Figure 1-2. Two pathways of ethanol production from pyruvate.....	17
Figure 1-3. Structure of thiamine pyrophosphate.....	18
Figure 1-4. Reactions and intermediates in pyruvate-processing TPP-dependent enzymes.....	20
Figure 1-5. Catalytic mechanism of POR and intermediates involved.....	28
Figure 1-6. Spatial organization of the [4Fe-4S] clusters in the POR of <i>Desulfovibrio africanus</i>	29
Figure 2-1. General steps involved in PDC activity assay.....	51
Figure 2-2. Gene organization of <i>por/vor</i> gene cluster in <i>T. guaymasensis</i>	55
Figure 2-3. Intercistronic sequences in <i>por/vor</i> operon of <i>T. guaymasensis</i>	57
Figure 2-4. Multiple sequence alignment of part of PorB from various bacteria and archaea.....	58
Figure 2-5. Rooted phylogenetic tree based on amino acid sequences of various Thermococcales POR subunits.....	60
Figure 2-6. Analysis of purified enzyme from <i>T. guaymasensis</i>	64
Figure 2-7. Analysis of purified enzyme from <i>P. furiosus</i>	65
Figure 2-8. Co-elution of POR and PDC activities during chromatography steps.....	66
Figure 2-9. pH dependency of POR and PDC activities of the enzyme from <i>T. guaymasensis</i>	70
Figure 2-10. Oxygen sensitivity of POR and PDC activities of <i>T. guaymasensis</i>	71
Figure 2-11. Temperature dependence of <i>T. guaymasensis</i> POR and PDC activities.....	72
Figure 2-12. Schematic pathway of ethanol production in <i>T. guaymasensis</i>	80
Figure 3-1. General steps involved in PDC activity assay.....	98
Figure 3-2. Schematic representation of <i>por</i> ORF organization in Thermotogales.....	102
Figure 3-3. A rooted phylogenetic analysis of POR subunits from various bacteria and archaea.....	104
Figure 3-4. Multiple sequence alignment of part of PorD subunit from Thermotogales.....	105
Figure 3-5. Analysis of purified POR/PDC from <i>T. maritima</i> and <i>T. hypogea</i>	109
Figure 3-6. Co-elution of PDC activity in <i>T. maritima</i>	111
Figure 3-7. pH dependency of POR and PDC activities of POR/PDC from <i>T. maritima</i>	112
Figure 3-8. pH dependency of POR and PDC activities of POR/PDC from <i>T. hypogea</i>	113
Figure 3-9. Oxygen sensitivity of POR and PDC activities of <i>T. maritima</i> and <i>T. hypogea</i>	118
Figure 3-10. Temperature dependence of <i>T. maritima</i> PDC activity.....	119
Figure 3-11. Temperature dependence of <i>T. hypogea</i> POR and PDC activities.....	120
Figure 3-12. Thermal stability of POR and PDC activities of purified ThPOR.....	121

Figure 4-1. Reactions catalyzed by anabolic AHAS and catabolic AHAS	134
Figure 4-2. Biosynthesis pathways of branched chain amino acids and the butanediol pathway	135
Figure 4-3. Construction of expression plasmids for <i>T. maritima</i> AHAS.....	144
Figure 4-4. Construction of expression plasmids for <i>P. furiosus</i> AHAS	145
Figure 4-5. General steps of AHAS activity assay	149
Figure 4-6. General steps of PDC activity assay for the AHAS.....	151
Figure 4-7. Relatedness of AHAS catalytic subunits	156
Figure 4-8. Relatedness of AHAS regulatory subunits	157
Figure 4-9. Gene organization of the <i>ilv</i> gene cluster in <i>T. maritima</i> and <i>P. furiosus</i>	158
Figure 4-10. Intercistronic sequences in the <i>ilv</i> operon of <i>T. maritima</i>	160
Figure 4-11. Conserved motifs in AHASs.....	162
Figure 4-12. AHAS activity in CFEs of different hyperthermophilic bacteria and archaea	164
Figure 4-13. Oxygen sensitivity of AHAS activities in CFEs of <i>T. maritima</i> and <i>P. furiosus</i>	165
Figure 4-14. Coding sequences of catalytic and regulatory subunits of TmAHAS	167
Figure 4-15. Analysis of over-expression of different clones at 37°C.....	168
Figure 4-16. Analysis of the effect of temperatures on expression of MI-pET30a	170
Figure 4-17. Effect of the expression temperature on AHAS activity of MI-pET30a.....	171
Figure 4-18. Effect of the expression temperature on AHAS activity of Mc-pET30a.....	172
Figure 4-19. Analysis of the effect of heat-treatment on purification of MI-pET30a	175
Figure 4-20. Effect of heat-treatment of crude extract on AHAS activity	176
Figure 4-21. Analysis of purified catalytic subunit of TmAHAS	180
Figure 4-22. Analysis of purified recombinant regulatory subunit of TmAHAS.....	181
Figure 4-23. pH dependency of AHAS and PDC activities of recombinant TmAHAS.....	183
Figure 4-24. Dependence of AHAS and PDC activities on pyruvate concentration.....	185
Figure 4-25. Oxygen sensitivity of recombinant TmAHAS when AHAS was measured.....	188
Figure 4-26. Oxygen sensitivity of recombinant TmAHAS when PDC was measured.....	189
Figure 4-27. Thermal stability of synthase and decarboxylase activities.....	190
Figure 4-28. Determination of optimal temperatures of AHAS and PDC activities of TmAHAS	191
Figure 4-29. Effect of TmAHAS reconstitution on AHAS and PDC activities	193
Figure 4-30. Gel-filtration chromatography of AHAS subunits.....	194
Figure 4-31. Proposed acetoin production pathway in hyperthermophiles	204

List of Tables

Table 1-1. List of the species described in the order Thermotogales	6
Table 1-2. List of the species described in the order Thermococcales	10
Table 1-3. PORs isolated and characterized from different microorganisms.....	25
Table 2-1. Composition of trace mineral solution used for the growth of <i>T. guaymasensis</i>	41
Table 2-2. Composition of 100X vitamin solution used for small-scale growth of <i>T. guaymasensis</i> ..	42
Table 2-3. The primers used for the sequencing of the <i>por/vor</i> operon of <i>T. guaymasensis</i>	44
Table 2-4. Purification of bifunctional POR/PDC from <i>P. furiosus</i>	62
Table 2-5. Purification of bifunctional POR/PDC from <i>T. guaymasensis</i>	63
Table 2-6. Kinetic parameters of POR and PDC of <i>T. guaymasensis</i> and <i>P. furiosus</i>	68
Table 2-7. Structure and activities of PORs and VORs from various organisms.....	75
Table 2-8. Properties of commonly-known PDCs characterized from various organisms	77
Table 3-1. The primers used for the sequencing of the <i>por</i> operon of <i>T. hypogea</i>	92
Table 3-2. Purification of bifunctional POR/PDC from <i>T. hypogea</i>	107
Table 3-3. Purification of POR/PDC from <i>T. maritima</i>	108
Table 3-4. Kinetic parameters for POR and PDC activities of <i>T. hypogea</i> and <i>T. maritima</i>	115
Table 3-5. Kinetic properties of some characterized PORs.....	125
Table 4-1. Search of the genome sequences of some hyperthermophiles against the commonly-known PDCs.....	131
Table 4-2. General properties of anabolic and catabolic AHASs.....	133
Table 4-3. Amino acid requirements of Thermotogales and Thermococcales	138
Table 4-4. Oligonucleotide primers used for amplification of the coding sequences of the putative catalytic and regulatory subunits of <i>ilvB</i> and <i>ilvN</i> genes from <i>T. maritima</i> and <i>P. furiosus</i>	143
Table 4-5. Homologs of <i>ilv</i> operon in Thermotogales and Thermococcales.....	155
Table 4-6. AHAS activity in cell-free extracts of different hyperthermophiles	163
Table 4-7. Properties of recombinant proteins as deduced from their primary structures	169
Table 4-8. Survey of heat-precipitation temperatures for some recombinant hyperthermophilic proteins expressed in <i>E. coli</i>	174
Table 4-9. Purification of recombinant catalytic subunit of TmAHAS.....	179
Table 4-10. Apparent kinetic parameters for AHAS and PDC activities of TmAHAS	184
Table 4-11. Catalytic and structural properties of AHAS activity from different organisms	196
Table 5-1. POR/PDC and AHAS/PDC activities in hyperthermophiles	207

List of Abbreviations

ACDH	Acetaldehyde dehydrogenase
ACS	Acetyl-CoA synthase
ADH	Alcohol dehydrogenase
ADP	adenosine diphosphate
AHAS	Acetohydroxyacid synthase
ATP	adenosine triphosphate
BCAA	Branched chain amino acid
CAPS	3-(Cyclohexylamino)-1-propanesulfonic acid
CFE	Cell-free extract
CoA	Coenzyme A
DTT	dithioeritol
EDTA	Ethylenediaminetetraacetic acid
EPDS	N-(2-hydroxyethyl)-piperazine-N'-(3-propanesulfonic acid)
FAD	Flavin adenine dinucleotide
FPLC	Fast performance liquid chromatography
HEPES	4-(2-Hydroxyethyl)-1-piperazineethanesulfonic acid
HPLC	High performance liquid chromatography
HTCE	Heat-treated cell-free extract
IPCR	Inverse polymerase chain reaction
KOR	2-keto acid ferredoxin oxidoreductase
MV	Methyl viologen
NAD ⁺	Nicotinamide adenine dinucleotide
NADP ⁺	Nicotinamide adenine dinucleotide phosphate
PCR	polymerase chain reaction
PDC	Pyruvate decarboxylase
PfPOR	<i>Pyrococcus furiosus</i> pyruvate ferredoxin oxidoreductase
POR	pyruvate ferredoxin oxidoreductase
SDT	Sodium dithionite
TgPOR	<i>Thermococcus guaymasensis</i> pyruvate ferredoxin oxidoreductase

TmAHAS	<i>Thermotoga maritima</i> Acetohydroxyacid synthase
TPP	Thiamine pyrophosphate
Tris	2-Amino-2-hydroxymethyl-1,3-propanediol
VOR	2-ketoisovalerate ferredoxin oxidoreductase

Chapter 1 General introduction

1.1 Hyperthermophiles

Extremophiles are microorganisms that require extreme conditions for optimal growth. These “extreme” parameters may include physical conditions, for instance, high temperature (thermophiles), high hydrostatic pressure (piezophiles), and high radiation doses (radiophiles). These conditions also encompass geo-chemical environments, including high salinity (halophiles), low pH (acidophiles), high pH (alkaliphiles), or even combinations of any of these conditions (van den Burg 2003).

Thermophilic microorganisms can be further categorized into several groups: moderate thermophiles, or simply thermophiles, are those that grow optimally between 50-64°C, extreme thermophiles are those with optimal growth temperatures between 65-79°C. Finally, the organisms that can grow optimally above 80°C are called hyperthermophiles. Hyperthermophiles can survive at room temperature for long periods of time, but cannot propagate at temperatures lower than 50°C (Wiegel 1990; Stetter 1996; Charlier and Droogmans 2005; Stetter 2006; Lebedinsky *et al.* 2007; Wagner and Wiegel 2008).

Some hyperthermophiles can endure multiple extreme conditions at the same time; for example, the anaerobic hyperthermophilic piezophilic archaeon *Thermococcus barophilus* not only grows optimally at 85°C but also has a shorter doubling time when provided with strong hydrostatic pressures (Marteinsson *et al.* 1999). The same is also true for the moderate thermophilic bacterium *Natranaerobius thermophilus*, which can grow optimally at temperatures of 53°C, pH of 9.5 and in sodium ion concentrations of 3.3-3.9 M (Mesbah *et al.* 2007).

The first hyperthermophilic organism (*Sulfolobus acidocaldarius*) was discovered in 1972 in a hot spring in Yellowstone National Park (Brock *et al.* 1972). Examples of the natural habitats for extremely thermophilic and hyperthermophilic microorganisms include but are not limited to marine and terrestrial environments like shallow deep-sea hydrothermal vents at the ocean floor (also known as “black smokers”) and volcanic or geo-thermally heated environments like hot springs, terrestrial solfataric fields (solfatares), mud pools, and oil reservoirs (Vieille and Zeikus 2001; Charlier and Droogmans 2005; Stetter 2006; Wagner and Wiegel 2008).

Many of these environments naturally contain very low levels of oxygen or are completely anoxic, for several reasons, including the low solubility of oxygen at high temperatures and sometimes at high salt concentrations; the high concentration of reducing gasses; such as H₂ and H₂S; being distant from the surface area, resulting in restricted access to oxygen; and consumption of the limited

available oxygen by the aerobic populations. Consequently, many of these organisms are adapted to survive in completely anaerobic conditions or in the presence of very limited oxygen (aero-tolerant) (Stetter *et al.* 1990; Stetter 1996; Wagner and Wiegel 2008).

Other than a few thermophilic members (Maheshwari *et al.* 2000; Baumgartner *et al.* 2003), so far there has been no report on the presence of hyperthermophilic members in the *Eukarya* domain. Only a few bacterial lineages, including *Thermotogaceae*, *Aquificaceae* and *Thermodesulfobacteriaceae*, contain hyperthermophilic members. Most of the known hyperthermophiles (and other extremophiles) are members of *Archaea*, within which the families containing hyperthermophilic taxa include *Methanopyraceae*, *Methanothermaceae*, *Methanocaldococcaceae*, *Thermococcaceae*, *Archaeoglobaceae*, *Sulfolobaceae*, *Desulfurococcaceae*, *Pyrodictiaceae*, *Thermofilaceae*, and *Thermoproteaceae* (Stetter 2006; Lebedinsky *et al.* 2007; Wagner and Wiegel 2008). Hyperthermophiles (both bacteria and archaea) are presented at the deepest and shortest branch of the tripartite 16S rRNA phylogenetic tree of life (**Figure 1-1**) with *Eukarya* (also known as *Eucarya*), *Bacteria*, and *Archaea* (Woese and Fox 1977; Woese *et al.* 1990). While a highly controversial evolutionary topic [for example see (Glansdorff *et al.* 2008; Gribaldo *et al.* 2010)], the aforementioned data suggest (Woese 1998; Forterre 2002) that they might be the closest organisms to the last universal common ancestor (LUCA).

Hyperthermophilic microorganisms are widely studied for their remarkable scientific values and industrial potential. It is generally accepted that hyperthermophilic enzymes have very similar functions and catalytic mechanisms to their mesophilic homologs. However, most of the hyperthermophilic enzymes characterized so far have optimum temperatures close to the host organism's requirements; thus, due to their intrinsic properties, the enzymes are stable and active under conditions that are detrimental to their mesophilic counterparts. Interestingly, enzymes from extremophiles usually show increased stability not to one, but to several environmental factors. There are a number of advantages for using the hyper/thermophilic enzymes (especially for industrial applications) over their mesophilic partners, including the reduced risk of contamination during industrial processes, the possibility of self-distillation of the products at high temperatures, decreased viscosity and increased solubility/bioavailability of both the enzyme and the substrate(s) leading to minimization of the diffusion limitations, and elimination of the costly transportation under cold

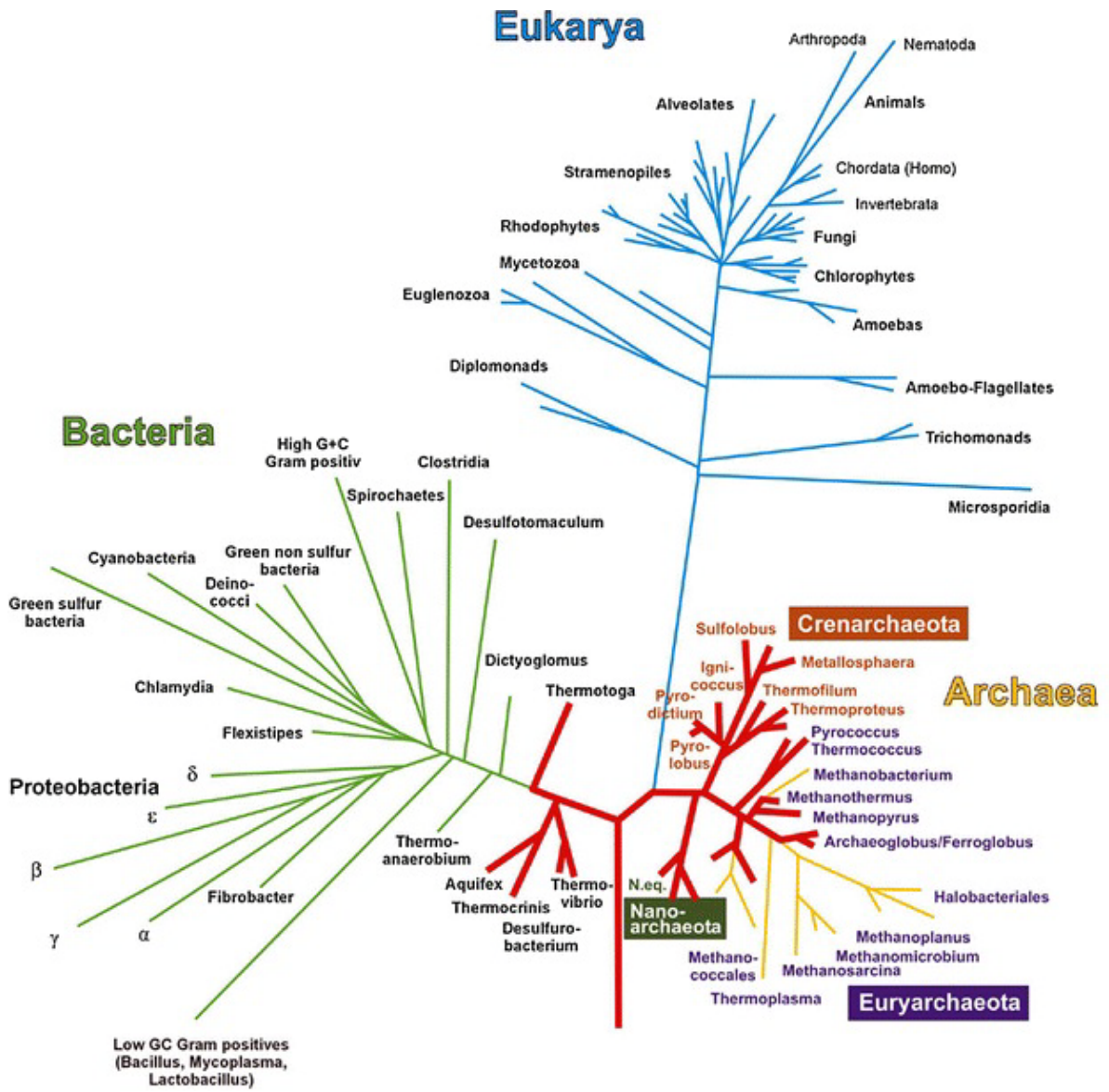


Figure 1-1. Universal phylogenetic tree based on small-subunit rRNA sequence. The bulky lineage represents hyperthermophiles (Stetter 2006).

temperature-controlled environment (Vieille and Zeikus 2001; Haki and Rakshit 2003; Sommer *et al.* 2004; Egorova and Antranikian 2005; Morozkina *et al.* 2010).

The aforementioned properties along with high demand from the biotech industries for the development of tailor-made bio-catalysts have created significant attention on the biochemistry and physiology of these organisms. Enzymes such as proteases, polymerases, hydrolases, isomerases, lipases, and oxidases are studied for their potential biotechnological exploitation, with the ultimate goal of using the whole organisms or their products (mainly enzymatic) for biotechnological applications.

It is also appealing to determine the molecular, biochemical, physiological, and evolutionary mechanisms that enable these organisms to adapt to such hostile environments. Furthermore, hyperthermophilic proteins serve as models to study enzyme evolution, structure-function relationships and catalytic mechanisms. The findings of these studies can benefit the design of highly stable and active enzymes to be used for many different applications (van den Burg 2003; Morozkina *et al.* 2010; Atomi *et al.* 2011).

Hyperthermophiles survive and grow under conditions that are believed to resemble those of the primal earth, under which life began; thus, studying these organisms may provide clues on how life started (Glansdorff *et al.* 2008; Brazelton *et al.* 2010). These types of studies, generally known as “origin-of-life” studies, as well as astrobiological studies (Cavicchioli 2002; Tung *et al.* 2005) covet the enormous advantages of archaea, specifically hyperthermophiles.

1.1.1 The order Thermotogales

The order Thermotogales contains anaerobic, heterotrophic, extremely thermophilic and hyperthermophilic bacteria that have an outer sheath-like structure called the “toga” which surrounds the cell and is visible during all phases of growth. Thermotogales represent a slowly evolving and deep branch of the phylogenetic tree of life, along with *Aquificales* (**Figure 1-1**). Although the members of Thermotogales are widespread and can thrive in many diverse thermal environments, most of them were originally isolated from deep sub-surface oil reservoirs (**Table 1-1**) and almost all of them are strict anaerobes. The Thermotogales include a single family *Thermotogaceae* which contains seven genera: *Kosmotoga* (Nunoura *et al.* 2010), *Petrotoga*, *Geotoga*, *Marinitoga*, *Fervidobacterium*, *Thermosipho*, and *Thermotoga* (Huber and Hanning 2006; Wagner and Wiegel 2008). The species representing different genera of Thermotogales are presented in **Table 1-1**. The

Table 1-1. List of the species described in the order Thermotogales

Species	Growth temp. [optimum] (°C)	pH range [optimum]	Original isolation	Reference	Genome sequence*
<i>Geotoga subterranea</i>	30–55 [50]	5.5–9 [6.5]	Oil reservoir	Jeanthon <i>et al.</i> 1995a	-
<i>Geotoga petraea</i>	30–60 [45]	5.5–9 [6.5]	Oil reservoir	Jeanthon <i>et al.</i> 1995a	-
<i>Marinitoga camini</i>	25–65 [55]	5–9 [7]	deep-sea hydrothermal chimney	Wery <i>et al.</i> 2001	DOE-JGI
<i>Marinitoga piezophila</i>	45–70 [65]	5–8 [6]	deep-sea hydrothermal chimney	Alain <i>et al.</i> 2002	DOE-JGI
<i>Marinitoga hydrogenitolerans</i>	35–65 [60]	4.5–8.5 [6]	deep-sea hydrothermal chimney	Postec <i>et al.</i> 2005	-
<i>Marinitoga okinawensis</i>	30–70[55–60]	5.0–7.4 [5.5–5.8]	deep-sea hydrothermal chimney	Nunoura <i>et al.</i> 2007	-
<i>Marinitoga litoralis</i>	45–70 [60]	5.5–7.5 [6]	Hot spring	Postec <i>et al.</i> 2010	-
<i>Petrotoga mexicana</i>	25–65 [55]	5.8–8.5 [6.6]	Oil reservoir	Miranda-Tello <i>et al.</i> 2007	-
<i>Petrotoga miotherma</i>	35–65 [55]	5.5–9 [6.5]	Oil reservoir	Miranda-Tello <i>et al.</i> 2007	Integrated Genomics
<i>Petrotoga olearia</i>	37–60 [55]	6.5–8.5 [7.5]	Oil reservoir	L'Haridon <i>et al.</i> 2002	-
<i>Petrotoga sibirica</i>	37–55 [55]	6.5–9.4 [8]	Oil reservoir	L'Haridon <i>et al.</i> 2002	-
<i>Petrotoga mobilis</i>	40–65 [58–60]	5.5–8.5 [6.5–7]	Oil reservoir	Lien <i>et al.</i> 1998	DOE-JGI
<i>Petrotoga halophila</i>	45–65 [55–60]	5.6–7.8 [6.7–7.2]	Oil reservoir	Miranda-Tello <i>et al.</i> 2007	-
<i>Thermosipho atlanticus</i>	45–80 [65]	5–9 [6]	deep-sea hydrothermal chimney	Urios <i>et al.</i> 2004	-
<i>Thermosipho melanesiensis</i>	45–80 [70]	3.5–9.5 [6.5–9.5]	deep-sea hydrothermal chimney	Antoine <i>et al.</i> 1997	DOE-JGI
<i>Thermosipho geolei</i>	45–75 [70]	6–9.4 [7.5]	Oil reservoir	L'Haridon <i>et al.</i> 2001	-
<i>Thermosipho japonicus</i>	45–80 [72]	5.3–9.3 [7.2]	deep-sea hydrothermal chimney	Takai and Horikoshi 2000	-
<i>Thermosipho africanus</i>	35–77 [75]	6–8 [7.2]	deep-sea hydrothermal chimney	Ravot <i>et al.</i> 1996	Dalhousie University
<i>Thermosipho globiformans</i>	40–75 [68]	5–8.2[6.8]	deep-sea hydrothermal chimney	Kuwabara <i>et al.</i> 2011	-
<i>Thermosipho affectus</i>	37–75[70]	5.6–8.2[6.6]	deep-sea hydrothermal chimney	Podosokorskaya <i>et al.</i> 2010	-
<i>Fervidobacterium gondwanense</i>	[65–68]	[7]	Geo-thermally heated water	Andrews and Patel 1996	-
<i>Fervidobacterium islandicum</i>	50–80 [65]	6–8 [7]	Continental solfatara	Huber <i>et al.</i> 1990	-
<i>Fervidobacterium nodosum</i>	41–79 [70]	6–8 [7]	Hot spring	Patel <i>et al.</i> 1985	DOE-JGI
<i>Fervidobacterium pennavorans</i>	50–80 [70]	5.5–8.0 [6.5]	Hot spring	Friedrich and Antranikian 1996	DOE-JGI*
<i>Fervidobacterium changbaicum</i>	55–90 [75–80]	6.3–8.5 [7.5]	Hot spring	Cai <i>et al.</i> 2007	-
<i>Thermotoga lettingae</i>	50–75 [65]	6–8.5 [7]	Methanol-degrading bioreactor	Balk <i>et al.</i> 2002	DOE-JGI
<i>Thermotoga elfii</i>	50–72 [66]	5.5–8.7 [7.5]	Oil reservoir	Ravot <i>et al.</i> 1995	-
<i>Thermotoga hypogea</i>	56–90 [70]	6.1–9.1 [7.3–7.4]	Oil reservoir	Fardeau <i>et al.</i> 1997	-
<i>Thermotoga subterranea</i>	50–75 [70]	6–8.5 [7]	Oil reservoir	Jeanthon <i>et al.</i> 1995b	-
<i>Thermotoga thermarum</i>	55–84 [70]	5.5–9 [7]	Continental Solfataric spring	Windberger <i>et al.</i> 1989	DOE-JGI
<i>Thermotoga maritima</i>	55–90 [80]	5.5–9 [6.5]	Geo-thermally heated sea floor	Huber <i>et al.</i> 1986	TIGR
<i>Thermotoga petrophila</i>	47–88 [80]	5.2–9 [7]	Oil reservoir	Takahata <i>et al.</i> 2001	Dalhousie University

Species	Growth temp. [optimum] (°C)	pH range [optimum]	Original isolation	Reference	Genome sequence*
<i>Thermotoga naphthophila</i>	48–86 [80]	5.4–9 [7]	Oil reservoir	Takahata <i>et al.</i> 2001	DOE-JGI
<i>Thermotoga neapolitana</i>	55–90 [80]	5.5–9 [7]	Submarine thermal vent	Takahata <i>et al.</i> 2001	Genotech Corp.
<i>Kosmotoga oleriae</i>	20-80 [65]	5.5-8 [6.8]	Oil reservoir	DiPippo <i>et al.</i> 2009	DOE-JGI
<i>Kosmotoga arenicorallina</i>	50-65 [60]	6.2-8 [7.1]	submarine hot spring	Nunoura <i>et al.</i> 2010	-
<i>Kosmotoga shengliensis</i>	47-75 [65]	6-8 [7]	Oil reservoir	Feng <i>et al.</i> 2010; Nunoura <i>et al.</i> 2010	-

*DOE-JGI: The U.S. Department of Energy (DOE) Joint Genome Institute (JGI); TIGR, The Institute for Genomic Research

genome sequences are available for eight members of the *Thermotoga* genus, including *Thermotoga maritima*, *Thermotoga petrophila*, *Thermotoga naphthophila*, *Thermotoga thermarum*, *Thermotoga lettingae*, *Thermotoga neapolitana*, and *Thermotoga* sp. strain RQ2. The organism shares many orthologous genes with Archaeal hyperthermophiles, suggesting the occurrence of horizontal gene transfer between these two domains (Nelson *et al.* 1999).

Thermotogales can use sulfurous compounds as terminal electron acceptors. Members of the order Thermotogales have a great hydrolytic capacity and are able to utilize complex carbohydrates and proteins. All of the organisms under this order can produce hydrogen to some extent. In addition to their extensive supply of hydrolytic enzymes, the Thermotogales are particular interest to researchers for their high potential as hydrogen producers (Bronnenmeier *et al.* 1995; Balk *et al.* 2002; Kluskens *et al.* 2003; Yang *et al.* 2006; Chou *et al.* 2008). The type strain of Thermotogales is *T. maritima* which was originally isolated from the geothermally heated marine sediments at Vulcano, Italy. *T. maritima* utilizes glucose, maltose, xylose, galactose, glycogen, sucrose, ribose, starch, yeast extract, and whole cell extracts of bacteria (and archaea) for growth; it has also been investigated in more detail than have other members of Thermotogales and other hyperthermophilic bacteria (Huber *et al.* 1986).

The existence of a new subclass of mesophilic “mesotoga” was lately postulated based on the metagenomics information (Nesbø *et al.* 2006). The first member of this proposed genus was recently cultivated and shown to have an optimal growth temperature of 37°C, with a doubling time of about 16.5 h on xylose (Ben Hania *et al.* 2011). It was shown that *Mesotoga prima* uses sulfur as terminal electron acceptor. The full sequence of its genome was made available recently (Nesbø *et al.* 2012).

1.1.2 The order Thermococcales

The domain archaea initially contained two kingdoms Crenarchaeota and Euryarchaeota (Zwickl *et al.* 1990). Since then, based on the isolation of new microorganisms and sequencing of the 16S rRNA, more kingdoms (phyla) have been proposed under the domain Archaea (**Figure 1-1**), including *Nanoarchaeota* (Huber *et al.* 2002), *Korarchaeota* (Elkins *et al.* 2008), and *Thaumarchaeota* (Brochier-Armanet *et al.* 2008). However, it is worth mentioning that there is a general consensus only on the first two kingdoms and that the classification of the latter kingdoms is still an ongoing debate, as some studies support the new potential kingdoms becoming new clades of either Euryarchaeota or Crenarchaeota (Robertson *et al.* 2005; Pace 2009).

Euryarchaeota is the most diverse kingdom and contains all of the methanogenic and extremely halophilic archaea including Thermococcales, *Methanomicrobiales*, *Methanosarcinales*, *Archaeoglobales*, and *Halobacteriales*. *Crenarchaeota* consists of *Sulfolobales*, *Thermoproteales*, and *Desulfurococcales*. There has been no *Korarchaeon* isolated to date in pure culture, and the kingdom is proposed based solely on culture-independent methods such as amplification of small subunit rRNA from environmental samples. *Nanoarchaeota* contain only one isolate: *Nanoarchaeum equitans* (**Figure 1-1**). *Thaumarchaeota* consists mainly of mesophilic archaea, and so far there has been only one report of isolation of the two marine members (Muller *et al.* 2010) reported and the rest of the members are only assigned based on culture-independent methods (Cavicchioli 2011).

Members of the order Thermococcales are the most commonly isolated hyperthermophiles and mainly consist of strictly anaerobic sulfur-reducing chemoorganotrophic *euryarchaea*. The optimum growth temperature for members of the genera *Pyrococcus* and *Thermococcus* are between 95-100°C and 80-90°C, respectively (**Table 1-2**). They are found in different thermal environments, including deep sea hydrothermal vents, marine and terrestrial solfatares, as well as oil reservoirs.

The majority of Thermococcales are sulfur-reducers and require sulfur for optimal growth. In view of the growth substrates, the general preferences of Thermococcales seem to be mostly polymeric substrates including proteins and peptide-related substrates; they may also utilize carbohydrates, although less frequently (Erauso *et al.* 1993). The hydrogen molecules produced during fermentation of proteins or carbohydrates are transferred into elemental sulfur which serves as a terminal electron acceptor leading to hydrogen sulfide (H₂S) production (Dworkin *et al.* 2006a).

1.2 Microbial production of ethanol

Demand for biofuel as a substitute for oil-based fuels is increasing due to concerns related to national security, economic stability, environmental impacts, and global warming. The national research council of the United States has predicted that, by 2020, half of organic chemicals and materials will be produced by bioconversion. Bio-ethanol can also be used as a precursor for many other commodity chemicals, such as acetaldehyde, acetic acid and their derivatives (Lynd *et al.* 1999; Zaldivar *et al.* 2001; Mabee and Saddler 2010).

Table 1-2. List of the species described in the order Thermococcales

Species	Growth temp. [optimum] (°C)	pH range [optimum]	Carbon source	Growth on amino acids	Effect of Sulfur	Reference	Genome sequence†
<i>Palaeococcus ferrophilus</i>	60–88 [83]	4.0–8.0 [6]	Complex substrates	n.d.	R	Takai <i>et al.</i> 2000	DOE-JGI
<i>Palaeococcus helgesonii</i>	45-85 [80]	5-8 [6.5]	Yeast or beef extract, tryptone, peptone	n.d	S	Amend <i>et al.</i> 2003	-
<i>Pyrococcus furiosus</i>	3870-103 [100]	5–9 [7]	Complex substrates, maltose, starch, pyruvate, and casamino acids	Yes	R	Fiala and Stetter 1986	Utah Genome Center
<i>Pyrococcus abyssi</i>	67-100 [96]	4–8.5 [6.8]	Complex substrates, maltose, starch, pyruvate, and casamino acids	Yes	S	Erauso <i>et al.</i> 1993	Genoscope
<i>Pyrococcus woesei</i> DSM 3773	70-105 [100-103]	n.d.	Yeast extract, tryptone, glycogen, and gellan	Yes	S	Zillig <i>et al.</i> 1987	-
<i>Pyrococcus endeavori</i>	80-110 [98]	4–8 [7]	Casamino acids	Yes	S	Holden and Baross 1993	-
<i>Pyrococcus horikoshii</i>	80-102 [98]	5–8 [7]	Complex substrates	Yes	S	González <i>et al.</i> 1998	NITE
<i>Pyrococcus glycovorans</i>	75-104 [95]	2.5–9.5 [7.5]	Complex substrates, and glucose	Yes	S	Barbier <i>et al.</i> 1999	-
<i>Pyrococcus yayanosii</i>	80-108 [98]	6.0-9.5 [7.5-8.0]	yeast extract, peptone, casein, sucrose, starch, chitin, pyruvate, acetate ,glycerol	No	S	Birrien <i>et al.</i> 2011	Shanghai JiaoTong University
<i>Thermococcus celer</i>	Up to93 [88]	n.d. [5.8]	Peptides stimulated by sucrose	Yes	S	Zillig <i>et al.</i> 1983	-
<i>Thermococcus kodakaraensis</i>	65-100 [95]	5–9 [7]	Complex substrates, and peptides	Yes	S	Morikawa <i>et al.</i> 1994; Atomi <i>et al.</i> 2004	Kyoto University, Japan
<i>Thermococcus litoralis</i>	65-95 [88]	6.2–8.5 [7.2]	Peptides, pyruvate	No	S	Neuner <i>et al.</i> 1990	New England Biolabs, Inc.
<i>Thermococcus stetteri</i>	60-85 [75]	5.7–7.2 [6.5]	Starch, pectin, and peptides	No	R	Miroshnichenko <i>et al.</i> 1989	-
<i>Thermococcus profundus</i>	50-90 [80]	4.5–8.5 [7.5]	Peptides, pyruvate, starch, maltose	n.d.	R	Kobayashi <i>et al.</i> 1994	-
<i>Thermococcus peptonophilus</i>	60-100 [85]	4–8 [6]	Peptides	n.d.	S	González <i>et al.</i> 1995	-
<i>Thermococcus aggregans</i>	60-94 [88]	4.6–7.9 [7]	Peptides, Casein, dextrose, and maltose	n.d.	S	Canganella <i>et al.</i> 1998	-

Species	Growth temp. [optimum] (°C)	pH range [optimum]	Carbon source	Growth on amino acids	Effect of Sulfur	Reference	Genome sequence†
<i>Thermococcus pacificus</i>	70-95 [80-88]	6–8 [6.5]	Complex substrates	n.d.	S	Miroshnichenko <i>et al.</i> 1998	-
<i>Thermococcus guaymasensis</i>	56–90 [88]	5.6–8.5 [7.2]	Peptides, Casein, dextrose, and maltose	No	S	Canganella <i>et al.</i> 1998	-
<i>Thermococcus gorgonarius</i>	68-95 [80-88]	3.4–9 [7]	Proteins, peptides	No	R	Miroshnichenko <i>et al.</i> 1998	-
<i>Thermococcus hydrothermalis</i>	53-100 [85]	2–10 [7]	Casein, peptides, and maltose	Yes	S	Godfroy <i>et al.</i> 1997	-
<i>Thermococcus zilligii</i>	[75]	n.d. [7.4]	Casein	n.d.	S	Ronimus <i>et al.</i> 1997	Korea Research Institute of Bioscience and Biotechnology
<i>Thermococcus acidaminovorans</i>	45-93 [85]	5–9.5 [9]	Peptides	Yes	S	Dirmeier <i>et al.</i> 1998	-
<i>Thermococcus aegeicus</i>	50-90 [88]	4–9 [6]	Starch	No	S	Arab <i>et al.</i> 2000	-
<i>Thermococcus barophilus</i>	75-95 [85]	4.5–9.5 [7]	Yeast extract, and peptone	No	S	Marteinsson <i>et al.</i> 1999	Moore Foundation
<i>Thermococcus barossii</i>	60-92 [82.5]	3–9 [6.5-7.5]	Tryptone, yeast extract, and malto-oligosaccharides	No	R	Duffaud <i>et al.</i> 1998	-
<i>Thermococcus chitinophagus</i>	60-93 [85]	3.5–9 [6.7]	Complex substrates, and chitin	No	S	Huber <i>et al.</i> 1995	-
<i>Thermococcus siculi</i>	50-93 [85]	5.0–9.0 [7]	Peptides	Yes	S	Grote <i>et al.</i> 1999	-
<i>Thermococcus alcaliphilus</i>	54-91 [85]	6.5–10.5 [9]	Peptides	Yes	S	Keller <i>et al.</i> 1995	-
<i>Thermococcus waiotapuensis</i>	60-90 [85]	5–8 [7]	Complex substrates, starch, maltose, and pyruvate	Yes	R	González <i>et al.</i> 1999	-
<i>Thermococcus fomiculans</i>	73-103 [90]	4.5–9.5 [8.5]	Complex substrates, and pyruvate	Yes	S	Godfroy <i>et al.</i> 1996	-
<i>Thermococcus sibiricus</i>	40-88 [78]	5.8–9 [7.5]	Peptides	n.d.	S	Miroshnichenko <i>et al.</i> 2001	NCBI
<i>Thermococcus atlanticus</i>	70-95 [85]	4–9 [7]	Peptides	No	S	Cambon-Bonavita <i>et al.</i> 2003	-
<i>Thermococcus gammatolerans</i>	55-95 [88]	5.5-6.5 [6]	Yeast extract, tryptone, peptone	No	R	Jolivet <i>et al.</i> 2003	IGM/ Universit Paris-Sud, France
<i>Thermococcus marinus</i>	55-95 [88]	4-8.5 [6]	Yeast extract, peptone	Yes	R	Jolivet <i>et al.</i> 2004	-
<i>Thermococcus</i>	55-95 [88]	4-8.5 [6]	Yeast extract, peptone	No	R	Jolivet <i>et al.</i> 2004	-

Species	Growth temp. [optimum] (°C)	pH range [optimum]	Carbon source	Growth on amino acids	Effect of Sulfur	Reference	Genome sequence†
<i>radiotolerans</i>							
<i>Thermococcus thio-reducens</i>	55-94 [83-85]	5-8.5 [7]	Yeast extract, peptone, Bacto-tryptone casamino acid	No	R	Pikuta <i>et al.</i> 2007	-
<i>Thermococcus coalescens</i>	57-90 [87]	5.2-8.7 [6.5]	Yeast extract, tryptone	n.d	S	Kuwabara <i>et al.</i> 2005	-
<i>Thermococcus celericrescens</i>	50-85 [80]	5.6-8.3 [7]	Yeast extract, tryptone	n.d	S	Kuwabara <i>et al.</i> 2007	-
<i>Thermococcus onnurineus</i>	63-90 [80]	5.0-9.0 [8.5]	Starch, casein	Yes	R	Bae <i>et al.</i> 2008	NCBI

n.d: Not determined; S: stimulatory for growth, R: required for growth; DOI-JGI, U.S. Department of Energy (DOE) Joint Genome Institute (JGI); NITE, National Institute of Technology and Evaluation; NCBI, National Centre for Biotechnology Information; IGM, Institut deGénétique et Microbiologie, Université Paris-Sud

The most commonly used ethanologenic organisms being intensively studied or already being used for industrial-scale production plants are *Zymomonas mobilis*, *Saccharomyces cerevisiae*, *Escherichia coli*, and *Klebsiella oxytoca*. Substantial attention and effort have been dedicated to redirecting the metabolic pathways of these -and others- towards ethanol production, by means of metabolic engineering (Dien *et al.* 2003).

However, the lack of industrially suitable microorganisms that can efficiently convert the raw biomaterials to bio-ethanol has been one of the main obstacles to widespread use of bio-fuels. In addition to the ability to ferment a wide variety of sugars, some other features must be considered when choosing an organism for industrial-scale bio-ethanol production. These important features include but are not limited to the ability to produce high ethanol yield, tolerance to fermentation products/by-products, simple growth requirements, and the ability to grow under conditions that prevent contaminating organisms from growing (Zaldivar *et al.* 2001; Dien *et al.* 2003).

Production of bio-ethanol using thermophilic and hyperthermophilic organisms is the focus of many researchers. Extermophiles in general and hyperthermophiles in particular are stout organisms that produce highly stable enzymes due to their natural habitats, and many of them are able to tolerate changes in environment; making them good candidates for bio-ethanol production (Taylor *et al.* 2009).

1.2.1 Ethanol production by thermophiles

Several distinct advantages are associated with using thermophiles over mesophiles, including high temperatures and the mostly anaerobic nature of thermophilic organisms, that result in elimination of oxygenation and cooling of the fermenter. Another aspect is improved solubility of many reaction components at elevated temperatures (Bustard *et al.* 2000). In addition, the high temperature of the process leads to lowering the viscosity of reaction mixtures, causing improved production yields. Various thermophiles can ferment hexose and/or pentose sugars, as well as more complex substrates such as cellulose and xylan in some cases. Many of these organisms and their enzymes are relatively resistant to sudden pH or temperature changes and high concentrations of solvents (Huber and Stetter 1998; Schiraldi and De Rosa 2002). High temperatures can result in lower gas solubility and significantly decrease the risk of process failure and product loss due to contamination which is the common problem in the yeast-based fermentation system. At the same time, high temperatures lower the cost of ethanol recovery due to the high volatility of ethanol at high fermentation temperatures (Lamed and Zeikus 1980; Klapatch *et al.* 1994; Zaldivar *et al.* 2001; Sommer *et al.* 2004; Taylor *et*

al. 2009). However, there are some disadvantages associated with using the hyperthermophiles, the most important one being their intrinsic low substrate and product/by-product tolerance. Moreover, some of these organisms are mixed-fermenters which results in production of sometimes too many various products during growth (Zaldivar *et al.* 2001; Dien *et al.* 2003).

Application of metabolic engineering approaches has great impacts on elimination of the problems associated with using thermophiles, and led to development of strains with bio-ethanol yields that are almost equal to those of the yeast-based systems. Members of the genus *Clostridium*, especially thermophilic members such as *Clostridium thermocellum*, have been studied intensively due to their competence in production of substantial amounts of ethanol, butanol and hydrogen (Lamed and Zeikus 1980; Demain *et al.* 2005; Barnard *et al.* 2010). Members of the genus *Thermoanaerobacter*, including *Thermoanaerobacter ethanolicus* and *Thermoanaerobacter tengcongensis*, are extremely thermophilic bacteria that are well studied for their high ethanol production potential especially from pentoses (Shaw *et al.* 2008; Yao and Mikkelsen 2010a; Yao and Mikkelsen 2010b). The genus *Geobacillus* has been studied widely for bio-ethanol production potential (Thompson *et al.* 2008; Cripps *et al.* 2009; Taylor *et al.* 2009; Barnard *et al.* 2010). Production of ethanol, although at lower concentrations, has also been reported for the extremely thermophilic *Caldicellulosiruptor* species that includes *Caldicellulosiruptor owensensis* (Huang *et al.* 1998), *Caldicellulosiruptor kristjanssonii* (Bredholt *et al.* 1999), and *Caldicellulosiruptor saccharolyticus* (van Niel *et al.* 2003).

1.2.2 Ethanol production by hyperthermophiles

Compared to the thermophilic ethanol producers, very little is known about the ethanol production levels and pathways in the extremely thermophilic and hyperthermophilic microorganisms. It was shown that the peptide- and carbohydrate-fermenting hyperthermophilic archaeon *Pyrococcus furiosus* can produce H₂, CO₂, acetate, alanine, and small amounts of ethanol (Kengen *et al.* 1994). The strictly anaerobic archaeon *Thermococcus* sp. strain ES1 produced some ethanol and butanol when cultures were grown at low concentrations of elemental sulfur (Ma *et al.* 1995). The production of ethanol as an end product of fermentation was also shown in the hyperthermophilic anaerobic archaeon *Thermococcus guaymasensis* (Ying and Ma 2011) and more recently in the autotrophic hyperthermophile, *Thermococcus onnurineus* (Moon *et al.* 2012). Within the bacterial hyperthermophiles, traces of ethanol were reported in cultures of different Thermotogales including *Thermotoga hypogea* (Fardeau *et al.* 1997), *Thermotoga lettingae* (Balk *et al.* 2002), *Thermotoga*

neapolitana (de Vrije *et al.* 2009), *Kosmotoga olearia* (DiPippo *et al.* 2009), and *Thermosiphon affectus* (Podosokorskaya *et al.* 2011).

The key enzyme in both ethanol production pathways is alcohol dehydrogenase (**Figure 1-2**). Alcohol dehydrogenases are members of the oxidoreductase family and are present in all three domains of life (Reid and Fewson 1994; Littlechild *et al.* 2004). They belong to the dehydrogenase/reductase superfamily and can catalyze an expansive spectrum of reactions using a broad range of substrates, which are the reversible inter-conversion of alcohols to corresponding aldehydes or ketones. ADHs can be classified based on the cofactor requirements: I) the flavin adenine di-nucleotide (FAD)-dependent ADHs, II) the pyrrolo-quinoline quinone (PQQ), heme or cofactor F₄₂₀ dependent ADHs, and III) NAD (P) dependent ADHs (Reid and Fewson 1994; Radianingtyas and Wright 2003). They can also be divided into three major groups based on their molecular size and metal contents: the first group is known as zinc-dependent long chain alcohol dehydrogenase; which have sizes of 300-900 amino acids, the second group is the short chain alcohol dehydrogenase: which contain no metal ions and have approximate lengths of 250 amino acids; and the third group is the long-chain iron dependent ADHs; with a length of 385-900 residues (Reid and Fewson 1994; Korkhin *et al.* 1998; Littlechild *et al.* 2004)

Many different ADHs have been characterized from various thermophilic and hyperthermophilic bacteria and archaea, with a majority of them being NAD(P)-dependent. Some of the more recently characterized hyper/thermophilic ADHs are those from *P. furiosus* (Ma and Adams 1999; van der Oost *et al.* 2001; Machielsen *et al.* 2006), *Thermococcus hydrothermalis* (Antoine *et al.* 1999), *Thermococcus kodakaraensis* (Bashir *et al.* 2009; Bowyer *et al.* 2009), *Thermococcus sibiricus* (Lyashenko *et al.* 2010; Stekhanova *et al.* 2010), *Thermococcus guaymasensis* (Ying and Ma 2011), *Sulfolobus acidocaldarius* (Pennacchio *et al.* 2010), *Thermococcus* strain ES1 (Ying *et al.* 2009), *Aeropyrum pernix* (Guy *et al.* 2003), and *Thermotoga hypogea* (Ying *et al.* 2007).

Although there is a relatively long list of ADHs isolated and characterized from thermophilic and hyperthermophilic archaea and bacteria, with the physiological roles of several proposed to be in the reduction of aldehydes to alcohols, other enzymes involved in the ethanol production pathways are not well characterized, especially the enzyme that was implicated in acetaldehyde production. In other words, it is known that some of these organisms are able to produce ethanol as an end product, which inevitably means acetaldehyde must be produced in a metabolic pathway; however, the origin of this acetaldehyde needs to be further explored.

1.3 Acetaldehyde production pathways

Pyruvate is an intermediate in the central metabolism of carbohydrates (Verhees *et al.* 2003; Siebers and Schönheit 2005); it can be converted to acetaldehyde that will be reduced to ethanol *via* one of the following two pathways:

1) A two-step pathway that is used by yeast and a few bacteria like *Zymomonas mobilis* (Buchholz *et al.* 1987) and *Sarcina ventriculi* (Canale-Parola 1970). Pyruvate is non-oxidatively decarboxylated to acetaldehyde and carbon dioxide, which is catalyzed by pyruvate decarboxylase (PDC). Acetaldehyde is then converted to ethanol which is catalyzed by ADH (**Figure 1-2**).

2) A three-step pathway that is more widespread in bacteria. Pyruvate is oxidatively decarboxylated to acetyl-coenzyme A (acetyl-CoA) by the metalloenzyme pyruvate ferredoxin oxidoreductase (POR) and/or pyruvate formate lyase (PFL). In the following steps, acetyl-CoA is converted to acetaldehyde by a CoA-dependent-acetylating acetaldehyde dehydrogenase (AcDH). Finally acetaldehyde is reduced to ethanol by ADH. In both pathways, ADH is the enzyme that converts acetaldehyde to ethanol (**Figure 1-2**).

The key metabolite for the two known pathways is acetaldehyde. Thiamine pyrophosphate (TPP)-dependent enzyme pyruvate decarboxylase is the only enzyme proficient at direct conversion of pyruvate to acetaldehyde. Interestingly, a majority (but not all) of the enzymes which are involved in the acetaldehyde production pathways are members of the superfamily of TPP-dependent enzymes, which includes PDC, POR, and PFL (Duggleby 2006; Costelloe *et al.* 2008).

1.3.1 TPP-dependent enzymes

TPP, also known as thiamine diphosphate (ThDP), is composed of an aromatic methylaminopyrimidine ring, linked to a methyl thiazolium ring *via* a methylene group with a pyrophosphate group attached to a hydroxyethyl side chain (**Figure 1-3**). TPP is derived from the water-soluble vitamin B1 and is the most common cofactor for enzymes that catalyze the cleavage and formation of carbon-carbon bonds next to a carbonyl group; hence it encompasses a wide range of metabolic pathways. Unlike many other cofactors (*e.g.* nicotinamide adenine dinucleotide, NADH) which are basically co-reactants, TPP remains at the enzymes catalytic centre and is directly involved in the catalysis of the reaction with different proteins, providing the specificity toward various

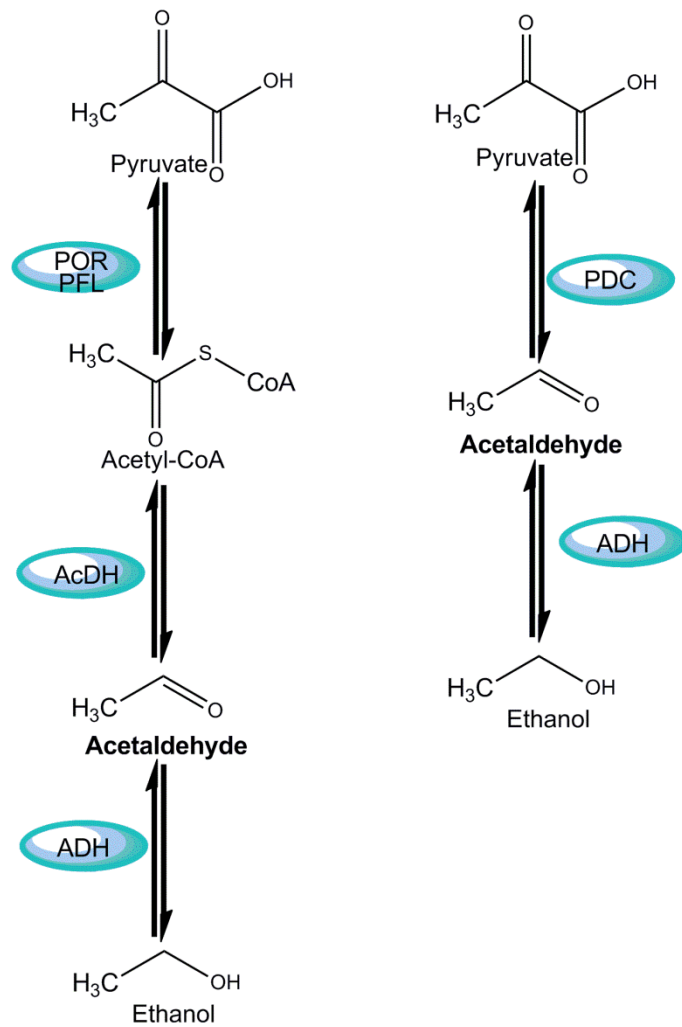


Figure 1-2. Two pathways of ethanol production from pyruvate

POR; Pyruvate ferredoxin oxidoreductase; PFL; Pyruvate formate lyase, AcDH; Acetaldehyde dehydrogenase, ADH; Alcohol dehydrogenase, PDC; pyruvate decarboxylase.

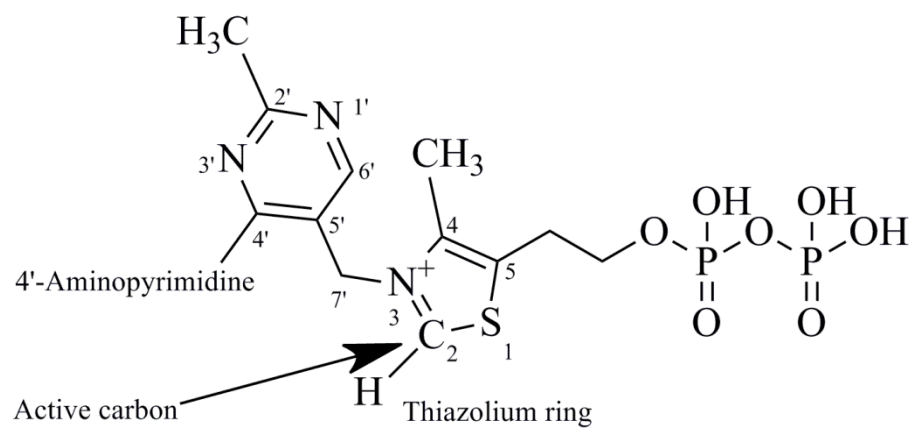


Figure 1-3. Structure of thiamine pyrophosphate (TPP)

substrates (Kluger and Tittmann 2008). The reactions catalyzed by TPP-dependent enzymes can be divided into at least three groups (Schellenberger 1998): the oxidative reactions, non-oxidative reactions (**Figure 1-4**), and carbonylation reactions.

1.3.1.1 TPP-binding motif and cation requirement

The structure of TPP was first described by Lohmann and Schuster in 1937, although Langenbeck (1930) suggested earlier that the primary amines may have a catalytic role in decarboxylation of the α -keto acids (Krampitz 1969; Iding *et al.* 1998). The suggested role of amine groups in the catalysis mechanism was ruled out later (Stern and Melnick 1939; Stern and Melnick 1940), and the actual catalytic site of TPP was found to be the C₂ carbon of the thiazolium ring (see sections 1.3.2.1 and 1.3.3.2).

The family of TPP-dependent enzymes encompasses a wide variety of enzymes catalyzing many different reactions (Mizuhara and Handler 1954; Reed *et al.* 2011). Despite their differences, they all share some common structural and mechanistic similarities. All TPP-dependent enzymes contain a TPP-binding motif and all require divalent metal ions (mostly Mg²⁺ or Ca²⁺) as cofactor. There is a suggested conserved motif of approximately 30 residues in all TPP-dependent enzymes, which is based on the sequence alignment of many TPP-dependent enzymes (Hawkins *et al.* 1989). This motif starts with the highly conserved sequence GDG and ends at the highly conserved sequence NN (GDG(X)₂₆NN or NCN), which may adopt a $\beta\alpha\beta$ fold (Hawkins *et al.* 1989). Later, it was predicted that these residues serve as ligands to metal ions based on data acquired from crystal structures, which themselves function as a platform for the binding (through a diphosphate side chain) of TPP (**Figure 1-3**). Site-directed mutagenesis experiments confirmed essential roles of these residues for TPP-dependent enzyme activity. The experiments also showed that binding of the metal ion takes place before the binding of the TPP (Muller *et al.* 1993; Schellenberger 1998; Jordan 2003).

1.3.1.2 The “V” coenzyme binding configuration

Another common aspect of all TPP-dependent enzymes (at least to all enzymes with an X-ray structure available) is the binding configuration. The presence of the so-called “V” shaped configuration is a common feature of all TPP-dependent enzymes, and is shown by X-ray structural analysis. The “V” configuration can be observed as a disposition of the aromatic 4-aminopyrimidine and thiazolium rings, with respect to the bridging methylene group. This configuration is unlike that

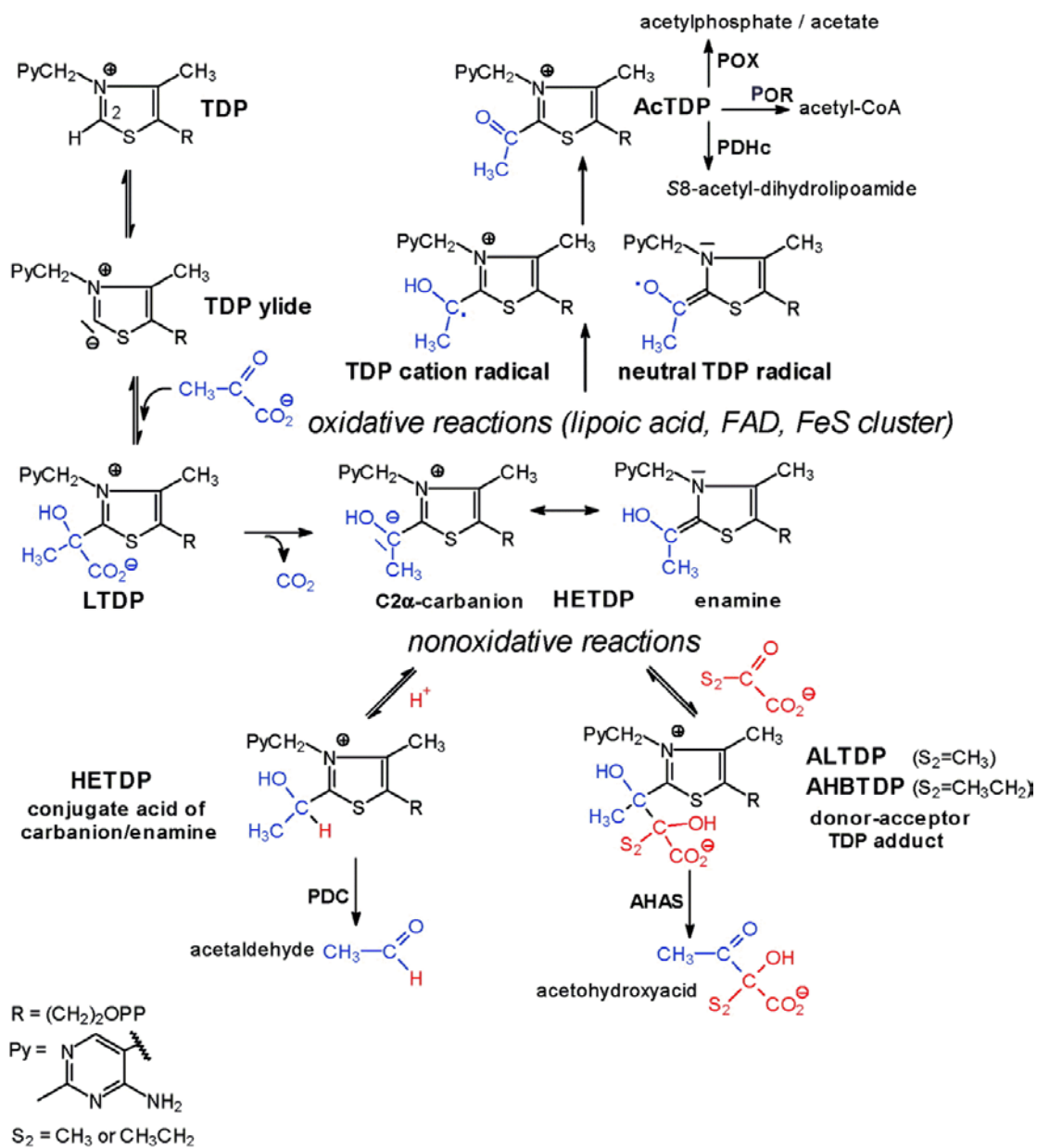


Figure 1-4. Reactions and intermediates in different pyruvate-processing TPP-dependent enzymes

TDP, Thiamine di-phosphate; HETDP, 2-(1-hydroxyethyl)-TDP, AcTDP, acetyl-dithiamine diphosphate intermediate; ALTDP, 2-[(1,2-dihydroxy-2-carboxy-1,2-dimethyl)-ethyl]-TDP POX, pyruvate oxidase; LTDP, 2-(2-lactyl)-TDP; POR, Pyruvate ferredoxin oxidoreductase; PDC, Pyruvate decarboxylase; PDHc, pyruvate dehydrogenase complex, AHAS, Acetoxyhydroxyacid synthase; FAD, flavin adenine dinucleotide. Reprinted with permission from Kluger and Tittmann 2008, American Chemical Society.

of free TPP (**Figure 1-3**), in which the two aromatic rings can rotate with respect to the connecting methylene group (which is known as F conformation). TPP is always located at the interface of the two subunits *via* the attachment by pyrophosphate groups and aminopyrimidine moieties in different anchored enzyme subunits. For this reason, dimers are the minimal functional unit for all TPP-dependent enzymes (Muller *et al.* 1993; Jordan 2003).

1.3.2 Pyruvate decarboxylase (PDC)

The decarboxylation of pyruvate to acetaldehyde was first described for fermenting yeast (*S. cerevisiae*) by Neuberg and Karczag in 1911. In 1922, the same research group detected the potential of yeast in the formation of C-C bonds in 1921. Neuberg named the new enzyme “carbolicase”, and assumed it to exist apart from “ α -carboxylase” (PDC) in yeast (Iding *et al.* 1998). However, the preliminary characterization of cofactors of the enzyme was delayed until 1937, when Lohmann and Schuster analyzed the complete structure of the cofactor of the enzyme pyruvate decarboxylase as “cocarboxylase” or “aneurinpyrophosphate” or thiamin diphosphate (Schellenberger 1998).

The enzyme catalyzes non-oxidative decarboxylation of α -keto acids to produce a corresponding aldehyde and carbon dioxide. The most extensively examined enzymes of this group are the ones from *Saccharomyces cerevisiae* and its bacterial counterpart *Z. mobilis*. In addition to decarboxylation of pyruvate, PDC also catalyzes the enantio-selective formation of 2-hydroxy ketons *via* carbolicase side reactions.

PDC, or its gene (*pdh*), is found to be widely distributed in fungi and higher plants but it is relatively rare in prokaryotes and unknown in animals. In fungi, PDC is found in *Saccharomyces cerevisiae*, *Saccharomyces carlsbergensis* (also known as *S. pastorianus*) and *Saccharomyces uvarum*, *Neurospora crassa*, members of the *Kluyveromyces* species, members of the *Aspergillus* species, *Hanseniaspora uvarum*, *Schizosaccharomyces pombe*, and in *Candida (Torulopsis) glabrata*. PDC is present in a variety of plants, including maize (*Zea mays*), parsnip, orange, pea (*Pisum sativum*), jack bean, sweet potato, wheat, cotton wood, soybean and rice (*Oryza sativa*). In prokaryotes, PDC is found and studied in *Z. mobilis*, *Sarcina ventriculi*, *Clostridium botulinum*, *Acetobacter* species, *Zymobacter palmae*, and in *Erwinia amylovora* (Bringer-Meyer *et al.* 1986; Raj *et al.* 2001; Talarico *et al.* 2001; Raj *et al.* 2002; Wang *et al.* 2004). So far there have been no reports on finding PDC/*pdh* homologs in thermophilic or hyperthermophilic bacteria or in any of the members of the third major evolutionary lineage of life, archaea as a whole (Raj *et al.* 2001; Talarico *et al.* 2001; Raj *et al.* 2002).

PDCs from different organisms show at least a 30% identity at the amino acid level and most of them are composed of subunits of 562-610 amino acid residues long. The holoenzyme is usually composed of four identical or non-identical subunits of approximately 60 kDa (ensuing in a total mass of about 240 kDa) in which every two subunits binds tightly (but not covalently) to a set of cofactors including TPP and Mg^{2+} ion. PDCs with four subunits are often arranged as a dimer of dimers, with multiple close contacts within the dimers and several contacts between the dimers. The contact area between two related dimers forms the “V” conformation that is a common property of all TPP-dependent enzymes studied so far (see section 1.3.1.2), and it also has an essential role in cofactor binding for this group of enzymes (Dobritzsch *et al.* 1998; Jordan 2003).

1.3.2.1 Catalytic mechanism of PDC

The catalytic mechanism of PDC for the most part follows the principles of catalytic mechanisms of other TPP-dependent enzymes: in brief, carbonyl addition of pyruvate to the reactive C2 atom of the cofactor thiazolium ring (**Figure 1-3**) yields the intermediate 2-(2-lactyl)-TDP (LTDP). The subsequent release of carbon dioxide produces resonating carbanion/enamine forms of 2-(1-hydroxyethyl)-TDP (HETDP, also known as hydroxyethylidene-TPP). The resonating form is considered to be a central and highly reactive intermediate state in TPP-dependent enzymes acting on pyruvate (**Figure 1-4**). However, unlike most other TPP-dependent enzymes in which the intermediate is oxidized, the carbanion/enamine in PDC is protonated at the C2 α position, yielding C2 α -hydroxyethylthiamine diphosphate (HETDP) before the final release of acetaldehyde completes the reaction (Kluger 1987; Candy and Duggleby 1998; Kluger and Tittmann 2008).

Crystal structures of several pyruvate decarboxylases are solved particularly from yeasts and *Z. mobilis* (Arjunan *et al.* 1996; Dobritzsch *et al.* 1998; Siegert *et al.* 2005). The active sites of these enzymes are also studied comprehensively using site-directed mutagenesis (Pohl 1997; Candy and Duggleby 1998; Liu *et al.* 2001b).

1.3.2.2 Carbolygation reaction

PDCs from various organisms have been studied for many years, mainly with respect to the mechanism of non-oxidative decarboxylation reactions. Neuberg and Hirsch first showed for the first time that when benzaldehyde is added to a growth medium, *S. cerevisiae* can produce phenylacetylcarbinol as an end product of fermentation (Iding *et al.* 1998). Many years later, in 1988, it was further shown that PDC was able to catalyze an enantio-selective carbolygation reaction in

which two aldehyde molecules are subjected to a condensation reaction, resulting in chiral 2-hydroxy ketones, which are essential building blocks of organic and pharmaceutical chemistry and used as precursors for the synthesis of vitamin E and anti-fungal compounds (Bringer-Meyer *et al.* 1986; Crout *et al.* 1991; Iding *et al.* 1998). The carboligase activity of the yeast PDC has been used for decades in the production of *R*-phenylacetylcarbinol, which is also known as *R*-PAC (Iding *et al.* 1998; Sprenger and Pohl 1999; Goetz *et al.* 2001; Pohl *et al.* 2002). *R*-PAC is an important precursor for production of some central pharmaceutical products with α and β adrenergic properties, such as L-ephedrine, pseudoephedrine, and norephedrine (Pohl 1997; Iding *et al.* 1998). It is still unclear whether the carboligase activity has any physiological importance or is just a remnant property from an ancestral protein (Siegert *et al.* 2005).

Two main steps are involved in the condensation reaction: the first step is the decarboxylation of pyruvate and the second step is ligation of the ThDP-bound acetaldehyde to benzaldehyde. Like other TPP-dependent catalytic mechanisms, the reaction starts with a nucleophilic attack on the carbanion of TPP to the keto group of α -keto acids. The resulting double-negative intermediate is then stabilized by elimination of carbon dioxide, producing the carbanion/enamine intermediate. During the carboligation reaction, the intermediate will be protonated by reacting with a second molecule of aldehyde, leading to production of 2-hydroxyl ketone (Pohl 1997; Pohl 1998; Siegert *et al.* 2005). Interestingly, unlike the PDC from yeast, decarboxylation of the pyruvate is not a prerequisite for carboligase activity from *Z. mobilis*; the enzyme is instead able to use acetaldehyde directly (Meyer *et al.* 2010). Numerous studies were conducted to improve the activity towards 2-hydroxy ketone production (carboligase activity) instead of acetaldehyde (PDC activity). In recent progress, a single mutation in the active site of *Zymomonas* PDC appears to cause a 100-fold increase toward carboligation activity over decarboxylation activity (Meyer *et al.* 2010).

1.3.3 Pyruvate ferredoxin oxidoreductase (POR)

The enzyme pyruvate ferredoxin oxidoreductase (also known as pyruvate synthase as the reaction is reversible) is one of the best studied members of the 2-oxoacid oxidoreductase family (Raeburn and Rabinowitz 1971; Uyeda and Rabinowitz 1971b; Uyeda and Rabinowitz 1971a; Rabinowitz 1975). The enzyme catalyzes coenzyme A and TPP-dependent oxidative decarboxylation of pyruvate to acetyl-CoA, releasing a molecule of CO₂ and transferring the reducing equivalents to the electron acceptor ferredoxin or flavodoxin. Alternatively, in other pyruvate oxidizing enzymes, the reducing equivalents are transferred to NAD⁺ or NADH (in the case of pyruvate dehydrogenase using lipoate

as oxidizing agent for the production of acetyl-CoA), to molecular-oxygen-producing hydrogen peroxide (in the case of pyruvate oxidase), or to the carbonyl groups producing formate (in case of pyruvate formate lyase) (Ragsdale 2003; Ragsdale and Pierce 2008; Tittmann 2009). In acetaldehyde and ethanol producing organisms, acetyl CoA is usually converted to acetaldehyde *via* the CoA-dependent (acetylating) acetaldehyde dehydrogenase.

POR uses iron-sulfur cluster chemistry to catalyze the pyruvate decarboxylation and release of acetyl-CoA. POR is an ancient molecule, and it seems to have existed even before the divergence of the domains of the bacteria and archaea (Kletzin and Adams 1996). The enzyme is present in all three domains of life. All archaea catalyze the conversion of pyruvate to acetyl-CoA using POR, and all of the archaeal genomes sequenced so far contain hetero-tetrameric PORs, which have been proposed to be the closest to the POR common ancestor (Kletzin and Adams 1996; Zhang *et al.* 1996).

POR is prevalent mainly in anaerobic bacteria and infrequently found in anaerobic protozoa, for example, in *Giardia duodenalis* (Townson *et al.* 1996) and *Entamoeba histolytica* (Horner *et al.* 1999; Pineda *et al.* 2010). The enzyme has been isolated and studied from many different anaerobic or microaerophilic microorganisms (see the full list in **Table 1-3**) including anaerobic bacteria like the genera *Clostridium* (Wahl and Orme-Johnson 1987), *Moorella thermoacetica* (Meinecke *et al.* 1989) and anaerobic sulphate-reducing bacteria *Desulfovibrio africanus* (Pieulle *et al.* 1995; Pieulle *et al.* 1997; Pieulle *et al.* 1999a; Pieulle *et al.* 1999b). In hyperthermophiles, PORs are characterized from the hyperthermophilic bacterium *Thermotoga maritima* (Blamey and Adams 1994) and hyperthermophilic archaea *Pyrococcus furiosus* (Blamey and Adams 1993) and *Archaeoglobus fulgidus* (Kunow *et al.* 1995), as well as the methanogenic archaea *Methanosarcina barkeri* (Bock *et al.* 1994; Bock *et al.* 1996) and *Methanobacterium thermoautotrophicum* (Tersteegen *et al.* 1997).

1.3.3.1 Structure and subunit organization

The quaternary oligomeric structure of the POR is variable depending on the source microorganism (**Table 1-3**) and can be homo-dimeric (*e.g.* most bacterial PORs), hetero-dimeric (*e.g.* POR of *Halobacterium salinarium*), hetero-tetrameric (archaeal PORs), and heteropentameric (anabolic PORs), although all of the PORs studied so far, regardless of their source and structure, seem to be phylogenetically related and derived from a common archaeal-type heterotetrameric ancestor (Kletzin and Adams 1996; Zhang *et al.* 1996; Ikeda *et al.* 2010).

Table 1-3. PORs isolated and characterized from different microorganisms and their oligomeric structures^a

Source organism	POR structure	Native Molecular weight (kDa)	Reference
<i>Anabaena cylindrica</i> (<i>Nostoc Sp.</i>)	Homodimeric	240	Bothe <i>et al.</i> 1974; Neuer and Bothe 1982
<i>Anabaena variabilis</i>	Homodimeric	NR	Leach and Carr 1971
<i>Archaeoglobus fulgidus</i>	Heterotetrameric	120	Kunow <i>et al.</i> 1995
<i>Clostridium acetobutylicum</i> (<i>Moorella thermoacetica</i>)	Homodimeric	246	Meinecke <i>et al.</i> 1989
<i>Clostridium thermoaceticum</i>	Homodimeric	240	Drake <i>et al.</i> 1981
<i>Desulfovibrio africanus</i>	Homodimeric	256	Pieulle <i>et al.</i> 1995
<i>Desulfovibrio vulgaris</i>	Homo-octameric	1000	Garczarek <i>et al.</i> 2007
<i>Entamoeba histolytica</i>	Homodimeric	ND	Horner <i>et al.</i> 1999; Pineda <i>et al.</i> 2010
<i>Giardia duodenalis</i>	Homodimeric	135	Townson <i>et al.</i> 1996
<i>Giardia intestinalis</i>	Homodimeric	138	Emelyanov and Goldberg 2011
<i>Halobacterium salinarium</i> (<i>halobium</i>)	Heterodimeric	256	Kerscher and Oesterhelt 1981b; Plaga <i>et al.</i> 1992
<i>Helicobacter pylori</i>	Heterotetrameric	NR	Hughes <i>et al.</i> 1995
<i>Hydrogenobacter thermophilus</i>	Heterotetrameric	265	Yoon <i>et al.</i> 1997; Ikeda <i>et al.</i> 2006; Ikeda <i>et al.</i> 2009
<i>Klebsiella pneumoniae</i> ^b	Homodimeric	240	Shah <i>et al.</i> 1983; Wahl and Orme-Johnson 1987
<i>Methanobacterium thermoautotrophicum</i>	Heterotetrameric	NR	Tersteegen <i>et al.</i> 1997
<i>Methanococcus maripaludis</i>	Heteropentameric	210	Lin <i>et al.</i> 2003
<i>Methanosarcina barkeri</i>	Heterotetrameric	130	Bock <i>et al.</i> 1994; Bock <i>et al.</i> 1996
<i>Pyrococcus furiosus</i>	Heterotetrameric	250	Blamey and Adams 1993; Smith <i>et al.</i> 1994
<i>Rhodobacter capsulatus</i>	Homodimeric	270	Yakunin and Hallenbeck 1998
<i>Rhodobacter rubrum</i>	Homodimeric	252	Brostedt and Nordlund 1991
<i>Sulfolobus</i> sp. strain 7	Heterodimeric	103	Iwasaki <i>et al.</i> 1995; Zhang <i>et al.</i> 1996
<i>Thermotoga maritima</i>	Heterotetrameric	113	Blamey and Adams 1994; Smith <i>et al.</i> 1994
<i>Trichomonas vaginalis</i>	Homodimeric	240	Williams <i>et al.</i> 1987; Meza-Cervantez <i>et al.</i> 2011

^a NR; not reported

^b Pyruvate flavodoxin oxidoreductase

The crystal structures of several POR have been determined. PORs from *Desulfovibrio africanus* (with and without bound substrate) and *Desulfovibrio vulgaris* (Chabrière *et al.* 1999; Chabriere *et al.* 2001; Garczarek *et al.* 2007) are among the most extensively studied PORs. POR is a metalloenzyme. All PORs studied contain between one and three [4Fe-4S] clusters arranged in a spatial order from the TPP located at the active center of the enzyme toward its surface, suggesting that they are part of an electron transfer pathway (Bock *et al.* 1997; Charon *et al.* 1999).

POR can also catalyze the reaction to form pyruvate from acetyl-CoA and carbon dioxide, which is the basis of the carbon dioxide fixation in many autotrophic microorganisms (Shiba *et al.* 1985). This type represents the so called “anabolic” PORs that are studied from the thermophilic facultative aerobic bacterium *Hydrogenobacter thermophilus* (Ikeda *et al.* 2006; Ikeda *et al.* 2009; Ikeda *et al.* 2010; Yamamoto *et al.* 2010), as well as the hydrogenotrophic methanoarchaeon *Methanococcus maripaludis* (Lin *et al.* 2003; Lin and Whitman 2004). In the case of the heteropentameric POR of *M. maripaludis*, four subunits are very closely related to the archaeal heterotetrameric (ancestral) PORs, the fifth subunit has no known homologue within PORs.

1.3.3.2 Catalytic mechanism of PORs

The general steps of the POR catalytic reactions follow the same principles as those of other TPP-dependent enzymes. However, the enzyme is unique in one aspect: unlike most other TPP-dependent enzymes, POR takes advantage of free radical chemistry to catalyze the decarboxylation reaction (**Figure 1-4**).

The formation of a stable radical intermediate during the course of the catalytic cycle of POR was first shown in early 1980s for the enzyme from the halophilic, facultative anaerobic archaeon *Halobacterium salinarium* (formerly known as *Halobacterium halobium*). The enzyme was chosen for study due to its relative stability toward oxygen compared to other PORs that are generally from anaerobic microorganisms and show high levels of sensitivity toward oxygen (Cammack *et al.* 1980; Kerscher and Oesterhelt 1981a; Kerscher and Oesterhelt 1982). Although there are some reports pertaining to the absence of the radical intermediate in some other PORs, for example, the one from *Clostridium (Moorella) thermoacetica* (Wahl and Orme-Johnson 1987; Smith *et al.* 1994), its absence can be simply attributed to its rapid decay and the transient nature of the radicals, which most possibly prevented its identification (Menon and Ragsdale 1997). The radical is generally stable, particularly when just pyruvate is present in the reaction mixture, indicating the effect of CoA addition and its role in fast decay of the radical intermediate (as further discussed in section 1.3.3.3).

The presence of the radical intermediate was also confirmed by the study of crystal structures of the POR isolated from the anaerobic, sulfate-reducing bacterium *Desulfovibrio africanus* in which the intermediate seems to be very stable. This stability can indeed be attributed to the enzyme's relative oxygen insensitivity (Charon *et al.* 1999; Pieulle *et al.* 1999a; Chabriere *et al.* 2001).

Although initial steps of the POR catalytic reaction, including the addition of a substrate to TPP and subsequent decarboxylation of HETDP, takes place in two-electron steps, the oxidation of HETDP to acetyl-CoA and regeneration of TPP takes place in two sequential one-electron steps *via* a chain of [4Fe-4S] clusters. The catalytic mechanism of the enzyme then can be viewed in three distinct steps (**Figure 1-4** and **Figure 1-5**): I) a reaction between pyruvate, TPP and the enzyme leading to the production of HETDP intermediate, II) a redox reaction leading to the production of the HETDP radical intermediate, by transfer of one electron to the proximal iron-sulfur cluster (**Figure 1-6**), and III) a reaction of the HETDP with coenzyme A, resulting in its decay and reduction of a second iron-sulfur cluster (Menon and Ragsdale 1997; Buckel and Golding 2006; Tittmann 2009).

In the course of catalytic activity, after binding of the pyruvate to TPP and the enzyme causing subsequent decarboxylation, the HETDP will be oxidized by the transfer of one electron to the [4Fe-4S] cluster that is proximal to the TPP (**Figure 1-6**, cluster A). This electron will then be transferred through the iron-sulfur cluster cascade all the way from the buried active site of the enzyme to the surface, where the electron will eventually be transferred to small iron-sulfur proteins ferredoxin or FMN containing molecules of flavodoxin. In the resulting complex of enzyme-acetyl-TDP radical, the acetyl group (coming from pyruvate) remains tightly bound to the abovementioned structure, until reaction with coenzyme A takes place. When coenzyme A is present, the intermediate will be oxidized once more by transferring the electron to an intra-molecular iron-sulfur cluster, leading to the release of acetyl-coA and zwitterionic TPP (**Figure 1-5**). The iron-sulfur cluster will be re-oxidized again by cluster-to-cluster hopping of the electrons finally arriving at the electron acceptor molecules ferredoxin or flavodoxin (**Figure 1-6**) (Kerscher and Oesterhelt 1981a; Menon and Ragsdale 1997; Buckel and Golding 2006; Tittmann 2009).

Although, using free radical chemistry for the catalysis provides POR a unique feature amongst TPP-dependent enzymes, it comes with a cost, due to the highly reactive nature of free radicals (resulting from the presence of a single electron in search of another electron to pair with). Radical

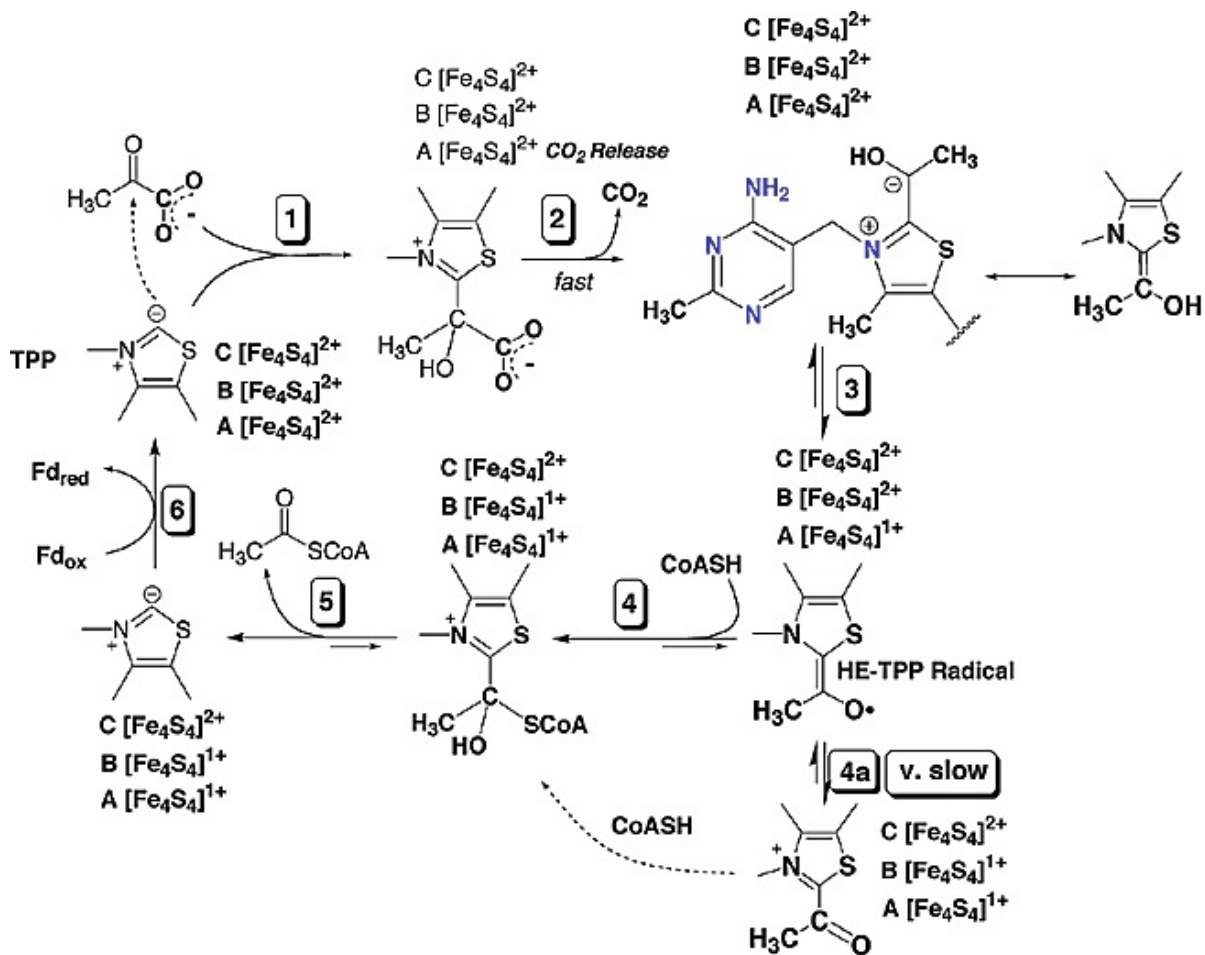


Figure 1-5. Catalytic mechanism of POR and intermediates involved in the reaction (Ragsdale 2003)

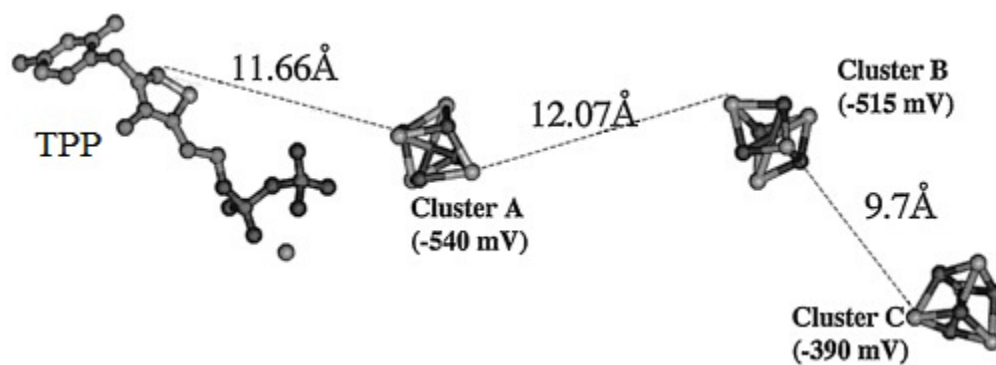


Figure 1-6. Spatial organization of the [4Fe-4S] clusters in the POR of *Desulfovibrio africanus* (Furdui and Ragsdale 2002)

intermediates are always avid to react with small bi-radical molecules of dioxygen, which results in irreversible inactivation of the enzymes. Therefore, radical enzymes are rather uncommon in aerobic organisms, and oxygen sensitivity seems to be a typical property of almost all PORs (Buckel and Golding 2006).

The oxygen sensitivity of PORs also stems from a structural reason. It has been suggested that when the cells are exposed to oxygen, the [4Fe-4S] cluster nearest to the enzyme surface (**Figure 1-6**) is oxidized and converted from a stable [4Fe-4S]²⁺ state to an unstable [4Fe-4S]³⁺ form. The reaction causes the release of an iron atom, converting the cluster to [3Fe-4S]¹⁺, which is not functional and causes failure in the enzymes catalytic activities (Imlay 2006).

Unlike most other PORs, the native homodimeric POR from the strictly anaerobic bacterium *D. africanus* is relatively oxygen-stable, and when isolated under aerobic conditions, it can remain stable for several days (Pieulle *et al.* 1995; Chabrière *et al.* 1999). Data from studies of the recombinant enzyme expressed in anaerobically grown *E. coli* report that the enzyme retained about 90% of its activity after six days of exposure to oxygen at 4°C. Deletion mutation studies also confirmed an important role of an about 60-residue extension at the C-terminal of the protein (Pieulle *et al.* 1997). This was further verified by determination of the crystal structures of the enzyme (Pieulle *et al.* 1999a; Pieulle *et al.* 1999b), confirming the presence of an extra domain (domain VII) that is absent from other studied PORs. This domain protects the terminal (close to the enzyme surface) iron-sulfur cluster from oxidation, presumably by blocking the access of oxygen or by preventing the decay of the over oxidized iron-sulfur cluster. Deletion of this domain leads to restoration of oxygen sensitivity (Pieulle *et al.* 1997; Chabrière *et al.* 1999; Charon *et al.* 1999; Imlay 2006). It was shown that a single disulfide bound in the structure of the enzymes played a crucial role in the process of iron-sulfur cluster protection. The bond was important because it could switch the enzyme between two states: highly active/oxygen sensitivity and low active/oxygen resistance (Vita *et al.* 2008). Accordingly, a thioredoxin-dependent thiol/disulfide redox system was characterized and was shown to interact with POR in *D. vulgaris* (Pieulle *et al.* 2011). Another much less studied example of POR oxygen insensitivity can be illustrated by the enzyme from *H. salinarium* (Kerscher and Oesterhelt 1981a; Pieulle *et al.* 1997). Although there is no structural data available for this enzyme, it is hypothesized that the architecture of the protein has an essential role in stabilizing of the protein against molecular oxygen (Kerscher and Oesterhelt 1981a).

1.3.3.3 Role of coenzyme A in POR reaction

Using electron paramagnetic resonance (EPR) spectroscopy, it has been shown that the presence of coenzyme A increases the rate of oxidation (decay) of the HETDP radical intermediate by 10^5 times, which subsequently reduces the half-life of the radical intermediate tremendously (Furdui and Ragsdale 2002). Accordingly, in the absence of coenzyme A, the lifetime of the intermediate is about two minutes. Three major mechanisms are suggested to explain possible role of coenzyme A in acceleration of HETDP radical intermediate oxidation.

In the first mechanism, known as the “kinetic coupling mechanism”, the thiol group of coenzyme A performs a nucleophilic attack on the HETDP radical intermediate that leading to the generation of an anion radical with high reducing power. Compared to the HETDP radical intermediate, this new radical has a much higher driving force for electron transfer to the adjacent iron-sulfur cluster. The thiol group of coenzyme A then has a critical role in catalysis of the electron transfer, hence replacement of coenzyme A with desulfocoenzyme A will decrease the rate of the reaction by about 10^6 -fold compared with the time of coenzyme A presence (Menon and Ragsdale 1997; Furdui and Ragsdale 2002).

In the second mechanism, known as the bi-radical mechanism, electron transfer from the thiol group of coenzyme A to one of the intramolecular iron-sulfur clusters will generate a thiyl radical. Interactions between the HETDP radical intermediate and the thiyl radical leads to the release of acetyl-CoA and zwitterionic TPP that will eventually be protonated to TPP (Menon and Ragsdale 1997; Buckel and Golding 2006).

In the third mechanism, known as the “wire mechanism”, coenzyme A functions like a wire between the HETDP radical intermediate and the intramolecular [Fe-S] cluster, improving the efficiency of electron transfer. However, this mechanism cannot be considered as the same rate enhancing mechanism for coenzyme A because, if it is, replacement with desulfocoenzyme A should not slow down the reaction to such a large extent (Menon and Ragsdale 1997). It is also possible that more than one mechanism is involved in the electron transfer rate enhancement, and there might even be a combination of the above-mentioned mechanisms involved in the process.

1.3.4 POR/PDC bifunctional enzyme

In 1997, it was reported that the POR was also capable of converting pyruvate to acetaldehyde in the hyperthermophilic anaerobic archaeon *Pyrococcus furiosus* (Ma *et al.* 1997). Unlike the commonly-known PDC; which employ chemical rather than radical intermediates and therefore are oxygen insensitive, the reported PDC activity was highly oxygen sensitive. Both the POR and PDC activities of the hyperthermophilic enzyme were TPP- and coenzyme A- dependent. By using the coenzyme A analogue (desulfocoenzyme A) showed that coenzyme A has only a structural, not a catalytic role in the catalyzed PDC reaction. Consequently, a “switch” mechanism was proposed for the enzyme’s bifunctionality, suggesting the conversion of active aldehyde to either acetyl-CoA or acetaldehyde, depending on the binding of CoA. According to the proposed model, binding of coenzyme A causes conformational changes in the intermediate structure, causing its protonation and generation of hydroxyethyl-TPP (HETDP). This reaction leads to the release of acetaldehyde, allowing for the regeneration of TPP and possible release of CoA (Ma *et al.* 1997). To date there has been no further study on the bifunctionality of the POR enzyme or its physiological relevance for any other organisms. It is not clear whether this bifunctionality is a trait of only *Pyrococcales* POR or a common property of hyperthermophilic PORs.

1.3.5 Acetaldehyde dehydrogenase (CoA acetylating)

Acetaldehyde dehydrogenase (CoA acetylating, EC 1.2.1.10) is a member of a very divergent superfamily of enzymes known as the “aldehyde dehydrogenases”. The prototype enzyme (*adhE*) was first discovered in *Escherichia coli* and is required for its anaerobic growth (Rudolph *et al.* 1968). It was then discovered in the strictly anaerobic bacterium *Clostridium kluyveri* (Lurz *et al.* 1979). The enzyme is responsible for the conversion of acetyl-coenzyme A (acetyl-CoA) to acetaldehyde that is then converted into ethanol. Two forms of the enzyme are available: one is the monofunctional enzyme with only AcDH activity (*mhpF*) and the other is the bifunctional enzyme with both AcDH and ADH activities (*adhE*). The latter group is composed of an ADH active C-terminal and an AcDH active N-terminal, a structure believed to be the result of gene fusion between the genes encoding for each single enzyme (Nair *et al.* 1994; Toth *et al.* 1999).

Reports are available on isolation and characterization of the bifunctional NADP-dependent alcohol/acetaldehyde dehydrogenase (CoA-acetylating) from mesophilic microorganisms including *Giardia lamblia* (Sánchez 1998) and *Entamoeba histolytica* (Bruchhaus and Tannich 1994; Pineda

et al. 2010). They are also present in some thermophiles, including *Thermoanaerobacter ethanolicus* (Burdette and Zeikus 1994), *Thermoanaerobacter mathranii* (Yao and Mikkelsen 2010b) and members of the genus *Geobacillus* (Taylor *et al.* 2009). However, no mono- or bi-functional AcDH activity was characterized from hyperthermophiles. Survey of the fully sequenced genomes of hyperthermophilic archaea and bacteria has shown no *adhE* or *mhpF* homologue either (present study).

1.3.6 Acetohydroxy acid synthase (AHAS)

The enzyme acetohydroxyacid synthase (AHAS, sometime referred to as acetolactate synthase, EC 2.2.1.6) is another TPP-dependent enzyme that acts on pyruvate. The enzyme catalyzes the condensation of two molecules of pyruvate or a molecule of pyruvate and a molecule of 2-ketobutyrate, leading to production of 2-acetolactate or 2-aceto-2-hydroxybutyrate, respectively. The enzyme is present in all of the plants, fungi, bacteria, and archaea that are capable of *de novo* biosynthesis of the branched chain amino acids (BCAAs), and they are absent from animals. The enzyme is always composed of two subunits: a larger (60-70 kDa) catalytic subunit and smaller (9.5-54 kDa) regulatory subunits. Although, in contrast to the regulatory subunit, the catalytic subunit is active by itself, the full activity of the enzyme requires the combination of the two subunits (Duggleby and Pang 2000; Chipman *et al.* 2005).

There has been no study of the AHAS activity of any hyperthermophilic organisms and in the case of the mesophilic enzymes; they have never been shown to be connected to acetaldehyde production. However, the primary structures of AHASs show the highest similarity to the commonly-known (typical) PDCs in hyperthermophiles (Chapter 4). These high levels of relatedness along with some structural similarity to commonly-known PDCs raise the question of whether AHASs can be involved in the biosynthesis of acetaldehyde.

1.3.7 Objectives of the present study

The objectives were to determine the presence and the characterization of acetaldehyde-producing enzymes in hyperthermophiles. Three types of activities were chosen for investigations pyruvate decarboxylase (PDC), CoA-dependent acetylating acetaldehyde dehydrogenase (AcDH), and other possible acetaldehyde-producing enzymes, such as acetolactate synthase (ALS, which shows the highest sequence homology to commonly-known PDC in hyper/thermophiles).

The presence of these activities was investigated in different extremely thermophilic and hyperthermophilic organisms, including the strictly anaerobic hyperthermophilic archaeon *Thermococcus guaymasensis*, and in bacteria *Thermotoga maritima* and *Thermotoga hypogea*. The specific goals were the following:

- 1) To determine the presence of the *pdc* coding sequences or its homologs in an increasing inventory of genomics and proteomics data available from various thermophilic and hyperthermophilic bacteria and archaea. The released genome sequences were studied in an attempt to characterize the commonly-known (classical) *pdc* gene homologs or the candidate genes encoding possible pyruvate decarboxylase. The primary focus was the genomes of heterotrophic hyperthermophilic bacteria and archaea capable of producing ethanol, especially members of the orders Thermotogales and Thermococcales.
- 2) To determine the activities of pyruvate decarboxylase, acetaldehyde dehydrogenase (CoA-acetylating), pyruvate ferredoxin oxidoreductase and acetohydroxyacid synthase in cell-free extracts of the hyperthermophilic microorganisms under study.
- 3) To clone and heterologously express the recombinant acetohydroxyacid synthase (AHAS), selected from the hyperthermophilic bacterium *T. maritima* and archaeon *P. furiosus*, in the mesophilic host (*E. coli*), for further characterization.
- 4) To purify the native or recombinant enzymes with non-oxidative pyruvate decarboxylase (acetaldehyde-producing) activities using fast performance liquid chromatography (FPLC) approaches under strictly anaerobic conditions.
- 5) To determine the biochemical and biophysical characteristics of the purified enzymes, including optimal pH, temperature and ionic strength, thermal stability, oxygen sensitivity, and substrate specificity. The kinetic parameters (K_m , V_{max} , and k_{cat}) of the enzymes were also determined by altering the concentration of cofactors and substrates.
- 6) Using their gene sequences to analyze molecular and genetic properties of the enzymes, including their similarity, phylogeny, regulatory sequences (such as promoter and ribosome binding sequences), and conserved motifs.

**Chapter 2 Characterization of a bifunctional
POR/PDC from the hyperthermophilic archaeon
*Thermococcus guaymasensis***

2.1 Overview

Thermococcus guaymasensis is a strictly anaerobic hyperthermophilic archaeon with an optimal growth temperature of 88°C. Ethanol is produced in these organisms as an end-product of metabolism, and an ADH that is likely involved in ethanol production has previously been purified and characterized. However, the enzyme that would catalyze the formation of acetaldehyde, the substrate for the ethanol production, is not known. Therefore, identification and characterization of a *Thermococcus guaymasensis* (*T. guaymasensis*) enzyme with both pyruvate ferredoxin oxidoreductase (POR) and pyruvate decarboxylase (PDC) activities was carried out.

The bifunctional enzyme was purified from *T. guaymasensis* grown on glucose and peptides using fast performance liquid chromatography (FPLC) system under strictly anaerobic conditions. Both POR and PDC enzyme activities were co-eluted during different steps of chromatography and the specific activities were increased to the same extent after each chromatography step. The purified enzyme was a hetero-tetrameric protein consisting of 46, 35, 26 and 12 kDa subunits (as estimated by SDS-PAGE). The native enzyme had an apparent molecular weight of 258,043±5650 Da, which was suggestive of a dimeric structure of the four subunits. The purified enzyme had specific activities of 20.2±1.8 and 3.8±0.22 U_{mg}⁻¹ for POR and PDC activities, respectively. The optimal pH for POR and PDC activities was 8.4 and 9.5, respectively. The optimal temperature for POR activity was above 95°C and the optimum for the PDC activity was 85°C. The activities were sensitive to air exposure and lost half of the POR and PDC activities within 40 and 30 min, respectively. Coenzyme A was essential for both PDC and POR activities. Enzyme kinetic parameters were determined for both activities. For POR, the apparent K_m values for pyruvate and CoA were 0.53 mM and 69 μM, respectively. For PDC activity, the apparent K_m values for pyruvate and CoA were determined to be 0.25 mM and 13 μM, respectively.

The sequences of the genes encoding the subunits of the bifunctional POR/PDC were determined using primer-walking and inverse PCR (IPCR) strategies. It was found that the genes encoding the subunits of POR and closely related enzyme 2-ketoisovalerate ferredoxin oxidoreductase (VOR) were organized in a single operon as *por/vorG-vorD-vorA-vorB-porD-porA-porB* in which the *vor/porG* gene product was shared between the two enzymes, a common feature conserved among members of Thermococcales. The released genome sequences of different hyperthermophiles were searched for the presence of the gene encoding the CoA-acetylating acetaldehyde dehydrogenase (AcDH); however, there were no gene homologs present in any of the bacterial or archaeal hyperthermophiles

examined. The AcDH assay on the cell-free extracts of different hyperthermophiles was also indicative of the absence of such activity in hyperthermophiles. It was concluded that a bifunctional POR and PDC enzyme was present in the hyperthermophilic archaeon *T. guaymasensis*.

2.2 Introduction

Hyperthermophiles are microorganisms with optimal growth temperatures $\geq 80^{\circ}\text{C}$ (Stetter *et al.* 1990; Stetter 1996; Wagner and Wiegel 2008). Thermococcales are represented by three genera of *Pyrococcus*, *Thermococcus* and *paleococcus*, which are typically anaerobic chemoorganotrophic microorganisms capable of growing on complex proteinaceous substrates (*e.g.*, yeast extract and tryptone) or carbohydrates (*e.g.* maltose, starch, and cellobiose) using a modified version of the Embden-Meyerhof pathway (Schönheit and Schafer 1995; Siebers and Schönheit 2005). The growth rates of most Thermococcales are stimulated by addition of the elemental sulfur (S^0) to the growth medium.

Thermococcus guaymasensis has an optimal growth temperature of 88°C and uses starch, glucose, casein, chitin, dextrose and maltose as growth substrates to produce acetate, CO_2 , and also propionate, isobutyrate, isovalerate and H_2S when grown on trypticase, yeast extract and elemental sulfur (Canganella *et al.* 1998)

In most anaerobic hyperthermophilic archaea, the oxidative decarboxylation of pyruvate catalyzed by pyruvate ferredoxin oxidoreductase (POR), leads to production of acetyl-coenzyme A which is then converted to acetate as an end-product *via* the enzyme acetyl-coenzyme A synthase (Ma *et al.* 1997; Fukui *et al.* 2005; Zivanovic *et al.* 2009). Several hyperthermophiles are able to produce ethanol (Kengen *et al.* 1994; Ma *et al.* 1995; Balk *et al.* 2002; de Vrije *et al.* 2009; DiPippo *et al.* 2009; Podosokorskaya *et al.* 2011), but the enzymes and pathways involved in the process are not well studied.

Among Thermococcales it is shown that the sulfur-reducing hyperthermophilic archaea *T. guaymasensis* (Ying and Ma 2011) and *T. onnurineus* (Moon *et al.* 2012) are able to produce ethanol as an end-product of metabolism. *T. guaymasensis* can produce millimolar levels of ethanol and an NADP-dependent zinc-containing alcohol dehydrogenase (ADH) with broad substrate range is purified and characterized from this organism (Ying and Ma 2011). Similar to several other ADHs characterized from hyperthermophiles, this novel zinc-containing ADH shows lower apparent K_m

values for aldehydes. These findings help in understanding of the metabolic pathway for alcohol production in hyperthermophiles (Machielsen *et al.* 2006; Ying *et al.* 2007; Ying and Ma 2011).

There are two pathways for ethanol production from pyruvate and in both pathways acetaldehyde is a key intermediate. In the two-step pathway, pyruvate is converted to acetaldehyde by the enzyme pyruvate decarboxylase (PDC, EC 4.1.1.1) and in the three-step pathway pyruvate is transformed into acetyl-CoA that is then reduced to acetaldehyde. Alcohol dehydrogenase (ADH) is the enzyme responsible for the ethanol production from acetaldehyde. However, the origin of the acetaldehyde in hyperthermophiles is not well understood. Pyruvate decarboxylase (encoded by *pdh* gene) catalyzes the non-oxidative decarboxylation of pyruvate to acetaldehyde. Within Bacteria the enzyme is shown to be present in *Sarcina ventriculi* and *Zymomonas mobilis*. CoA-acetylating enzyme, acetaldehyde dehydrogenase (AcDH, EC 1.2.1.10), is present in few prokaryotes (*e.g.* *Clostridium* sp.) and some mesophilic protozoa such as *Giardia lamblia* and *Entamoeba histolytica*, catalyzes the conversion of acetyl-CoA to acetaldehyde.

Since the genome sequence of *T. guaymasensis* is not available yet, it is not possible to determine if the *pdh* gene is present in this organism. A survey of databases containing hyperthermophilic genomes released to date, indicated that none of the hyperthermophilic genome sequences released – including any of the 17 fully sequenced genomes of Thermococcales (as of Aug 2012) - bears a gene homologue to any of the well known acetaldehyde-producing enzymes PDC or AcDH (CoA-acetylating).

A bifunctional pyruvate ferredoxin oxidoreductase (POR, EC 1.2.7.1)/pyruvate decarboxylase (PDC) was discovered to be present in the hyperthermophilic archaeon *Pyrococcus furiosus* (*P. furiosus*) (Ma *et al.* 1997). The bifunctional enzyme is active in both oxidative and non-oxidative decarboxylation of pyruvate to produce acetyl-CoA and acetaldehyde, respectively. POR seems to be the right candidate to elucidate the unexplained origin of the acetaldehyde in *P. furiosus*.

POR is a ferredoxin-dependent iron-sulfur protein catalyzing the reversible oxidative decarboxylation of pyruvate to acetyl-coenzyme A and CO₂ with the sequential transfer of the reducing equivalents to ferredoxin molecules, which can be used toward the reduction of the sulfate, N₂, or protons (Menon and Ragsdale 1996; Menon and Ragsdale 1997; Furdui and Ragsdale 2002; Ragsdale 2003). POR is ubiquitous in archaea and has a strong prevalence in bacteria and is present

in some amitochondriate protists. In aerobic organisms the same reaction is catalyzed *via* the large enzyme complex pyruvate dehydrogenase (PDH, EC 1.2.4.1). Unlike POR, the reaction catalyzed by PDH is irreversible, NAD⁺-dependent and uses the lipoate and flavin as prosthetic groups (Kerscher and Oesterhelt 1982; Ragsdale 2003; Reed *et al.* 2011).

Although POR is the only 2-keto acid oxidoreductase characterized in mesophilic and hyperthermophilic bacteria as well as anaerobic protozoa, different types of coenzyme A-dependent oxidoreductases, with broad range and sometimes overlapping substrate specificities are isolated and characterized from various hyperthermophilic archaea. The main alternative 2-keto acid oxidoreductases in hyperthermophilic archaea include 2-ketoisovalerate ferredoxin oxidoreductase (VOR) that oxidizes mainly branched-chain 2-keto acids derived from branched chain amino acids (BCAAs) valine, leucine, and isoleucine (Adams and Kletzin 1996; Heider *et al.* 1996; Ozawa *et al.* 2005), indolepyruvate ferredoxin oxidoreductase (IOR) that preferentially oxidizes 2-keto acids generated from the aromatic amino acids (Mai and Adams 1994), and 2-ketoglutarate ferredoxin oxidoreductase (KGOR) that specifically uses 2-ketoglutarate as the substrate (Mai and Adams 1996a). It is suggested that an “alternative keto acid oxidoreductase” activity is present in the flagellated protozoan *Trichomonas vaginalis* (Brown *et al.* 1999) and some other anaerobic protists (Upcroft and Upcroft 1999). However, it is shown recently that the detected activity was an artifactual non-enzymatic reaction resulted from the reduction of the indicator dye and not an enzyme-catalyzed reaction (Zedníková *et al.* 2012).

In hyperthermophiles, PORs are purified and characterized from the hyperthermophilic archaea *P. furiosus* (Blamey and Adams 1993) and *Archaeoglobus fulgidus* (Kunow *et al.* 1995). Within hyperthermophilic bacteria, *Thermotoga maritima* (*T. maritima*) is the only bacterium with its POR purified and characterized (Blamey and Adams 1994). It is unclear if the bifunctional POR/PDC is only a property of the *Pyrococcus* metabolic system, or it is a general trait of all Thermococcales. In this study, the bifunctional POR/PDC enzyme was purified from another member of the order Thermococcales, the hyperthermophilic archaeon *T. guaymasensis*, and characterized at molecular and biochemical levels.

2.3 Materials and Methods

2.3.1 Reagents and chemicals

Sodium pyruvate, isobutyraldehyde, thiamine pyrophosphate (TPP), dichloromethane, coenzyme A (CoASH), HEPES, CAPS, EPPS, lysozyme and methyl viologen (MV) were purchased from Sigma-Aldrich Canada Ltd. (ON, Canada). Desulfocoenzyme A was synthesized Dr. E. J. Lyon, Chemistry Department at Bellarmine University, USA. DNaseI for the cell lysis buffer preparation was purchased from Roche (Roche Applied Science, QC, Canada). The chemicals used in the growth media were all commercially available. Yeast extract was acquired from EMD (EMD Chemicals, Inc. NJ, USA) and trypticase soy broth (TSB) was purchased from Becton-Dickinson (BD Bioscience, Mississauga, ON, Canada). All of the FPLC columns and chromatographic media were purchased from GE Healthcare (QC, Canada).

2.3.2 Microorganisms and growth conditions

Thermococcus guaymasensis DSM11113 and *Pyrococcus furiosus* (DSM 3638) were obtained from DSMZ- Deutsche Sammlung von Mikroorganismen und Zellkulturen (Braunschweig, Germany). The medium was supplemented with trace minerals (**Table 2-1**) and vitamin solutions (**Table 2-2**) prepared as previously described by Balch and coworkers (1979).

T. guaymasensis was cultivated anaerobically at pH 7.0 and 88°C. The growth medium was based on tryptone, yeast extract, glucose and a mixture of trace minerals in the absence of elemental sulfur (Canganella *et al.* 1998; Ying and Ma 2011). The medium contained (per liter) KCl, 0.33 g; MgCl₂·6H₂O, 2.06 g; MgSO₄·7H₂O, 3.4 g; NH₄Cl, 0.25 g; CaCl₂·2H₂O, 0.14; K₂HPO₄, 0.14 g; Na₂SeO₃, 0.01 mg; NiCl₂·6H₂O, 0.01 mg; NaHCO₃, 1.0 g; NaCl, 18.0 g; resazurin, 1.0 mg; cysteine-HCl, 0.5 g; Na₂S·9H₂O, 0.5 g; yeast extract, 5.0 g; trypticase soy broth, 5.0 g; glucose, 5.0 g; HEPES, 5.2 g; vitamin solution, 10 ml (**Table 2-1**) and trace minerals (**Table 2-2**) 10 ml. For the large scale (15 L) growth, HEPES and vitamin solution were omitted from the media composition. The pH of the medium was adjusted to 7.0 before autoclave. The growth substrate (glucose) was sterilized by filtration using a syringe filter and added to the medium before inoculation with the starter culture.

Table 2-1. Composition of trace mineral solution used for the growth of *T. guaymasensis*

Chemical	g/L
Nitritotrioacetic acid	1.5
MgSO ₄	1.46
MnSO ₄ .H ₂ O	0.45
NaCl	1.0
FeSO ₄	0.055
CoCl ₂ .6H ₂ O	0.2
CaCl ₂ .2H ₂ O	0.1
ZnSO ₄ .7H ₂ O	0.18
CuSO ₄ .5H ₂ O	0.01
AlK(SO ₄) ₂ .12H ₂ O	0.018
H ₃ BO ₃	0.01
Na ₂ MoO ₄ .2H ₂ O	0.01
H ₂ O	to 1L

Table 2-2. Composition of 100X vitamin solution used for small-scale growth of *T. guaymasensis*

Vitamin	g/100 ml
Pyridoxine hydrochloride	0.02
Thiamine hydrochloride	0.01
Riboflavin	0.01
Nicotinic acid	0.01
DL-calcium pantothenate	0.01
Lipoic acid	0.01
Biotin	0.004
Folic acid	0.004
Cyanocobalamin	0.0002
Water	to 100ml

P. furiosus was grown on maltose, yeast extract, and tryptone at 95°C using the procedure described previously (Fiala and Stetter 1986). The medium for the growth of *P. furiosus* contained (per liter) KCl, 0.33 g; MgCl₂·6H₂O, 2.75 g; NH₄Cl, 1.2 g; NaCl, 13.8 g; KH₂PO₄, 0.5 g; CaCl₂·2H₂O, 0.75 g; NaBr, 0.05 g; KI, 0.05 g; H₃BO₃, 0.015 g; SrCl, 7.5 mg; citric acid, 5.0 mg; maltose, 5.0 g; yeast extract, 5.0 g; Na₂S·9H₂O, 0.5 g and resazurin 1 mg. The pH of the medium was adjusted to 6.8.

For media preparation the chemicals were added sequentially each after complete dissolving the previous one. After media preparation, 50 ml aliquots were dispensed in 160 ml serum bottles, covered with aluminum foil for autoclave sterilization. After autoclave, the media were capped with stoppers and aluminum seals under aseptic conditions and were degassed using anaerobic manifold by following the procedure described elsewhere (see section 2.3.4). Before inoculation the media were reduced using Na₂S (0.024%) and cysteine hydrochloride (0.0042%). The media were inoculated with late log-phase starter cultures and vitamin solutions. The growth in each culture bottle was monitored by sampling and direct microscopic cell count using a Petroff-Hausser cell counting chamber (1/400 mm², 0.02 mm deep; Hausser Scientific, Horsham, PA) and a Nikon Eclipse E600 phase-contrast light microscope (Nikon Canada, ON, Canada).

Large scale cultures were grown in 20 L glass carboys (15 L media per carboy) and under anaerobic conditions. After the cultures grown to late log-phase, the media were cooled down in a bucket of ice slurry and centrifuged at 13,000 ×g using Sharples continuous centrifugation system (Sharples equipment division, PA, USA) at 150-200 mlmin⁻¹. The cell paste obtained was snap-frozen in liquid nitrogen and then stored at -76°C until use.

2.3.3 Sequencing of *por/vor* operon

Since the genome sequence of *T. guaymasensis* is not available, the genes encoding both POR and VOR were sequenced using a primer walking strategy. To achieve this amino acid sequences of the subunits containing the conserved motifs including TPP-binding motif, CoA-binding motif, and [4Fe-4S] cluster-binding motif were aligned and the corresponding nucleotide sequences were chosen to design degenerative primers used for primer walking (**Table 2-3**). The PCR products with sizes close to the expected PCR product (estimated based on the closely related species) were sequenced in both (forward and reverse) directions. The identity of newly sequenced stretches of DNA was confirmed by searching the database for homologous sequences and then used to design next set of primers for amplification of the new fragments of genomic DNA. Genomes in the NCBI microbial genome database (http://www.ncbi.nlm.nih.gov/genomes/MICROBES/microbial_taxtree.html) were used to

Table 2-3. The primers used for the sequencing of the *por/vor* operon of *T. guaymasensis*

Name	Sequence ^a	Length	Tm (°C) ^b	Size (bp) ^c
GPORGF	5'- TCACACTTACCCAAAGACGCCTG -3'	23	71.1	727
GPORGR	5'- CTCCCCAAACAGCGTGTTCAAAC -3'	23	72.7	
GPORDF	5'- AGGTCTTCGGCTGAGCTTTCG-3'	21	70.4	611
GPORDR	5'- CACCAACACAGGCGGAGATAGC -3'	22	71.2	
GPORA1F	5'- GACTACTGTAAGGGCTGTGGCATC -3'	24	69.3	798
GPORA1R	5'- CGATGACCTTCTTTGCATTCTCG -3'	23	70.9	
GPORB1F	5'- ACGGTGAGGAGTTTGATGAGGTC -3'	23	68.9	719
GPORB1R	5'- ACCTGGACGAAAGCCGGACC -3'	20	72.5	
GPORB2F	5'- TGCCCACCAGGTTCCGTACG -3'	20	72.7	661
GPORB2R	5'- CCTCGTCTCCGGGTTTCTTCTC -3'	22	71.1	
GVORB2F	5'- AACCGCTGACATTGGCCTTC -3'	20	69.0	696
GVORB2R	5'- CTCTCTATGTCGGCCTTAAACGG-3'	23	69.9	
GVORA1F	5'-GCWGTKGCAAAGGCCACAGG-3'	20	67	798
GVORA1R	5'- GTGGAGCATCTCGTGCATGAG-3'	21	67.5	
GVORB1F	5'- GGTGCGCTGGTTCAGGCC -3'	18	70.5	705
GVORB1R	5'- GTAGAGAGCATCGTGGCCCCT -3'	21	69.8	

^a Primers were designed based on the sequences of the fully-sequenced closely related organisms of the genus *Thermococcales*

^b Melting temperature of the primers as determined using GeneRunner (Hasting software Inc., 1994)

^c expected size of the PCR products based on the sequence of the corresponding fragment in closely related organisms

retrieve the amino acid and nucleotide sequences of PORs from various hyper/thermophiles. The deduced amino acid sequences were compared to protein sequences retrieved from NCBI, Swiss Prot and EMBL. The search in these databases were carried out using the programs FASTA, BLAST, and PROSITE. The ClustalW version 2.0 (Thompson *et al.* 1994) was used for DNA and/or protein sequence alignments and comparisons.

After sequencing of each fragment, overlapping primers were designed within the sequenced fragment to get the neighboring DNA sequence. In some cases, when using the primer walking strategy failed to produce a positive PCR product, inverse PCR (IPCR) was used to get the sequences of the neighboring known parts.

2.3.4 Anaerobic techniques

All of the buffers and reagents were degassed in vials and flasks sealed with red rubber sleeved stoppers. The stoppers were punctured with needles to allow the alternate exposure between vacuum and nitrogen (N₂) using a manifold. The nitrogen gas (Praxair, ON, Canada) was deoxygenated by passing through a heated column containing a BASF catalyst (BASF, NJ, USA). Assay and purification buffers were degassed in magnetically-stirred flasks for 30 min, followed by three cycles of vacuum/flushing (each 3 min). Then a second needle was inserted to flush out N₂ to ensure an oxygen-free head space in the container (even if there would be residual O₂ contamination in the manifold system). The vials and flasks were kept under a nitrogen positive pressure (~3 psi). All of the purification buffers contained 2 mM sodium dithionate (SDT) and 2 mM dithiotheritol (DTT) to remove traces of oxygen contamination.

2.3.5 Preparation of cell-free extracts

To purify the native PORs from *T. guaymasensis* and *P. furiosus*, cell-free extracts (CFEs) were prepared from the cells grown to late log-phase. All operations were performed under strictly anaerobic conditions and at room temperature, unless otherwise specified

Cell pellets stored at -76°C (50 g of *T. guaymasensis* and 20 g of *P. furiosus*) were re-suspended in anaerobic lysis buffer [50 mM Tris-HCl, 5% glycerol, 2 mM DTT, and 2 mM SDT, 0.1 mgml⁻¹ lysozyme, and 0.01 mgml⁻¹ DNaseI, pH 7.8] in a pre-degassed flask. The ratio of the lysis buffer to cells (wet weight) was 1:6 (w/v) for *T. guaymasensis* and 1:4 (w/v) for the cell-free extract for *P. furiosus*. The cell suspensions were then incubated at 37°C while stirring for 2 h and subsequently were centrifuged anaerobically at 10,000 ×g for 30 min at 4°C. The supernatant designated as cell-

free extracts (CFEs) and was transferred to anaerobic serum bottle using a syringe pre-rinsed with anaerobic buffer A (50 mM Tris-HCl, 5% glycerol, 2 mM dithiotheritol, and 2 mM sodium dithionite with the pH adjusted to 7.8) and used directly as starting materials for the following purification steps.

2.3.6 Enzyme purification

Due to high levels of the oxygen sensitivity of both PfPOR (POR from *P. furiosus*) and TgPOR (POR from *T. guaymasensis*), all purification steps were carried out using a FPLC system (GE Healthcare, QC, Canada) at ambient temperatures and under strictly anoxic conditions to protect the enzyme from exposure to air. During the purification, the POR and PDC activities were monitored in chromatography fractions using each corresponding assay methods (sections 2.3.11 and 2.3.12) to further confirm the co-elution of the activities all through purification steps. At each step the purity of the active fractions were determined by running an aliquot of the eluted fraction on SDS-PAGE. The buffer A was used throughout the purification.

To purify TgPOR, the CFE was loaded on a diethylaminoethyl (DEAE)-sepharose column (5.0×10 cm) pre-equilibrated with anaerobic buffer A. The column was washed with 3 column volumes of buffer A and then a gradient (0-0.5 M NaCl) of buffer B [50 mM Tris-HCl, 5% glycerol, 1 M sodium chloride, 2 mM DTT, and 2 mM SDT, pH 7.8] was applied at a flow rate of 8.0 mlmin⁻¹. The active fractions (160-220 mM NaCl) were pooled together and applied to a hydroxyapatite (HAP, 2.6×15 cm) column pre-equilibrated with buffer A. After loading of the active fractions, the column was washed with 100 ml of buffer A and then the absorbed proteins were eluted with a gradient (0-0.5 M potassium phosphate) of buffer C [50 mM Tris-HCl, 5% glycerol, 0.32 M K₂HPO₄, 0.18 M KH₂PO₄, 2 mM DTT, and 2 mM SDT pH 7.8] at a flow rate of 2.5 mlmin⁻¹. The active fractions (110-145 mM potassium phosphate) were pooled together and loaded on a phenyl sepharose column (PS, 2.6×10 cm) pre-equilibrated with 0.8 M ammonium sulphate in buffer A. The column was washed with two column volume of 0.8M buffer A and then a linear gradient (0.8-0 M ammonium sulphate) of buffer D [50 mM Tris-HCl, 5% glycerol, 2 M ammonium sulphate, 2 mM DTT, and 2 mM SDT pH 7.8] was applied at a flow rate of 2.5 mlmin⁻¹.

The purified POR was eluted as 440-290 mM ammonium sulphate was applied based on SDS-PAGE. The purified fractions were then desalted and concentrated under anaerobic conditions using an ultrafiltration device (Advantec MFS, Inc., CA, USA) with a 44.5 mm membrane of

polyethersulfone and nominal molecular weight limit (NMWL) of 50,000 (Millipore, MA, USA) and under pressure of nitrogen. After concentration, the purified POR was stored as protein balls in liquid nitrogen until use.

To purify the bifunctional POR/PDC from *P. furiosus*, the CFE was loaded on a DEAE-sepharose column (5.0×10 cm) pre-equilibrated with anaerobic buffer A. The column was washed with 2.5 column volume of anaerobic buffer A and then a gradient (0-0.5 M NaCl) of buffer B [50 mM Tris-HCl, 5% glycerol, 1 M sodium chloride, 2 mM DTT, and 2 mM SDT, pH 7.8] was applied to the column at a flow rate of 5.0 mlmin⁻¹. The collected fractions were tested for the POR activity and the active fractions (162-198 mM NaCl) with POR specific activity higher than 5 Umg⁻¹ were pooled together and loaded on a phenyl sepharose column (2.6×10 cm) pre-equilibrated with 1 M ammonium sulphate in buffer A. The column was washed with 1.5 column volume of 1M ammonium sulphate and then a linear gradient (1-0 M ammonium sulphate) of buffer D [50 mM Tris-HCl, 5% glycerol, 2 M ammonium sulphate, 2 mM DTT, and 2 mM SDT pH 7.8] was applied to the column at a flow rate of 3.0 mlmin⁻¹. The PfPOR was eluted from the phenyl sepharose column as 900-700 mM ammonium sulphate applied to the column. The active fractions were pooled together, desalted and concentrated using an ultrafiltration device (Advantec MFS, Inc., CA, USA). The ultrafiltration was carried out using a 44.5 mm membrane of polyethersulfone and nominal molecular weight limit (NMWL) of 50,000 (Millipore, MA, USA) under anaerobic conditions and pressure of nitrogen. The concentrated fraction was then loaded onto a HiLoad Superdex-200 (GE healthcare, QU, Canada) gel-filtration chromatography column (2.6×60 cm) pre-equilibrated with buffer E (50 mM Tris, 5% glycerol, 100 mM KCl, pH 7.8) and eluted from the column at the flow rate of 2 mlmin⁻¹. The active fractions then were pooled and loaded on a hydroxyapatite (2.6×15 cm) column equilibrated with buffer A at 4.0 mlmin⁻¹. After loading of the active fractions, the column was washed with 100 ml of buffer A and then eluted with a gradient (0-0.5 M potassium phosphate) of buffer C [50 mM Tris-HCl, 5% glycerol, 0.32 M K₂HPO₄, 0.18M KH₂PO₄, 2 mM DTT, and 2 mM SDT pH 7.8]. The purified PfPOR (as judged by SDS-PAGE) was eluted from the HAP column at 90-139 mM phosphate concentration. The purified POR was desalted and concentrated again and stored in liquid nitrogen until use.

2.3.7 Protein concentration determination

The protein concentration was routinely determined using Bradford dye-binding method (Bradford 1976) using the Bradford reagent purchased from Bio-Rad Laboratories (ON, Canada). Bovine serum albumin (BSA) was used for obtaining a standard curve as instructed by the manufacturer.

2.3.8 SDS-PAGE

The sodium dodecyl sulfate polyacrylamide gel electrophoresis (SDS-PAGE) was used to determine the enzyme purity and apparent subunit molecular weights. SDS-PAGE was performed according to Laemmli (1970) with acrylamide and molecular weight standards from Bio-Rad (ON, Canada) using a Hoefer™ Mighty small system (Hoefer Inc., MA, USA) with the gels (8×10 cm) prepared and stained with Coomassie Brilliant Blue R250. The de-staining was carried out by storing the gel in the de-staining solution (12% 2-propanol and 7% acetic acid) with moderate shaking overnight.

2.3.9 Estimation of native molecular mass

The molecular weight of TgPOR subunits was estimated by loading the concentrated protein (approximately 1 mg) on a HiLoad Superdex-200 size-exclusion chromatography column of (2.6×60cm, GE Healthcare, QC, Canada) pre-equilibrated with buffer E (50 mM Tris, 5% glycerol, 100 mM KCl, pH 7.8) at the flow rate of 2.5 mlmin⁻¹. The following standards from Pharmacia protein standard kit (pharmacia, NJ, USA) were applied to the column: blue dextran (2,000,000 Da), thyroglobulin (669,000 Da), ferritin (440,000 Da), catalase (232,000 Da), aldolase (158,000, Da), bovine serum albumin (67,000, Da), ovalbumin (43,000 Da), chymotrypsinogen A (25,000 Da) and ribonuclease A (13,700 Da).

2.3.10 AcDH assay

CoA-dependent acetaldehyde dehydrogenase activity was determined in CFEs of *T. guaymasensis* and *P. furiosus*. The assays were carried out at 80°C in an assay mixture (2 ml) composed of glycine buffer (50 mM, pH 10.5), 1 mM MgCl₂, 1 mM DTT, 0.1 mM coenzyme A, and 1.5 mM NAD⁺ or NADP⁺ and different amounts of the CFEs were used as the source of the activity. The anaerobic assay buffer was transferred to a pre-degassed assay cuvette using syringes rinsed (three times) with anaerobic buffer. The cuvette was incubated in a water-jacketed cuvette holder on a Genesys 10 UV-Vis spectrophotometer (Thermo Scientific, MA, USA) and pre-warmed to the assay temperature

(80°C) for 4 min. After temperature equilibration, it was taken out and the assay components (other than enzyme) were added using pre-rinsed Hamilton gas-tight syringe (Hamilton Company, Reno, NV, USA) in rapid succession and cuvette was placed back in the holder for another 30 seconds. Then the reaction was started by adding the acetaldehyde and monitoring the absorbance change at 340 nm.

2.3.11 POR activity assay

The spectrophotometric measurement of pyruvate- and coenzyme A-dependent reduction of the benzyl (or methyl) viologen was used to assay the POR activity as previously described (Wahl and Orme-Johnson 1987).

The catalytic activities of purified PORs were assayed in duplicate and under strictly anaerobic conditions unless otherwise mentioned. The sodium pyruvate was routinely used as substrate (electron donor) and methyl viologen (MV) replaced ferredoxin as electron acceptors. The assays were carried out at 80°C in an assay mixture (2 ml) composed of 100 mM EPPS, pH 8.4, 1 mM MgCl₂, 5 mM sodium pyruvate, 0.4 mM TPP, 100 μM coenzyme A, 1 mM of methyl viologen (MV), and enzyme in stoppered optical glass cuvettes with 1cm light path (Starna cells, Inc., Atascadero, CA, USA). In addition, small amount of sodium dithionite (SDT) was added to the assay mixture (until a light blue color appeared) to scavenge residual oxygen and slightly reduce the assay mixture before the addition of the enzyme to start the reaction (section 2.3.4).

The anaerobic assay buffer was transferred to pre-degassed assay cuvette using a syringe pre-rinsed with anaerobic buffer for at least three times. The cuvette was incubated in a water-jacketed cuvette holder on a Genesys 10 UV-Vis spectrophotometer (Thermo Scientific, MA, USA) and pre-warmed to the assay temperature (80°C) for 4 min, then it was taken out and the assay components (all but the enzyme) were added using a pre-rinsed Hamilton gas-tight syringe (Hamilton company, Reno, NV, USA) in a rapid succession. Subsequently, the cuvette was placed back in the holder for another 30 seconds. The reaction was started by adding the enzyme fraction and the absorbance change at 578 nm was monitored. An extinction coefficient of $\epsilon_{578} = 9.8 \text{ mM}^{-1}\text{cm}^{-1}$ (Yoon *et al.* 1997; Schut *et al.* 2001a) was used for calculation of the activity. The oxidation of one pyruvate would release two electrons. The activity was determined based on the initial linear part of enzymatic reaction progress curve, and one unit of enzyme activity was defined as the oxidation of 1 μmol of the substrate or the reduction of 2 μmol methyl viologen per minute. Linear correlation between the activity and the

amount of protein in assay was determined to ensure that all activities were within the linear range of measurement.

2.3.12 PDC activity assay

Pyruvate decarboxylase activity (PDC) was determined by measuring the rate of acetaldehyde production. In principle, acetaldehyde produced during the enzymatic reaction (**Figure 2-1**, step A) was derivatized with a freshly prepared acidic solution of 2, 4-dinitrophenylhydrazine (DNPH) also known as Brady's reagent (**Figure 2-1**, step B). The reaction of the reagent with aldehyde groups creates a yellow-reddish color resulting from the formation of the corresponding hydrazone derivative. Subsequent to liquid-liquid phase extraction with a solvent (**Figure 2-1**, step C), the acetaldehyde-DNPH complex was quantified by reverse-phase high performance liquid chromatography (RP-HPLC). The general procedures and main steps involved in the assay are presented in **Figure 2-1**.

The enzymatic reactions were carried out in duplicate in stoppered 8 ml vials under anaerobic conditions at 80°C unless otherwise specified. The standard assay mixture (1 ml final volume) containing EPPS buffer (100 mM, pH 8.4), 1 mM MgCl₂, 0.1 mM thiamine pyrophosphate (TPP), 10 mM sodium pyruvate, and 1 mM coenzyme A (CoASH) was pre-warmed by incubation at 80°C water bath for 4 min. When specified, sodium pyruvate was replaced with 10 mM of 2-ketoisovalerate. The reaction was started by adding the enzyme (or enzyme containing fraction). Tests were carried out to make sure that there would be a linear correlation between the activity and the amount of enzyme in the assay. Unless specified, the enzyme reaction was stopped after 20 min by transferring the assay vials on the ice and adding of 2 ml of freshly prepared saturated DNPH solution in 2 N HCl (stirred at room temperature and dark for 1hr). The vials were then incubated overnight at room temperature with shaking (150-200 rpm) to allow derivatization of acetaldehyde with the DNPH. The resulting hydrazone (acetaldehyde-DNPH) derivative was then extracted with 1 ml of dichloromethane (DCM) by vigorous shaking at room temperature for 15 min. the extraction was then repeated for one more time. The organic (lower) phase was then transferred to a new clean vial covered with a piece of Parafilm M[®] membrane with few holes on it. The assay vials were placed in a vacuum desiccator covered with aluminum foil (to protect from the light), which was connected to a water pump to evaporate the DCM in a fume hood. After evaporation of DCM (about 3-4 h), the

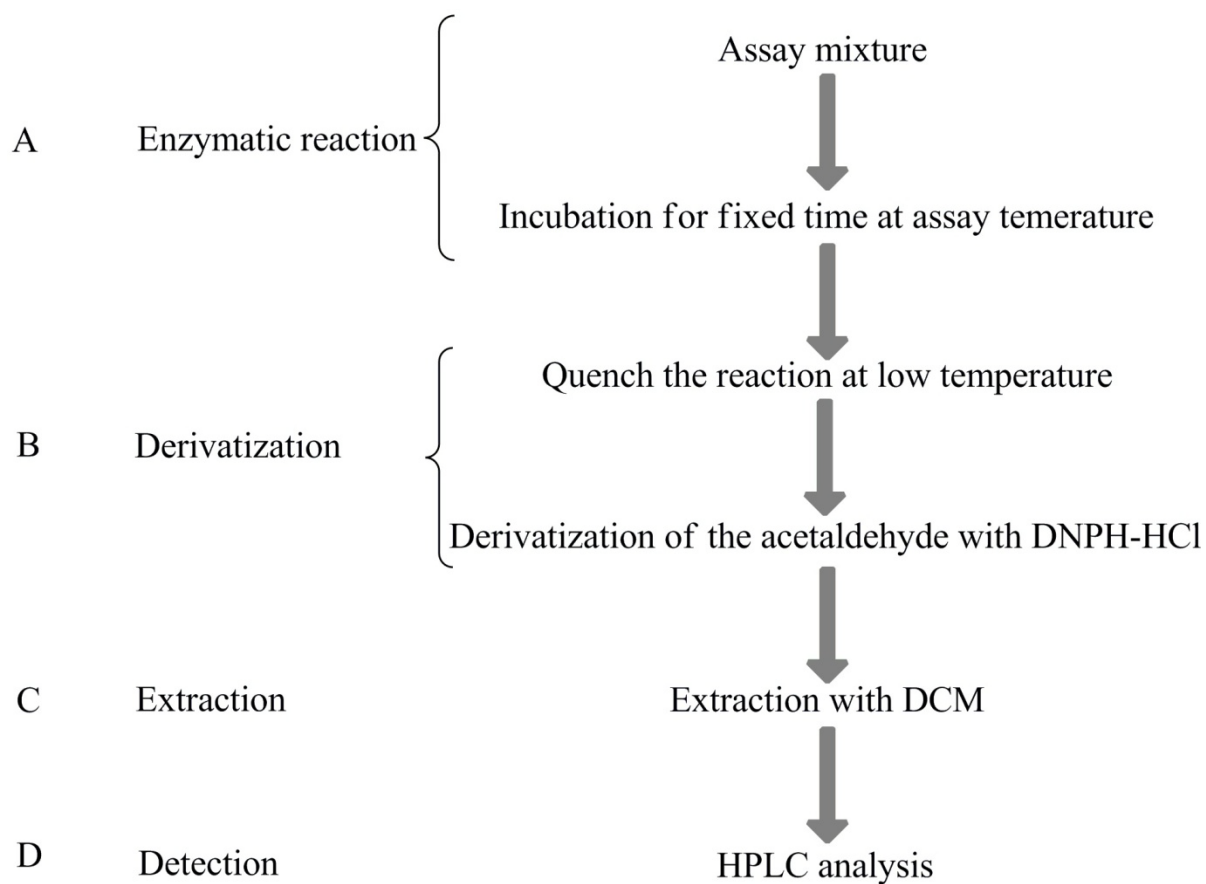


Figure 2-1. General steps involved in PDC activity assay

DNPH-HCl, hydrochloridric acid solution saturated with dinitrophenylhydrazine; DCM, dichloromethane; HPLC, high performance liquid chromatography. All assays were carried out at 80°C and under strictly anaerobic conditions; the buffer routinely used for the assay was glycine (100 mM, pH 9.5) unless specified.

resulting yellowish-red powder was dissolved in 4 ml of pure (HPLC grade) acetonitrile by incubation at 4°C overnight.

An aliquot of the assay product was filtered through a 0.2 µm nylon syringe filter (National Scientific, Rockwood, TN, USA), and the filtered sample was then analyzed using a Perkin-Elmer LC series 4 HPLC system (Norwalk, CT, USA) fitted with a reversed-phase Allure C18 column (150×4.6 mm, 5 µm, 60Å). Isocratic elution conditions with a mobile phase of acetonitrile/water (80:20 v/v) were used at a flow rate of 1 mlmin⁻¹. A micrometrics model 788 dual variable wavelength detector (Norcross, GA, USA) was used and operated at 365 nm. The sample was applied using a Rheodyne Model 7125 injection valve (Rheodyne Inc., CA, USA) with a 20 µl sample loop. The HPLC system was operated at room temperature. The final concentration of acetaldehyde and isobutyraldehyde were determined using a calibration curve prepared by linear regression plotting of known concentrations of each product which was processed under the same assay conditions.

2.3.13 Determination of PDC of pyruvate dehydrogenase (PDH)

To determine the ability of pyruvate dehydrogenase to catalyze the production of acetaldehyde from pyruvate, PDC enzyme assays were carried out using the procedure described previously (section 2.3.12). The porcine heart PDH was purchased from Sigma-Aldrich Canada Ltd. (ON, Canada). The PDC assays were carried out under aerobic conditions and at different pHs of 6.2 and 7.5 (sodium phosphate), 8.4 (EPPS), and 10.2 (CAPS) with a concentration of 100 mM. The standard assay mixture (1 ml final volume) containing 1 mM MgCl₂, 2.4 mM NAD, 0.3 mM dithiotheritol, 0.5 mM thiamine pyrophosphate (TPP), 5 mM sodium pyruvate, and 0.5 mM coenzyme A (CoASH) was pre-incubated in water bath (30°C) for 4 min. The reactions started by adding the enzyme and continued for 90 min. After the enzymatic reaction time, the vials were transferred on ice, and stopped by addition of 3 ml of freshly prepared and filtered saturated DNPH-HCl. The rest of the procedures including solvent extraction and HPLC analysis were followed using the procedure described in section 2.3.12 without deviations. Control assays were performed, which included reactions with no enzyme, no CoA, and no substrate (pyruvate), respectively.

2.3.14 Biochemical and biophysical characterization

To determine the pH dependence of each activity, assays were carried out in duplicate, at different pH values ranging from 6.0 to 11. The optimal pH (pH dependence) was determined for both activities using purified POR/PDC from *T. guaymasensis*. All assays were carried out at 80°C, under strictly

anaerobic conditions using degassed buffers (100 mM) as previously described. The pH values expressed throughout this manuscript were adjusted and measured at room temperature unless specified differently. The buffers used were sodium phosphate buffer (pK_a 7.20, $\Delta pK_a/^\circ C = -0.0028$) for pH values of 6.0, 7.0, and 7.5, EPPS buffer [N-(2-Hydroxyethyl)-piperazine-N'-3-propanesulfonic acid, pK_a 8.0, $\Delta pK_a/^\circ C = -0.015$] for pH values of 7.5, 8.0, 8.4 and glycine buffer (pK_a 9.55, $\Delta pK_a/^\circ C = -0.0025$) for pH values of 8.5, 9.0, 9.5, 10.0, 10.5 and finally CAPS buffer [3-(Cyclohexylamino)-propanesulfonic acid, pK_a 10.40, $\Delta pK_a/^\circ C = -0.009$] for pH values of 10.0, 10.5, and 11.0.

Steady-state kinetic parameters (K_m and V_{max}) were determined for each activity at the optimal pH and under strictly anaerobic conditions. All of the kinetic experiments were carried out at 80°C. The kinetic parameters were determined for pyruvate (substrate), TPP and coenzyme A (cofactor) and the artificial electron acceptor methyl viologen (MV) by applying various concentrations of each component and keeping the concentration of other assay components invariable. All of the assays were performed in duplicate. The kinetic parameters were calculated from best fit of data to Michaelis-Menten equation by non-linear regression using the SigmaPlot® software (SYSTAT Software Inc., CA, USA).

To investigate oxygen sensitivity of each activity, an aliquot of the enzyme was exposed to air at 4°C by gentle stirring. Enzyme activities were then measured at different time points and compared to a control preparation that was kept on ice and under anaerobic conditions (unexposed control).

The temperature dependencies of both activities were determined by assaying the enzyme activity at different temperatures from 30°C to 95°C under standard assay conditions. The POR assays were carried out in 100 mM EPPS buffer containing 10 mM $MgCl_2$, at pH 8.4. To determine the half-life of the enzyme at 80°C, the residual activities at different time points were determined and compared to un-heated control.

To determine the ability of the enzyme to use 2-ketoisovalerate in the oxidation or decarboxylation reactions, 2-ketoisovalerate was replaced for pyruvate in the assay mixture. To quantify the product of the decarboxylase activity, a standard curve was prepared using various concentrations of isobutyraldehyde. The whole assay procedures described for the PDC activity assay were followed. The assay mixtures for the standard preparations contained no enzyme and as limited amounts of 2-

ketoisovalerate was available, pyruvate was incorporated into the assay mixtures instead of the 2-ketoisovalerate. The final products were measured *via* HPLC as previously described (section 2.3.12).

2.4 Results

2.4.1 Growth of *T. guaymasensis*

T. guaymasensis cells were grown on glucose, yeast extract, tryptone without adding elemental sulfure (S^0). When cultures were in the late log phase-early stationary phase after 18-20 h of growth, the cells were harvested by continuous centrifugation. The cell density of the cultures at the time of harvest was approximately $5.5\text{-}6.5 \times 10^8$ cellsml⁻¹, which resulted in a final cell yield of 0.6 ± 0.17 g (wet weight) per liter of culture ($n=21$).

2.4.2 Sequencing of the *por/vor* gene cluster in *T. guaymasensis*

A total of 6.7 kbp of the genome of *T. guaymasensis* was sequenced using primer walking and inverse PCR strategies. The primers were designed based on highly conserved regions (including CoA-binding motif, TPP-binding motif, and [4Fe-4S] cluster-binding motifs) within *por/vor* operons of released coding sequences of the Thermococcales genomes including *T. kodakaraensis*, *P. furiosus*, *P. horikoshii*, and *P. abyssi*. The sequences obtained encompassed genes encoding all of the subunits of POR and VOR. Parts of the neighboring sequences were also retrieved using the aforementioned strategies. By analysis of the sequence information from the *por/vor* gene cluster in *T. guaymasensis* and comparison with other hyperthermophilic *por/vor* sequences from different databases, the gene organization in *T. guaymasensis* was determined (**Figure 2-2**). The deduced nucleotide sequences encoded for proteins of 186, 105, 391, 311, 105, 394, and 332 amino acid residues in lengths.

The subunit gamma (Por/VorG) was shared between POR and VOR, which is a common property of the gene organization in Thermococcales *por-vor* operons (Kletzin and Adams 1996). The subunits delta (*vorD*), alpha (*vorA*) and beta (*vorB*) of VOR were located downstream of the common subunit gamma gene (*por/vorG*) and then the subunit delta (*porD*), alpha (*porA*) and beta (*porB*) of POR were located downstream of the *vor* genes.

Interestingly, three coding sequences encoding for the subunits delta, alpha, and beta of each VOR and POR, had overlapping intercistronic regions. That is the start codon of the adjacent gene (coding the next subunit of the same enzyme) was separated by only few base pairs from the translation

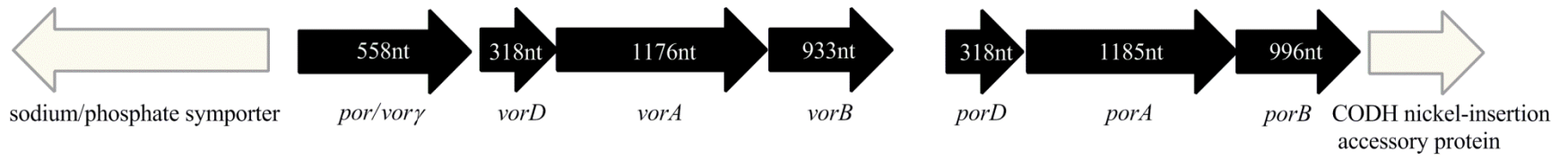


Figure 2-2. Gene organization of *por/vor* gene cluster in *T. guaymasensis*

por, pyruvate ferredoxin oxidoreductase; *vor*, 2-ketoisovalerate ferredoxin oxidoreductase; CODH, carbon monoxide dehydrogenase

termination sequence of the next subunit, then the ribosome binding site (RBS) of the next (distal) subunit is located in the coding sequence of the previous (proximal) subunit (**Figure 2-3**).

This was observed for some other proteins in bacteria and phages and was suggested to be a mechanism to assure all of the genes involved in making a multisubunit enzyme or the genes that are involved in the same biological pathway are being transcribed together and to the same level (Nichols and Yanofsky 1979; Schoner *et al.* 1984). Based on the transcription start and termination sequences identified, it was concluded that the genes were expressed as three independent transcriptional units, expressing the *por/vorG*, *vorDAB*, and *porDAB* (**Figure 2-2**), respectively. Each of the transcripts seemed to start from their own transcription initiation sequences. It seems to be a mechanism to assure that the shared subunit (PorG) is being expressed independent of each enzyme POR and VOR, and it might be suggestive that the POR and VOR are not necessarily being expressed at the same time.

TgPOR contained 15 conserved cysteine residues. Subunits PorA, PorB, and PorD contained 1, 6, and 8 cysteine residues, respectively. Unlike PORs of Thermotogales, which contained two highly conserved cysteine residues per PorG, there were no cysteines present in Thermococcales PorD. The primary sequence analysis confirmed the presence of two typical highly conserved cysteine-rich ferredoxin type [4Fe-4S] cluster binding motifs (CXXCXXCXXXCP) in the subunit delta. There were four highly conserved cysteine residues in the subunit beta, which were believed to be involved in the coordination of the third iron-sulfur cluster for the electron transfer to low molecular weight ferredoxin molecules (Kletzin and Adams 1996). Additionally two other cysteine residues were found to be conserved in all Thermococcales (with except for *T. sibiricus* and *T. barophilus*). The subunit beta (PorB) also contained the conserved TPP-binding motif (**Figure 2-4**), which is the common feature of all TPP-dependent enzymes and is known to be involved in Mg²⁺-TPP cofactor binding (Hawkins *et al.* 1989; Muller *et al.* 1993).

2.4.3 Searching for AcDH (CoA acetylating) activity in hyperthermophiles

The extensive database search to find a gene or protein homolog of the CoA-dependent AcDH in hyperthermophilic archaea and bacteria failed. The available genome sequences from different archaeal and bacterial hyperthermophiles were searched based on both the annotations and the homology to the known *adhE* and *mhpF* sequences. CoA-dependent acetaldehyde dehydrogenase activity under the conditions examined (different pHs and buffers, different amounts of CFEs, and using NAD⁺ and NADP⁺ as cofactors) was not detectable in CFEs of two hyperthermophilic archaea,

AGAGAAGT <u>GAGGTGATATAA</u> ATGCC	<i>vorD-vorA</i>
ACCTTA <u>AGAGGTG</u> AGAAC ATGG	<i>vorA-voaB</i>
GGGAGACCAAGT <u>GAGGTG</u> GTGAAG ATG	<i>porD-porA</i>
<u>GAAGGA</u> GATCCTGT <u>GAGGTGAGGAAA</u> ATG	<i>porA-porB</i>

Figure 2-3. Intercistronic sequences in *por/vor* operon of *T. guaymasensis*

The translation initiation (start) codons of the distal genes are indicated in bold, the ribosome-binding site (RBS) of the distal gene is boxed, and the translation terminations of the proximal genes are underlined.

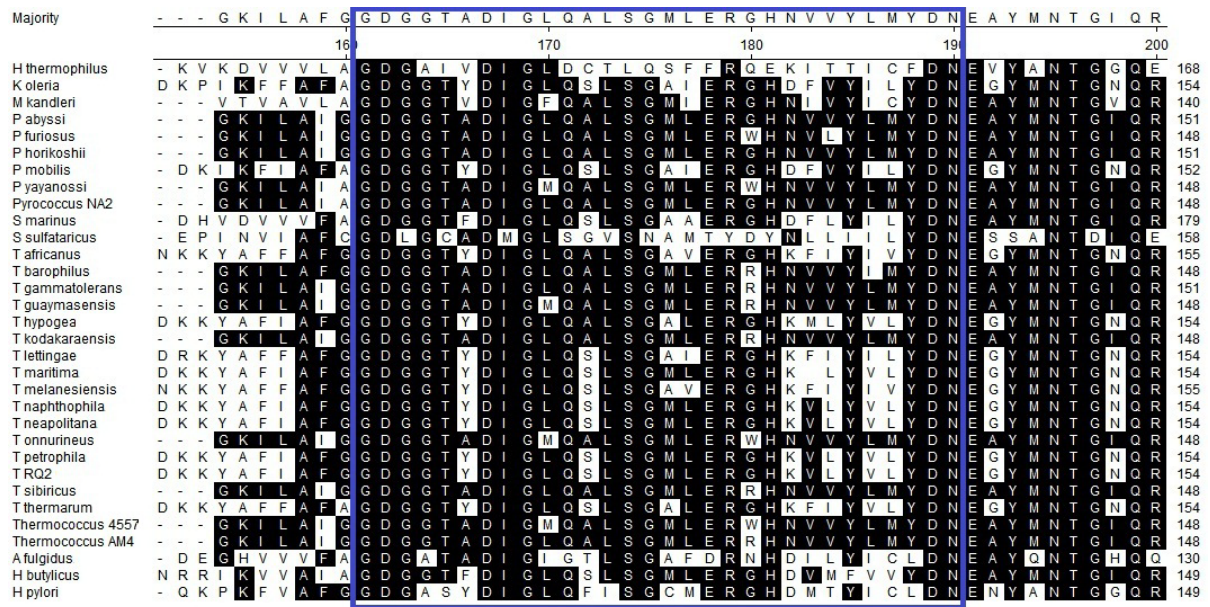


Figure 2-4. Multiple sequence alignment of part of PorB from various bacteria and archaea

The amino acid sequences of PorB were retrieved from GenBank and aligned using MegAlign software (Lasergene, DNASTar, Madison, USA). The TPP-binding motif (GDGX₂₄₋₂₇NN) is boxed.

A. fulgidus, *Archaeoglobus fulgidus*; *H. pylori*, *Helicobacter pylori*, *H. butylicus*, *Hyperthermus butylicus*; *K. oleriae*, *Kosmotoga oleriae*; *M. kandleri*, *Methanopyrus kandleri*; *P. mobilis*, *Petrotoga mobilis*; *P. mobilis*, *Petrotoga mobilis*; *P. abyssii*, *Pyrococcus abyssii*; *P. furiosus*, *Pyrococcus furiosus*; *P. horikoshii*, *Pyrococcus horikoshii*; *Pyrococcus NA2*, *Pyrococcus* species strain NA2; *P. yayanossii*, *Pyrococcus yayanossii*; *S. marinus*, *Staphylothermus marinus*; *S. solfataricus*, *Sulfolobus solfataricus*; *T. africanus*, *Thermosipho africanus*; *T. melanesiensis*, *Thermosipho melanesiensis*; *Thermococcus AM4*, *Thermococcus* species strain AM4; *T. barophilus*, *Thermococcus barophilus*; *T. naphthophila*, *Thermotoga naphthophila*; *T. lettingae*, *Thermotoga lettingae*; *T. neapolitana*, *Thermotoga neapolitana*, *T. hypogea*, *Thermotoga hypogea*; *T. thermarum*, *Thermotoga thermarum*; *T. maritima*, *Thermotoga maritima*; TRQ2, *Thermotoga* species strain RQ2; *Thermococcus 4557*, *Thermococcus* species strain 4557; *T. sibiricus*, *Thermococcus sibiricus*; *T. gammatolerance*, *Thermococcus gammatolerance*; *T. kodakaraensis*, *Thermococcus kodakaraensis*

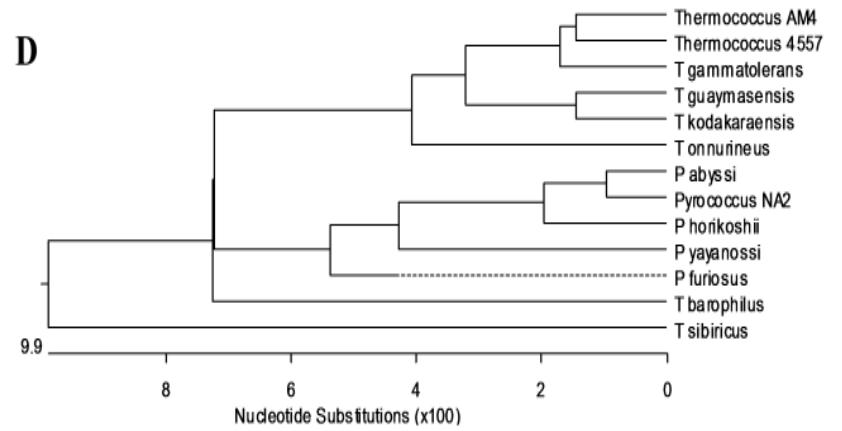
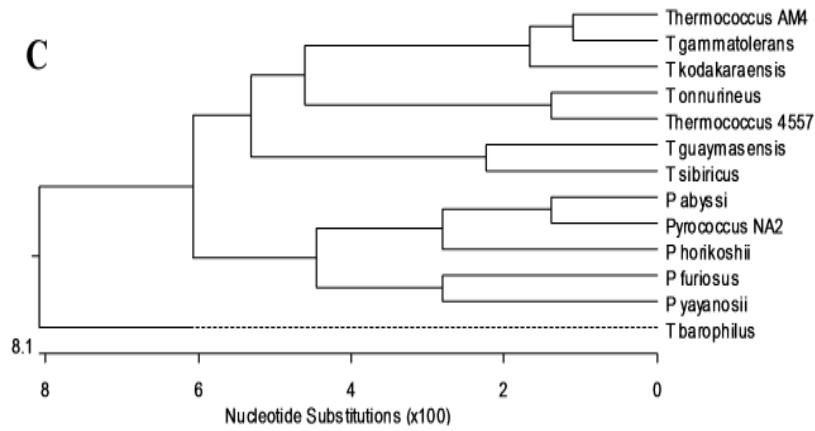
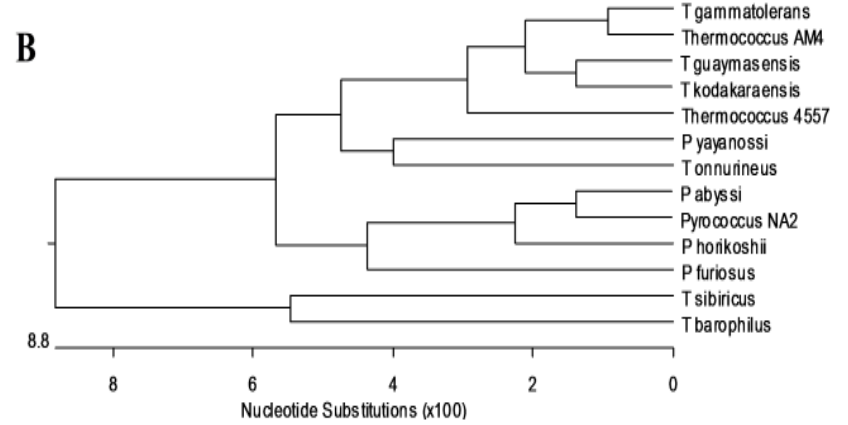
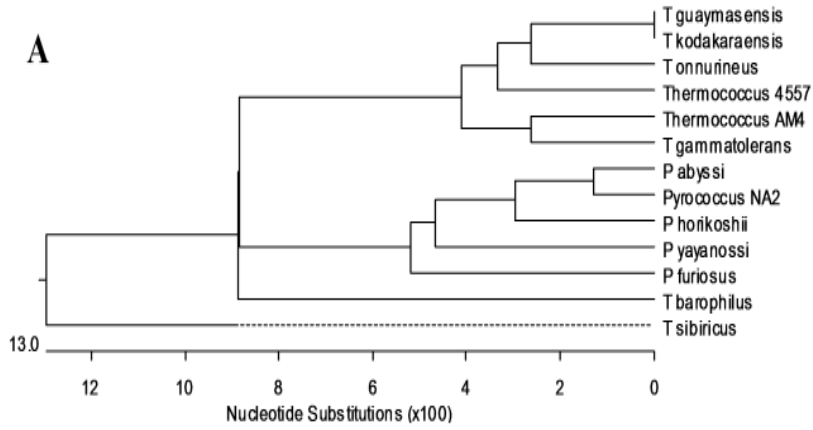


Figure 2-5. Rooted phylogenetic tree based on amino acid sequences of various Thermococcales POR subunits

The amino acid sequences of subunit alpha (**A**), subunit beta (**B**), subunit gamma (**C**), and subunit delta (**D**) of Thermococcales PORs were aligned. The amino acid sequences used for the generation of tree were retrieved from the genome databases as described in the Materials and Methods (section 2.3.3). In the case of TgPOR, the amino acid sequences were determined by translation of the nucleotide sequences retrieved by primer walking and inverse PCR (section 2.3.3). The sequences homology and the phylogenetic trees were prepared using MegAlign software (Lasergene, DNASTar, Madison, USA). The numbers at the bottom of each tree indicate the number of the amino acid substitutions. A dotted line on the phenogram indicates a negative branch length, a common result of averaging.

P. abyssi, *Pyrococcus abyssi*; *P. furiosus*, *Pyrococcus furiosus*; *P. horikoshii*, *Pyrococcus horikoshii*; *Pyrococcus* NA2, *Pyrococcus* species strain NA2; *P. yayanosii*, *Pyrococcus yayanosii*; *Thermococcus* AM4, *Thermococcus* sp. strain AM4; *T. barophilus*, *Thermococcus barophilus*; *Thermococcus* 4557, *Thermococcus* species strain 4557; *T. sibiricus*, *Thermococcus sibiricus*; *T. gammatolerance*, *Thermococcus gammatolerance*; *T. kodakaraensis*, *Thermococcus kodakaraensis*; *T. guaymasensis*, *Thermococcus guaymasensis*.

T. guaymasensis and *P. furiosus* (and some bacterial hyper/thermophiles including *Thermotoga hypogea* and *T. maritima*).

2.4.4 Purification

Both bifunctional POR/PDC enzymes were present in the CFEs of *T. guaymasensis* and *P. furiosus* indicating that they are cytoplasmic. The typical purification steps for the enzymes from *P. furiosus* (**Table 2-4**) and *T. guaymasensis* (**Table 2-5**) resulted in a relatively low (about 7-8%) recovery yield. Both of proteins were purified to the homogeneity as judged by SDS-PAGE analysis (**Figure 2-6** and **Figure 2-7**). The purified proteins from both organisms had a brownish color, which is the common characteristic of the iron-sulfur containing proteins.

CFE of *T. guaymasensis* showed a POR specific activity typically in the range of 2.6 U mg^{-1} and a PDC activity of approximately 0.04 U mg^{-1} . CFE of *P. furiosus* had POR and PDC of about 3.2 and 0.03 U mg^{-1} , respectively. The final preparation of the purified enzyme from *T. guaymasensis* had specific activities of 20.2 \pm 1.8 U mg^{-1} and 3.8 \pm 0.22 U mg^{-1} for oxidation and decarboxylation reactions, respectively. The POR and PDC activities were co-eluted throughout different steps of chromatography purification (**Figure 2-8**). Interestingly, on the final column (PS) there are two peaks of the POR and PDC activities with the larger one most likely belonging to POR and the second one belonging to the VOR activity (as confirmed by corresponding enzyme assay on both fractions), which is apparently able to catalyze the oxidative and non-oxidative decarboxylation of the pyruvate, albeit with a lower rate. The purified enzyme of *P. furiosus* had POR specific activity of 22.3 U mg^{-1} and PDC activity of 3.8 U mg^{-1} using pyruvate as the substrate.

Purification of PfpOR resulted in a specific activity increase of 7.8-fold over that of CFE. This was in agreement with the previously reported 7-fold increase with a specific activity of 21 U mg^{-1} (Blamey and Adams 1993; Schut *et al.* 2001a).

Table 2-4. Purification of bifunctional POR/PDC from *P. furiosus*^a

Step	Total protein ^b (mg)	Total activity ^c (units)	Specific activity ^d (Umg ⁻¹)	Purification (fold)	Recovery (%)
Cell-free extract	1267	8442	3.2	1	100
DEAE sepharose	386	2016	5.2	1.7	23.8
Phenyl sepharose	80	1031	13.1	4.1	12.2
Gel filtration	28.2	495	19.1	6.0	5.8
Hydroxyapatite	21	392	22.3	7.0	4.6

^a CFE was prepared from 20 g (wet weight) of *P. furiosus* cells

^b As determined by Bradford assay using BSA as the standard protein as described in the Materials and Methods section

^c POR activity assay as described in the material and methods (section 2.3.11)

^d One unit was defined as micromoles of pyruvate oxidized per min

Table 2-5. Purification of bifunctional POR/PDC from *T. guaymasensis*^a

Step	Total protein ^b (mg)	Total activity ^c (units)	Specific activity ^d (Umg ⁻¹)	Purification (fold)	Recovery (%)
Cell-free extract	1358	3434	2.6	1	100
DEAE sepharose	322	1748	5.6	2.2	50.9
Hydroxyapatite	84	580	7.5	2.9	16.9
Phenyl sepharose	17.9	363	20.2±1.8	7.8	10.6

^a CFE was prepared from 25 g (wet weight) of *T. guaymasensis* cells

^b As determined by Bradford assay using BSA as the standard protein as described in the Materials and Methods (section 2.3.7).

^c The POR activity assay as described in the material and methods (section 2.3.11)

^d One unit was defined as micromoles of pyruvate oxidized per min

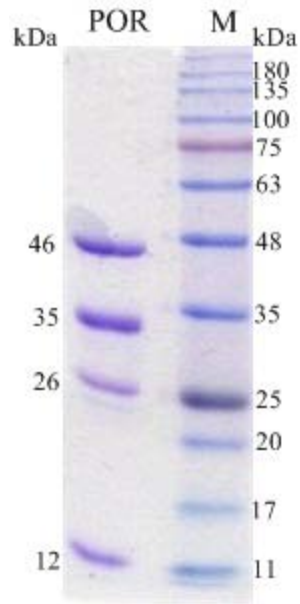


Figure 2-6. Analysis of purified enzyme from *T. guaymasensis* using SDS-PAGE (12.5%)

Lane 1, 5 μ g of the purified protein; lane 2, BLUeye pre-stained protein ladder (Froggibio, ON, Canada)

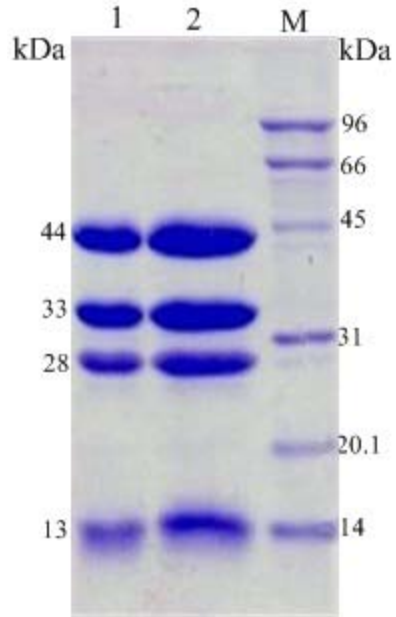


Figure 2-7. Analysis of purified enzyme from *P. furiosus* using SDS-PAGE (12.5%)

Lane 1, 8 µg of the purified protein; lane 2, 12 µg of the purified protein; lane M, molecular weight standard marker. The numbers on the right side indicate the molecular weight of the maker bands and the numbers on the left side indicate the estimated molecular weights calculated based on the SDS-PAGE.

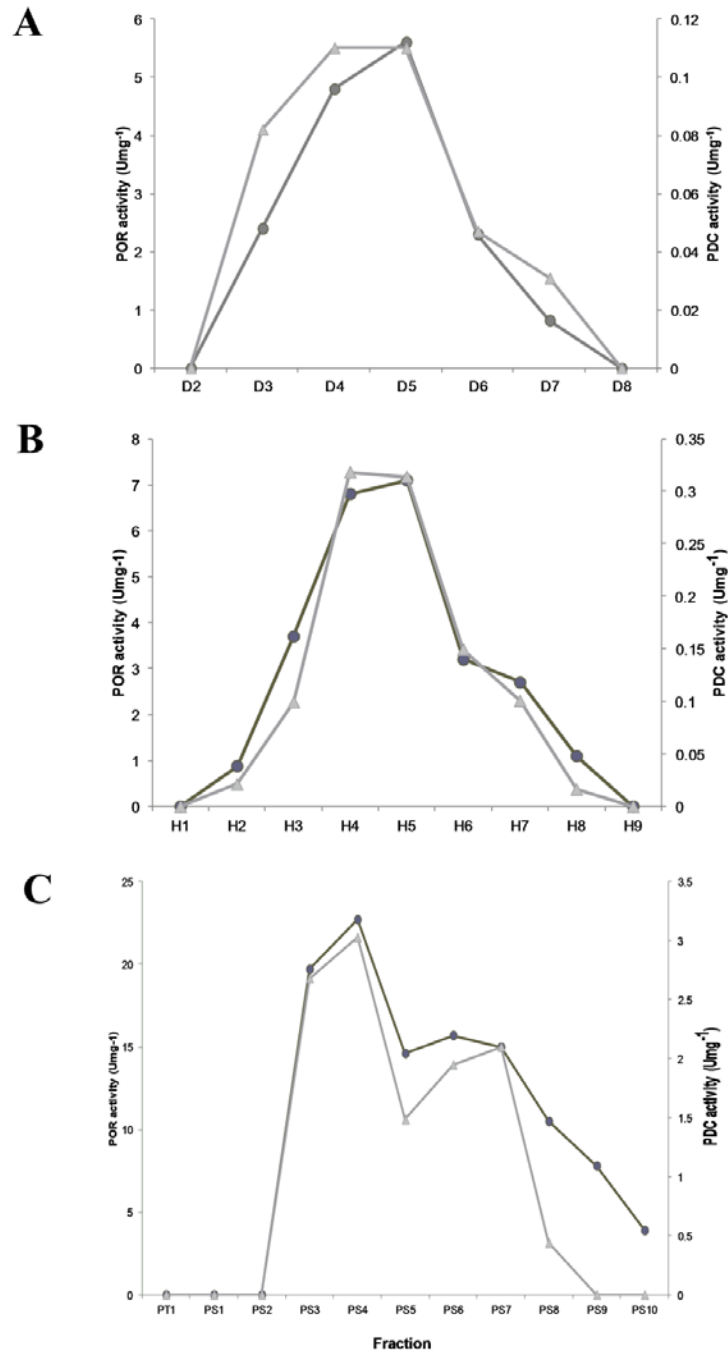


Figure 2-8. Co-elution of POR and PDC activities during chromatography steps

Different fractions from DEAE-sepharose (A) Hydroxyapatite (B), and Phenyl-sepharose (C) chromatography columns for *T. guaymasensis*. The fractions from each chromatography step were assayed for both PDC and POR activities. All assays were carried out under strictly anaerobic conditions and at 80°C as described in Material and Methods (sections 2.3.11 and 2.3.12). The filled and open symbols represent POR and PDC activities, respectively.

2.4.5 Estimation of native molecular mass

The apparent molecular weight of the purified POR was determined to be 258,043±5650 Da ($n=3$) by running approximately 0.5 mg of the purified protein on a gel-filtration chromatography column. The SDS-PAGE analysis of the purified enzyme after gel-filtration column (**Figure 2-6**) revealed that the enzyme was composed of four different subunits with estimated molecular weights of 12, 26, 35, and 46 kDa, respectively. These were further verified by estimation made by the amino acid sequences deduced from the nucleotide sequence of each subunit (11.9, 19.9, 36.1, and 43.8 kDa). Overall, the subunit molecular weights are suggesting the native molecule is a dimer of heterotetramers ($\alpha_2\beta_2\gamma_2\delta_2$ -type).

2.4.1 Catalytic properties of the enzymes

Both activities were highly CoA-dependent and no oxidation or decarboxylation of pyruvate was catalyzed when CoA was omitted from the assay mixture. To see if other chemicals with structural similarities to CoA can be substituted for this cofactor, while preserving the enzyme activity, PDC assays were carried out by substituting CoA with different candidate chemicals including adenosine triphosphate (ATP), adenosine monophosphate (AMP), pantothenic acid, combination of ATP and pantothenic acid, and combination of ADP and pantothenic acid, all of which were at a final concentration of 0.1 mM. The complete POR assay containing coenzyme A was used as positive control. No pyruvate oxidation or decarboxylation was catalyzed with any of the above mentioned compounds, indicating that they could not replace CoA in the POR or PDC assays. Desulfo-CoA a known coenzyme A analog was able to replace CoA in the non-oxidative decarboxylation of pyruvate for both enzymes from *T. guaymasensis* and *P. furiosus*.

Enzyme kinetic parameters were calculated from the non-linear regression of Michaelis-Menten plots (**Table 2-6**). When necessary, the bifunctional POR/PDC enzyme from *P. furiosus* (Blamey and Adams 1993; Ma *et al.* 1997) was used as control or for comparison. Both the oxidation and decarboxylation reactions displayed a typical Michaelis-Menten progress curve for pyruvate, CoA, and the artificial electron acceptor methyl viologen (MV).

Table 2-6. Kinetic parameters of POR and PDC of *T. guaymasensis* and *P. furiosus*

Source	activity	Pyruvate ^a		CoA ^b		Specific activity ^c
		Apparent K_m (mM)	Apparent V_{max} (Umg ⁻¹)	Apparent K_m (mM)	Apparent V_{max} (Umg ⁻¹)	
<i>T. guaymasensis</i>	POR	0.53±0.03	18±0.23	69±10	21.8±0.8	20.2±1.8
	PDC	0.25±0.05	3.8±0.14	12.3±1.8	3.3±0.09	3.8±0.22
<i>P. furiosus</i>	POR ^d	0.46	23.6	110	39.9	22.0
	PDC ^e	1.1	4.3±0.3	0.11	4.3±0.3	4.3±0.3

^a For POR measured at 0.1 mM CoA, 1 mM MV, 0.4 mM TPP, and for PDC at 1mM CoA, 0.1mM TPP

^b For POR measured at 5 mM pyruvate, 1 mM MV, 0.4 mM TPP, and for PDC at 10mM pyruvate, 0.1mM TPP

^c Expressed as micromoles of pyruvate oxidized per min per milligram of enzyme

^d Values reported by Blamey *et al.* (1993) measured using EPPS (50 mM, pH 8.4) at 80°C

^e Values reported by Ma *et al.* (1997) measured using CAPS (50 mM, pH 10.2) at 80°C

The effect of pH on both oxidation and decarboxylation reactions was determined using a set of 100 mM buffers (pH 6.0 to 11.0). TgPOR showed a significant (more than 75%) activity in a relatively wide pH range from 7.5 to 10, with the highest at pH 8.4 (**Figure 2-9A**). The optimal pH for non-oxidative decarboxylation of pyruvate (PDC activity) displayed a relatively sharp optimum at pH 9.5 (**Figure 2-9B**), indicating the optimal pH for the PDC activity was higher than that of the POR activity.

Both oxidative and non-oxidative decarboxylation reactions were oxygen sensitive. The time required for a 50% loss of POR activity ($t_{1/2}$) of the purified enzyme [1.3 mgml⁻¹ in 50 mM Tris-HCl (pH7.8) containing 2 mM SDT and 2 mM DTT] was about 40 min at 4°C (**Figure 2-10A**). The time required for the PDC activity [0.8 mgml⁻¹ in 50 mM Tris-HCl (pH7.8) containing 2 mM SDT and 2 mM DTT) was approximately 30 min (**Figure 2-10B**). Ideally the sensitivity of both activities should have determined on the same batch of the enzyme; however, due to technical difficulties (different assay procedures, preparations ...etc.), it was not possible to determine the oxygen sensitivity on the same batch of the enzymes. Therefore, the differences in the time might be simply reflective of the different contents for the reducing agents (SDT/DTT) in the enzyme preparations.

The optimal temperature for both POR and PDC activities were determined by conducting corresponding assays at different temperatures. The reaction rates of both POR and PDC reactions increased along with the increasing assay temperature. The optimal temperature for POR activity seems to be above 95°C (**Figure 2-11**). In the case of the PDC activity though, the reaction rate increased constantly with increasing the reaction temperature, starting at 50°C and all the way up to 85°C. PDC activity decreased at assay temperatures above 85°C (**Figure 2-11**).

The the bifunctional POR/PDC from *T. guaymasensis* was able to use 2-ketoisovalerate as substrate for both oxidative and non-oxidative decarboxylation reactions, although with a lower rate. The rates of oxidative and non-oxidative decarboxylation of 2-ketoisovalerate were 32% (specific activities of 6.5 Umg⁻¹) and 44% (specific activity of 1.7 Umg⁻¹) compared to that of pyruvate, respectively. The enzyme purified from *P. furiosus* was also examined for its ability of using 2-ketoisovalerate; however, it was unable to use it as substrate for oxidative and non-oxidative reactions.

The results of the PDC assay on the commercially purchased porcine PDH indicated the inability of the enzyme for production of acetaldehyde. There were some residual amounts of acetaldehyde detected in each vial; however, this residual activity was lower than the amount detected in the negative controls, which contained no enzyme and/or no CoA. These trace amounts of acetaldehyde can be attributed to the non-enzymatic decarboxylation of pyruvate in the presence of reducing agents, which was reported previously (Constantopoulos and Barranger 1984).

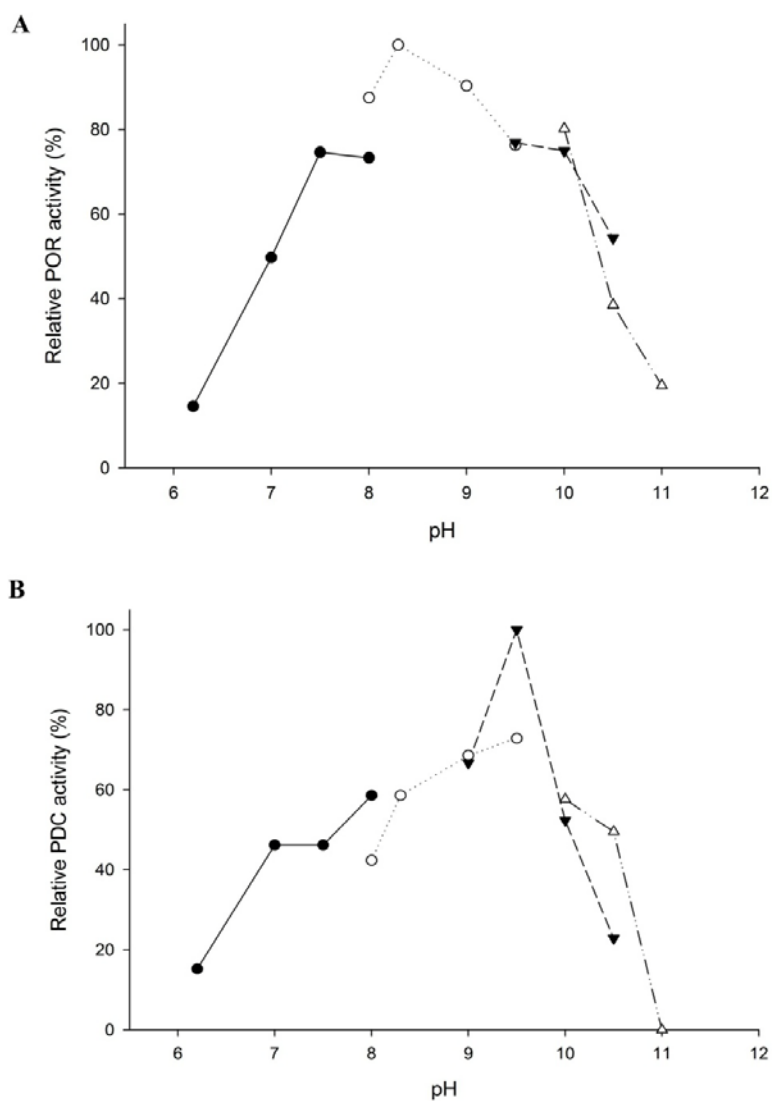


Figure 2-9. pH dependency of POR (A) and PDC (B) activities of the enzyme from *T. guaymasensis*

The activities of POR (A) and PDC (B) were measured as described previously (sections 2.3.11 and 2.3.12) under strictly anaerobic conditions and at 80°C. The relative activities of 100% equals to highest measured specific activities (17.4 U_{mg}⁻¹ and 2.6 U_{mg}⁻¹ for POR and PDC, respectively). The POR assay mixtures contained 100 mM buffers at different pHs, 1 mM magnesium chloride, 5 mM sodium pyruvate, 0.4 mM thiamine pyrophosphate (TPP), and 0.1 mM CoA. The PDC assay mixture contained 100 mM buffers at different pHs, 1 mM magnesium chloride, 10 mM sodium pyruvate, 0.1 mM thiamine pyrophosphate (TPP), and 1 mM CoA. The filled circles represent the reactions with sodium phosphate buffers (pH 6.2, 7.0, 7.5, and 8.0); the open circles represent the reactions with EPPS buffer (pH 8.0, 8.4, 9.0, and 9.5); the filled triangles represent glycine buffer (pH 9.5 and 10); and open triangles represent the CAPS buffer (pH 10.5 and 11.0).

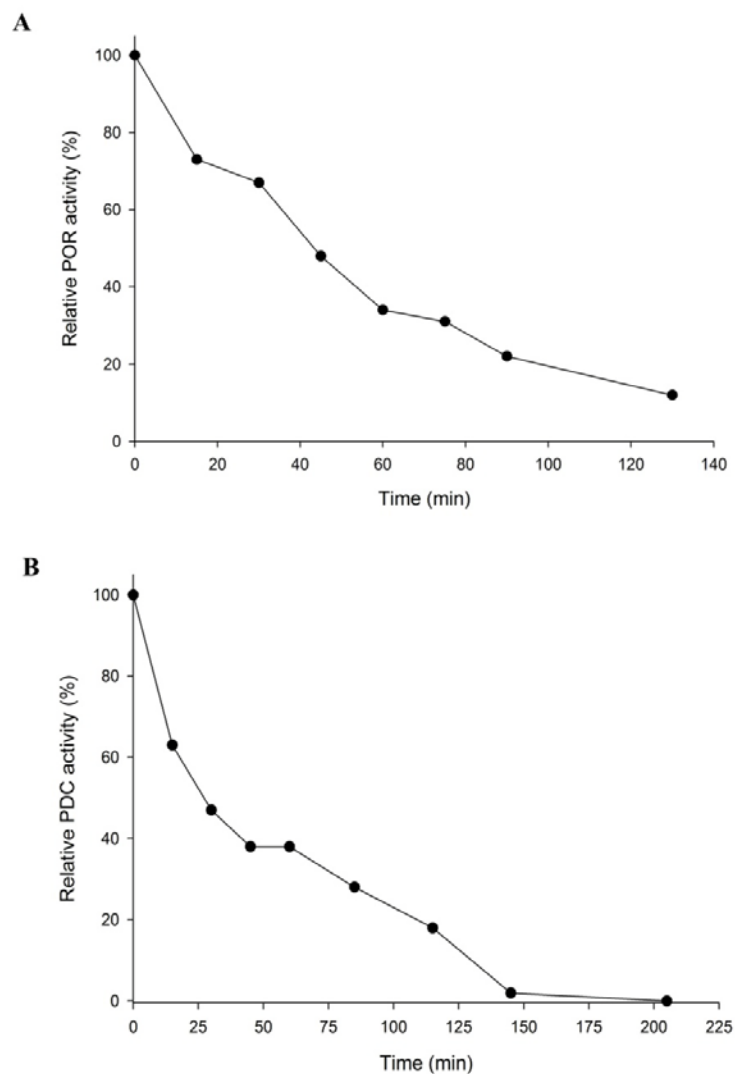


Figure 2-10. Oxygen sensitivity of POR and PDC activities of *T. guaymasensis*

The activities of pyruvate oxidation (**A**) and decarboxylation (**B**) reactions were measured at different time points in enzyme aliquots exposed to air while stirring. The enzyme assays were conducted as described previously (section 2.3.11 and 2.3.12) under strictly anaerobic conditions. The POR assay mixtures (2 ml) contained 100 mM EPPS buffer, pH 8.4, 1 mM magnesium chloride, 5 mM sodium pyruvate, 0.4 mM thiamine pyrophosphate (TPP), and 0.1 mM CoA. The assay mixture for the PDC assay (1 ml) contained 100 mM glycine buffer, pH 9.5, 1 mM magnesium chloride, 10 mM sodium pyruvate, 0.1 mM thiamine pyrophosphate (TPP), and 1 mM CoA. The relative activities of 100% equals to highest measured specific activity at time zero with no exposure to air (16.2 U mg^{-1} and 2.2 U mg^{-1} for POR and PDC activities, respectively).

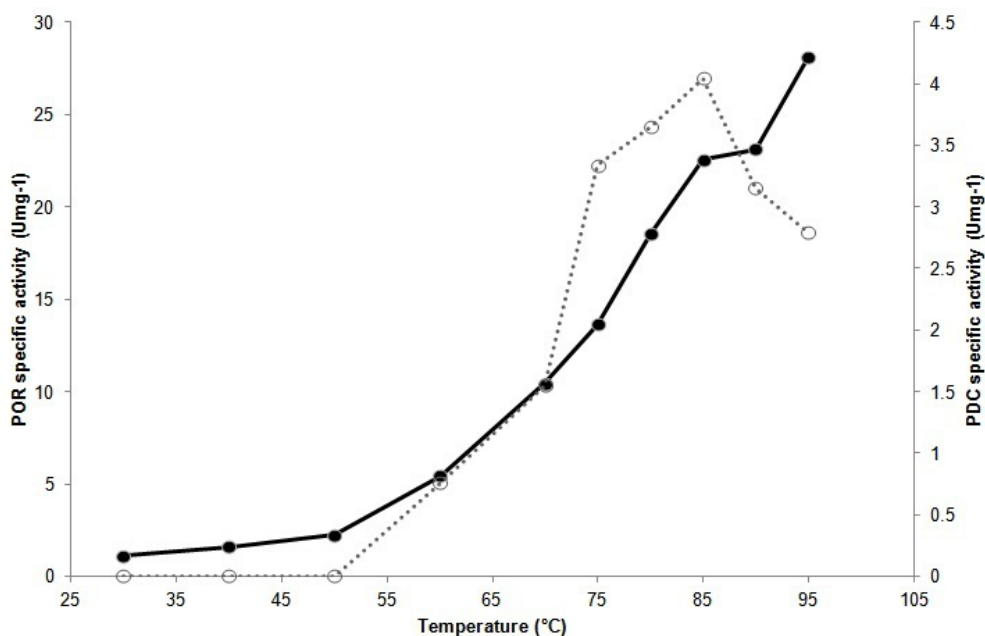


Figure 2-11. Temperature dependence of *T. guaymasensis* POR and PDC activities

The POR and PDC assays were conducted as described in the material and methods (section 2.3.11 and 2.3.12, respectively) under standard assay conditions except the temperatures were varied. The vials containing the standard assay mixture were pre-incubated at each temperature for 4min. The assay reactions were started by adding the enzyme. The POR assay mixtures (2 ml) contained 100 mM EPPS buffer, pH 8.4, 1 mM magnesium chloride, 5 mM sodium pyruvate, 0.4 mM thiamine pyrophosphate (TPP), and 0.1 mM coenzyme A. The PDC assay mixture (1 ml) contained 100 mM glycine buffer, pH 9.5, 1 mM magnesium chloride, 10 mM sodium pyruvate, 0.1 mM thiamine pyrophosphate (TPP), and 1 mM coenzyme A. The filled circles indicate the POR activity and the open circles are indicative of PDC activity. The filled circles represent the POR and the open circles represent the PDC activity.

2.5 Discussion

The absence of the commonly-known pyruvate decarboxylase (PDC) is a perplexing feature of hyperthermophiles, especially considering that some of them have the ability to carry out fermentation at high temperatures and produce ethanol as an end-product (Karakashev *et al.* 2007). Many of these hyperthermophiles can grow on peptides and/or sugars *via* a fermentative-type metabolism (Adams *et al.* 1992; Adams 1993; Kelly and Adams 1994; Dworkin *et al.* 2006a). As expected, several alcohol dehydrogenases are found to be present in different ethanogenic hyper/thermophiles, including, *T. hypogea* (Ying *et al.* 2007), *Thermococcus* strain species ES1 (Ying *et al.* 2009), *T. guaymasensis* (Ying and Ma 2011) and *T. onnurineus* (Moon *et al.* 2012). PDC is widely distributed in plants and fungi, but limited in bacteria. The enzyme is not detected in animals (Konig 1998). The only PDC activity that has been reported from hyperthermophiles is a bifunctional POR/PDC isolated from the heterotrophic hyperthermophilic archaeon *P. furiosus* (Ma *et al.* 1995; Ma *et al.* 1997). The current study provided evidence confirming that POR of *T. guaymasensis* was also able to catalyze the non-oxidative decarboxylation of pyruvate to produce acetaldehyde.

As in other studies pertaining to hyperthermophilic proteins, obtaining sufficient amounts of cells for enzyme purification and characterization is a major challenge. Factors such as limited availability of information on physiology, generation of large amounts of hydrogen sulfide and other gases, low cell yields, and growth under anaerobic conditions, are considered to be potential difficulties in studying such organisms and their enzyme (Verhagen *et al.* 2001). Some heterotrophic hyperthermophiles (mostly Thermococcales and Thermotogales) can grow without addition of elemental sulfur to the medium, which makes them appropriate candidates for purification and characterization of their native thermostable proteins. Low biomass yield of *T. guaymasensis* (0.6 ± 0.17 g cell paste per liter of culture), made the growth of sufficient biomass an immense challenge.

Nucleotide sequence of *por/vor* cluster in *T. guaymasensis* indicated that POR or VOR was encoded by four genes, with one of them (*por/vorG*) shared between the two enzymes (**Figure 2-2**). These findings were in accordance with the gene organization and enzyme structure of other archaeal hyperthermophiles studied so far (Kletzin and Adams 1996; Ragsdale 2003). Bacterial hyperthermophiles, including *T. hypogea* and *T. maritima* (Chapter 3), do not have the VOR and only the four subunits of POR were present that have similar gene organization to that of their archaeal

counterparts (*porG*, *porD*, *porA*, and *porB*). Amino acid sequences of TgPOR subunits were remarkably similar to the corresponding subunits of other 2-keto acid oxidoreductases, especially to PORs from various hyperthermophiles (**Figure 2-5**).

The purification scheme of TgPOR (**Table 2-5**) was similar to previously published reports (Blamey and Adams 1993; Schut *et al.* 2001a) on purification of the similar enzyme from a closely related archaeon *P. furiosus* (**Table 2-4**). The purified enzyme of *T. guaymasensis* was eluted out as a single peak from a Superdex-200 gel-filtration column, indicating the purity of the protein preparation. When it was loaded on SDS-PAGE, four subunits with apparent molecular weights of 46, 35, 26, and 12 kDa were revealed (**Figure 2-6**) which was in accordance with genetics information acquired from the nucleotide sequencing (**Figure 2-2**), and also the subunit composition of similar enzymes from various organisms (**Table 2-7**). Both enzymes purified from *T. guaymasensis* and *P. furiosus* were heterotetrameric proteins, with native molecular weights of approximately 260 kDa, which was indicative of the native protein being a dimer of tetramers ($\alpha_2\beta_2\gamma_2\delta_2$ structure).

POR and PDC activities were absolutely dependent on CoA, and no activity was observed when it was omitted from the assay mixture. No other components (ATP, ADP, pantothenic acid, and different combinations of these could be used to substitute for CoA, indicating an essential role of the cofactor in the catalytic mechanisms of both reactions. It was shown that desulfo-CoA was completely inhibitory for the oxidation (POR) reaction, but not for the decarboxylation (PDC) reaction. When desulfo-CoA was substituted for CoA in the PDC assay, the enzymes from *P. furiosus* and *T. guaymasensis* exhibited approximately 75% and 80% of the complete activities with CoA, respectively. The ability of the PDC activity to utilize desulfo-CoA instead of CoA as cofactor supported the previously suggested (Ma *et al.* 1997) structural role of CoA rather than a catalytic role in the pyruvate decarboxylation reaction.

Like other archaeal PORs characterized so far, including *P. furiosus* (Blamey and Adams 1993; Schut *et al.* 2001a) and *A. fulgidus* (Kunow *et al.* 1995), addition of TPP to the standard assay mixture had no effect on the rate of pyruvate oxidation or decarboxylation when the enzymes were assayed in the crude extracts or CFEs of *T. guaymasensis*. Additional TPP also had no impact on the PDC activity of the bifunctional enzyme from *P. furiosus* (Ma *et al.* 1997 and this study). However, incorporation of TPP to the assay mixtures led to a 20-25% stimulation of both oxidation and

Table 2-7. Structure and activities of PORs and VORs from various organisms^a

Organism	Enzyme ^a	Subunit					Specific activity (U/mg) ^b	Reference
		Subunit α (kDa)	Subunit β (kDa)	Subunit γ (kDa)	Subunit δ (kDa)	Subunit ϵ (kDa)		
<i>Archaeoglobus fulgidus</i>	POR	45	33	25	13	-	74	Kunow <i>et al.</i> 1995
<i>Desulfovibrio africanus</i>	POR	45	33	24	13	-	14	Pieulle <i>et al.</i> 1997
<i>Helicobacter pylori</i>	POR	47	36	24	14	-	2.5	Hughes <i>et al.</i> 1995
<i>Hydrogenobacter thermophilus</i>	POR	46	31.5	29	24.5	-	3.5	Yoon <i>et al.</i> 1997
<i>Methanococcus maripaludis</i>	POR	47	33	25	13	21.5	79	Lin <i>et al.</i> 2003
<i>Methanosarcina barkeri</i>	POR	48	30	25	15	-	25	Bock <i>et al.</i> 1997
<i>Pyrococcus furiosus</i>	POR	45 44	31 36	24 20	13 12	-	20	Blamey and Adams 1994 Blamey and Adams 1993; Menon <i>et al.</i> 1998
<i>Thermococcus litoralis</i>	VOR	47	34	23	13	-	46	Heider <i>et al.</i> 1996
<i>Thermococcus litoralis</i>	KGOR	43	29	23	10	-	22.3	Mai and Adams 1996a
<i>Thermococcus guaymasensis</i>	POR	46	35	26	12	-	20.2	this study
<i>Thermococcus profundus</i>	VOR	45	31	22	13	-	128	Ozawa <i>et al.</i> 2005
<i>Thermotoga hypogea</i>	POR	44	39	25	13	-	96.7	this study
<i>Thermotoga maritima</i>	POR	45 42	37 36	22 29	12 14	-	87.4 90	Blamey and Adams 1994 this study

^a POR, Pyruvate ferredoxin oxidoreductase; VOR, 2-ketoisovalerate ferredoxin oxidoreductase; KGOR, 2-ketoglutarate ferredoxin oxidoreductase

^b Expressed as micromoles of pyruvate oxidized per min per milligram of enzyme

decarboxylation reactions catalyzed by the purified enzyme from *T. guaymasensis*. This observation was presumably due to a partial dissociation of the TPP from the enzyme during the purification steps which is a common feature of bacterial PORs but exceptional within archaeal PORs. Considering that even in the absence of additional TPP the enzyme exhibited a significant portion of its POR and PDC activities, the apparent kinetic parameters for TPP were not determined.

The pyruvate oxidation reaction displayed an activity optimum at pH 8.4, which was in accordance with the previous findings on the closely related archaeon *P. furiosus* (Blamey and Adams 1993) as well as the hyperthermophilic bacteria *T. hypogea* and *T. maritima* (Chapter 3). However, PDC activity, displayed an optimal pH of 9.5 (**Figure 2-9**), which was close to the value reported for the similar bifunctional enzyme from *P. furiosus*. Bifunctional POR/PDC enzymes of Thermotogales showed optimal pH for both oxidation and decarboxylation reactions at pH 8.4 (Chapter 3). The physiological significances of these differences are not clear. The pH optima for both groups (bacterial and archaeal bifunctional PDCs) were higher than that those of the commonly-known bacterial and fungal PDCs, which (as summarized in **Table 2-8**) work more efficiently at slightly acidic pHs (Raj *et al.* 2001; Talarico *et al.* 2001; Raj *et al.* 2002).

Optimal temperature for the POR activity of TgPOR was determined to be above 95°C (**Figure 2-11**), which was similar to those of *P. furiosus* and *T. maritima* with growth temperature optima of about 100°C and 80°C, respectively (Blamey and Adams 1993; Blamey and Adams 1994). However, PDC activity of the enzyme had an optimal temperature of 85°C (**Figure 2-11**). This was not in accordance with that of *T. maritima* and *P. furiosus*, which both have their temperature optima above 95°C. The difference between the pH optima for oxidation and decarboxylation activities was also observed for the bacterial POR/PDC isolated from *T. hypogea* (Chapter 3). As in many other studies, the temperature ranges higher than 95°C was not investigated due to instability of the assay components at such high temperatures as well as the technical difficulties of conducting assays at such higher temperatures. The difference between the minimum limit of the decarboxylase reaction detection for the POR and PDC activities is presumably reflective of the lower sensitivity limits of each corresponding assay.

Table 2-8. Properties of commonly-known PDCs characterized from various organisms

Source	K_m for pyruvate (mM)	Pyruvate kinetics ^a	Specific activity ^b	Thermal stability ^c	Optimal Temp.	Optimal pH	Enzyme	reference
<i>Zymobacter palmae</i>	0.24	N	130 66	60°C (100%)	55°C	5.5-6.0	Recombinant Native	Raj <i>et al.</i> 2002
<i>Sarcina ventriculi</i>	13.0	S	103	N/A	42°C	6.3-7.6	Native	Lowe and Zeikus 1992
<i>Sarcina ventriculi</i>	2.8	S	67	42°C (100%)	42°C	6.3-7.6	Recombinant	Talarico <i>et al.</i> 2001; Raj <i>et al.</i> 2002
<i>Acetobacter pasteurianus</i>	0.39	N	71	60°C (65%)	65°C	5.0-5.5	Native	Raj <i>et al.</i> 2001; Raj <i>et al.</i> 2002
<i>Zymomonas mobilis</i>	0.3	N	160 ^c	60°C (65%)	60°C	6.0	Recombinant Native	Hoppner and Doelle 1983; Neale <i>et al.</i> 1987
<i>Saccharomyces cerevisiae</i>	3.75	S	40	50°C	43°C	5.8-6.0	Native	Liu <i>et al.</i> 2001a; Gocke <i>et al.</i> 2009a
<i>Zea mays</i>	0.9	S	96	NR	NR	5.8-6.0	Native	Lee and Langston-Unkefer 1985
<i>Torulopsis glabrata</i>	0.8	S	40	NR	30°C	6.0-6.5	Recombinant Native	Wang <i>et al.</i> 2004

^a N, normal Michaelis-Menten kinetics; S, sigmoidal kinetics; NR, not reported

^b One unit of enzyme activity was defined as the amount of enzyme that generates 1 μ mol of acetaldehyde per min.

^c Enzymes were incubated at different temperatures ranging from 30-70°C and residual activity measured at 25°C, as described in (Raj *et al.* 2002). When provided, the values in parentheses show the residual relative activity.

^d Determined at 60°C.

Both oxidation and decarboxylation reactions catalyzed by the bifunctional enzyme isolated from *T. guaymasensis* were highly oxygen sensitive, that is a typical characteristic of the majority of PORs isolated and characterized and in contrary to the commonly-known PDCs. Upon exposure to air, the bifunctional POR/PDC of *T. guaymasensis* lost 50% of its POR activity within 40 min. The time taken to lose 50% of the PDC activity of the same enzyme was estimated to be about 30 min (**Figure 2-10**).

Interestingly, only one type of KOR enzyme (*i.e.* POR) is present in bacterial hyper/thermophiles. PORs are purified and characterized from the hyperthermophilic bacterium *T. maritima* and the extremely thermophilic bacterium *T. hypogea*, which have specific activities of approximately $90.8 \pm 11 \text{ U mg}^{-1}$ and $96.7 \pm 15.1 \text{ U mg}^{-1}$, respectively (Blamey and Adams 1994 and this study). The physiological significance of having single type of KOR is not understood.

KORs including POR, VOR, KGOR, and IOR play central roles in amino acid degradation pathways of majority of sulfur-dependent hyperthermophilic archaea (Schönheit and Schafer 1995). Other than POR, which is involved in the metabolism of both sugars and amino acids, other enzymes of the KOR family are found only in hyper/thermophilic heterotrophic and methanogenic archaea (Schäfer *et al.* 1993; Heider *et al.* 1996; Mai and Adams 1996a; Ozawa *et al.* 2005). When grown on peptides, 2-keto acids produced from transamination of different amino acids are oxidized by the corresponding KORs. The 2-ketoglutarate (KGOR), aromatic amino acids (IOR), the keto acids derived from the branched chain amino acids (VOR) and pyruvate (POR) are oxidized to the corresponding aryl- or acyl-CoA compounds, with concomitant release of CO₂, and finally to organic acids. The final step in archaea is catalyzed by the enzymes acetyl-coenzyme A synthase I and II (ACS) coupling energy conservation in the form of ATP (Schönheit and Schafer 1995; Mai and Adams 1996b; Schut *et al.* 2001a; Zivanovic *et al.* 2009). Generally, KORs do not have a broad substrate range and act very specifically (Schut *et al.* 2001a) although some levels of overlapping substrate specificity exist, particularly between the Thermococcales POR and VOR (Heider *et al.* 1996; Ozawa *et al.* 2005).

The microarray studies show a constitutive transcription of KORs, including the *por* and *vor*, when *P. furiosus* is grown on peptides (Schut *et al.* 2001b; Schut *et al.* 2003). Even when the organism is cultivated on maltose, the transcription of the genes encoding four POR subunits displays no major change (unlike other KOR genes, which show decreased transcription), which is most likely due to the role of POR in the metabolism of pyruvate produced from glycolysis (Schut *et al.* 2001a; Schut *et*

al. 2003). This is also in accordance with the gene organization of the *por/vor* operon determined in *T. guaymasensis*, in which three transcription units were identified: the *por/vorG*, *vorDAB*, and *porDAB*. Then for each expression of each enzyme (POR or VOR), two of the transcription units would be transcribed and eventually translated. Transcription levels of the POR subunit encoding genes is not affected during the early (1-2 h) and late (5 h) cold-shock (72°C) response, which is consistent with no change in POR activity (Weinberg *et al.* 2005).

It is shown that within Thermococcales, *P. furiosus* (Kengen *et al.* 1994), *Thermococcus* species strain ES1 (Ma *et al.* 1995), *T. guaymasensis* (Ying and Ma 2011), and *T. onnurineus* (Moon *et al.* 2012) are capable of producing ethanol. Thermococcales have a modified Embden-Meyerhof pathway for glycolysis using various novel enzymes including an ADP-dependent glucokinase and glyceraldehyde-3-phosphate ferredoxin oxidoreductase (Verhees *et al.* 2003; Sakuraba 2004). Different alcohol dehydrogenases with possible roles in catalysis of aldehyde reduction and alcohol production were characterized from these organisms (Ma *et al.* 1994; Li and Stevenson 1997; Antoine *et al.* 1999; Ying and Ma 2011). ADH isolated and characterized from *T. guaymasensis* is suggested to be involved in the NADP⁺ regeneration by concomitant production of acetoin and ethanol (Ying and Ma 2011). Nevertheless, no commonly-known acetoin-producing enzyme is characterized in members of the genus *Thermococcus*. The enzymes involved in generation of acetoin in various organisms (including bacteria and plants) are anabolic acetohydroxyacid synthases (AHASs). Survey of genomes of the members of the genus *Thermococcus* indicated the absence of AHAS-encoding gene homologs from these microorganisms (Chapter 4). Intriguingly, acetoin can be detected in spent cultures of *T. guaymasensis* (Ying and Ma 2011). In current study, an AHAS activity was detected in CFE of *T. guaymasensis* and *T. kodakaraensis* (Chapter 4). Purification and characterization of enzyme catalyzing this activity would be highly valuable in determining how acetoin would be produced in hyperthermophiles.

The proposed pathway for producing ethanol in *T. guaymasensis* is presented in **Figure 2-12**. There are two possible pathways for production of acetaldehyde, which are a) the consecutive function of POR and/or pyruvate formate lyase (PFL) followed by AcDH (CoA-dependent) and b) the direct production of acetaldehyde from pyruvate by the enzyme PDC (**Figure 2-12**). Genes encoding AcDH (CoA-acetylating) were absent from the released genome sequences of hyperthermophiles (this study).

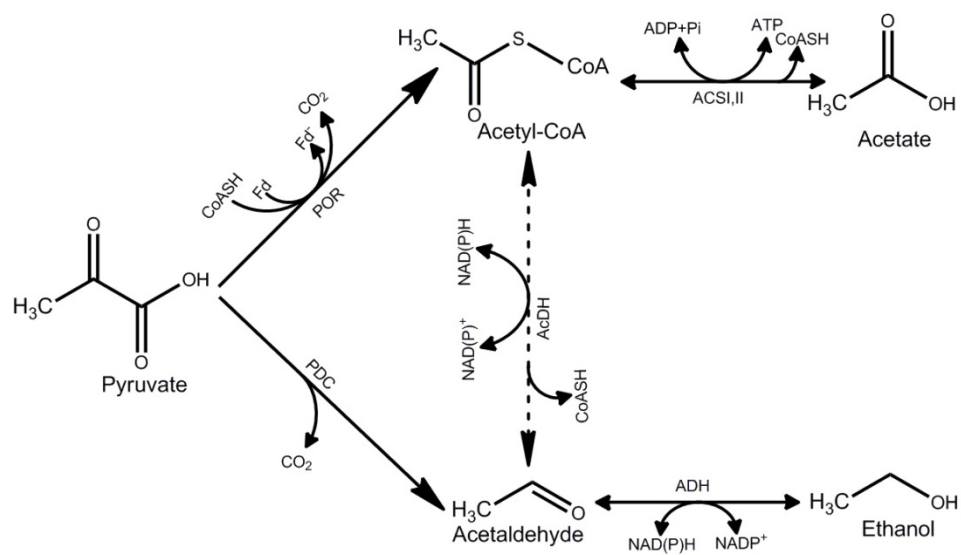


Figure 2-12. Schematic pathway of ethanol production in *T. guaymasensis*

AcDH; acetaldehyde dehydrogenase; ACS, acetyl-CoA synthase I and II both types are involved in the ADP-dependent formation of acetate with different substrate specificities); ADH; alcohol dehydrogenase; PDC, pyruvate decarboxylase; POR, pyruvate ferredoxin oxidoreductase. The dashed arrow indicates the speculated pathway, while the solid arrows indicate the steps confirmed by enzyme assays.

CFEs of different hyperthermophilic bacteria and archaea indeed displayed no CoA-dependent AcDH activity when examined under different assay conditions (this study). PDC activity catalyzed by the bifunctional POR/PDC that was characterized here would complete our understanding of ethanol production in Thermococcales. Considering the very high activity of the zinc-containing ADH characterized from *T. guaymasensis* (223 U_{mg}⁻¹ in the aldehyde/ketone reduction direction) and relatively low PDC activity of the enzyme characterized here (3.8 U_{mg}⁻¹), it appears that PDC activity is the limiting factor and the reason for low ethanol yield of hyperthermophiles. Although the PDC reaction of archaeal hyperthermophiles display higher specific activities compared to bacterial hyperthermophiles (Chapter 3), the extents of the PDC activities are residual compared to the activities of most commonly-known PDCs from yeasts and bacteria (**Table 2-8**). In hyperthermophiles, pyruvate is most likely catabolized by POR reaction, leading to production of acetyl-CoA, which is either used for biosynthesis purposes or converted to acetate by acetyl-CoA synthase due to the absence of CoA-dependent AcDH activity (Jenney and Adams 2008). The production of acetate is coupled to energy conservation in the form of ATP (**Figure 2-12**).

Surprisingly, despite having specialized enzymes for oxidation of different 2-keto acids such as 2-ketoisovalerate (VOR, 2-ketoisovalerate ferredoxin oxidoreductase), the purified POR from *T. guaymasensis* was able to catalyze the oxidative and non-oxidative decarboxylation of 2-ketoisovalerate. However, there is always possibility of residual contamination of purified enzyme with the closely related VOR. Due to their very high sequence and size similarities it is possible that the two activities were not completely separated from each other during different chromatography steps. Such residual contamination was not detected by loading the purified POR on size-exclusion chromatography column.

The PORs isolated and characterized from *P. furiosus* (Blamey and Adams 1993), *A. fulgidus* (Kunow *et al.* 1995), and *Methanosarcina barkeri* (Bock *et al.* 1996) cannot use 2-oxoglutarate, phenyl pyruvate, indole pyruvate, and hydroxy pyruvate as a substrate for oxidation reaction. PfPOR was also shown to be unable to use 2-ketoisovalerate as substrate for oxidative decarboxylation (Schut *et al.* 2001a and this study) or non-oxidative decarboxylation (this study). Interestingly, VOR isolated from the hyperthermophilic archaeon *Thermococcus litoralis*, can use 2-ketoisovalerate as the best substrate while pyruvate is used as a substrate with a lower (8.5%) activity (Schut *et al.* 2001a).

Catalytic mechanisms of oxidative decarboxylation of pyruvate by PORs are studied in detail, and it is well known that POR uses radical chemistry for the catalysis, which is a distinctive characteristic of PORs within the family of the TPP-dependent enzymes (Ragsdale 2003; Buckel and Golding 2006). Using radical chemistry is also the reason for the extraordinary oxygen sensitivity of almost all of PORs studied from different organisms, and the only exception so far, are the enzymes characterized from the sulfate-reducing bacterium *D. africanus* (Pieulle *et al.* 1995; Pieulle *et al.* 1999a; Pieulle *et al.* 1999b) and the halophilic archaeon *H. salinarium* (Kerscher and Oesterhelt 1981a; Kerscher and Oesterhelt 1981b; Plaga *et al.* 1992). The free-radical chemistry is absent from the catalytic mechanism of the analogous aerobic enzyme pyruvate dehydrogenase (PDH), which uses lipoic acid and flavin chemistry to catalyze the reaction of hydroxyethyl-TPP (HETPP) and CoA (Witzmann and Bisswanger 1998; Tittmann 2009).

Since PDC activity of bifunctional enzymes characterized from the hyperthermophiles is highly CoA-dependent and oxygen-sensitive (Ma *et al.* 1997 and this study), it is hypothesized that the reaction is using a modified version of the free-radical chemistry for the catalysis (Ma *et al.* 1997 and this study), which is different from that of the commonly-known PDCs. In commonly-known PDCs, acetaldehyde is released following protonation of the HETPP intermediate, a reaction that is not sensitive to oxygen, nor is CoA-dependent (Kluger 1987; Arjunan *et al.* 1996; Kluger and Tittmann 2008). Ma *et al.* (1997) proposed a “switch mechanism” for the control of acetaldehyde production by the bifunctional POR/PDC isolated from *P. furiosus*, a mechanism that seems to be expandable to the newly characterized activities from *T. guaymasensis* (this study) and the isolated bacterial counterparts from *T. hypogea* and *T. maritima* (Chapter 3). In the proposed mechanism, TPP activation follows the steps similar to other pyruvate utilizing TPP-dependent enzymes, especially the typical example of this group, PDC. Protonation of the N1 atom of the pyrimidine ring by the highly conserved glutamine residue results in the induction a 1', 4' -iminotautomer. Due to the common “V-conformation”, the 4-imino group is located in the proximity of the C₂ catalytic centre of the AHAS, which results in de-protonation of the C₂ atom. The proton abstraction step gives rise to formation of a highly reactive ylide (Kern *et al.* 1997; Lie *et al.* 2005; McCourt and Duggleby 2006). The nucleophilic attack of ylide on the carbonyl group of pyruvate, results in production of 2-(2-lactyl)-TPP (also known as L-TPP or L-TDP). Binding of CoA at this step is hypothesized to result in decarboxylation of L-TPP and production of the resonating carbanion/enamine forms of 2-(1-hydroxyethyl)-TPP (HETPP), which is a central and highly reactive intermediate state common in

TPP-dependent enzymes that act on pyruvate (Candy and Duggleby 1998; Tittmann *et al.* 2003; Kluger and Tittmann 2008). This step is followed by the release of acetaldehyde and possibly CoA and regeneration of TPP (Ma *et al.* 1997). The decarboxylation reaction is suggested to be independent of the redox state of the enzyme; however, since the oxidation of HETPP takes place in two sequential one-electron steps *via* a chain of [4Fe-4S] clusters, then the POR activity of the enzyme is dependent on the redox state of the enzyme, which is in fact reliant on the redox state of the [4Fe-4S] clusters. The latter is determined by the overall redox potential of the cytoplasm that is, in turn, dependent on the physiological growth conditions and stages (Ma *et al.* 1997).

POR has many general features of moonlighting enzymes, which are generally defined as multifunctional proteins that can perform multiple -often unrelated- functions (Piatigorsky *et al.* 1988; Jeffery 1999); it is a highly conserved ancient enzyme (Kletzin and Adams 1996; Zhang *et al.* 1996; Ragsdale 2003) which is involved in the sugar metabolism and constitutively expressed (Schut *et al.* 2003) under different environmental and metabolic conditions (Jeffery 2003; Pomel *et al.* 2008; Huberts and van der Klei 2010). Besides POR/PDC functions, POR is shown to be involved in other metabolic (catalytic) and structural (non-catalytic) processes. For instance, in some sulfate-reducing bacteria it is shown that POR can function as a hydrogenase in the absence of external electron carriers (Menon and Ragsdale 1996). In the pathogenic protozoan, *Trichomonas vaginalis* it is shown that there is a surface-associated version of POR, which although lacking the POR activity, but is involved in the trichomonal cell-surface binding to host cells (Meza-Cervantez *et al.* 2011). In the Gram-positive anaerobic pathogenic bacterium *Clostridium perfringens* and the pathogenic protist *Entamoeba histolytica*, the enzyme is shown to be involved in the pathogenesis, serving as a virulence factor (Thammapalerd *et al.* 1996; Kulkarni *et al.* 2007; Kulkarni *et al.* 2008; Lee *et al.* 2011).

An intriguing feature of the sequenced part of the *T. guaymasensis* genome was a homologous gene encoding a carbon monoxide dehydrogenase-associated protein located downstream of *porB* encoding sequence (**Figure 2-2**). The protein is an accessory nickel-insertion protein that is involved in the maturation of the metalloenzyme carbon monoxide dehydrogenase (CODH, EC 1.2.99.2). The enzyme CODH is a metalloenzyme involved in the reversible conversion of carbon monoxide (CO) to carbon dioxide (CO₂) and is a prerequisite for the autotrophic life.

Proteins with high levels of similarity (more than 85% amino acid homology to the retrieved sequence) to the identified accessory protein sequence in *T. guaymasensis* could be found in the genomes of *Thermococcus* sp. strain AM4 (TAM4_1296) and *Thermococcus gammatolerans* (TGAM_0231). The enzyme CODH is not common within the members of the order Thermococcales and the genes annotated as CODH and found only in genomes of *T. onnurineus* (TON_1019), *T. gammatolerans* (TGAM_0824), *T. barophilus* (TERMP_01183), and *Thermococcus* sp. strain AM4 (TAM4_0582). Accordingly, capability of lithotrophic growth under a carbon monoxide atmosphere was shown for *Thermococcus* sp. strain AM4 (Sokolova *et al.* 2004; Oelgeschläger and Rother 2008; Oger *et al.* 2011) and *T. onnurineus* (Lee *et al.* 2008; Yun *et al.* 2011; Bae *et al.* 2012). However, in the case of *T. guaymasensis*, the preliminary growth experiments using carbon monoxide as a sole carbon source were not conclusive and need to be continued.

**Chapter 3 POR/PDC bifunctional enzyme from
Thermotoga maritima and *Thermotoga hypogea***

3.1 Overview

Bifunctional pyruvate ferredoxin oxidoreductase (POR)/ pyruvate decarboxylase (PDC) enzymes from two hyper/thermophilic bacteria *Thermotoga maritima* (Tm) and *Thermotoga hypogea* (Th) were purified to apparent homogeneity using fast performance liquid chromatography (FLPC) under strictly anaerobic conditions. Both purified enzymes shared structural properties that are common to the hyperthermophilic PORs and were composed of four different subunits of approximately 45, 35, 22, and 12 kDa and native molecular masses of approximately 160 kDa suggesting a heterotetrameric native structure. The nucleotide sequences of the genes encoding the bifunctional enzyme of *T. hypogea* were determined *via* primer walking and inverse PCR (IPCR). The amino acid sequence showed similarity to other known bacterial and archaeal PORs.

Both TmPOR and ThPOR had PDC activities were highly coenzyme A-dependent because no acetyl-CoA or acetaldehyde was produced when CoA was omitted from the assay mixture. Addition of TPP to the assay mixture stimulated both activities. The purified enzymes displayed POR specific activities of $96.7 \pm 15.1 \text{ U mg}^{-1}$ (PDC specific activity $1.82 \pm 0.44 \text{ U mg}^{-1}$) and $90.8 \pm 11 \text{ U mg}^{-1}$ (PDC specific activity 1.4 ± 0.15) for *T. hypogea* and *T. maritima*, respectively. Both activities were highly oxygen sensitive with a half-life ($t_{1/2}$) of less than 15 min upon exposure to air. The optimal pH for the POR and PDC activities of the enzyme purified from both bacteria were 8.4. The optimal temperature for the POR and PDC activities of the enzyme from *T. maritima* was above 95°C , while the optimal temperatures for the POR and PDC activities of the enzyme purified from *T. hypogea* were 90°C and 80°C , respectively. The POR and PDC activities of the enzyme from *T. hypogea* were thermostable, with $t_{1/2}$ of 180 min and 130 min, respectively. The steady-state kinetics parameters were determined for both activities of each enzyme. Both of the enzymes had consistently lower apparent K_m values for pyruvate in the POR activities compared to their PDC activities. On the other hand, the apparent K_m for PDC activity was much lower compared to that of the POR activities.

The results showed that POR/PDC bifunctionality was indeed present in bacterial hyper/thermophiles. The bifunctional POR/PDC activity along with the previously reported alcohol dehydrogenases (ADHs) would be most likely involved in the alcohol fermentation pathway in bacterial hyper/thermophiles.

3.2 Introduction

The genus *Thermotoga* is comprised of a group of Gram-negative heterotrophic bacteria belonging to the order Thermotogales. Members of the order Thermotogales are generally characterized by the presence of an outer sheath-like structure surrounding the cells called “toga” (Conners *et al.* 2006; Dworkin *et al.* 2006b). They are mainly isolated from habitats with elevated temperatures, including volcanically or geothermally heated terrestrial environments. They are also typically extreme thermophiles with optimal growth temperature of 65-79°C or hyperthermophiles that can grow optimally at $\geq 80^\circ\text{C}$ (Wagner and Wiegel 2008). However, a more recent study has proposed a new subclass of the mesophilic “mesotoga” (Nesbø *et al.* 2006) with the first member of this genus cultivated (Ben Hania *et al.* 2011) and fully sequenced (Nesbø *et al.* 2012). The representatives of the genus *Thermotoga* have been investigated extensively during the last two decades, mainly for their abundance of hydrolyzing enzymes and their ability to use a wide range of substrates, in particular both simple and complex carbohydrates including, but not limited to, hexoses, pentoses, xylan, pectin, chitin, amorphous cellulose, starch, ...etc. (Bronnenmeier *et al.* 1995; Chhabra *et al.* 2003; Conners *et al.* 2005; Chou *et al.* 2008; Frock *et al.* 2012) Thermotogales are also being studied as model organisms for the study of the adaptation to high temperatures (Huber *et al.* 1986; Conners *et al.* 2006).

The growth substrates in Thermotogales (predominantly oligosaccharides or oligopeptides) are metabolized *via* the conventional Embden-Meyerhof (EMP) and Entner-Doudoroff (ED) pathways to pyruvate and the major products of fermentation are acetate, lactate, alanine, CO₂ and H₂, (Schröder *et al.* 1994; Schönheit and Schafer 1995; Selig *et al.* 1997; Conners *et al.* 2006). It is shown that some heterotrophic extreme thermophiles and hyperthermophiles including some members of the order Thermotogales, namely *Thermotoga hypogea* (Fardeau *et al.* 1997), *Thermotoga lettingae* (Balk *et al.* 2002), *Thermotoga neapolitana* (de Vrije *et al.* 2009), *Kosmotoga olearia* (DiPippo *et al.* 2009), and *Thermosipho affectus* (Podosokorskaya *et al.* 2011) are able to produce ethanol. However, the pathways and enzymes leading to the production of ethanol are not well understood. Several NADPH-dependent alcohol dehydrogenases have been isolated and characterized from different hyperthermophiles including the extremely thermophilic bacterium *T. hypogea* with kinetics data suggesting that -at least some of them- are active in the direction of aldehyde reduction and alcohol production (Hirakawa *et al.* 2004; Machielsen *et al.* 2006; Ying *et al.* 2007; Ying and Ma 2011).

Two enzyme activities are known to be able to produce acetaldehyde from pyruvate: pyruvate decarboxylase (PDC, EC 4.1.1.1), which is the enzyme that directly converts pyruvate to acetaldehyde *via* non-oxidative decarboxylation, and coenzyme A-dependent acetaldehyde dehydrogenase (AcDH, EC 1.2.1.10) that converts acetyl-coenzyme A to acetaldehyde. The presence of at least one of these two activities seem to be essential for any of the biological alcohol production pathways in which the enzyme alcohol dehydrogenase (ADH, EC 1.1.1.1) reduces the aldehydes to the corresponding alcohols.

No pyruvate decarboxylase or acetaldehyde dehydrogenase (CoA acetylating) has ever been detected from any extremely thermophilic or hyperthermophilic bacterium. In accordance with the missing activities, no *pdh* or *acd* gene homologue could be found in the fully sequenced genomes of any hyperthermophilic organism (this study). The question rises about how acetaldehyde is produced.

There is a report on a bifunctional pyruvate ferredoxin oxidoreductase/pyruvate decarboxylase of the hyperthermophilic archaeon *Pyrococcus furiosus* (Ma *et al.* 1997). Pyruvate ferredoxin oxidoreductase (POR, EC 1.2.7.1) is a metalloenzyme that catalyzes the ferredoxin-dependent oxidative decarboxylation of pyruvate to acetyl-coenzyme A (and *vice versa*) in a TPP and CoA-dependent reaction. Although pyruvate is the best substrate, the enzyme is indeed able to bind and use other 2-keto acids as substrates (Assary and Broadbelt 2011). The redox equivalents during the reaction are transferred to low potential single electron carrier oxidants, ferredoxin or flavodoxin. POR is widespread in all three different domains of life and is isolated and characterized from different archaea, bacteria, and protozoa (Townson *et al.* 1996; Horner *et al.* 1999; Pineda *et al.* 2010).

The majority of the PORs isolated from bacteria and protists have homodimeric structures, unlike a majority of the archaeal PORs, which are heterotetrameric. There are exceptions in each group, the mesophilic bacterium *Helicobacter pylori* and all of the extremely thermophilic and hyperthermophilic bacteria contain the heterotetrameric-type POR (Hughes *et al.* 1995). Alternatively, in halophilic archaeon *Halobacterium halobium*, POR is a heterodimeric molecule composed of two different subunit types (Kerscher and Oesterhelt 1981b; Plaga *et al.* 1992). It has been suggested that mesophilic monomeric and dimeric PORs are results of the fusion of four ancestral subunits, which are now present in the hyperthermophilic bacteria and archaea (Kletzin and Adams 1996; Zhang *et al.* 1996).

POR was isolated and characterized from the hyperthermophilic fermentative archaeon *P. furiosus* (Blamey and Adams 1993), the sulfate-reducing hyperthermophilic archaeon *Archaeoglobus fulgidus* (Kunow *et al.* 1995), the hyperthermophilic anaerobic bacterium *T. maritima* (Blamey and Adams 1994) the extremely thermophilic bacterium *Hydrogenobacter thermophilus* (Yoon *et al.* 1997) as well as the hyperthermophilic archaeon *T. guaymasensis* (Chapter 2). Both types of the PORs are TPP- and CoA-dependent and contain at least two [4Fe-4S] clusters. Hyperthermophilic PORs are composed of four distinct subunits with holoenzyme being heterotetrameric and molecular weights of approximately 120 kDa. However, the POR/PDC bifunctionality was only shown for the enzyme from *P. furiosus*. It was unclear if such POR/PDC bifunctionality was only a property of the POR from Pyrococcales or if it would be a universal property of all hyperthermophilic PORs. If such bifunctionality exists in the thermophilic and hyperthermophilic bacterial (*e.g.* Thermotogales) enzymes, it would still be intriguing to study the possible contributions of each activity to the physiology of the corresponding microorganism. In this study, the bifunctional POR/PDCs were purified from two members of the genus *Thermotoga*, the hyperthermophilic bacterium *T. maritima* and the extremely thermophilic bacterium *T. hypogea* and the properties of both activities were studied. Although the catalytic properties of the POR activity from *T. maritima* were mostly characterized in a previous study (Blamey and Adams 1994), some of the characterization experiments (the optimal pH determination) would be carried out to be compared with the PDC activities.

3.3 Materials and Methods

3.3.1 Reagents and chemicals

Sodium pyruvate, isobutyraldehyde, thiamine pyrophosphate (TPP), dichloromethane, coenzyme A (CoASH), HEPES, CAPS, EPPS, lysozyme and methyl viologen (MV) were purchased from Sigma-Aldrich Canada Ltd. (ON, Canada). Desulfocoenzyme A was kindly synthesized Dr. E. J. Lyon, Chemistry Department at Bellarmine University, USA. DNaseI for the cell lysis buffer preparation was purchased from Roche (Roche Applied Science, QC, Canada). The chemicals used in the growth media were all commercially available. Yeast extract was acquired from EMD (EMD Chemicals, Inc. NJ, USA) and trypticase soy broth (TSB) was purchased from Becton-Dickinson (BD Bioscience, Mississauga, ON, Canada). All of the FPLC columns and chromatographic media were purchased from GE Healthcare (QC, Canada).

3.3.2 Microorganisms and growth conditions

Thermotoga maritima (DSMZ 3109) and *Thermotoga hypogea* (DSMZ 11164) were obtained from DSMZ- Deutsche Sammlung von Mikroorganismen und Zellkulturen (Braunschweig, Germany) and were grown routinely under anaerobic conditions in 20 L glass carboys, and small scale starter cultures were grown in the media supplemented with vitamin solutions and no vitamin mixture was used for large scale (15L) growth.

T. maritima was grown anaerobically on glucose and yeast extract at 80°C as described by Huber *et al.* (1986) with modifications as previously described (Yang and Ma 2010). The medium contained (per liter) KCl, 2.0 g; MgCl₂·6H₂O, 1.42 g; MgSO₄·7H₂O, 1.8 g; CaCl₂·2H₂O, 0.05 g; NaCl, 20 g; (NH₄)₂CO₃, 1.14 g; KH₂PO₄, 0.05 g; resazurin 0.05 mg, trace minerals [prepared as described by Balch *et al.* (1979)], 10 ml, Yeast extract 2.5 g, and glucose, 4.0 g. The pH of the medium was adjusted to 6.8 before autoclave.

T. hypogea was grown under anoxic conditions at 70°C as described previously (Fardeau *et al.* 1997) with some modifications of the procedure as described elsewhere (Yang and Ma 2005). The media contained (per liter) KCl, 0.1 g; MgCl₂·6H₂O, 0.2 g; CaCl₂·2H₂O, 0.1 g; NaCl, 20 g; NH₄Cl, 1.0 g; KH₂PO₄, 0.3 g; K₂HPO₄, 0.3 g; resazurin 0.05 mg, trace minerals [prepared as described by Balch *et al.* (1979)], 10 ml, Yeast extract 2.0 g, and trypticase, 2.0 g. The pH of the medium was adjusted to 7.3 prior to autoclave (Yang and Ma 2005).

The cell density and growth phases of the large-scale cultures were monitored by direct sampling using Petroff-Hausser cell counting chamber (1/400 mm², 0.02 mm deep; Hausser Scientific, Horsham, PA) and a Nikon Eclipse E600 phase-contrast light microscope (Nikon Canada, ON, Canada). After the growth reached to the late log-phase the cultures were cooled down in an ice slurry bucket and centrifuged at 13,000 ×g using a Sharples continuous centrifugation system (Sharples equipment division, PA, USA) at 150-200 mlmin⁻¹. The biomasses were snap-frozen in liquid nitrogen and subsequently stored at -76°C freezer until use.

3.3.3 Sequencing of *por* genes of *T. hypogea*

The genome sequence is not available for *T. hypogea*. The genes encoding the four subunits of POR as well as the promoter regions and parts of the neighboring genes were sequenced using a primer walking strategy. The primers were designed based on highly conserved regions within *por* operon of the *Thermotoga* species released by the time of the study, including *T. maritima*, *T. petrophila*, and *T. lettingae*. To achieve this amino acid sequences of subunits containing the conserved motifs including TPP-binding motif, CoA-binding motif, and [4Fe-4S] cluster-binding motif were aligned and the corresponding nucleotide sequences were chosen to design the degenerative primers (**Table 3-1**). The primers were used for amplification of the unknown sequence of DNA from genomic DNA of *T. hypogea*. The PCR products with sizes close to the expected PCR product (estimated based on the closely related species) were sequenced in both (forward and reverse) directions. The identity of newly sequenced stretches of DNA was confirmed by searching the database for homologous sequences. And then used to design the next set of the primers for amplification of the new fragments of genomic DNA. After sequencing of each fragment, overlapping primers were designed within the newly sequenced fragment to be used for amplification and sequencing of the neighboring DNA sequence. The overlapping sequenced segments were subsequently assembled manually.

Genomes in the NCBI microbial genome database (http://www.ncbi.nlm.nih.gov/genomes/MICROBES/microbial_taxtree.html) were used to retrieve the amino acid and nucleotide sequences of PORs from various hyper/thermophiles. The deduced amino acid sequences were compared to protein sequences retrieved from NCBI, Swiss Prot and EMBL. The search in these databases were carried out using the programs FASTA, BLAST, and PROSITE. ClustalW version 2.0 (Thompson *et al.* 1994) was used for DNA and/or protein sequence alignments and comparisons.

Table 3-1. The primers used for the sequencing of the *por* operon of *T. hypogea*

Name	Sequence ^a	Length	T _m (°C) ^b	Size(bp) ^c
HPORGF	5'-CGTCGTTGTGGTGATCGATG-3'	20	66.2	652
HPORGR	5'-AAACTCWGTYTCAGGTCTCATCTC-3'	24	57.0	
HPORA1F	5'-AGCGATGACAGCAACCAGTGC -3'	67.5	21	683
HPORA1R	5'-TCGGGAATGGTCTGAACATCC-3'	68.4	21	
HPORG2F	5'- CAGAAGAAATGATTCAGGCGAAC -3'	67.9	23	770
HPORG2R	5'- ATCCAACCCGAATCTCTCACC -3'	67	21	
HPORG1R	5'- TCTTGACACGCCAATCACCG-3'	20	68.7	646
HPORG1F	5'- GAAATMMGRTGGCACKSWAGAGC-3'	23	63	
HPORA2F	5'- ATGGTTGCTCTGGGATCTTCC-3'	21	67.1	749
HPORA2R	5'- CATACTGTTCCWCCRTCTCCACC -3'	22	67.7	
HPORBF	5'- TACAGGGCGTTGAAGAAGGC -3'	20	67.0	668
HPORBR	5'- CCAGTGTRAGYARTCTTTCCCATCTT -3'	26	64.1	

^a Primers were designed based on the sequences of the fully-sequenced closely related organisms of the genus *Thermococcales*

^b Melting temperature of the primers as determined using GeneRunner (Hasting software Inc., 1994)

^c expected size of the PCR products based on the sequence of the corresponding fragment in closely related organisms

3.3.4 Anaerobic techniques

All of the buffers and reagents were degassed in containers sealed within red rubber sleeved stoppers. The stoppers were punctured with needles to allow the alternate exposure to vacuum and nitrogen (N₂) using a manifold. The nitrogen gas (Praxair, ON, Canada) was deoxygenated by passing through a heated column containing a BASF catalyst (BASF, NJ, USA). Assay and purification buffers were degassed in magnetically stirred flasks for 30 min, followed by three cycles of flushing/vacuum (each 3 min). Then a second needle was inserted to flush out more N₂ to ensure oxygen-free head space in the container (even if there is residual O₂ contamination in the manifold system). The containers were kept under nitrogen pressure (~3 psi). All of the purification buffers contained 2 mM sodium dithionate (SDT) and 2 mM dithiothreitol (DTT) to remove traces of oxygen contamination.

3.3.5 Preparation of cell-free extracts

To purify the bifunctional POR/PDC from *T. maritima* and *T. hypogea*, the cell-free extract (CFE) were prepared from the biomass grown to the late log-phase. Unless otherwise noted all operations were performed under anoxic conditions and on ice.

The cell pellets (50 g of frozen *T. hypogea* and 60 g of frozen *T. maritima* biomass) were re-suspended in the anaerobic lysis buffer [50 mM Tris-HCl, 5% glycerol, 2 mM DTT, and 2 mM SDT, 0.1 mgml⁻¹ lysozyme, and 0.01 mgml⁻¹ DNaseI, pH 7.8] in a pre-degassed flask. The ratio of the lysis buffer to the biomass was 1:5 (v/w) for *T. hypogea* and 1:4 (w/v) for *T. maritima*. The cell suspensions were incubated at 37°C with stirring for two hours and subsequently were centrifuged at 10,000 ×g for 30 min at 4°C. The supernatants were designated as cell-free extracts and were transferred to anaerobic serum bottles using a syringe pre-rinsed with anaerobic buffer A (50 mM Tris-HCl, 5% glycerol, 2 mM DTT, and 2 mM SDT with pH adjusted to 7.8) and used directly as starting materials for the following purification steps.

3.3.6 Enzyme purification

Protein purifications were carried out using anaerobic multistep chromatography and at ambient temperature. The columns were run using a fast performance liquid chromatography (FPLC) system and all the materials were obtained from GE Healthcare (GE Healthcare, QC, Canada). Similar purification steps were followed for the purification of the POR/PDC bifunctional enzyme from *T. maritima* and *T. hypogea*. All of the purification steps were conducted under strictly anaerobic

conditions and by following the POR activity (since the assay is faster compared to the PDC assay) as well as the SDS-PAGE analysis of the chromatography fractions at each step. In the case of *T. maritima* the co-elution of both activities were followed throughout FPLC purification steps by assaying both POR and PDC activities. The buffer A was used throughout the purification, which was consisted of 50 mM Tris-HCl, 5% glycerol, 2 mM DTT, and 2 mM SDT and pH 7.8.

The CFEs were diluted two times before being loaded on a diethylaminoethyl (DEAE)-sepharose column (5.0×10 cm) pre-equilibrated with anaerobic buffer A. The column was washed with 300 ml buffer A and after that a gradient (0-0.5 M NaCl) of buffer B [50 mM Tris-HCl, 5% glycerol, 1 M sodium chloride, 2 mM DTT, and 2 mM SDT, pH 7.8] was applied to the column at a flow rate of 3.0 mlmin⁻¹. The collected fractions were tested for the POR activity. The active fractions (170-220 mM NaCl for *T. hypogea* and 180-240 mM sodium chloride for *T. maritima*) were combined and loaded on a hydroxyapatite (HAP, 2.6×15 cm) column pre-equilibrated with buffer A. After loading of the active fractions, the columns were washed with 100 ml of anaerobic buffer A and then eluted with a gradient (0-0.5 M potassium phosphate) of buffer C [50 mM Tris-HCl, 5% glycerol, 0.32 M K₂HPO₄, 0.18 M KH₂PO₄, 2 mM DTT, and 2 mM SDT pH 7.8] at a flow rate of 2.0 mlmin⁻¹. The active fractions (125-150 mM and 115-135 mM phosphate for *T. hypogea* and *T. maritima*, respectively) were pooled and loaded on a phenyl sepharose column (PS, 2.6×10 cm) pre-equilibrated with 0.8 M ammonium sulphate in buffer A. The column was washed with 50 ml of 0.8 M buffer D followed by a linear (decreasing) gradient (0.82-0 M ammonium sulphate) of buffer D [50 mM Tris-HCl, 5% glycerol, 2 M ammonium sulphate, 2 mM DTT, and 2 mM SDT pH 7.8] at flow rates of 2.0 mlmin⁻¹ for elution of proteins. The active enzymes from both *T. maritima* and *T. hypogea* were eluted from the column as 0.3-0.1 M ammonium sulphate applied to the column for the enzymes. The purified enzymes (as judged by SDS-PAGE) were desalted and concentrated using an ultrafiltration device (Advantech MFS, Inc., CA, USA) via a 44.5 mm membrane of polyethersulfone and nominal molecular weight limit (NMWL) of 50,000 (Millipore, MA, USA) under anaerobic conditions and pressure of nitrogen (10-15 Mpa). The concentrated purified protein was subsequently stored in liquid nitrogen until use.

3.3.7 Protein concentration determination

The protein concentrations were routinely determined using Bradford dye-binding method (Bradford 1976) *via* the reagent purchased from Bio-Rad Laboratories (ON, Canada). Bovine serum albumin (BSA) was used for preparation of the standard protein curve as instructed by the manufacturer.

3.3.8 SDS-PAGE

The sodium dodecyl sulfate polyacrylamide gel electrophoresis (SDS-PAGE) was used to determine the enzyme purity and apparent subunit molecular weights. The SDS-PAGE was performed according to Laemmli (1970) with acrylamide and molecular weight standards from Bio-Rad (ON, Canada). SDS-PAGE was run using a Hoefer™ Mighty Small System (Hoefer Inc., MA, USA) with the gels (8×10 cm) prepared and stained with Coomassie Brilliant Blue R250. The de-staining was carried out by storing the gel in the de-staining solution (12% 2-propanol and 7% acetic acid) with moderate shaking and overnight.

3.3.9 Estimation of native molecular masses

The molecular weights of the purified enzymes were estimated by loading the concentrated proteins on a size exclusion chromatography column (2.6×60 cm). The HiLoad Superdex-200 column (GE healthcare, QC, Canada) pre-equilibrated with buffer C (50 mM Tris, 5% glycerol, 100 mM KCl, pH 7.8) at the flow rate of 2 mlmin⁻¹. The following standards from Pharmacia protein standard kit (pharmacia, NJ, USA) were applied to the column: blue dextran (2,000,000 Da), thyroglobulin (669,000 Da), ferritin (440,000 Da), catalase (232,000 Da), aldolase (158,000 Da), bovine serum albumin (67,000 Da), ovalbumin (43,000 Da), chymotrypsinogen A (25,000 Da) and ribonuclease A (13,700 Da).

3.3.10 POR assay

The spectrophotometric measurement of pyruvate- and coenzyme A-dependent reduction of the benzyl (or methyl) viologen was used to assay the POR activity as previously described (Wahl and Orme-Johnson 1987).

The catalytic activities of the purified PORs were assayed in duplicate and under strictly anaerobic conditions unless otherwise mentioned. The sodium pyruvate was routinely used as the substrate (electron donor) and methyl viologen (MV) replaced ferredoxin as the electron acceptors. The assays

were carried out at 80°C in an assay mixture (2 ml) composed of 100 mM EPPS, pH 8.4, 1 mM MgCl₂, 5 mM sodium pyruvate, 0.4 mM TPP, 100 μM coenzyme A, 1 mM of methyl viologen (MV), and enzyme in stoppered optical glass cuvettes with 1cm light path (Starna cells, Inc., Atascadero, CA, USA). In addition, small amounts of sodium dithionate (SDT) were added to the assay mixture to scavenge the residual oxygen and slightly reduce the assay mixture before the addition of the enzyme to start the reaction (section 3.3.4).

The anaerobic assay buffer was transferred to the pre-degassed assay cuvette using a syringe pre-rinsed with anaerobic buffer for at least three times. The cuvette was incubated in a water-jacketed cuvette holder on a Genesys 10 UV-Vis spectrophotometer (Thermo Scientific, MA, USA) and pre-warmed to the assay temperature (80°C) for 4 min, then it was taken out and the assay components were added using a pre-rinsed Hamilton gas-tight syringe (Hamilton company, Reno, NV, USA) in a rapid succession the SDT was added at a very small amount until a light blue color appeared in the cuvette. Subsequently the cuvette was placed back in the holder for another 30 seconds. The reaction was started by adding the enzyme fraction and monitoring the absorbance change at 578 nm. An extinction coefficient of methyl viologen is $\epsilon_{578} = 9.8 \text{ mM}^{-1}\text{cm}^{-1}$ (Yoon *et al.* 1997; Schut *et al.* 2001a). The oxidation of pyruvate would release two electrons. The activity was determined based on the linear part of the enzymatic reaction progress curve and one unit of enzyme activity was defined as the oxidation of 1 μmol of the substrate or the reduction of 2 μmol MV per minute. Tests were done to determine the linear correlation between the activity and the amount of protein in the assay.

3.3.11 PDC activity assay

The pyruvate decarboxylase activity (PDC) was determined by measuring the rate of acetaldehyde production. In principle, the acetaldehyde produced during the enzymatic reaction (**Figure 3-1**, step A) was derivatized with a freshly prepared acidic solution of 2, 4-dinitrophenylhydrazine (DNPH) also known as Brady's reagent (**Figure 3-1**, step B). The reaction of the reagent with aldehyde groups creates a yellow-reddish color resulting from the formation of the corresponding hydrazone derivative. Subsequent to liquid-liquid phase extraction with a solvent (**Figure 3-1**, step C), the acetaldehyde-DNPH complex was quantified by reverse-phase high performance liquid chromatography (RP-HPLC). The general procedures and main steps involved in the assay are presented in **Figure 3-1**.

Enzymatic reactions were carried out in duplicate, in stoppered 8 ml vials under anaerobic conditions and 80°C unless specified. The standard assay mixture (1 ml final volume) containing EPPS buffer (100 mM, pH 8.4), 1 mM MgCl₂, 0.1 mM thiamine pyrophosphate (TPP), 10 mM sodium pyruvate, and 1 mM coenzyme A (CoASH) was pre-warmed by incubation at 80°C water bath for 4 min. When specified, sodium pyruvate was replaced with 10 mM of 2-ketoisovalerate. The reaction was started by adding the enzyme (or enzyme containing fraction). Tests were done to make sure that there is a linear correlation between the activity and the amount of enzyme in the assay. After the enzymatic reaction time (20 min), the reaction was stopped after 20 min unless specified by transferring the assay vials on the ice and adding 2 ml of freshly prepared saturated DNPH solution in 2 N HCl (stirred at room temperature and dark for 1 h). The vials were then incubated overnight at room temperature with shaking (150-200 rpm) to allow derivatization of acetaldehyde with the

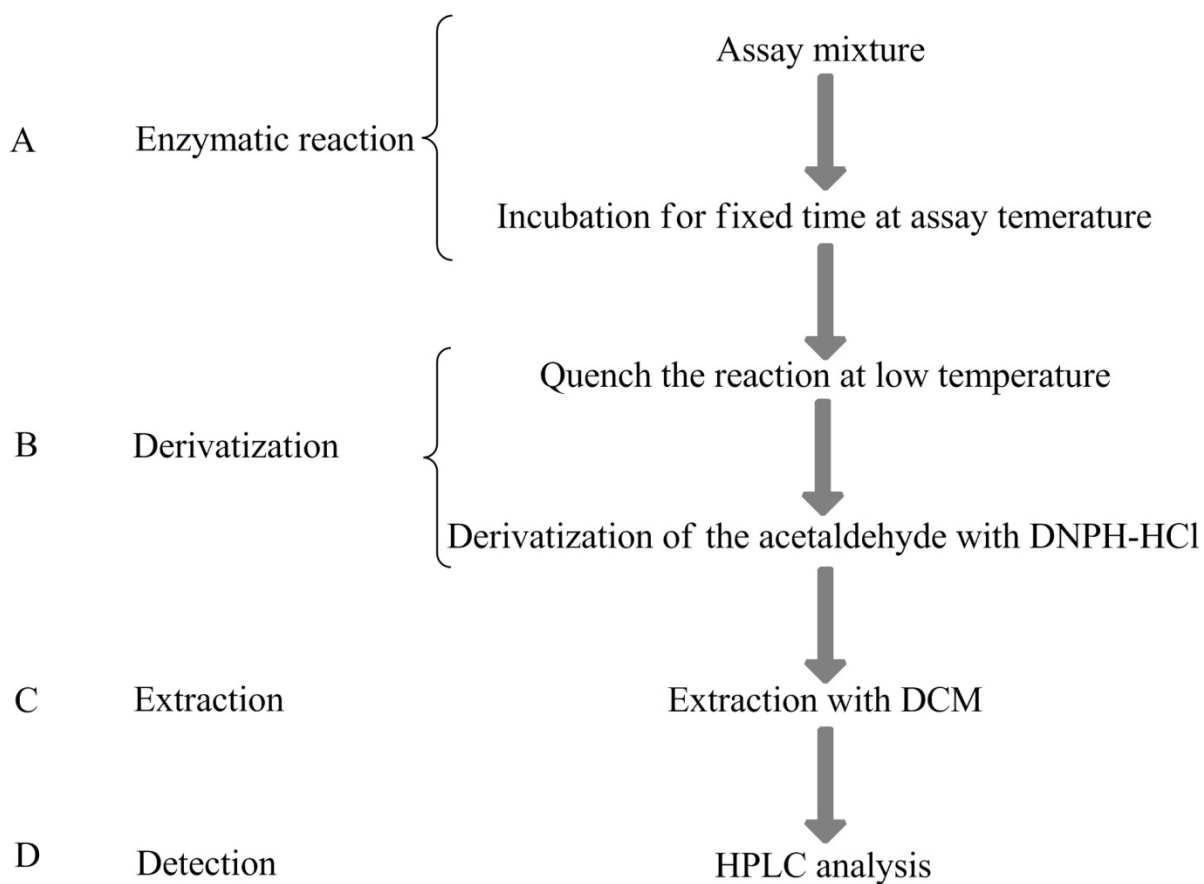


Figure 3-1. General steps involved in PDC activity assay

DNPH-HCl, hydrochloridric acid solution saturated with dinitrophenylhydrazine; DCM, dichloromethane; HPLC, high performance liquid chromatography. All assays were carried out at 80°C and under anaerobic conditions unless specified. The buffer routinely used for the assay was EPPS (100 mM, pH 8.4).

DNPH. The resulting hydrazone (acetaldehyde-DNPH) derivative was then extracted with 1 ml of dichloromethane (DCM) by vigorous shaking at room temperature for 15 min. The extraction was then repeated for one more time. The organic (lower) phase was then transferred to a new clean vial covered with a piece of Parafilm M[®] membrane with few holes on it. The assay vials were placed in a vacuum desiccator covered with aluminum foil (to protect from the light) which was connected to a water pump to evaporate the DCM in a fume hood. After evaporation of DCM (about 3-4 h), the resulting yellowish-red powder were dissolved in 4ml of pure (HPLC grade) acetonitrile by incubation at 4°C overnight.

An aliquot of the assay product was filtered through a 0.2 µm nylon syringe filter (National Scientific, Rockwood, TN, USA), and analyzed by a Perkin-Elmer LC Series4 HPLC system (Norwalk, CT, USA) fitted with a reversed-phase Allure C18 column (150×4.6 mm, 5µm, 60 Å). Isocratic elution conditions with a mobile phase of acetonitrile/water (80:20 v/v) were used at a flow rate of 1 mlmin⁻¹. A micrometrics model 788 dual variable wavelength detector (Norcross, GA, USA) was used and operated at 365 nm. The sample was applied using a Rheodyne Model 7125 injection valve (Rheodyne Inc., CA, USA) with a 20 µl sample loop. The HPLC system was operated at room temperature. The final concentration of acetaldehyde and isobutyraldehyde were determined using a calibration curve prepared by linear regression plotting of known concentrations of each product which was processed under the same assay conditions.

3.3.12 Biochemical and biophysical characterization

The optimal pH (pH dependence) was determined for the purified POR from both *T. maritima* and *T. hypogea*. Sodium pyruvate was used as the substrate for routine assays unless specified. The activity assays were carried out in minimum of duplicates, at different pH values ranging from 6.0 to 11. All buffers had a concentration of 100 mM. The pH values expressed throughout this manuscript were all adjusted and measured at room temperature unless specified differently. Sodium phosphate buffer (pKa 7.20, $\Delta pK_a/^\circ C = -0.0028$) was used for pH values 6.0, 7.0, and 7.5. HEPES buffer (pKa 7.39, $\Delta pK_a/^\circ C = -0.014$) covered pH values 7.5, 8.0, 8.5 and 9.0 and glycine buffer (pKa 9.55, $\Delta pK_a/^\circ C = -0.0025$) was used for the pH values 9.0, 9.5, 10.0, and 10.5. Finally, for the pH points of 10.0, 10.5, and 11.0 the CAPS buffer (pKa 10.40, $\Delta pK_a/^\circ C = -0.009$) was used.

Assays to determine the apparent kinetics parameters of the purified enzyme from *T. hypogea* and *T. maritima* were all carried out at 80°C and under standard assay conditions using the optimal pH for each activity (POR and PDC). The kinetic parameters were determined for pyruvate (substrate) and coenzyme A (cofactor) by applying various concentrations of each component and keeping the concentration of other assay components invariable. The kinetic parameters were also determined for the artificial electron

acceptor, methyl viologen, in the case of ThPOR. All of the assays were carried out in minimums of duplicate or triplicate. The activities were assayed with various concentrations and the kinetic parameters were calculated from the nonlinear best fit of data to the Michaelis-Menten equation by non-linear regression using the SigmaPlot® software (SYSTAT Software Inc., CA, USA).

The oxygen sensitivity of POR and PDC activities for both purified enzymes from *T. maritima* and *T. hypogea* were determined by exposing aliquots of each purified enzyme to the ambient atmosphere at 4°C by gentle stirring. At different time intervals the enzyme activities were determined and compared with the control preparation that was kept at 4°C and under anaerobic conditions and nitrogen pressure.

The temperature dependencies of both activities were determined by assaying the enzyme activities at different temperatures from 30°C to 95°C under anaerobic conditions. The assay mixtures were prepared as described previously. The mixture was pre-incubated at each corresponding temperature for four minutes, before starting the reaction by adding the enzymes. The enzymatic reaction time for PDC assays were 20 min. To determine the half-life of the activities at high temperature, the enzyme was incubated at 80°C and the residual activities at different time points were determined and compared to unheated control.

3.4 Results

3.4.1 Sequence analysis of *por* genes

The nucleotide sequences of about 4.9 kb including the POR-encoding genes of the genome of *T. hypogea* were determined using the primer walking strategy and inverse PCR. Four genes corresponding to subunits α , β , γ , and δ with 391, 324, 190, and 100 amino acid residues, were sequenced which showed similar gene arrangements as other Thermotogales. The sequenced genes are arranged in the *porG-porD-porA-porB* order. An overview of the POR open reading frame (ORF) gene arrangement in *T. hypogea* and other Thermotogales was shown in **Figure 3-2**.

A phylogenetic analysis of Tm- and ThPOR sequences indicated their close relatedness to each other and to other bacterial and archaeal PORs. Each of the subunits was orthologous to corresponding subunits in other Thermotogales PORs as well as other keto acid ferredoxin oxidoreductases which are present in hyperthermophilic archaea. The closest homologues of the ThPOR seem to be the PORs from *T. lettingae* and *T. thermarum* (**Figure 3-3**). Amino acid sequences of TmPOR subunits are highly similar to the one from *Thermotoga* sp. strain RQ2, *T. petrophila* and *T. naphthophila* (**Figure 3-3**). The Thermotogales POR subunit sequences were divergent from the Thermococcales counterparts, which were shown by their separate clustering as in **Figure 3-3**. The pairwise comparison of the amino acid sequences of the whole length PORs from *T. hypogea* and *T. maritima* indicated an overall 76% amino acid sequence identity.

ATG was identified to be the start codon for the translation of *porA*, *porB*, and *porG*, while GTG was the start codon for the translation of subunit delta (*porD*) in all Thermotogales. It was found that TmPOR contained 15 conserved cysteine residues per tetrameric structure which were all conserved within the PORs of the Thermotogales and other hyperthermophilic PORs. The subunits PorA, PorB, PorG, and PorD contain 1, 4, 2, and 8 conserved cysteine residues, respectively. However, there was an extra cysteine residue in ThPOR subunit alpha (in total two cysteine residues) which was also conserved within some (but not all) other members of Thermotogales, including *T. lettingae*, *T. thermarum*, and *K. oleriae*.

Sequence analysis confirmed the presence of two typical cysteine-rich ferredoxin type [4Fe-4S] cluster motifs (CXXCXXCXXXCP) in subunit delta of Thermotogales PORs as well as the PorD of *T. hypogea* (**Figure 3-4**). The presence of such motif is a conserved characteristic of all different types of oxidoreductases. There is an additional cysteine rich [4Fe-4S] cluster binding motif located in the subunit beta which is composed of four highly conserved cysteines. PorB also contains the typical TPP-binding motif (GDGX₂₄₋₂₇NN) which is a conserved feature of all TPP-dependent enzymes

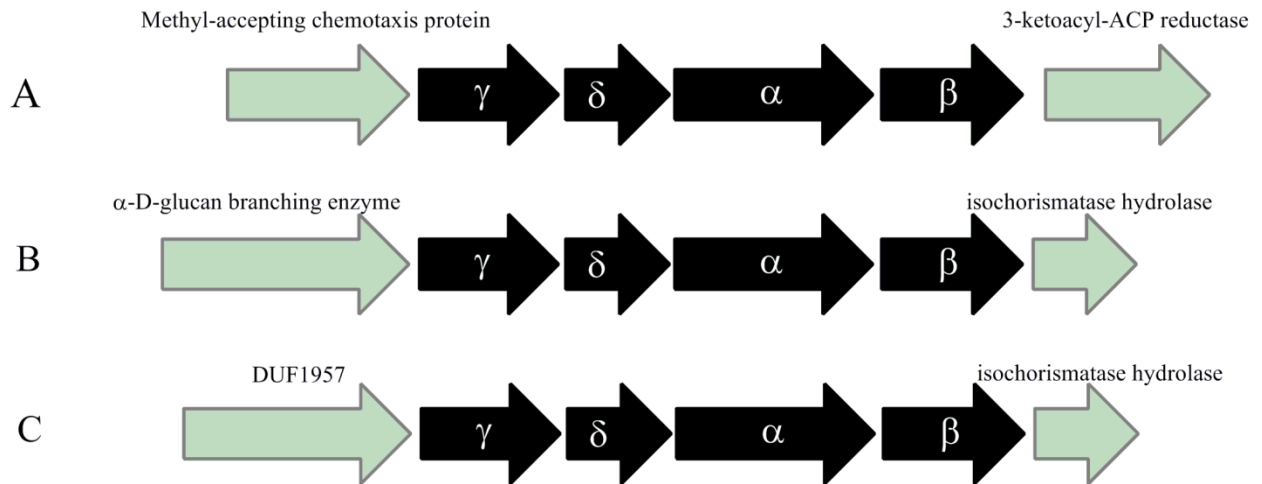


Figure 3-2. Schematic representation of *por* ORF organization in Thermotogales

ACP, acyl carrier protein; DUF, domain of unknown function

The genes encoding different subunits of POR are indicated with their corresponding names. The arrangement of the analogous genes are presented for *T. maritima*, *T. neapolitana*, *Thermotoga* species strain RQ2, *T. petrophila*, and *T. naphthophila* (A) *T. thermarum*; (B) *T. lettingae*; and *T. hypogea* (C).

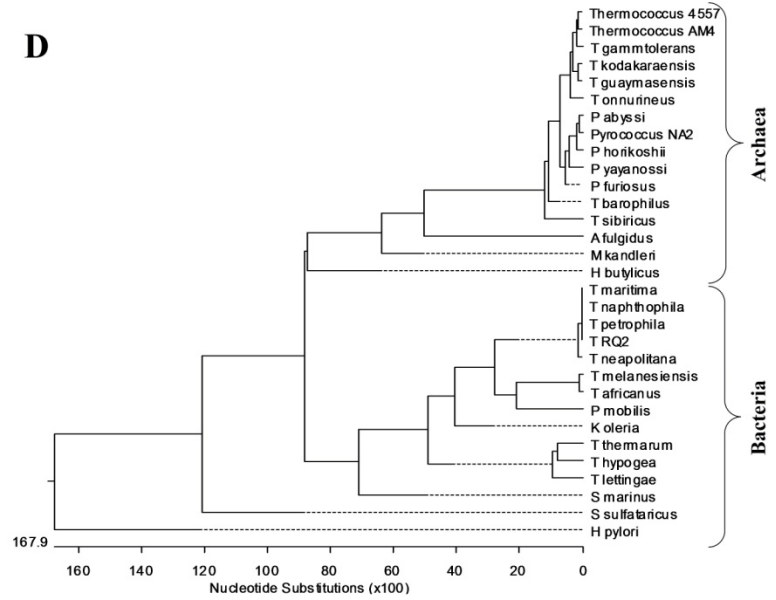
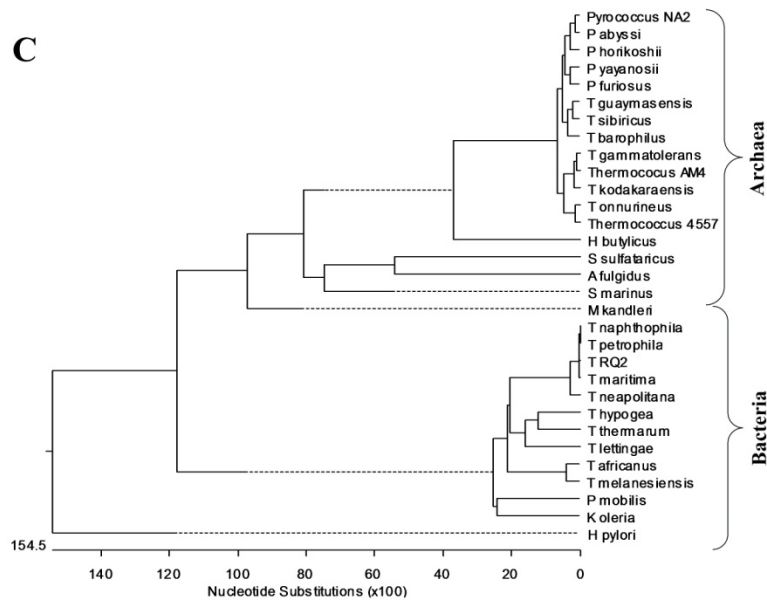
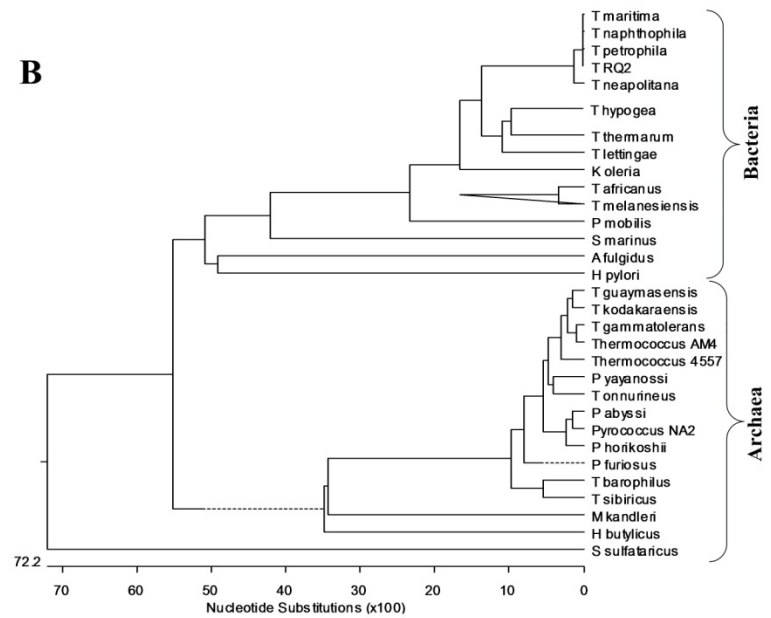
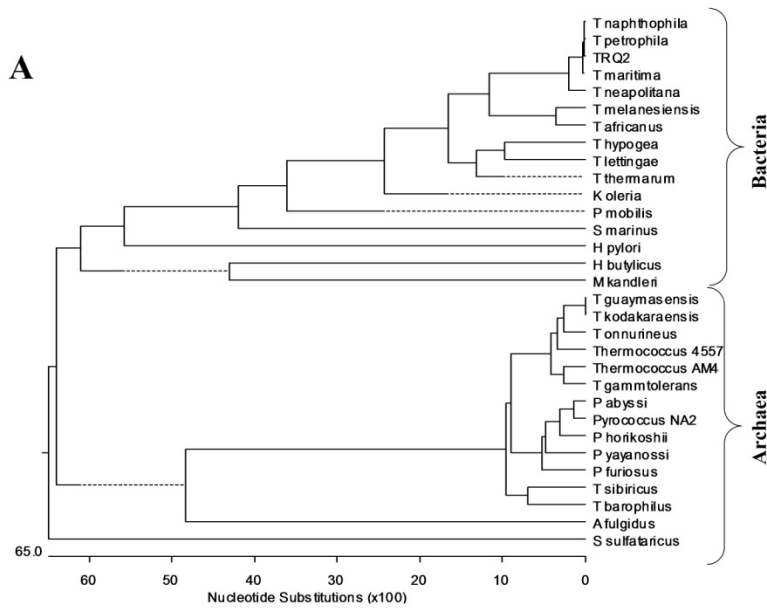


Figure 3-3. A rooted phylogenetic analysis of POR subunits from various bacteria and archaea

The amino acid sequences of subunit alpha (A), subunit beta (B), subunit gamma (C), and subunit delta (D) were aligned using the ClustalW multiple sequence alignment program. The amino acid sequences used for the generation of tree were retrieved from the genome databases as described in the Materials and Methods (section 3.3.3). The amino acid sequences of ThPOR were determined by translation of the nucleotide sequences retrieved by primer walking and inverse PCR (section 3.3.3). The numbers at the bottom of each tree indicate the number of the amino acid substitutions. A dotted line on the phenogram indicates a negative branch length, a common result of averaging.

A. fulgidus, *Archaeoglobus fulgidus*; *H. pylori*, *Helicobacter pylori*, *H. butylicus*, *Hyperthermus butylicus*; *K. oleriae*, *Kosmotoga oleriae*; *M. kandleri*, *Methanopyrus kandleri*; *P. mobilis*, *Petrotoga mobilis*; *P. mobilis*, *Petrotoga mobilis*; *P. abyssi*, *Pyrococcus abyssi*; *P. furiosus*, *Pyrococcus furiosus*; *P. horikoshii*, *Pyrococcus horikoshii*; *Pyrococcus* NA2, *Pyrococcus* species strain NA2; *P. yayanosii*, *Pyrococcus yayanosii*; *S. marinus*, *Staphylothermus marinus*; *S. solfataricus*, *Sulfolobus solfataricus*; *T. africanus*, *Thermosipho africanus*; *T. melanesiensis*, *Thermosipho melanesiensis*; *Thermococcus* AM4, *Thermococcus* species strain AM4; *T. barophilus*, *Thermococcus barophilus*; *T. naphthophila*, *Thermotoga naphthophila*; *T. lettingae*, *Thermotoga lettingae*; *T. neapolitana*, *Thermotoga neapolitana*, *T. hypogea*, *Thermotoga hypogea*; *T. thermarum*, *Thermotoga thermarum*; *T. maritima*, *Thermotoga maritima*; TRQ2, *Thermotoga* species strain RQ2; *Thermococcus* 4557, *Thermococcus* species strain 4557; *T. sibiricus*, *Thermococcus sibiricus*; *T. gammatolerance*, *Thermococcus gammatolerance*; *T. kodakaraensis*, *Thermococcus kodakaraensis*

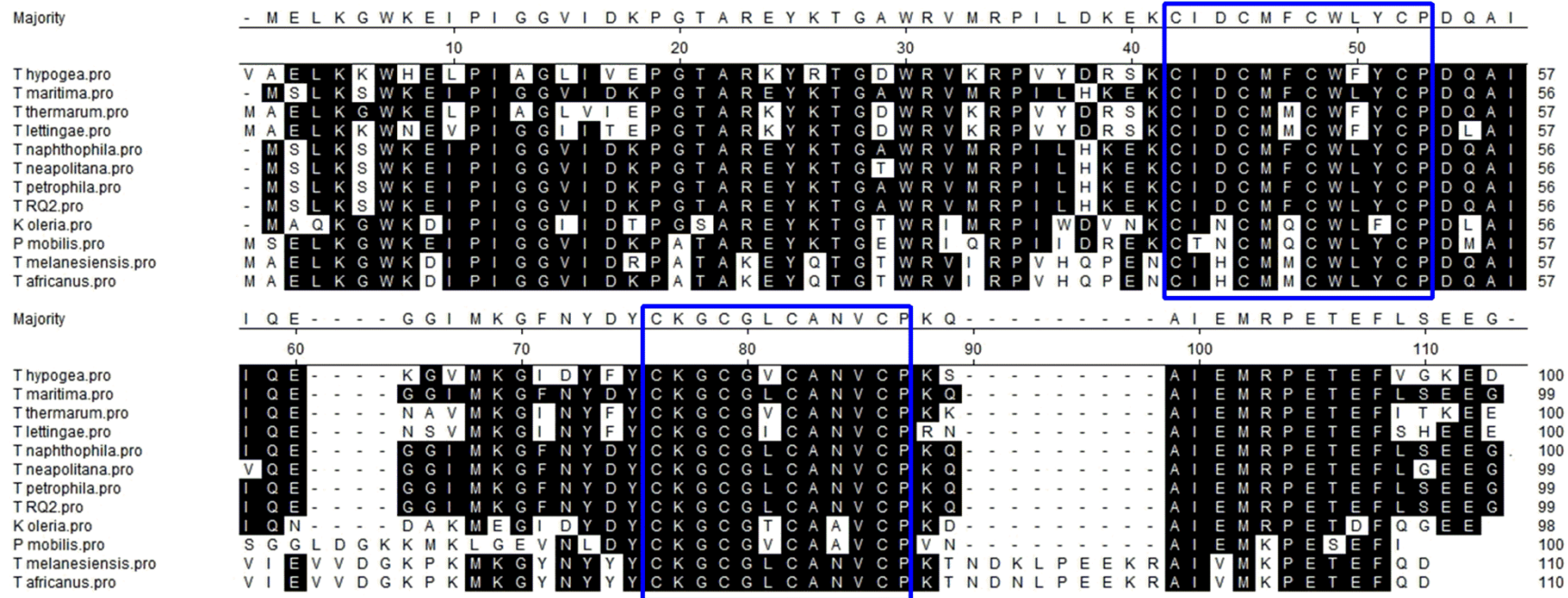


Figure 3-4. Multiple sequence alignment of part of PorD subunit from Thermotogales

The iron-sulfur binding motif (CXXCXXCXXXCP) is boxed. *Thermotoga hypogea*, *Thermotoga maritima*, *Thermotoga thermarum*, *Thermotoga lettingae*, *Thermotoga naphthophila*, *Thermotoga neapolitana*, *Thermotoga petrophila*, *Thermotoga* sp. strain RQ2, *Kosmotoga oleriae*, *Petrotoga mobilis*, *Thermosiphon melanesiensis*, and *Thermosiphon africanus*

(Hawkins *et al.* 1989; Muller *et al.* 1993). Subunit gamma (PorG) contains a highly conserved coenzyme A binding motif (GXXGXG) which is indeed a conserved feature of the hyperthermophilic 2-keto acid oxidoreductases.

For both *T. hypogea* and *T. maritima* POR operons, a typical putative Shine-Dalgarno sequence (RBS) is located upstream of the *porG*. The translational stop and start codons of *porG-porD*, *porD-porA*, and *porA-porB* are overlapping which is indicative of polycistronic transcription of POR operon in members of the order Thermotogales. Such polycistronic arrangement has been previously reported mostly in some phage and bacterial operons, for instance in tryptophan biosynthesis pathway of *E. coli* (*trp* operon). This manner of gene organization is particularly common in case of the multi-subunit enzymes or metabolically inter-related enzymes and seems to be a mechanism to assure all of subunits are being transcribed and translated simultaneously and to the same extent (Das and Yanofsky 1984; Schoner *et al.* 1984).

3.4.2 Purification of POR/PDC from *T. maritima* and *T. hypogea*

The bifunctional POR/PDC was purified from the CFEs of *T. hypogea* and *T. maritima*. Almost all of the POR/PDC activities were associated with the soluble fractions after anaerobic centrifugation which is consistent with previous finding regarding the solubility of PORs. CFEs of *T. hypogea* and *T. maritima* contained 2.6 and 5 U mg^{-1} of the POR, respectively. When assayed under the specified conditions (EPPS buffer, 100 mM, pH 8.4 and at 80°C), both CFEs exhibited PDC activity, with the specific activities of 0.08 and 0.12 U mg^{-1} for *T. hypogea* and *T. maritima*, respectively. Omitting coenzyme A from the assay mixture resulted in no PDC activity in CFE of *T. hypogea* and a residual PDC activity of about 0.012 U mg^{-1} in the CFE of *T. maritima*. The purified enzymes from both microorganisms exhibited a brownish color which is characteristic of the iron-sulfur containing proteins. Typical purification of the POR/PDC from *T. hypogea* and *T. maritima* were summarized in **Table 3-2** and **Table 3-3**, respectively.

A considerable part of activity was lost during hydroxyapatite (HAP) chromatography step which is similar to what observations reported previously for POR purifications from *T. maritima* and *P. furiosus* (Blamey and Adams 1993; Blamey and Adams 1994). The purity of the enzymes was judged by SDS-PAGE analysis (**Figure 3-5** A and B) and it had POR specific activities of about 96.7 \pm 15.1 and 90.8 \pm 11 U mg^{-1} for *T. hypogea* and *T. maritima*, respectively. The specific activity of the purified TmPOR was fairly close to the previously reported value of approximately 85 U mg^{-1} (Blamey and Adams 1994).

Table 3-2. Purification of bifunctional POR/PDC from *T. hypogea*^a

Step	Total protein ^b (mg)	Total activity ^c (U)	Specific activity ^d (Umg ⁻¹)	Purification (fold)	Recovery (%)
Cell-free extract ^a	1242	6189	5	1	100
DEAE sepharose	264	5890	22.8	4.6	95.2
Hydroxyapatite	32.2	3049	94.5	18.9	49.3
Phenyl sepharose	11.6	1617	119	23.8	26.2

^a CFE was prepared from 50 g of *T. hypogea* cells (wet weight)

^b As determined by Bradford assay using BSA as the standard protein as described in the Materials and Methods section 3.3.7

^c POR activity assays were conducted as previously described in the Materials and Methods (section 3.3.10)

^d One unit was defined as micromole of pyruvate oxidized per min

Table 3-3. Purification of POR/PDC from *T. maritima*^a

Step	Total protein ^b (mg)	Total activity ^c (units)	Specific activity ^d (Umg ⁻¹)	Purification (Fold)	Recovery (%)
Cell-free extract ^a	1094	3028	2.6	1	100
DEAE sepharose	348	2320	6.6	2.6	76.7
Hydroxyapatite	32.	556	17.4	6.7	18.3
Phenyl sepharose	4	268	78	30	8.9

^a CFE was prepared from 60 g of *T. maritima* cells (wet weight)

^b As determined by Bradford assay using BSA as the standard protein as described in Materials and Methods (section 3.3.7)

^c POR activity as described in the material and methods (section 3.3.10)

^d One unit was defined as micromoles of pyruvate oxidized per min

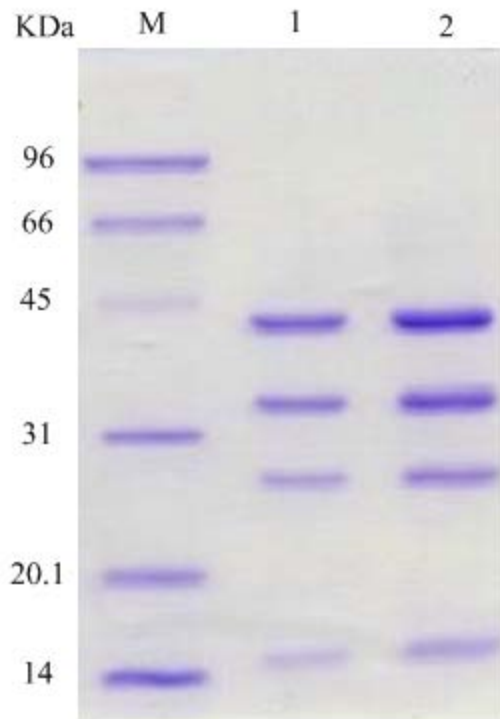
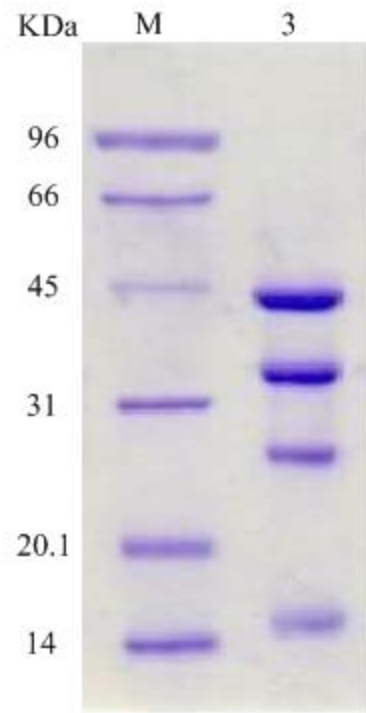
A**B**

Figure 3-5. Analysis of purified POR/PDC from *T. maritima* (A) and *T. hypogea* (B) using SDS-PAGE (12.5%)

lane1, 2 μg of purified POR from *T. maritima*; lane 2, 4 μg purified POR from *T. maritima*; lane 3, 6 μg purified POR from *T. hypogea*; lanes M, molecular weight standard markers (Bio-Rad Laboratories, ON, Canada)

In *T. maritima*, POR and PDC activities were co-eluted throughout different FPLC steps. Also, POR and PDC activities were increased to the same extent after each chromatography step (**Figure 3-6 A and B**). In *T. hypogea* only the elution of the POR activity was followed during different purification steps, and PDC activity was determined just on the resulting purified enzyme fraction. Purified TmPOR and ThPOR both catalyzed the non-oxidative decarboxylation of pyruvate with specific activities of $1.82 \pm 0.44 \text{ U mg}^{-1}$ and $1.4 \pm 0.15 \text{ U mg}^{-1}$ for *T. hypogea* and *T. maritima*, respectively.

3.4.3 Molecular mass determination

Each of the purified POR/PDC of *T. maritima* and *T. hypogea* showed four bands on 12.5 % SDS-PAGE (**Figure 3-5 A and B**) which is in accordance with the previously studied PORs from hyper/thermophilic bacteria and archaea. The estimated apparent molecular masses of the subunits were 46, 35, 23, and 13 kDa for *T. maritima* and 45, 35, 22, and 14 kDa for the enzyme from *T. hypogea*, which are similar to the previously purified and characterized PORs from *Archaeoglobus fulgidus*, *P. furiosus*, and *M. maripaludis* (Blamey and Adams 1993; Kunow *et al.* 1995; Lin *et al.* 2003). When separated on SDS-PAGE the protein bands had different staining densities, with the smallest band always stained very poorly compared to the other three bands (**Figure 3-5 A and B**). The same phenomenon was observed archaeal PORs purified from the hyperthermophilic archaeon *A. fulgidus* (Kunow *et al.* 1995).

To determine the apparent native molecular masses, aliquots of each purified enzyme was loaded on a Superdex-200 gel-filtration chromatography column. The enzymes were eluted as single peaks from gel filtration column. The apparent native molecular mass of the bifunctional POR/PDC was estimated to be $156,769 \pm 6,107 \text{ Da}$ for *T. hypogea* and $159,654 \pm 4,526 \text{ Da}$ for the enzyme purified from *T. maritima*, which suggested that both enzymes were heterotetramers ($\alpha\beta\gamma\delta$). These apparent molecular weights were in accordance with the previous report on the Thermotogales POR (Blamey and Adams 1994).

3.4.4 Catalytic properties of the enzymes

The biophysical and biochemical properties of the purified enzymes from *T. maritima* and *T. hypogea* were characterized based on their ability for both oxidative (POR) and non-oxidative (PDC) decarboxylation of pyruvate. The optimal pH for both POR and PDC activities of the enzyme from *T. maritima* was determined to be 8.4 (**Figure 3-7 A and B**, respectively). Repeating the optimal pH experiment for several times, resulted in the same activity trend, confirming that the higher activity observed at pH 8.4 is not an artifactual effect resulting from the poor anoxic conditions during buffer preparation steps. Similarly the optimal pH for both POR and PDC activities of *T. hypogea* was determined to be 8.4 (**Figure 3-8**).

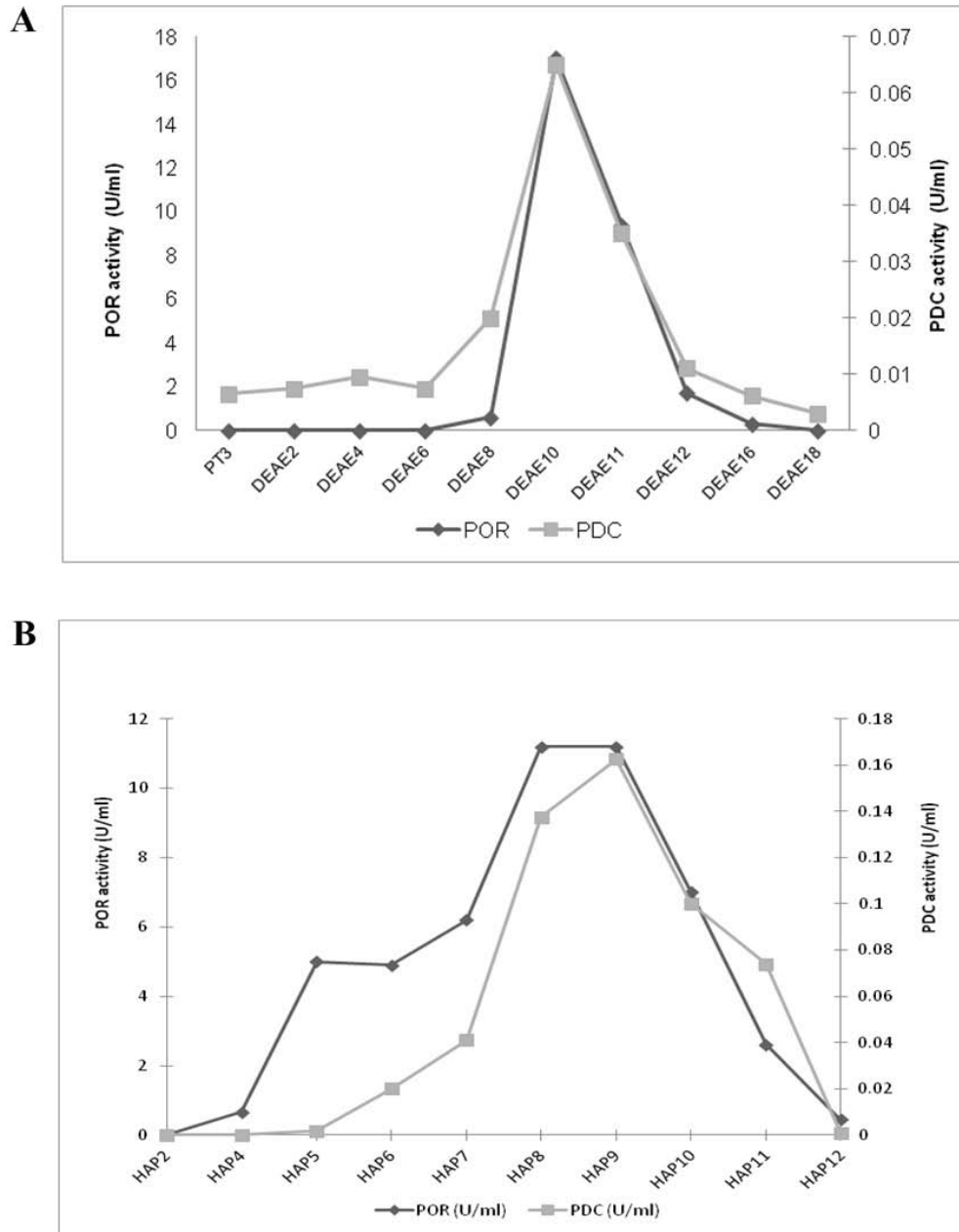


Figure 3-6. Co-elution of PDC activity in *T. maritima*

Different fractions from DEAE-sepharose (A) and Hydroxyapatite (B) chromatography during the purification of *T. maritima* POR. Fractions from each chromatography step were assayed for both the PDC and POR activities. All assays were carried out under anaerobic conditions and at 80°C as described in the material and methods sections 3.3.10 and 3.3.11.

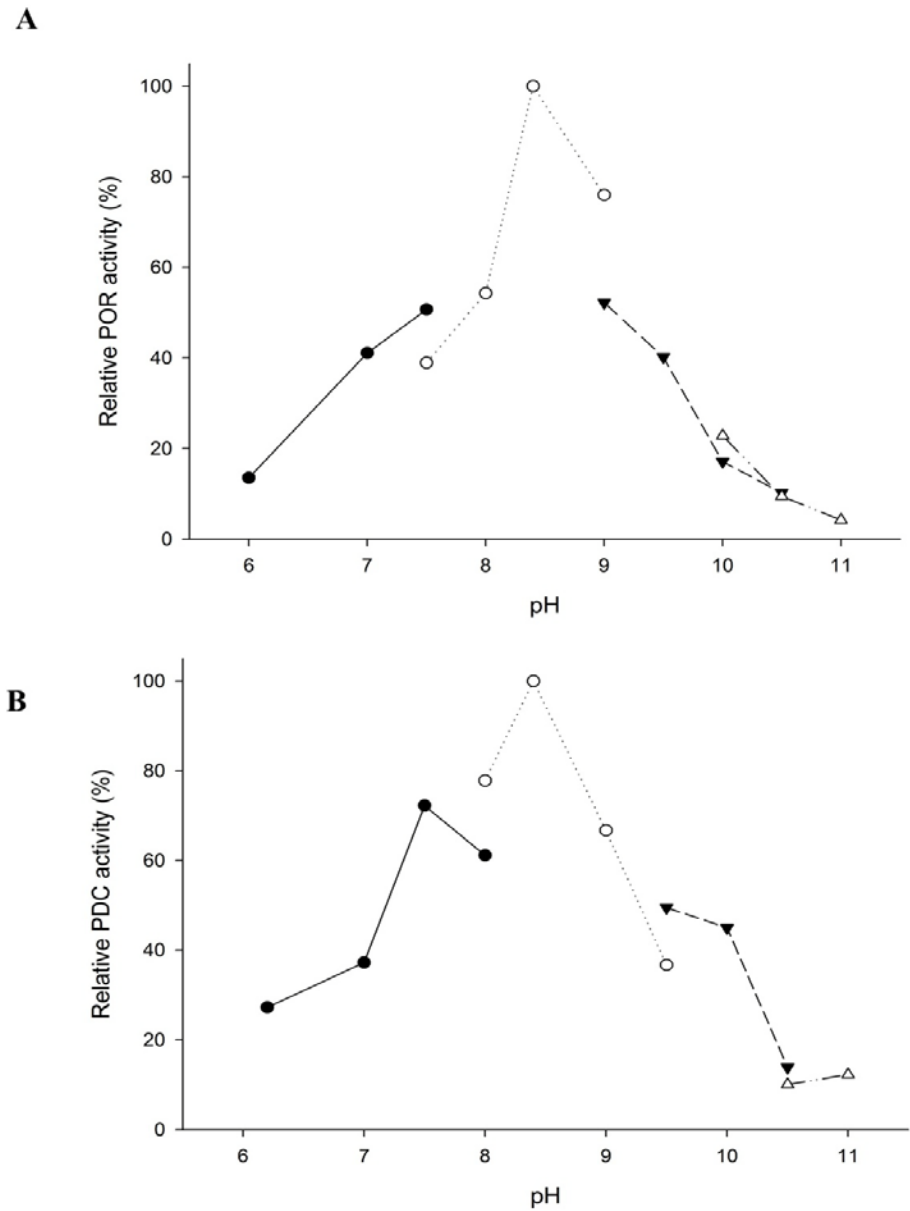


Figure 3-7. pH dependency of POR (A) and PDC (B) activities of bifunctional POR/PDC from *T. maritima*

POR and PDC activities were measured as described previously (sections 3.3.10 and 3.3.11) under strictly anaerobic conditions and at 80°C. The relative activities of 100% equals to highest measured specific activity for both enzymes at 80°C and in EPPS buffer, pH 8.4 (99.1 U_{mg}⁻¹ for POR and 1.8 U_{mg}⁻¹ for PDC activity). The filled circles represent the sodium phosphate buffers (pH 6.2, 7.0, 7.5, and 8.0); the open circles represent the EPPS buffer (pH 8.0, 8.4, 9.0, and 9.5); the filled triangles represent glycine buffer (pH 9.5 and 10); and open triangles represent the CAPS buffer (pH 10.5 and 11.0).

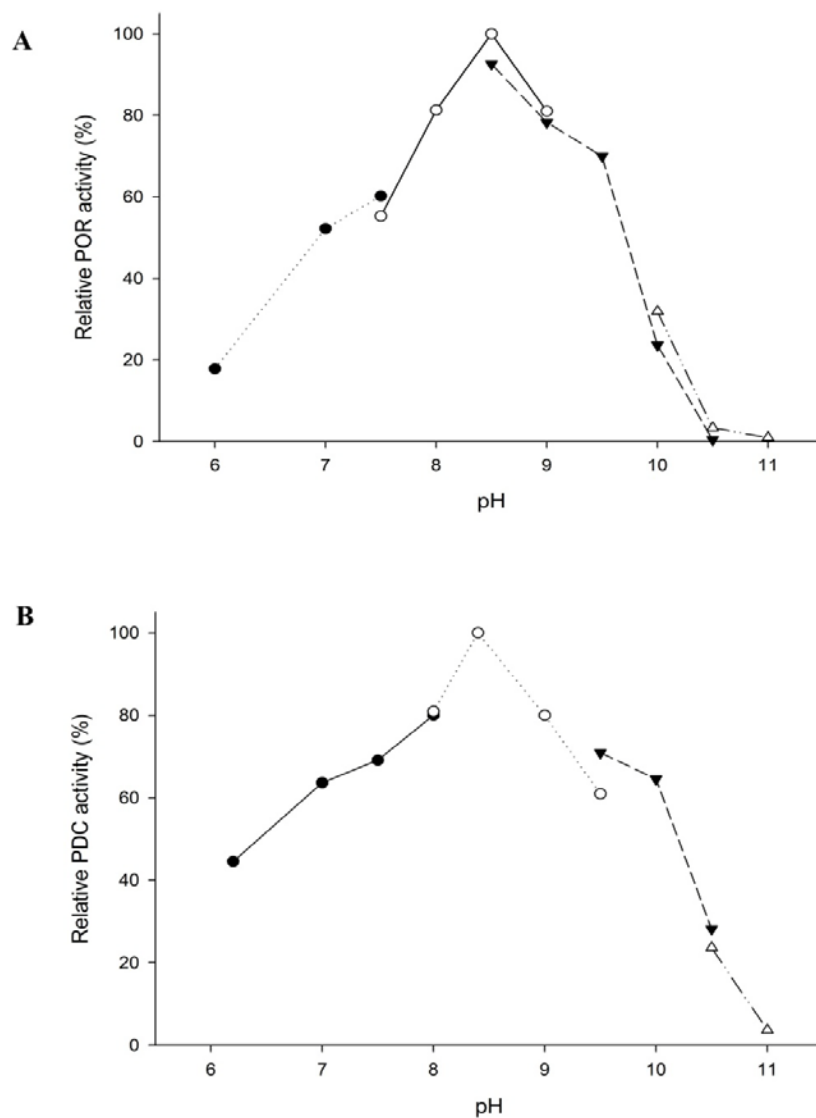


Figure 3-8. pH dependency of POR (A) and PDC (B) activities of the bifunctional POR/PDC from *T. hypogea*

POR and PDC activities were measured as described previously (sections 3.3.10 and 3.3.11) under strictly anaerobic conditions and at 80°C. The relative activities of 100% equals to highest measured specific activity for both enzymes at 80°C and in an assay mixture containing 100 mM EPPS buffer (pH 8.4), 1 mM magnesium chloride, 10 mM sodium pyruvate, 1 mM thiamine pyrophosphate (TPP), and 1 mM CoA (78.0 U μg^{-1} for POR and 1.8 U μg^{-1} for PDC activity). The filled circles represent the sodium phosphate buffers (pH 6.2, 7.0, 7.5, and 8.0); the open circles represent the EPPS buffer (pH 8.0, 8.4, 9.0, and 9.5); the filled triangles represent glycine buffer (pH 9.5 and 10); and open triangles represent the CAPS buffer (pH 10.5 and 11.0).

The kinetic constants were calculated using data fitted to the Michaelis-Menten equation for pyruvate, TPP, and CoA in the standard POR and PDC assay mixtures. The results of the kinetic studies were presented in **Table 3-4**. It is not clear that how valid are the apparent K_m values determined for TPP, as it is not a substrate for the enzyme and even without addition of the TPP to the assay mixture, both enzymes preserved considerable levels of the activity. In the absence of TPP in the assay mixture, the enzyme of *T. hypogea* and *T. maritima* showed 67% and 80% of the full activity, respectively.

The sensitivity toward molecular oxygen is a common property of majority of PORs. The only exceptions so far are the enzymes characterized from the halophilic bacterium *H. salinarium* (Kerscher and Oesterhelt 1981b; Plaga *et al.* 1992) and the mesophilic sulfate-reducing bacterium *D. africanus* (Pieulle *et al.* 1995; Pieulle *et al.* 1997; Pieulle *et al.* 1999b). In Thermotogales, both activities of TmPOR/PDC and ThPOR/PDC were extremely sensitive to oxygen. Exposure of the CFEs to air or the addition of trace amounts of air during the assay or purification resulted in a complete loss of both (POR and PDC) activities. Hence, all of the preparations that were used for the oxygen sensitivity experiment contained no extra SDT and DTT, other than the 2 mM SDT and DTT supplemented into the buffer used for enzyme dilution. This results in SDT and DTT final concentrations of approximately 0.5-1.0 mM. The previously reported half-life ($t_{1/2}$) of TmPOR at room temperature was about 70 min (Blamey and Adams 1994). The half-life ($t_{1/2}$) that was acquired in the course of the experiments in this study was less than 10 min for the POR and less than 15 min for the PDC activity in TmPOR (**Figure 3-9** panels A and C, respectively). The differences were presumably the result of differences in the amount of the reducing agents (SDT and/or DTT) present in the enzyme preparation as well as the difference in protein concentration of the enzyme preparations used for the experiment. The *T. hypogea* enzyme was exceedingly sensitive to oxygen with $t_{1/2}$ determined for POR and PDC activities to be at 5 min or less (**Figure 3-9** panels B and D, respectively).

The temperature dependence of the POR activity of *T. maritima* was investigated previously, TmPOR activity was detected at 35°C and the rate of the reaction constantly increased up to 95°C (Blamey and Adams 1994). There was POR activity detected at temperatures from 35°C and PDC activity was detected at temperatures from 60 to 95°C (**Figure 3-10**). Similar temperature dependence trend was observed for the enzyme isolated from *T. hypogea*. Optimal temperatures for POR and PDC were approximately 90°C and 80°C (**Figure 3-11**). The differences in the optimal temperatures were observed repeatedly and seemed to be reflective of differences between the stability of each activity.

Table 3-4. Kinetic parameters for POR and PDC activities of *T. hypogea* and *T. maritima*^a

Source	activity	Pyruvate ^b		TPP (μM) ^c		CoA (μM) ^d		MV (mM) ^e		Specific Activity ^f
		Apparent K_m (mM)	Apparent V_{max} (Umg ⁻¹)	Apparent K_m (mM)	Apparent V_{max} (Umg ⁻¹)	Apparent K_m (mM)	Apparent V_{max} (Umg ⁻¹)	Apparent K_m (mM)	Apparent V_{max} (Umg ⁻¹)	
<i>T. maritima</i>	POR ^g	0.4±0.09	81±6.2	43	NR	63±6.4	94±2.1	-	-	90.8±11
	PDC	0.92±0.28	1.4±0.04	-	-	3.1±1.2	1.3±0.03	NA	NA	1.4±0.15
<i>T. hypogea</i>	POR	0.13±0.03	99±2.9	14±2.2	58±2.5	21±2.3	73±3.6	0.14±0.03	81.4±5.5	96.7±15.1
	PDC	1.4±0.4	2.5±0.18	-	-	1.4±0.02	1.6±0.13	NA	NA	1.82±0.44

^a NA, not applicable; -, not determined

^b For POR measured at 0.1 mM CoA, 1 mM MV, 0.4 mM TPP, and for PDC at 1mM CoA, 0.1mM TPP

^c For POR measured at 0.1 mM CoA, 1 mM MV, and 5 mM pyruvate

^d For POR measured at 5 mM pyruvate, 1 mM MV, 0.4 mM TPP, and for PDC at 10mM pyruvate, 0.1mM TPP

^f Expressed as micromoles of pyruvate oxidized per min per mg of enzyme

^g Values reported by Blamey *et. al.* (1994), are 14.5 mM and 340 μM as K_m values for the pyruvate and CoA, respectively. The assays were conducted using EPPS (50 mM, pH 8.4) and at 80°C

The thermal stability was determined for the POR and PDC activities of the enzyme purified from *T. hypogea* by incubation of enzyme aliquots at 80°C and the residual activities were measured at different time intervals. Although ideally such assays needed to be done using the same batch of the enzyme for both activity assays, two different batches of the enzymes (but from the same purification round) were used for these assays, due to technical difficulties (different assay procedures for POR and PDC assays and time restraints). The results indicated that both activities were highly stable at 80°C. The time required for a 50% loss of POR activity ($t_{1/2}$) of the purified enzyme (1.7 mgml⁻¹ in 50 mM Tris-HCl [pH 7.8] containing 0.5-1.0mM SDT and 0.5-1.0mM DTT) was about 180 min (~3 h) at 80°C (**Figure 3-12A**). The half-life ($t_{1/2}$) for PDC activity of the same enzyme (0.9 mgml⁻¹ in 50 mM Tris-HCl [pH7.8], containing 0.5-1.0 mM SDT and 0.5-1.0 mM DTT) was about 130 min.

The ability of bifunctional Tm- and Th-POR/PDC to catalyze non-oxidative decarboxylation of 2-ketoisovalerate was also investigated. A standard curve was prepared under the same assay conditions as PDC assay (anaerobic conditions, 80°C) using various amounts of isobutyraldehyde, the product of the non-oxidative decarboxylation of 2-ketoisovalerate. ThPOR could catalyze non-oxidative decarboxylation of 2-ketoisovalerate with a rate of about 10% of the reaction with pyruvate (specific activity 0.14 Umg⁻¹ compared to 1.4 Umg⁻¹). *T. maritima* enzyme was also able to catalyze the non-oxidative decarboxylation of 2-ketoisovalerate with an activity of about 13% of the reaction with pyruvate (specific activity of 0.18 Umg⁻¹ compared to 1.4 Umg⁻¹).

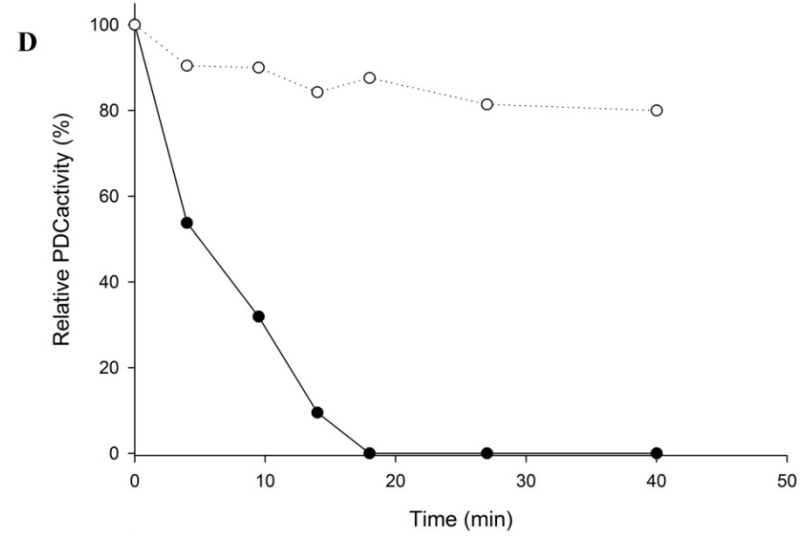
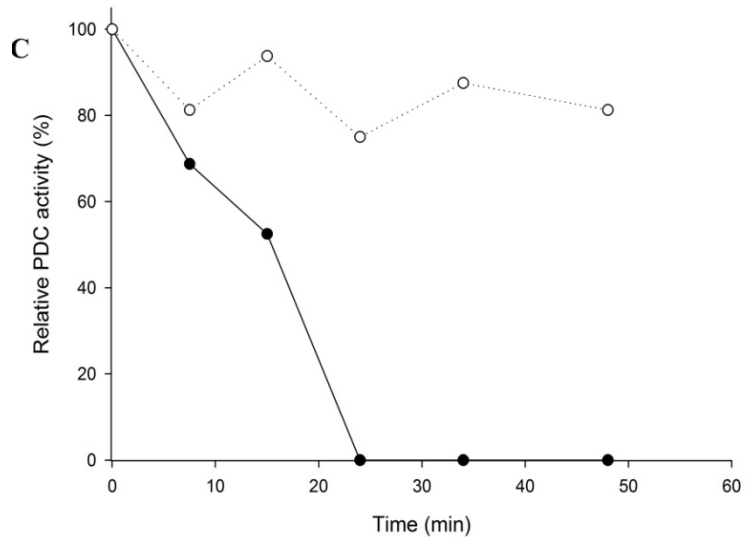
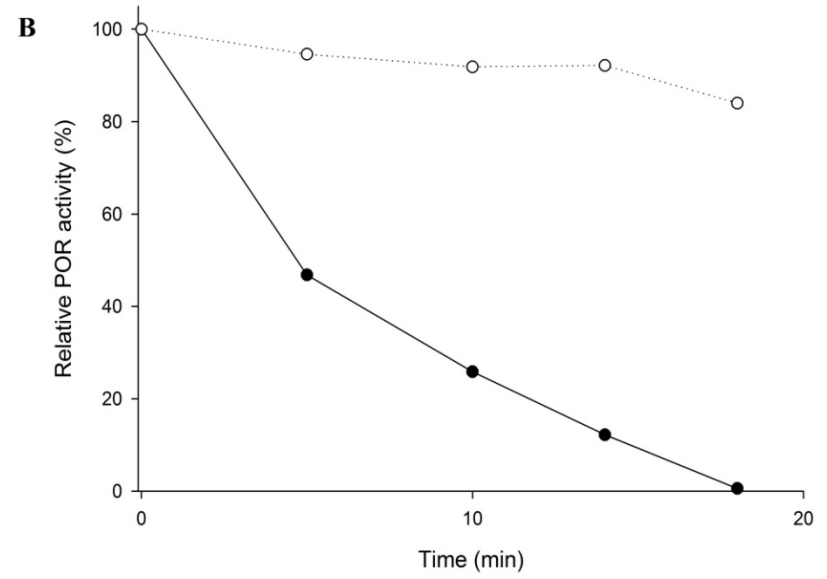
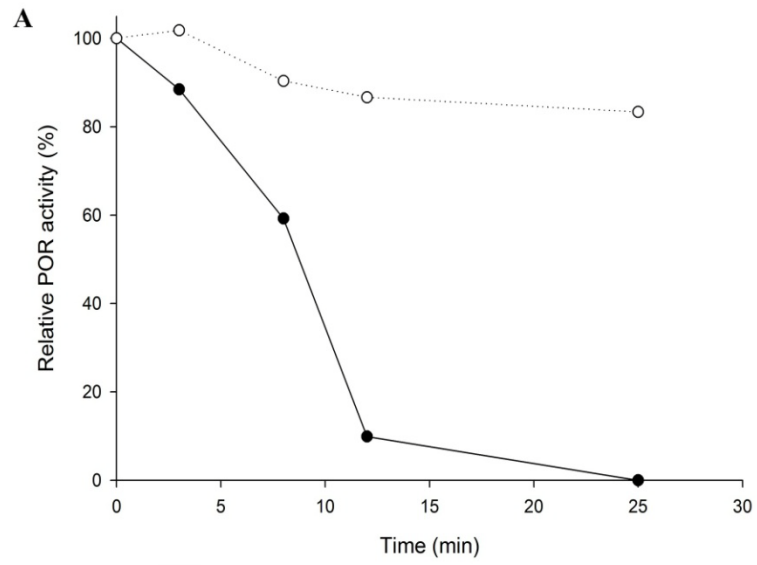


Figure 3-9. Oxygen sensitivity of POR and PDC activities of *T. maritima* and *T. hypogea*

TmPOR (A), ThPOR (B), TmPDC (C), and ThPDC (D) activities were measured in the samples exposed and un-exposed to air. The enzyme assays were conducted as described previously (section 3.3.10 and 3.3.11) under strictly anaerobic conditions. The assay mixtures for POR assay contained 100 mM EPPS buffer, pH 8.4, 1 mM magnesium chloride, 5 mM sodium pyruvate, 0.4 mM thiamine pyrophosphate (TPP), and 0.1 mM CoA. The assay mixture for the PDC assay contained 100 mM EPPS buffer, pH 8.4, 1 mM magnesium chloride, 10 mM sodium pyruvate, 0.1 mM thiamine pyrophosphate (TPP), and 1 mM coenzyme A. The relative activities of 100% equals to highest measured specific activity at time zero with no exposure to air (90 Umg^{-1} and 1.6 Umg^{-1} for *T. maritima* POR and PDC activities, respectively and 66.2 Umg^{-1} and 2.1 Umg^{-1} for *T. hypogea* POR and PDC activities, respectively). The filled circles indicate the exposed samples and the open circles indicate the un-exposed controls.

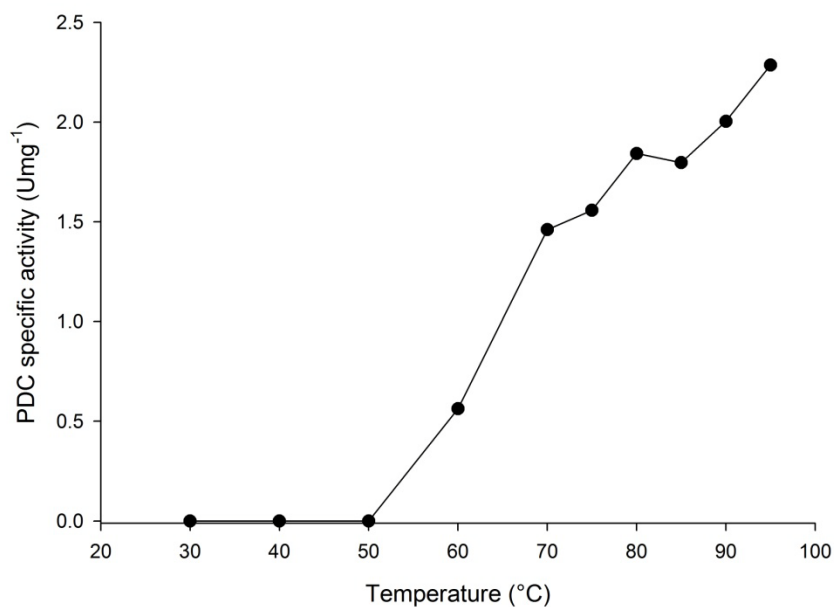


Figure 3-10. Temperature dependence of *T. maritima* PDC activity

PDC assays were conducted as described in Material and Methods (section 3.3.11) standard assay conditions, except temperature was varied. The vials containing the standard assay mixture were pre-incubated at each temperature for 4 min. The reactions were started by adding the enzyme. The assay mixtures (1 ml total volume) contained 100 mM EPPS buffer, pH 8.4, 1 mM magnesium chloride, 10 mM sodium pyruvate, 1 mM thiamine pyrophosphate (TPP), and 1 mM coenzyme A.

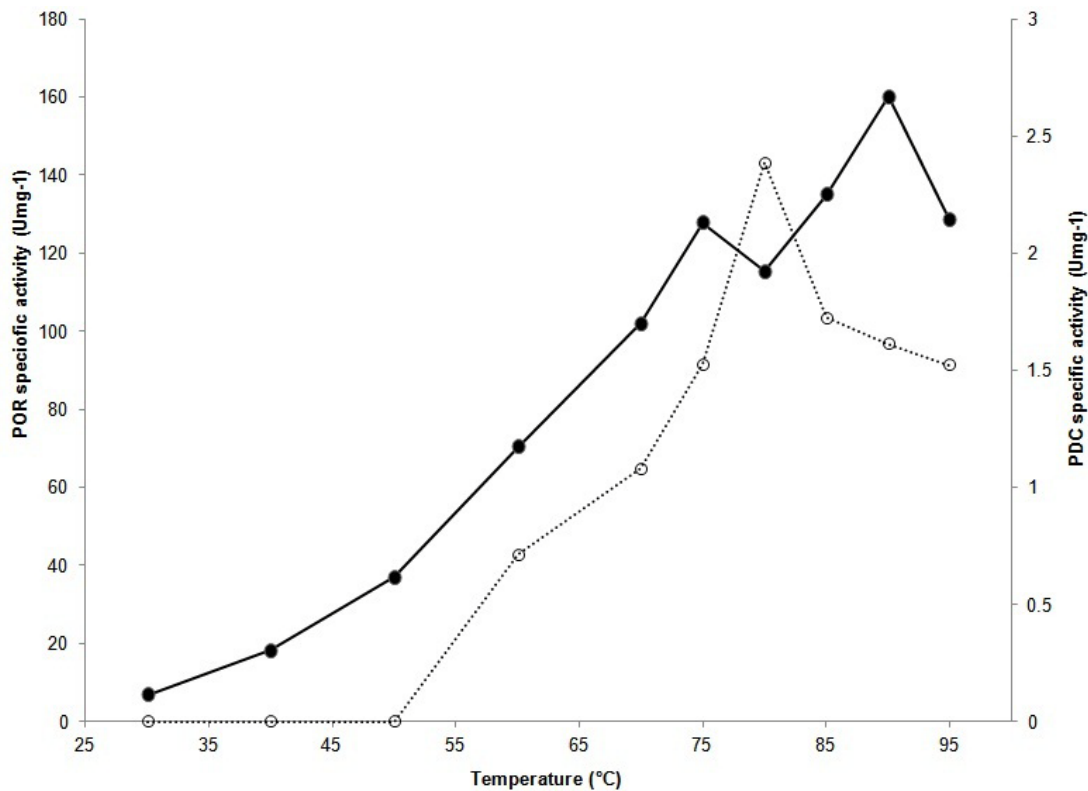


Figure 3-11. Temperature dependence of *T. hypogea* POR and PDC activities

POR and PDC assays were conducted as described in the material and methods (section 3.3.10 and 3.3.11, respectively) under standard assay conditions except the temperature was varied. The vials containing the standard assay mixture were pre-incubated at each temperature for 4 min. In each case the reactions were started by adding the enzyme. The assay mixtures for POR assay contained 100 mM EPPS buffer, pH 8.4, 1 mM magnesium chloride, 5 mM sodium pyruvate, 0.4 mM thiamine pyrophosphate (TPP), and 0.1 mM coenzyme A. The assay mixture for the PDC assay contained 100 mM EPPS buffer, pH 8.4, 1 mM magnesium chloride, 10 mM sodium pyruvate, 0.1 mM thiamine pyrophosphate (TPP), and 1 mM coenzyme A. Filled circles indicate the POR activity and the open circles indicate the PDC activity.

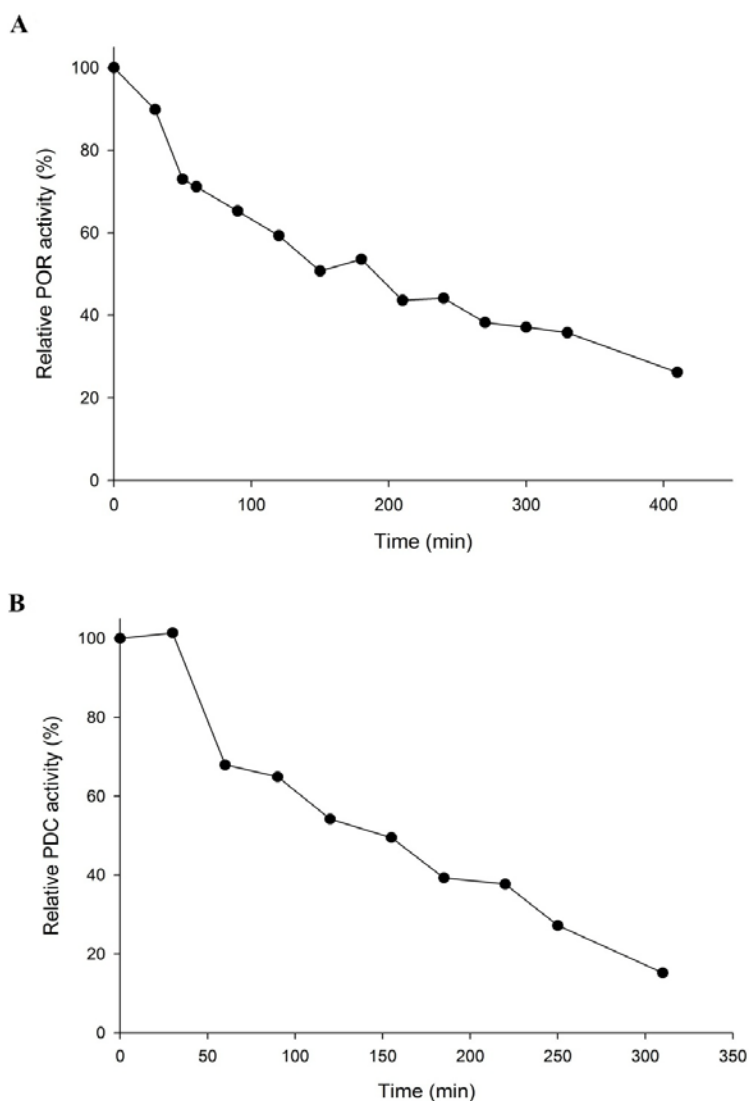


Figure 3-12. Thermal stability of POR (A) and PDC (B) activities of purified ThPOR

Aliquots (approximately 1 ml) of the enzyme were incubated at 80°C and at each time point the corresponding assay were conducted to assay the residual activity. All assays were carried out anaerobically and at 80°C. The assay mixtures for POR assay contained 100 mM EPPS buffer, pH 8.4, 1 mM magnesium chloride, 5 mM sodium pyruvate, 0.4 mM TPP, and 0.1 mM coenzyme A. The enzyme had 1.7 mgml⁻¹ protein in 50 mM Tris-HCl [pH 7.8] containing 2 mM SDT and 2 mM DTT. The assay mixture for the PDC assay contained 100 mM EPPS buffer, pH 8.4, 1 mM magnesium chloride, 10 mM sodium pyruvate, 0.1 mM TPP, and 1 mM coenzyme A. The enzyme preparation had 0.9 mgml⁻¹ protein in 50 mM Tris-HCl [pH 7.8] containing 2 mM SDT and 2 mM DTT. The relative activities of 100% equals to highest measured specific activity at time zero with no heat-treatment (69.1 U_{mg}⁻¹ for POR activity and 2.1 U_{mg}⁻¹ for PDC activity).

3.5 Discussion

The discovery of ethanologenic capabilities of a growing list of hyper/thermophiles has prompted an increasing attention on isolation and characterization of the enzymes that are involved in the alcohol production pathways. Although the list of the ADHs involved in the process is getting longer, there is not much progress in characterization of enzymes involved in production of aldehydes. Unlike the ADHs, which are widely distributed (Reid and Fewson 1994; Radianingtyas and Wright 2003), the enzymes that catalyze acetaldehyde production are quite rare in prokaryotes. There are two major classes of acetaldehyde-producing enzymes in various ethanologenic organisms: the commonly-known pyruvate decarboxylases, which are rare in bacteria and completely absent from the hyper/thermophiles, and the coenzyme A-dependent acetaldehyde dehydrogenases, which are present in mesophilic and some thermophilic bacteria like *Thermoanaerobacter* (Burdette and Zeikus 1994; Peng *et al.* 2008; Yao and Mikkelsen 2010b) and *Geobacillus* species (Taylor *et al.* 2009), but not in any hyperthermophilic bacterium or archaeon (this study).

POR catalyzes the oxidative decarboxylation of pyruvate to acetyl-CoA and CO₂, and the resulting reduced ferredoxins are usually re-oxidized by various [NiFe]- and/or [FeFe]-type hydrogenases (Ma *et al.* 1997; Ma *et al.* 2000; Joe Shaw *et al.* 2008; Schut and Adams 2009). The POR isolated from the hyperthermophilic archaeon *P. furiosus* can also catalyze the non-oxidative decarboxylation of pyruvate to produce acetaldehyde (Ma *et al.* 1997). It was shown that the same bifunctionality is also present in the PORs from the extremely thermophilic bacteria *T. hypogea* and *T. maritima*.

Comparison of the deduced nucleotide sequence of genes encoding the POR of *T. hypogea* with other POR-encoding genes from other fully sequenced members of the Thermotogales have provided a complete picture of the POR operon structure and gene organization (**Figure 3-2**). Unlike the POR/VOR operon in the hyperthermophilic archaea, which is transcribed as at least three transcripts, there seems to be only one transcript produced from the POR operon of Thermotogales (Kletzin and Adams 1996). The genes encoding all of the four subunits have overlapping intercistronic sequences, and the ribosome-binding sites (RBSs) are located in the coding sequence of the previous gene. This mechanism ensures that after its binding to first RBS (*porG*), the translation of next gene does not require detachment and re-attachment of the ribosome. This seems to be a mechanism to assure that all four subunits of the enzyme are being translated and eventually translated with the same ratio (Nichols and Yanofsky 1979; Schoner *et al.* 1984). That finding is further supportive of the 1:1 subunit stoichiometry of PORs suggested in previous studies (Kunow *et al.* 1995).

The deduced amino acid sequence of each subunit showed close relatedness of PORs of *T. hypogea* and *T. maritima* to other bacterial and archaeal PORs, especially within the members of the order Thermotogales (**Figure 3-3**). General biophysical properties of TmPOR and ThPOR were also quite similar to other hyper/thermophilic 2-keto acid oxidoreductases (Blamey and Adams 1993; Blamey and Adams 1994; Iwasaki *et al.* 1995; Ikeda *et al.* 2006). During purification, POR and PDC activities were co-eluted from various chromatography columns, and PDC to POR ratios were constant after each step (**Figure 3-6**) which is supportive of the bifunctionality of the enzymes. Both POR and PDC activities were extremely sensitive to exposure to air (**Figure 3-9**). PORs from *T. maritima* and *T. hypogea* were found to be heterotetramers ($\alpha\beta\gamma\delta$ structure) which is consistent with previously characterized PORs from hyperthermophiles (Blamey and Adams 1993; Blamey and Adams 1994). Thermotogales PORs were composed of four subunits with apparent molecular sizes of approximately 45, 35, 22 and 12 kDa, respectively (**Figure 3-5 A and B**) and a native molecular weight of approximately 155 kDa which are similar to previously characterized bifunctional POR/PDC isolated from the hyperthermophilic archaeon *P. furiosus*, and PORs from *A. fulgidus* and *M. maripaludis* (Blamey and Adams 1993; Kunow *et al.* 1995; Lin *et al.* 2003).

The optimal pH for POR activity of the enzyme from *T. maritima* was determined to be pH 8.4 (**Figure 3-7**), which is not in agreement with the value of 6.3 previously reported by Blamey and Adams (1994). The previous optimal pH was low compared to optimal pH values reported for other PORs (**Table 3-5**). The purified enzyme from *T. hypogea* showed an optimal pH for both POR and PDC activities at 8.4. The optimal pH for the PDC activity of the enzyme from *T. maritima* was also 8.4 (**Figure 3-7**). In the case of purified enzyme from *T. hypogea* the optimal pH for both POR and PDC activities was found to be 8.4 (**Figure 3-8**). These values were different from the bifunctional POR/PDCs characterized in archaea, where the PDCs generally had higher pH optima (pH 10.2 for *P. furiosus* and pH 9.5 for *Thermococcus guaymasensis*) compared to POR activities, which have optimal pHs closer to neutral (**Table 3-5**). Taking the effect of the temperature on pH of the buffers, the optimal pH for the bifunctional PDC activities (pH 7.5) at 80°C is still higher than most of the commonly-known PDCs from different mesophilic bacteria and yeasts, which generally have slightly acidic pHs (pH 5.5-6.5) for optimal activity (Raj *et al.* 2002). The only exception is the PDC from the Gram-positive bacterium *Sarcina ventriculi* with an optimal pH value higher than neutral pH with a range of pH of 6.3-7.6 (Lowe and Zeikus 1992; Talarico *et al.* 2001).

T. maritima POR is reported to be highly temperature-dependent, and has an optimal temperature above 95°C (Blamey and Adams 1994). Its PDC activity also followed a similar increasing trend, and had a maximal activity at above 95°C (**Figure 3-10**). However, POR and PDC activities of *T. hypogea* enzyme showed different thermal dependencies as the POR activity constantly increased, from 30°C to

90°C, while PDC activity showed an increasing trend starting from 60°C up to 80°C, and its activity decreased at temperatures higher than 80°C (**Figure 3-11**).

The difference between minimum temperatures determined for the activities might be attributed to the lower sensitivity limit of the PDC assay procedure compared to POR assay. The thermal liability of the assay components does not appear to be a factor, as both (POR and PDC) assay mixtures contains same components and, in fact, POR assay mixture contained fewer amounts of pyruvate and CoA and still showed full activity at temperatures higher than 80°C. Moreover, all of the assay components were relatively stable at high temperatures; the time required for a 1 mM solution of TPP (pH 8.0) to lose 50% of its cofactor activity is about 70 min at 80°C. Coenzyme A (1 mM, pH 8.0) is also resistant to heat-denaturation, with a half-life of about 90 min at 80°C (Adams and Kletzin 1996). Such temperature difference was not observed for TmPOR/PDC.

Bifunctional POR and PDC of *T. hypogea* were thermostable which was shown by their half-lives of about 3 h and 2 h at 80°C, respectively (**Figure 3-12 A and B**). The POR of *T. maritima* is also stable under anaerobic conditions with $t_{1/2}$ of 11 h, which made the enzyme the most thermostable POR characterized so far (Blamey and Adams 1994). PfPOR had $t_{1/2}$ of only 18 min at 80°C (Blamey and Adams 1993). Since both TmPOR and PfPOR are optimally active at above 90°C, the difference between their thermal stabilities is intriguing. However, considering the optimal growth temperature (T_{opt}) of 70°C for *T. hypogea*, and 80°C for *T. maritima* it was not unexpected that ThPOR would displayed less thermal stability than TmPOR.

Apparently most enzyme-bound TPPs were dissociated during purification of enzymes from *T. hypogea* and *T. maritima* which is similar to other reports on purification and characterization of PORs from *T. maritima* (Blamey and Adams 1994) and mesophilic bacteria (Wahl and Orme-Johnson 1987; Brostedt and Nordlund 1991). The addition of TPP, could result in a full recovery of both POR and PDC activities. Only negligible amounts of activity could be detected for both POR and PDC from *T. hypogea* enzyme, if TPP was omitted from the assay mixture (5% and 12% for POR and PDC activities, respectively). *T. maritima* enzyme displayed approximately 30% of its full activity of both POR and PDC.

When CoA was omitted from the enzyme assay mixture, CFE of *T. maritima* showed some residual PDC activity of about 0.012 Umg^{-1} . Such residual activity might be the result of uncharacterized PDC activities or the results of residual CoA remained in CFE. The *T. maritima* acetohydroxyacid synthase (AHAS) was found to be able to catalyze non-oxidative decarboxylation of 2-keto acid to

Table 3-5. Kinetic properties of some characterized PORs^a

Organism	Apparent K_m value for				Optimal pH	Specific activity ^b (Umg ⁻¹)	Reference
	Pyruvate (mM)	TPP (μ M)	CoA (μ M)	MV (μ M)			
<i>Trichomonas vaginalis</i>	0.14	-	2.5	-	7.0 ^c	18	Williams <i>et al.</i> 1987; Meza-Cervantez <i>et al.</i> 2011
<i>Archaeoglobus fulgidus</i>	0.3	-	20	100	7.5	74	Kunow <i>et al.</i> 1995
<i>Clostridium acetobutylicum</i>	0.33	-	3.7	-	7.5	25	Drake <i>et al.</i> 1981; Meinecke <i>et al.</i> 1989
<i>Desulfovibrio africanus</i>	2.5	-	0.5	500	9.0	14	Pieulle <i>et al.</i> 1995
<i>Halobacterium salinarium (halobium)</i>	1.1	-	NR	-	9.0	6	Kerscher and Oesterhelt 1981b
<i>Helicobacter pylori</i>	NR	-	NR	-	8	2.5	Hughes <i>et al.</i> 1995
<i>Hydrogenobacter thermophilus</i>	3.45	-	54	-	7.6	3.46	Yoon <i>et al.</i> 1997
<i>Klebsiella pneumonia</i> ^d	2.0	-	4	-	7.0	6.0	Shah <i>et al.</i> 1983; Wahl and Orme-Johnson 1987
<i>Methanosarcina barkeri</i>	0.07	-	6	70 ^e	7.0	25	Bock <i>et al.</i> 1996
<i>Pyrococcus furiosus</i>	0.46	-	110	-	8.0	21	Blamey and Adams 1993; Schut <i>et al.</i> 2001a
<i>Thermococcus guaymasensis</i>	0.53	-	70	90	8.4	22.3	this study
<i>Thermotoga hypogea</i>	0.13	14	21	140	8.4	96.7	this study
<i>Thermotoga maritima</i> ^f	0.4	43	63	-	8.4	90.8	Blamey and Adams 1994, this study
<i>Trichomonas vaginalis</i>	0.14	-	2.5	-	7	18.3	Williams <i>et al.</i> 1987

^a -, not reported

^b Expressed as micromoles of pyruvate oxidized per min per mg of enzyme

^c The optimal pH is not reported in the reference, and this is the pH used for the assay

^d Pyruvate flavodoxin oxidoreductase.

^e Benzyl viologen.

^f K_m values reported by Blamey *et al.* (1994) are 14.5 mM, 340 μ M, for pyruvate, CoA, respectively. The optimal pH is 6.3

corresponding aldehydes (Chapter 4). However, such “alternative PDC activity” was not present in the CFE of the closely related bacterium *T. hypogea*, that most likely lacks the AHAS (Chapter 4). Moreover, there might be some other acetaldehyde-producing activities not detectable under the conditions used for the assay.

The PDC to POR ratios of the enzymes from hyper/thermophilic bacteria *T. hypogea* and *T. maritima* were much lower (>10 times) than the ratios from the hyperthermophilic archaea *P. furiosus* (Ma *et al.* 1997 and this study) and *T. guaymasensis* (Chapter 2). The physiological implications of the higher POR activity levels (at least 4-fold) in Thermotogales (hyper/thermophile bacteria) compared to the same activity in the archaeal counterparts (Thermococcales) are not well understood.

Bifunctional *T. hypogea* POR/PDC had lower apparent K_m values for pyruvate in POR activity (0.13 mM) than the 1.4 mM for the PDC activity (**Table 3-4**), suggesting that under normal physiological conditions, POR is most likely the dominant catalytic activity. Apparent K_m values of TmPOR, are reported for both pyruvate and CoA (Blamey and Adams 1994) which are unusually high (14.5 mM and 340 μ M, respectively), compared to the corresponding K_m of the similar enzyme of the closely related *T. hypogea* POR as well as the other PORs (**Table 3-5**). Therefore, the kinetic parameters were determined again for pyruvate and CoA, for TmPOR. As expected, the K_m values were much closer to the apparent K_m values reported from the bacterial and archaeal PORs (0.4 mM and 63 μ M for pyruvate and CoA, respectively) (**Table 3-4**).

The PORs from hyper/thermophilic archaea and bacteria have higher (~10 times) apparent K_m values for CoA than their mesophilic counterparts (**Table 3-5**). The K_m values of the mesophilic PORs have at least an order of magnitude lower K_m values for CoA. This effect cannot be the result of the thermal lability of the CoA, since, as mentioned, CoA is quite stable at 80°C. Surprisingly, the bifunctional PDC activities from bacteria had a lower apparent K_m for CoA which was lower than that for the POR of the same enzyme (**Table 3-4**).

Among the only known PDCs characterized from Gram-negative bacteria *Z. mobilis* (Hoppner and Doelle 1983; Neale *et al.* 1987) and *Z. palmae* (Raj *et al.* 2002), *Acetobacter pastorianus* (Raj *et al.* 2001; Raj *et al.* 2002), and the Gram-positive bacterium *S. ventriculi* (Lowe and Zeikus 1992; Talarico *et al.* 2001), only the enzyme from *S. ventriculi* does not follow the Michaelis-Menten kinetics for pyruvate and displays a sigmoid saturation curve which is typical characteristic of fungal and plant PDCs (Lee and Langston-Unkefer 1985; Wang *et al.* 2004). The bifunctional POR/PDC studied from hyperthermophiles displayed Michaelis-Menten kinetics for pyruvate (Ma *et al.* 1997

and this study). The apparent pyruvate K_m values for pyruvate of the bacterial PDCs were all about 0.3 mM (Raj *et al.* 2001; Raj *et al.* 2002), which is lower than the values determined for PDCs from *T. hypogea* and *T. maritima*, which were 1.4 mM and 0.92 mM, respectively (**Table 3-4**).

Both bifunctional enzymes of *T. maritima* and *T. hypogea* were able to catalyze the non-oxidative decarboxylation of 2-ketoisovalerate in the presence of CoA, although at a much lower rate compared to pyruvate. When pyruvate was substituted with 2-ketoisovalerate in PDC assays, the enzymes from *T. maritima* and *T. hypogea* displayed approximately 13% and 10% of full activity with pyruvate, respectively. Surprisingly, none of these enzymes were able to catalyze the oxidative decarboxylation of 2-ketoisovalerate when measured in the oxidation direction. It was reported that TmPOR is unable to catalyze the oxidative decarboxylation of 2-oxoglutarate, indolyl pyruvate, and phenyl pyruvate (Blamey and Adams 1994), however, the ability of the enzyme to catalyze the oxidation of 2-ketoisovalerate was not examined at that time. Here, it was shown that TmPOR could catalyze the oxidative decarboxylation of 2-ketoisovalerate with only about 0.7% of the rate of POR oxidation, and ThPOR cannot catalyze the oxidative decarboxylation of the 2-ketoisovalerate. It is found that only one type of 2-keto acid oxidoreductase (*i.e.* POR) is present in prokaryotic and eukaryotic microorganisms which is different from the situation in hyperthermophilic archaea, which contain at least four types of the 2-keto acid ferredoxin oxidoreductases (namely POR, VOR, KGOR, and IOR). Therefore, it would be expected that the bacterial POR have a wider substrate range than the archaeal enzyme. However, TmPOR has strict substrate specificity for pyruvate. Similarly, ThPOR had a very low apparent K_m value for the pyruvate (**Table 3-5**) and could not use 2-ketoisovalerate as substrate in the oxidation direction implying the high affinity of the enzyme to use pyruvate as substrate.

T. hypogea is capable of producing ethanol (Fardeau *et al.* 1997). An iron-containing ADH with lower apparent K_m values for reducing acetaldehyde and butyraldehyde compared to that for ethanol and butanol was isolated from these bacteria suggesting (Ying *et al.* 2007) its physiological role in production of alcohols from aldehydes. However, no aldehyde-producing activity was known in *T. hypogea* or any other hyper/thermophilic bacterium. Here the PDC activities of both TmPOR and ThPOR were confirmed - for the first time- that are most likely involved in aldehyde production in hyperthermophilic bacteria. CFE of *T. hypogea* contains approximately 0.2 U mg^{-1} of ADH activity (Ying *et al.* 2007) compared to specific PDC activity in CFE of about 0.08 U mg^{-1} , indicating that the production of ethanol is limited by availability of aldehydes, the substrates used by ADH.

**Chapter 4 AHAS/PDC activities of recombinant AHAS
from *Thermotoga maritima***

4.1 Overview

Acetohydroxyacid synthase (AHAS) activity was determined to be present in the cell-free extracts of different archaeal and bacterial hyperthermophiles including *Thermococcus guaymasensis*, *Thermococcus kodakaraensis*, *Pyrococcus furiosus* (Pf), *Thermotoga maritima* (Tm), *Thermotoga hypogea*, and *Thermotoga neapolitana*. Higher AHAS activity was found in the organisms harboring the BCAA biosynthesis operon (*ilv* operon) with an optimum at neutral pH, and lower activity in members of the genus *Thermococcus* which have no *ilv* operon in their genomes at higher pH (pH 10.5), suggesting the presence of a possible alternative uncharacterized enzyme with AHAS activity.

T. maritima and *P. furiosus* cell-free extract showed AHAS specific activities of $100.2 \pm 9 \text{ mUmg}^{-1}$ and $73 \pm 6 \text{ mUmg}^{-1}$, respectively. The genes encoding the catalytic and regulatory subunits of AHAS from both organisms were cloned and over-expressed in an *Escherichia coli* strain containing a plasmid expressing tRNAs that are rare in *E. coli*. The recombinant proteins were purified using a simplified procedure including a heat-treatment step to precipitate *E. coli* proteins. The catalytic (large) subunit of *T. maritima* AHAS was purified approximately 30-fold following two chromatography steps, resulting in an AHAS activity of approximately 163 Umg^{-1} . Its native molecular mass was determined to be $156 \pm 6.2 \text{ kDa}$ suggesting a dimeric structure. The regulatory (small) subunit had no catalytic activity and was purified to homogeneity via denaturing immobilized metal affinity chromatography (IMAC). The purified regulatory subunit showed a native molecular mass of approximately $37.7 \pm 0.4 \text{ kDa}$, suggesting a dimeric structure. The recombinant *T. maritima* enzyme also had pyruvate decarboxylase (PDC) activity that catalyzed the reaction from pyruvate to acetaldehyde and CO_2 at a rate approaching 10% of AHAS activity. Reconstitution of the catalytic and regulatory subunits led to increased AHAS and PDC activities that were consistent with the findings on bacterial and fungal AHASs. The addition of both TPP and FAD in the assay mixture resulted in increased levels of both AHAS and PDC activities, indicating the cofactors (TPP and FAD) were partly dissociated from the recombinant enzymes during purification. Both activities had the same pH and temperature optima of 7.0 and 85°C , respectively. The recombinant AHAS/PDC was thermostable with a half-life of approximately 23 h at 80°C when incubated in sealed vials anaerobically without stirring. When stirred under aerobic conditions, both activities had a half-life ($t_{1/2}$) of approximately 30 min. Under anaerobic conditions the half-life of the enzyme was prolonged to approximately 85 min and 110 min for AHAS and PDC activities, respectively. Without stirring, it was quite stable and remained highly active even after 5 days at 4°C under anaerobic conditions, suggesting the destructive effect of stirring on the enzyme. This was the first characterization of a hyperthermophilic AHAS and the discovery of 2-keto acid decarboxylase activity in an anabolic AHAS.

4.2 Introduction

Hyperthermophiles are organisms that exhibit optimum growth temperatures of 80°C or above (Stetter 2006; Wagner and Wiegel 2008). During the last decade there has been enormous attention toward biotechnological and industrial applications of hyperthermophiles. One promising avenue is to use the organisms (or their metabolites) in bio-processing of various substrates toward production of value-added commodities (*e.g.*, alcohols). However, advances are hindered by the relatively poor understanding of the physiology and metabolic pathways of these organisms.

Ethanol has been detected as an end-product of fermentation in many extreme thermophiles and some hyperthermophiles (Kengen *et al.* 1994; Ma *et al.* 1995; Balk *et al.* 2002; de Vrije *et al.* 2009; DiPippo *et al.* 2009; Podosokorskaya *et al.* 2011; Ying and Ma 2011). Although some of the enzymes (*e.g.*, alcohol dehydrogenases) involved in the ethanol fermentation pathways have been isolated and characterized from hyper/thermophilic archaea and bacteria, there is limited information available about the other enzymes involved in these metabolic pathways. One of the essential questions about the ethanol production by hyper/thermophiles, is the source of the aldehydes which are the substrates for the alcohol dehydrogenases for the production of alcohols.

Acetaldehyde is the key precursor in the ethanol production pathway and it can be produced by either non-oxidative decarboxylation of pyruvate catalyzed by TPP-dependent enzyme pyruvate decarboxylase (PDC, EC 4.1.1.1) or the reduction of acetyl-CoA catalyzed by a CoA-dependent acetaldehyde dehydrogenase (AcDH, EC 1.2.1.10). However, search of the available genome sequences of the thermophilic and hyperthermophilic bacteria and archaea against the commonly-known (yeast and bacterial) PDC and AcDH amino acid sequences, failed to detect any orthologs (this study). Consequently, the potential role of alternative enzyme(s) for the catalysis of the acetaldehyde production from pyruvate was considered. One such enzyme was discovered to be the bifunctional pyruvate ferredoxin oxidoreductase/pyruvate decarboxylase (POR/PDC) enzyme, which was described first time in the hyperthermophilic archaeon *Pyrococcus furiosus*. This bifunctional enzyme was previously shown to be able to catalyze both oxidative and non-oxidative decarboxylation of pyruvate to produce acetyl-CoA and acetaldehyde, respectively (Ma *et al.* 1997) and the bifunctionality seems to be a universal trait of hyperthermophilic (archaeal and bacterial) PORs.

When the genome sequences of hyper/thermophilic archaea and bacteria were searched for the orthologues of the commonly-known PDCs, the closest hit (when present) is almost exclusively the enzyme acetoxyacid synthase (**Table 4-1**). Like PDC, acetoxyacid synthase is a thiamine pyrophosphate (TPP) - and Mg²⁺-dependent enzyme. Given the high homology levels of the AHAS to the

Table 4-1. Search of the genome sequences of some hyperthermophiles against the commonly-known PDC sequences^a

Organism	Annotation	<i>Saccharomyces cerevisiae</i>	<i>Sarcina ventriculi</i>	<i>Zea mays</i>	<i>Zymomonas mobilis</i>	<i>Aspergillus oryzae</i>	<i>Nicotiana tabacum</i>
<i>Archaeoglobus fulgidus</i>	acetolactate synthase III, (large subunit)	23.5	20.4	17.2	19.7	21.2	17.4
<i>Methanothermobacter thermoautotrophicus</i>	acetolactate synthase large subunit	21.9	21.3	18.8	19.9	20.6	16.8
	pyruvate dehydrogenase / acetolactate	18.1	16.6	18.2	18.1	16.6	13.9
	acetolactate synthase, large subunit	20.5	22.5	19.6	20.2	21.2	17.6
<i>Pyrococcus abyssi</i> GE5	acetolactate synthase, large subunit	22.1	22.8	20.5	22.8	22.5	14.8
<i>Pyrococcus furiosus</i>	acetolactate synthase	22.2	22.2	19.3	22.6	23.9	14.5
<i>Pyrococcus horikoshii</i> OT3	426aa long hypothetical protein	0.5	0.5	0.4	0.2	0.1	0.4
<i>Saccharomyces cerevisiae</i>	yeast PDC isozyme 1	100	36.9	31.0	29.6	47.0	24.5
<i>Sulfolobus acidocaldarius</i>	thiamine pyrophosphate enzyme	21.4	20.4	20.4	20.4	20.3	17.1
<i>Sulfolobus solfataricus</i>	acetolactate synthase large subunit	21.7	21.6	21.7	20.8	22.8	15.8
<i>Sulfolobus tokodaii</i> str.7	acetolactate synthase large subunit	21.4	20.5	21.0	20.4	22.4	16.0
<i>Thermoanaerobacter tengcongensis</i>	thiamine pyrophosphate-requiring enzyme [acetolactate synthase]	21.5	23	19.4	18.8	22.1	17.5
<i>Thermococcus kodakaraensis</i> KOD1	hypothetical protein TK1705	0.1	0.7	1.2	0.8	0.3	0.7
	hypothetical protein, DUF1102 family	3.7	0.5	3.0	1.4	0.2	0.8
<i>Thermotoga maritima</i>	acetolactate synthase, large subunit	21.6	19.4	17.4	19.6	21.4	15.0
<i>Thermus thermophilus</i>	acetolactate synthase large	22.2	20.3	20.3	20.4	22.5	17.7
<i>Zea mays</i>	maize PDC isozyme 1	31.0	28.8	100	39.4	32.4	54.9
<i>Zymomonas mobilis</i>	pyruvate decarboxylase	29.6	30.8	39.4	100	29.7	29.8

^a Genomes in the NCBI microbial genome database (http://www.ncbi.nlm.nih.gov/genomes/MICROBES/microbial_taxtree.html) were used to retrieve the amino acid and nucleotide sequences of PDCs from various organisms. The deduced amino acid sequences were compared to protein sequences retrieved from NCBI, Swiss Prot and EMBL. The search in these databases were carried out using FASTA, BLAST, and PROSITE.

commonly-known PDCs and considering the high frequency of multi-functionality in the superfamily of TPP-dependent enzymes, the question arises: can the enzyme AHAS also catalyze the non-oxidative decarboxylation of pyruvate to acetaldehyde?

Acetohydroxyacid synthase (AHAS, EC 2.2.1.6, formerly and EC 4.1.3.18) can be divided into two classes based on the metabolic/physiological roles, substrate specificity and cofactor (FAD) requirements, the anabolic and catabolic AHASs (Duggleby and Pang 2000; Duggleby *et al.* 2008). The general properties of anabolic and catabolic AHASs are summarized in **Table 4-2**.

The anabolic AHAS catalyzes the first common step in the biosynthesis of the branched-chain amino acids (valine, leucine, and isoleucine) as well as the precursors derived from the same biosynthetic pathway (*e.g.* coenzyme A and pantothenate). The enzyme is relatively prevalent in archaea, bacteria, fungi, algae, and plants, but is absent from animals (Umbarger and Brown 1958; Radhakrishanan and Snell 1960; Grimminger and Umbarger 1979). The anabolic AHAS catalyzes two parallel reactions during which one molecule of pyruvate is decarboxylated, and the resulting “active aldehyde” is condensed with either a second molecule of pyruvate or alternatively a molecule of 2-ketobutyrate producing acetolactate (precursor of valine and leucine) and 2-aceto-2-hydroxybutyrate (precursor of isoleucine), respectively (**Figure 4-1** and **Figure 4-2**).

The anabolic enzymes characterized contain one molecule of FAD per catalytic site (Chipman *et al.* 2005). In all of the cases studied to date, the enzyme is composed of two subunits: a larger active subunit known as catalytic subunit (generally 59-66 kDa) and a smaller (catalytically inactive) subunit known as regulatory subunit (generally 9-35 kDa). The regulatory subunit mediates the regulation of the catalytic subunit through the feedback regulation by one or more of the branched chain amino acids (Weinstock *et al.* 1992). In all of the anabolic AHASs studied to date, the holoenzyme (catalytic and regulatory subunits together) has the highest specific activity. Addition of the purified regulatory subunit to the catalytic subunit leads to at least a several-fold increase in the specific activity of the reconstituted holoenzyme (Chipman *et al.* 2005; McCourt and Duggleby 2006; Duggleby *et al.* 2008; Gedi and Yoon 2012).

The catabolic AHAS (also known as acetolactate synthase; ALS) is usually approximately 60 kDa in size, involved in channeling the excess pyruvate to the less inhibitory product 2-acetolactate and which is converted to 2, 3-butanediol under certain fermentation conditions and by the help of the enzyme acetoin decarboxylase (Störmer 1968b; Störmer 1968c; Störmer 1968a). Unlike the anabolic enzyme, the catabolic enzyme is composed of single subunit and is FAD-independent. Catabolic AHAS is less common compared to the anabolic enzyme and is only found in certain bacterial species including *Klebsiella*, *Bacillus* species, and some lactic acid bacteria (Duggleby and Pang 2000; Pang *et al.* 2004).

Table 4-2. General properties of anabolic and catabolic AHASs

Characteristics	Anabolic (AHAS)	Catabolic (ALS)
Structure	Two type of subunits	One type of subunit
Optimum pH	7-9	~6
FAD requirement	+	-
Inhibition by BCAAs	+	-
Inhibition by acetate	-	+
Prevalence	Many plants, algae, fungi, bacteria, and archaea	few bacteria including <i>Enterobacter</i> , some <i>Klebsiella</i> , <i>Serratia</i> and <i>Bacillus</i> species, certain lactic acid bacteria
Gene organization	In BCAA pathways operon	In butanediol operon

“+” means that the trait is present and “-“ means the trait is absent from each specific class of enzyme.

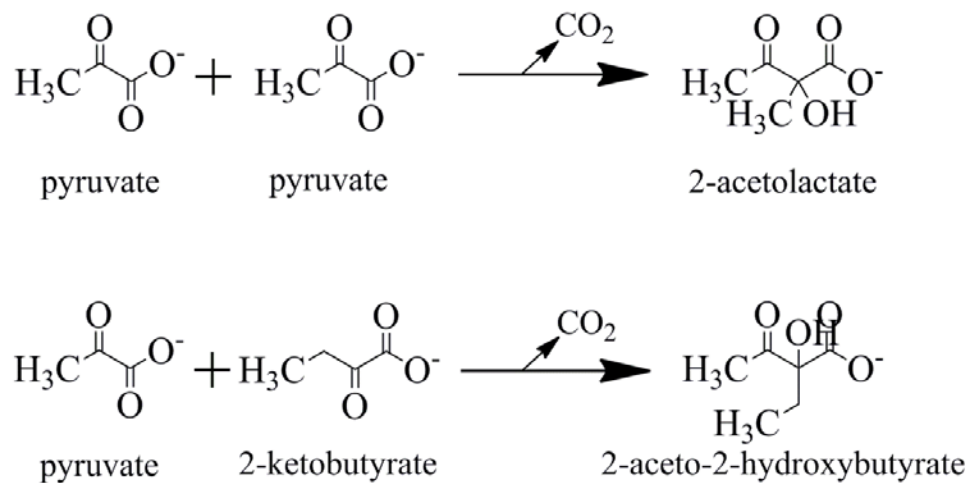


Figure 4-1. Reactions catalyzed by anabolic AHAS and catabolic AHAS (also known as ALS)

The upper reaction is catalyzed by both anabolic and catabolic acetohydroxyacid synthase and the lower reaction is only catalyzed by the anabolic enzyme

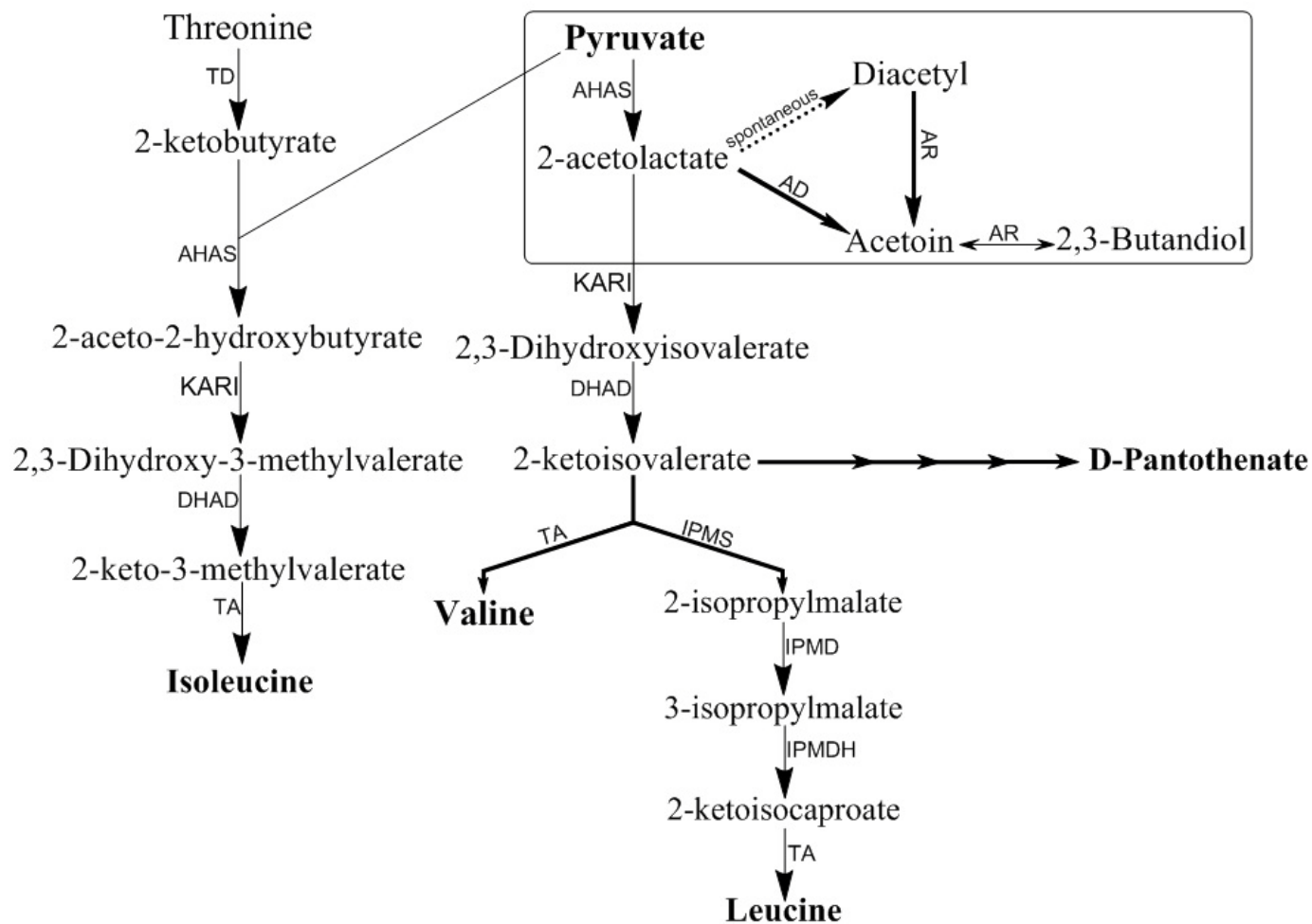


Figure 4-2. Biosynthesis pathways of branched chain amino acids and the butanediol pathway (Boxed)

TD, threonine deaminase (EC 4.3.1.19); KARI, ketol-acid reductoisomerase (EC 1.1.1.86); DHAD, dihydroxyacid dehydratase (EC 4.2.1.9) ; TA, transaminase (EC 2.6.1.42, EC 2.6.1.66, EC 2.6.1.6); IPMS, 2-isopropylmalate synthase (EC 2.3.3.13); IPMD, isopropylmalate dehydratase (EC 4.2.1.33); IPMDH, 3-isopropylmalate dehydrogenase (EC 1.1.1.85); AD, acetolactate decarboxylase (EC 4.1.1.5); AR, acetoin reductase (EC 1.1.1.4).

Unlike the anabolic enzyme (which produces both 2-acetolactate and 2-ketobutyrate), the catabolic enzyme reacts almost exclusively with pyruvate as the second substrate and is only able to produce 2-acetolactate (**Figure 4-1**). The unstable 2-acetolactate can be either decomposed to diacetyl (spontaneously) or be decarboxylated to acetoin by the enzyme acetolactate decarboxylase. The enzyme acetoin reductase (butanediol dehydrogenase) can catalyze the reversible conversion of acetoin to 2, 3-butanediol as well as the reduction of the diacetyl to acetoin (**Figure 4-2**).

Several anabolic AHASs from various organisms have been characterized including different isozymes (isozymes I, II, and III) from *Escherichia coli* (Sella *et al.* 1993; Vyazmensky *et al.* 1996; Hill *et al.* 1997), and *Salmonella* (Schloss *et al.* 1985), *Corynebacterium glutamicum* (Keilhauer *et al.* 1993), *Klebsiella pneumoniae* (Peng *et al.* 1992), different pathogenic mycobacteria species (Grandoni *et al.* 1998; Zohar *et al.* 2003; Choi *et al.* 2005; Singh *et al.* 2011), *Shigella sonnei* (Lim *et al.* 2011) and *Haemophilus influenzae* (Gedi *et al.* 2011), *Saccharomyces cerevisiae* (Pang and Duggleby 1999), *Arabidopsis thaliana* (Singh *et al.* 1991), and *Nicotiana tabacum* (Yoon *et al.* 2003). Considering the absence of the BCAA biosynthesis pathway in animal hosts, the anabolic AHAS has attracted great attention as a potential candidate for development of new antimicrobial drugs and herbicides and has been explored extensively during the last few years.

Very few AHASs have been investigated from the third domain of life (archaea) as well as the bacterial extremophiles. An oxygen-sensitive AHAS from the mesophilic archaeon *Methanococcus aeolicus* was previously isolated and characterized (Xing and Whitman 1994; Bowen *et al.* 1997). An AHAS with properties comparable with the bacterial counterparts has been purified and characterized from the halophilic archaeon *Haloferax volcanii* (Vyazmensky *et al.* 2000). The genes encoding a thermophilic AHAS have been expressed from the thermophilic bacterium *Bacillus stearothermophilus*. Like its non-thermophilic counterpart, the larger subunit is catalytically active and the holoenzyme can be reconstituted by titration with the regulatory subunit resulting higher specific activity at 55°C (Porat *et al.* 2004). However, to date no extreme- or hyperthermophilic AHAS have been studied *per se*, and the properties of the potential PDC activity have not been investigated.

The few bacterial lineages that contain extremely thermophilic or hyperthermophilic members include *Thermotogaceae*, *Aquificaceae*, and *Thermodesulfobacteriaceae*. The genus *Thermotoga* represents one of the deepest and most slowly evolving phylogenetic lineages within the domain Bacteria and is composed of rod-shaped anaerobic heterotrophs with an outer “sheath-like” envelops known as “toga” (Bocchetta *et al.* 2000). *Thermotoga maritima* is the model organism in the order of Thermotogales with a growth temperature range of 55-90°C and an optimum growth temperature of 80°C (Huber *et al.* 1986).

Thermotoga hypogea is an extremely thermophilic bacterium with an optimal growth temperature of 70°C and maximum growth temperature of 90°C (Fardeau *et al.* 1997).

The hyperthermophilic archaea are found in diverse archaeal lineages; members of the order Thermococcales are the most commonly isolated archaeal hyperthermophiles. *Pyrococcus furiosus* is the model organism of the genus *Pyrococcus* and is a strictly anaerobic organotrophic hyperthermophile with optimum growth temperature of 100°C. It is capable of growth on complex proteinaceous substrates including yeast extract supplemented with tryptone and few sugars including maltose (Fiala and Stetter 1986).

It has been shown that the *T. maritima* does not require addition of any BCAA to the growth medium for optimal growth, suggesting the organism is equipped for biosynthesis of these compounds (Rinker and Kelly 2000). However, characterization of the catalytic steps in BCAA production in hyperthermophilic anaerobic bacteria can certainly begin with an examination of the key enzyme of the pathway: AHAS.

None of the enzymes involved in the BCAA biosynthetic pathway has been studied in any other hyperthermophile. Also there are few studies pertaining to the amino acid requirement of hyperthermophiles (**Table 4-3**), and the results of existing studies are sometimes controversial or even contradictory (*e.g.* see the studies on *P. furiosus* in **Table 4-3**). These discrepancies presumably result from the use of different media compositions and growth conditions. In addition, in some cases the result of the minimal amino acid requirement studies are not in agreement with the information from the genome sequences. For instance, the results of the minimal amino acid requirement for *P. furiosus* is dissimilar in two independent studies conducted by Hoaki and coworkers (1994) and Ravenand coworkers (1997), with the earlier one being contradictory with that of the genomic information which confirmed the presence of a full *ilv* operon in *P. furiosus* (**see Table 4-3**).

In this study, AHAS activity was investigated in the cell lysates of different hyperthermophilic archaea and bacteria. The results were then compared with published genomic information (where available) concerning the presence or absence of BCAA biosynthesis operon and/or the results of the growth requirement experiments in the presence of different amino acids. The genes encoding the hypothetical catalytic and regulatory subunits of AHAS from the hyperthermophilic bacterium *T. maritima* and the hyperthermophilic archaeon *P. furiosus* were heterologously expressed in the mesophilic bacterial host *E. coli*. The presence of pyruvate decarboxylase activity was confirmed for the recombinant *T. maritima*'s enzyme; the general properties of both PDC and AHAS activities were characterized after purification.

Table 4-3. Amino acid requirements of Thermotogales and Thermococcales

Organism ^a	BCAA requirement ^b	BCAA operon ^c	Study type	Reference
<i>Pyrococcus furiosus</i>	Requires val and ile, poor growth w/o leu	+	Amino acid and growth requirement study,	Hoaki <i>et al.</i> 1993; Hoaki <i>et al.</i> 1994
<i>Pyrococcus furiosus</i>	Does not need any of BCAAs to grow	+	Minimum medium development	Raven and Sharp 1997
<i>Pyrococcus abyssi</i>	Minimal medium contains val, leu, and ile	+	Minimal amino acid requirement	Watrín <i>et al.</i> 1995
<i>Pyrococcus abyssi</i>	Requires val, leu, and ile	+	genome analysis, confirmed experimentally	Cohen <i>et al.</i> 2003
<i>Pyrococcus</i> strain GB-D	Requires val, leu, and ile	NA	Amino acid and growth requirement study	Hoaki <i>et al.</i> 1993; Hoaki <i>et al.</i> 1994
<i>Pyrococcus horikoshii</i>	The genes for val, leu, and ile are missing from the genome	-	Genomic data comparison	Maeder <i>et al.</i> 1999
<i>Thermococcus hydrothermalis</i>	Minimal medium contains val, leu, and ile	NA	Minimum medium development	Postec <i>et al.</i> 2004
<i>Thermococcus marinus</i>	BCAAs are essential for growth	-	Original paper on the species, experimental	Jolivet <i>et al.</i> 2004
<i>Thermococcus gammatolerans</i>	Requires val and leu, but not ile	-	Genome analysis and proteomics, experimental	Zivanovic <i>et al.</i> 2009
<i>Thermococcus celer</i>	Requires val, leu, and ile	NA	Amino acid and growth requirement study	Hoaki <i>et al.</i> 1993; Hoaki <i>et al.</i> 1994
<i>Thermococcus kodakaraensis</i>	The BCAA biosynthesis genes are missing; requires val, ile, and leu for growth	-	Genome analysis	Fukui <i>et al.</i> 2005
<i>Thermococcus onnurineus</i>	Lacks the genes for biosynthesis of BCAA, has the genes for their transport	-	Genome analysis	Lee <i>et al.</i> 2008
<i>Thermococcus litoralis</i>	Requires val, leu, and ile	NA	Amino acid and growth requirement study	Rinker and Kelly 2000
<i>Thermotoga maritima</i>	Does not need any amino acid in the minimal medium	+	Amino acid and growth requirement study	Rinker and Kelly 2000
<i>Thermotoga neapolitana</i>	Does not need any amino acid in the minimal medium	+	Amino acid and growth requirement study	Hoaki <i>et al.</i> 1993

^a The published studies for Thermococcales and Thermotogales were examined

^b BCAA, branched-chain amino acids; val, valine; leu, leucine; ile, isoleucine; “+”, the BCAA operon is present in the genome; “-”, the BCAA operon is not present; NA, the genome sequence is not available

^c The presence of the complete BCAA biosynthesis operon was examined in the available genomes

4.3 Materials and Methods

4.3.1 Reagents and chemicals

Sodium pyruvate, thiamine pyrophosphate and flavin adenine dinucleotide (FAD), acetoin (3-hydroxybutanone), isobutyraldehyde, 2-ketoisovalerate, and lysozyme were purchased from Sigma-Aldrich Canada Ltd. (ON, Canada). Other chemicals including isopropyl β -D-1-thiogalactopyranoside (IPTG) and dithiothreitol (DTT), alpha naphthol and creatine were all of reagent grade and purchased from Fisher Scientific (Ottawa, ON, Canada). The yeast extract was acquired from EMD (EMD Chemicals, Inc. NJ, USA) and Bacto-tryptone was purchased from Becton-Dickinson (BD Bioscience, Mississauga, ON, Canada). Proteinase K, restriction enzymes and markers for the agarose gel electrophoresis were all purchased from Fermentas (Ontario, Canada) and Phusion[®] High-Fidelity DNA polymerase (NEB, ON, Canada) was used for amplification of DNA.

4.3.2 Microorganisms and plasmids

Thermotoga maritima (DSMZ 3109), *Thermotoga hypogea* (DSMZ 11164), *Thermotoga neapolitana* 5068, *Thermococcus guaymasensis* DSM11113, and *Pyrococcus furiosus* (DSMZ 3638) were obtained from DSMZ- Deutsche Sammlung von Mikroorganismen und Zellkulturen (Braunschweig, Germany) and *Thermococcus kodakaraensis* KOD1, was acquired from the Japan type culture collection (RIKEN BioResource Center, Saitama, Japan). All of the organisms were grown routinely under anaerobic conditions in 20 L glass carboys. In all cases, the small scale starter cultures were grown in media supplemented with vitamin solutions and no vitamin mixture was used for large scale (15 L) growth.

The hyperthermophilic archaeon *T. guaymasensis* was grown in batch cultures under anaerobic conditions at 88°C on glucose, yeast extract and trypticase soy broth in the absence of elemental sulfur (Canganella *et al.* 1998; Ying and Ma 2011). The medium contained (per liter) KCl, 0.33 g; MgCl₂·6H₂O, 2.06 g; MgSO₄·7H₂O, 3.4; NH₄Cl, 0.25 g; CaCl₂·2H₂O, 0.14 g; K₂HPO₄, 0.14 g; Na₂SeO₃, 0.01 mg; NiCl₂·6H₂O, 0.01 mg; NaHCO₃, 1.0 g; NaCl, 18; resazurin, 1.0 mg; cysteine-HCl, 0.5g; Na₂S·9H₂O, 0.5g; yeast extract, 5.0 g; trypticase soy broth, 5.0 g; glucose, 5.0 g; HEPES, 5.2 g; vitamin solution, 10 ml and trace mineral, 10 ml [prepared as described previously by Balch *et al.* (1979)]; for large scale growth no HEPES and no vitamin solution was added to the medium. The pH of the medium was adjusted to 7.0 after preparation. The growth substrate (glucose) was sterilized by filtration using a syringe filter and added to the medium before inoculation with the starter culture.

T. kodakaraensis KOD1 was cultivated under anaerobic conditions at 85°C as described previously (Atomi *et al.* 2004) using sodium pyruvate as substrate and without addition of elemental sulfur and

vitamin supplements. The medium used for growing *T. kodakaraensis* contained (per liter): KCl, 0.33 g; MgCl₂·6H₂O, 2.8 g; MgSO₄·7H₂O, 3.4 g; NH₄Cl, 0.25 g; NaCl, 15 g; K₂HPO₄, 0.3 g; FeSO₄·7H₂O, 0.025 g; NaBr, 1 mg, Na₂S·9H₂O, 0.5 g; resazurin 1mg; yeast extract, 5.0 g; tryptone, 5.0 g and 10 ml of trace minerals [prepared as described by Balch *et al.* (1979)], the pH of the medium was adjusted to 7.0. The growth substrate was prepared separately and sterilized by filtration using a 0.45µm syringe filter, and added before inoculation to a final concentration of 0.5% (5.0 g per liter).

P. furiosus was grown on maltose, yeast extract, and tryptone and with elemental sulfur (S⁰) at 95°C using a procedure described previously (Fiala and Stetter 1986). The medium for the growth of *P. furiosus* contained (per liter) KCl, 0.33 g; MgCl₂·6H₂O, 2.75 g; NH₄Cl, 1.2 g; NaCl, 13.8 g; KH₂PO₄, 0.5 g; CaCl₂·2H₂O, 0.75 g; NaBr, 0.05 g; KI, 0.05 g; H₃BO₃, 0.015 g; SrCl, 7.5 mg, citric acid, 5.0 mg; maltose, 5.0 g; yeast extract, 5.0 g; Na₂S·9H₂O, 0.5 g and resazurin 1 mg. The pH of the medium was adjusted to 6.8.

The hyperthermophilic bacterium *T. maritima* was grown anaerobically on glucose and yeast extract at 80°C as described by Huber *et al.* (1986) with modifications as previously described (Yang and Ma 2010). The medium contained (per liter) KCl, 2 g; MgCl₂·6H₂O, 1.42 g; MgSO₄·7H₂O, 1.8 g; CaCl₂·2H₂O, 0.05 g; NaCl, 20 g; (NH₄)₂CO₃, 1.14 g; KH₂PO₄, 0.05 g; resazurin 0.05 mg, trace minerals [prepared as described previously by Balch *et al.* (1979)], 10 ml, yeast extract 2.5 g, and glucose, 4.0 g. Before autoclave the pH of the medium was adjusted to 6.8 using 1 M NaOH.

T. hypogea and *T. neapolitana* cell biomasses were from another study and was grown at 70°C and 77°C on glucose using the procedure modified from (Fardeau *et al.* 1997) as described by Yang and Ma (2005; 2010). In each case, growth was monitored by direct sampling from cultures and direct microscopic cell count using a Petroff-Hausser cell counting chamber (1/400 mm², 0.02 mm deep; Hausser Scientific, Horsham, PA) and a Nikon Eclipse E600 phase-contrast light microscope (Nikon Canada, ON, Canada). The late log-phase cultures were cooled down in an ice slurry bucket and centrifuged at 13,000 ×g using a Sharples continuous centrifugation system (Sharples equipment division, PA, USA) at 150-200 mlmin⁻¹. The resulting biomass was snap-frozen in liquid nitrogen and then stored at -76°C until the time of use.

Escherichia coli strains DH5α (BRL, CA, USA) was used for recombinant DNA propagation and *E. coli* BL21 (DE3) Rosetta 2 [F⁻ *ompT hsdSB (rB⁻ mB⁻) gal dcm pRARE27 (CamR)*] (Novagen, WI, USA) was used for overexpression of AHAS subunits under the control of T7 polymerase of the plasmid pET30a (+) (Novagen, WI, USA). The recombinant *E. coli* strains were grown in LB broth (10 g Bacto-Tryptone, 5.0 g yeast extract, 10 g NaCl per liter, pH 7.5) supplemented with kanamycin (30 µgml⁻¹) and

chloramphenicol ($34 \mu\text{gml}^{-1}$) for plasmid maintenance. All materials and columns for fast protein liquid chromatography (FPLC) were obtained from GE Health (Quebec, QC, Canada).

4.3.3 CFE preparation from hyperthermophiles

The procedure for cell-free extract preparation was carried out under anaerobic conditions and at 4°C unless specified otherwise. For each organism, the frozen biomass was thawed in a pre-degassed flask and then re-suspended in anaerobic lysis buffer (10 mM Tris-HCl, 5% glycerol, 2 mM SDT, 2 mM DTT, 0.01 mgml^{-1} DNase, and 0.1 mgml^{-1} lysozyme, pH 7.8) with 1:9 ratio (w/v). To study their impact on activity, TPP and FAD were included into the composition of the lysis buffer with the final concentrations of 0.1 mM and 0.01 mM, respectively. The suspension was incubated at 37°C for 1.5-2 h and then centrifuged at $10,000 \times g$ for 30 min. The supernatant was transferred to a new anaerobic serum bottle and used as the cell-free extract for further experiments. The success of cell lysis was confirmed by light microscopy under 400X magnification.

4.3.4 Genomic DNA isolation from *T. maritima* and *P. furiosus*

The genomic DNA of the native organisms was isolated for amplification of the genes encoding the catalytic and regulatory subunits of AHAS. The biomasses were prepared by harvesting logarithmic growth phase cultures and storing the harvested cells at -76°C until the time of use. For purification of chromosomal DNA, 0.1 g of each frozen biomass was transferred in a 1.5 ml tube and washed twice and each time with 500 μl of Tris-EDTA buffer (Tris-HCl, 10 mM and 1 mM EDTA, pH 7.5). After each wash, the cells were pelleted by centrifugation and the supernatant was decanted. To the pellet from the last wash 437 μl of Tris-EDTA buffer, 3 mg lysozyme (Sigma, ON, Canada) added and the mixture was incubated at 37°C for 1 h. Then, 0.6% SDS (Bio-Rad Laboratories, ON, Canada) and 60 μg of proteinase K (Fermentas, ON, Canada) were added. The tube was incubated for another 1hr at 37°C .

To remove the proteins and other contaminants from the preparations, 500 μl of the phenol: chloroform solution (1:1 v/v) added and mixed for 2-3 min. The tubes were centrifuged for 2 min at $10,000 \times g$ and then the upper phase containing the genomic DNA was transferred to a new 1.5ml tube using a clean Pasteur pipette. The genomic DNA was precipitated by adding 0.3 volumes of 10 M ammonium acetate and 0.6 volumes of 2-propanol and gently mixing the tube contents. The tubes were then centrifuged at $10,000 \times g$ and the supernatant was discarded. To the pellet, 500 μl of 70% ethanol was added and the centrifugation step repeated. The pellets were then re-suspended and dissolved in Tris-EDTA buffer (10 mM Tris-HCl, 1 mM EDTA, pH 7.5).

A NanoDrop spectrophotometer (Thermo Scientific, DE, USA) was used for quantification of the purified chromosomal DNAs as well as checking the quality. An absorbance ratio (A_{260}/A_{280}) of 1.8-2.0 was considered an indicator of the purity of the isolated genomic DNA.

4.3.5 Genome searches

The NCBI Microbial Genomes database (http://www.ncbi.nlm.nih.gov/genomes/MICROBES/microbial_taxtree.html) was searched for homologs of bacterial and plants pyruvate decarboxylase gene (*pdh*), catabolic AHAS genes (*als*) and anabolic AHAS genes (*ilv*). The putative hits were also examined for presence of the conserved motifs and binding sites.

4.3.6 Construction of expression plasmids

Standard procedures were followed for all DNA manipulation, competent cell preparation and transformation according to the methods described by Sambrook and Russell (2001). The coding sequences of the putative catalytic (TM0548, PF0935) and regulatory (TM0549, PF0934) subunits of AHAS were PCR-amplified using genomic DNA of *T. maritima* and *P. furiosus* and gene-specific primers (**Table 4-4**). For simultaneous amplification of coding sequence of the catalytic and regulatory subunits from *T. maritima*, the primers TMCSF and TMRSR were used as forward and reverse primers, respectively.

The amplified coding sequences of the putative catalytic and regulatory subunits were cloned separately into pET30a (+) inducible overexpression vector to produce fusion proteins with N-terminal histidine tags. The final plasmid constructs for *T. maritima* and *P. furiosus* putative genes are presented in **Figure 4-3** and **Figure 4-4**, respectively. The recombinant plasmids were transformed into *E. coli* DH5 α and subsequently were isolated again and introduced into *E. coli* BL21 (DE3) Rosetta 2 cells.

4.3.7 Purification of recombinant proteins

The expression conditions were optimized by varying the induction temperatures. Induction in LB medium was carried out at 18°C; room temperature (24°C), 30°C and 37°C with shaking at 180-200 rpm for about 18-24 h. Cells were lysed in the cell lysis buffer and resulting lysates were loaded polyacrylamide gels for SDS-PAGE to determine the optimal temperature for production of each soluble recombinant protein. Three different preparations were electrophoresed depending on the extent of treatment: the crude extract (CE) resulted from lysis of cells in the cell lysis buffer, the cell-free extract (CFE) was the supernatant from centrifugation of crude extract; and heat-treated crude extract (HTCE) was supernatant resulting from centrifugation of heat-treated (80°C for 1 h) crude extract.

Table 4-4. Oligonucleotide primers used for amplification of the coding sequences of the putative catalytic and regulatory subunits of *ilvB* and *ilvN* genes from *T. maritima* (Tm) and *P. furiosus* (Pf)

Primer name	Sequence ^a	Restriction site
TMCSF	5'-ATACA TAT GGTTCACGTGAAGATGAAAGG-3'	<i>NdeI</i>
TMCSR	5'- TACTCGAGT CTTTTCATCACCTCTCCTGCTCT-3'	<i>XhoI</i>
TMRSF	5'-ATACA TAT GACGGACCAGATTTCGAGAGC-3'	<i>NdeI</i>
TMRSR	5'- ATCTCGAG GAATCCCTCCCCTTCTTTTACG-3'	<i>XhoI</i>
PFCSF	5'-ATACA TAT GGAAATGTCCGGTGCAAAAGCC-3'	<i>NdeI</i>
PFCSR	5'- ATCTCGAG ATACCTTGTCACAACGTTTGAGATG-3'	<i>XhoI</i>
PFRSF	5'-ATACA TAT GGAGTTCGAAGCCATGAAG-3'	<i>NdeI</i>
PFRSR	5'- ATCTCGAG GTACCTATTCATCATATTTCTCAATATGT-3'	<i>XhoI</i>

^a Nucleotide sequences added to incorporate the restriction sites are indicated in bold

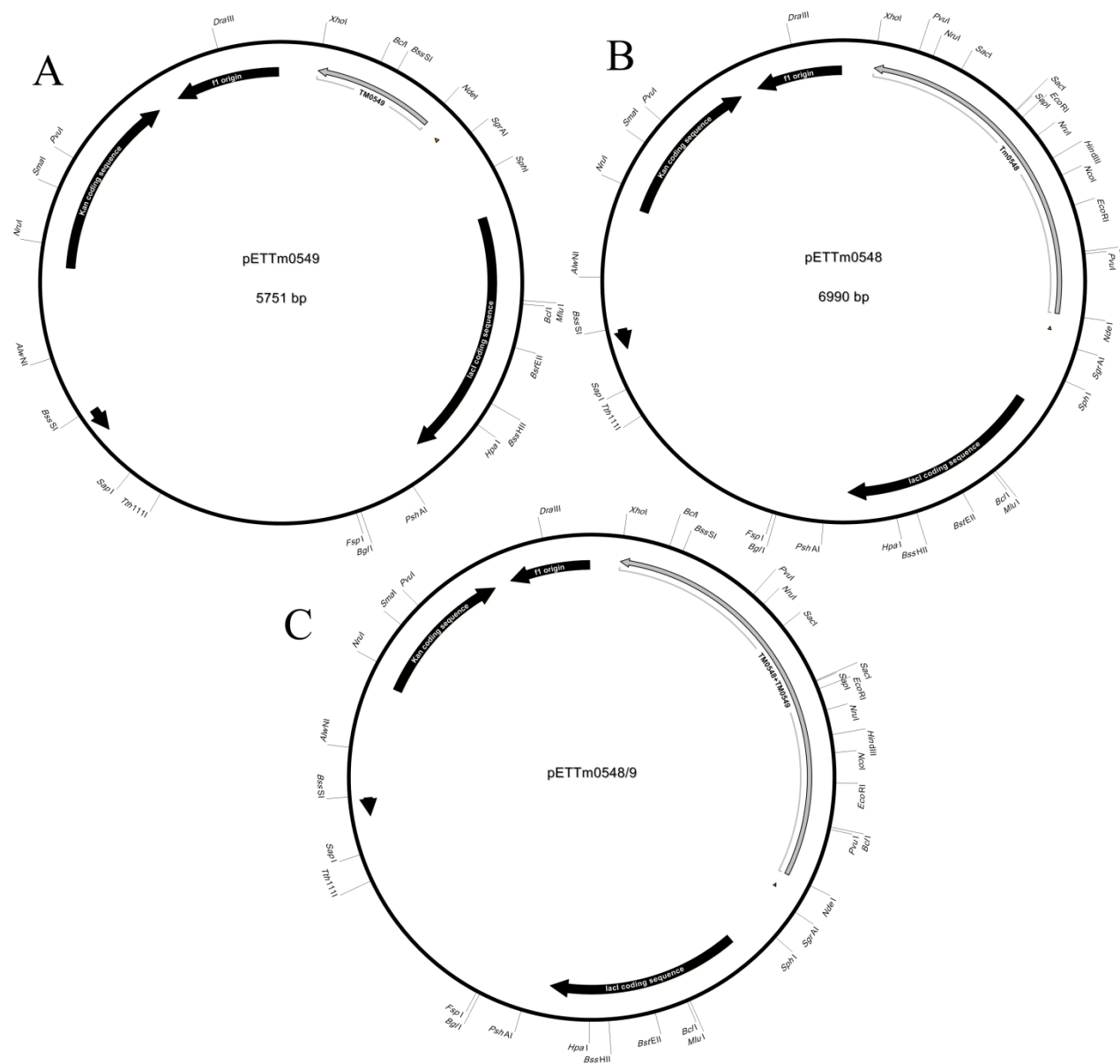


Figure 4-3. Construction of expression plasmids for *T. maritima* AHAS

Plasmids containing *ilvN*, the putative regulatory subunit (**A**), *ilvB*, the putative catalytic subunit (**B**), and (*ilvB-ilvN*) the coupled catalytic and regulatory subunits (**C**) of acetohydroxyacid synthase from *T. maritima*. For each clone, the coding sequences and their transcription direction is indicated with grey arrows; in all cases the amplified coding sequences were digested with *NdeI-XhoI* and inserted into the pET30a(+) vector; the plasmid pETTm0548/9 was constructed by insertion of the consecutive catalytic and regulatory subunits (*ilvB-ilvN*) in their natural order. The plasmid maps were generated using the SeqBuilder software (Lasergene, DNASTar, Madison, USA).

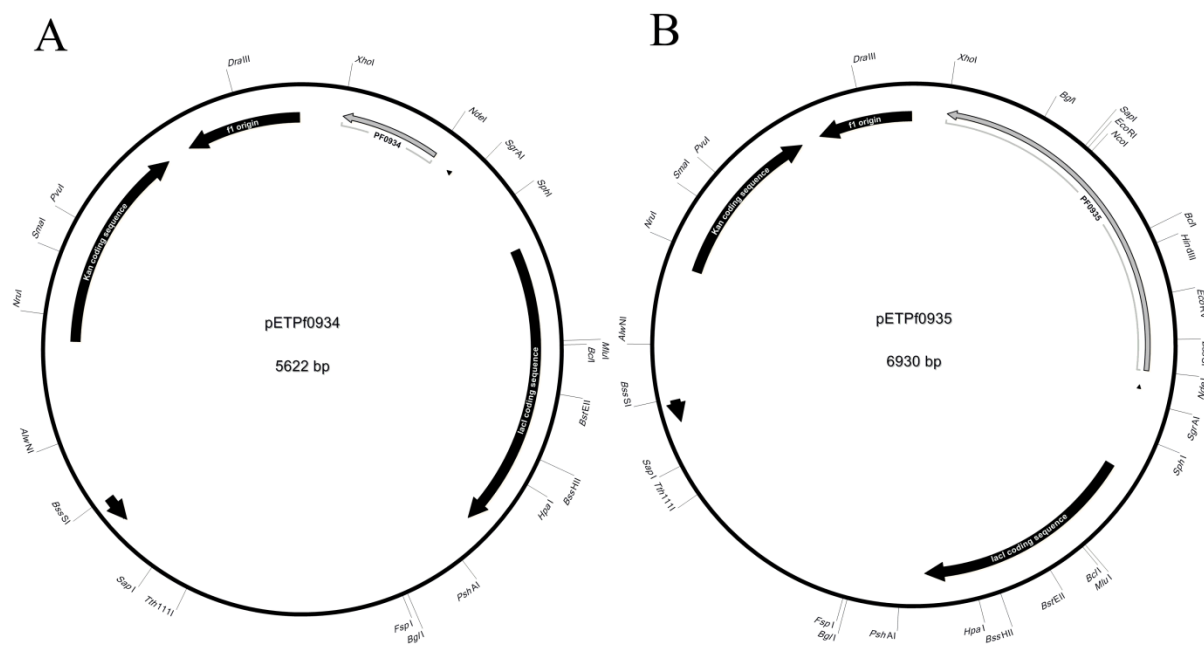


Figure 4-4. Construction of expression plasmids for *P. furiosus* AHAS

Plasmids containing the *ilvN* gene encoding a putative regulatory subunit (A) and *ilvB* gene encoding a putative catalytic subunit (B) of acetohydroxyacid synthase from *P. furiosus*; for each clone, the coding sequences and their transcription direction is indicated with grey arrows; in both cases the amplified coding sequences were digested with *NdeI-XhoI* and inserted into the pET30a vector. The plasmid maps were generated using the SeqBuilder software (Lasergene, DNASTar, Madison, USA).

The recombinant proteins were purified from the corresponding recombinant strains. The *E. coli* Rosetta 2 cells harboring the recombinant plasmids were grown in a 4 L flask at 37°C with shaking at 200rpm until the OD₆₀₀ reached 0.6-0.8. The cultures were then induced with 0.4 mM of isopropyl β-D-1-thiogalactopyranoside (IPTG) as recommended by the manufacturer of the vector. The induced cultures were then incubated at 37°C overnight. The biomass of the recombinant strain was then harvested by centrifugation at 10,000 ×g for 30 min at 4°C using a RC6-plus centrifuge in a SLA-3000 rotor (Thermo Scientific, MA, USA). After collection and weighing, the cell-pellets were snap-frozen in liquid nitrogen and stored at -76°C until use.

During purification steps when necessary, the eluted fractions containing the recombinant proteins were concentrated using an ultrafiltration device (Advantec MFS, Inc., CA, USA). The ultrafiltration was carried out under anaerobic conditions and pressure of nitrogen (10-25 PSi). The purified proteins were subsequently stored in liquid nitrogen until use.

Since small subunit of TmAHAS has no detectable activity, the presence of desired protein and its purity was checked by subjecting the chromatography fractions to SDS-PAGE. The cell lysis and purification steps were all carried out under anaerobic conditions. No activity could be detected in the cell lysates (prepared under different conditions including crude extract, heat-treated crude extract, and cell-free extract (CFE) with and without heat-treatment as well as the CFE prepared under denaturing conditions and re-natured by dilution in non-denaturing buffer. There was no detectable activity present in the recombinant clones expressing catalytic and regulatory subunits of PfAHAS either alone or mixed together and hence the purification was not further pursued for these two clones.

4.3.7.1 Heat-denaturation of the native *E. coli* proteins

To determine the optimum temperature for denaturation of the native *E. coli* (host) proteins, the crude extract was prepared from the strain expressing the catalytic subunit of TmAHAS. The crude extract was then heat-treated under anaerobic conditions for different time periods (0, 0.5, 1, 1.5 h) and at two different temperatures of 70°C and 80°C. The preparations then were centrifuged at 10,000 ×g and the supernatant (HTCE) was transferred to a new anaerobic container. The protein concentration (Bradford assay) and purity (SDS-PAGE), as well as the AHAS activity (AHAS activity assay) was determined and compared for each time point.

4.3.7.2 Purification of recombinant catalytic subunit

The purification steps were carried out at room temperature and under anaerobic conditions unless otherwise specified. SDS-PAGE and AHAS activity assay were used to determine the purity of the proteins at each step. The cell lysis was achieved by thawing the cell pellet in anaerobic lysis buffer [(10

mM Tris-HCl, 1 mM EDTA, 50 mM sodium chloride, 5% (v/v) glycerol, 0.5 mgml⁻¹, 1 mM sodium dithionite (SDT) and 1 mM dithiothreitol (DTT), 1 mM TPP, and 10 µM FAD, pH 7.8] under nitrogen pressure. The suspension was incubated at room temperature for 90 min to promote the cell lysis and then 0.01 mgml⁻¹ DNase I and 5 mM MgCl₂ were added. Incubation continued for another 30 min. The lysate was then heat-treated to denature the unwanted native proteins from the expressing host (the recombinant *E. coli* Rosetta 2 strain). Cell lysis was verified by examining a sample of the prepared lysate under a light microscope to confirm the absence of intact cells as an indicator of complete cell lysis. The cell debris and denatured proteins were removed by centrifugation (10,000 ×g for 30 min) and the supernatant was transferred to a new anaerobic container.

The heat-treated CFE was loaded on a Ni Sepharose™ High Performance (GE Healthcare, QC, Canada) column pre-equilibrated with anaerobic binding buffer (20 mM phosphate buffer, 0.5 M sodium chloride, 10 mM imidazole, and 5% glycerol, 1 mM SDT, 1 mM DTT, pH 8.0) and eluted with an increasing linear gradient of imidazole from 10 to 250 mM.

4.3.7.3 Purification of recombinant regulatory subunit

The recombinant regulatory (small) subunit was expressed mostly in the form of insoluble inclusion bodies (IBs) under normal growth conditions in accordance with a previous report (Petkowski *et al.* 2007). The recombinant small subunit was purified by denaturing immobilized nickel affinity chromatography followed by on column renaturation as described previously (Petkowski *et al.* 2007). All purification steps were carried out at 4°C unless otherwise mentioned and SDS-PAGE was used to determine the purity of the proteins at each step. To solubilize the IBs, 5 M urea was incorporated into the composition of the lysis buffer [(10 mM Tris-HCl, 1 mM EDTA, 50 mM Sodium chloride, 5% (v/v) glycerol, 0.5 mgml⁻¹ lysozyme, 1 mM SDT and 1 mM DTT, 1 mM TPP, and 10 µM FAD, pH 7.8] and buffer A (50 mM phosphate buffer, 20 mM Tris, 0.5 M NaCl, 5 M urea, 10 mM imidazole, 5% glycerol, 1 mM SDT, and 1 mM DTT, pH 8.0). The cells were lysed using the same procedure as for catalytic subunit.

After the heat precipitation step (80°C for 1hr), the CFE was loaded on Ni Sepharose™ High Performance (GE Healthcare, QC, Canada) column equilibrated with buffer A (50 mM phosphate buffer, 20 mM Tris, 0.5 M NaCl, 5 M urea, 10 mM imidazole, 5% glycerol, 1 mM SDT, and 1 mM DTT, pH 8.0). On column refolding was carried out by applying a linear gradient of urea from 5M (Buffer A) to 0 M (Buffer B: 50 mM phosphate buffer, 20 mM Tris, 0.5 M NaCl, 10 mM imidazole, 5% glycerol, 1 mM SDT, and 1 mM DTT, pH 8.0), and then the recombinant protein was eluted by applying a gradient of

imidazole from 10 mM (Buffer B) to 250 mM (Buffer C: 50 mM phosphate buffer, 20 mM Tris, 0.5 M NaCl, 250 mM imidazole, 5% glycerol, 1 mM SDT, and 1mM DTT, pH 8.0).

4.3.8 Protein determination

The protein concentration was determined using the Bradford dye-binding assay (Bradford 1976) with reagent purchased from Bio-Rad Laboratories (ON, Canada). Bovine serum albumin (BSA) was used for preparation of the standard with modifications of the protocol as supplied by the manufacturer.

4.3.9 SDS-PAGE

Sodium dodecyl sulfate polyacrylamide gel electrophoresis (SDS-PAGE) was used to determine the enzyme purity and apparent subunit molecular weights. SDS-PAGE was performed according to Laemmli (1970) with acrylamide and molecular weight standards from Bio-Rad (ON, Canada) using a Hoefer™ Mighty Small System (Hoefer Inc., MA, USA). Gels (8×10 cm) were prepared and stained with Coomassie Brilliant Blue R250. The de-staining was carried out by storing the gel in de-staining solution (12% 2-propanol and 7% acetic acid) with moderate shaking and overnight.

4.3.10 AHAS activity assay

The AHAS activity assay procedure was a modification of the discontinuous colorimetric method of Singh *et al.* (1988). The AHAS activity was determined by measuring the production of acetolactate from pyruvate (**Figure 4-5**, step A), upon its decarboxylation (**Figure 4-5**, step B) to acetoin or diacetyl under high temperature and acidic condition. The products of decarboxylation (acetoin and diacetyl) will react with the guanidino groups of creatine under alkaline conditions creating a cherry red colored complex (Westerfeld 1945), which can be measured at 525 nm (**Figure 4-5**, step C). The enzymatic reactions were carried out in duplicate; in stoppered 8 ml vials under strictly anaerobic conditions (as described in section 4.3.12) at 80°C unless otherwise specified. CFEs prepared from *E. coli* Rosetta 2 strain (the expression host) transformed with an empty pET30a vector were used as blank for each set of assays.

The anaerobic assay mixture (1 ml final volume) containing 100 mM sodium phosphate (pH7.0), 10 mM MgCl₂, 2.5 mM thiamine pyrophosphate (TPP), 50 mM sodium pyruvate, and 10 μM FAD was pre-heated by incubation in a 80°C water bath for 4 min. The final concentration of 2-acetolactate was determined using a calibration curve prepared by linear regression plotting of known concentrations of acetoin and processed under same assay conditions.

The vial containing the assay mixture was pre-incubated in a water bath at assay temperature for 4min and then the reaction was started by adding the enzyme (or enzyme-containing fraction) using a pre-rinsed Hamilton gas-tight syringe (Hamilton company, Reno, NV, USA). Care was taken to ensure a

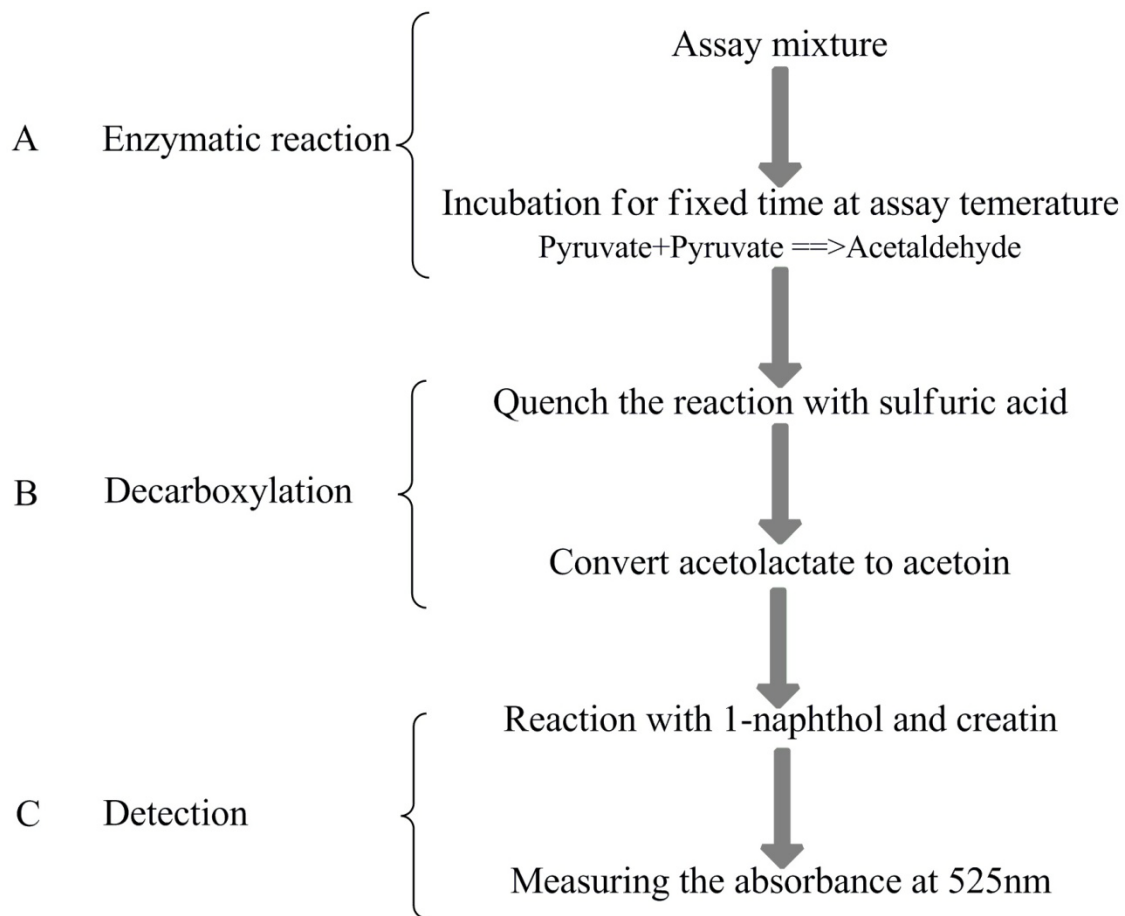


Figure 4-5. General steps of AHAS activity assay

All assays were carried out at 80°C and under anaerobic conditions, the buffer routinely used for the assays were sodium phosphate (100 mM, pH 7.0) unless specified otherwise.

linear correlation between the activity and the amount of protein sample in the assay. The assay vials were incubated in the water bath (80°C) for 30min after adding the enzyme and then the reaction was quenched by adding sulfuric acid (50% v/v) to a final concentration of 0.85%. The assay solution then was incubated at 60°C for 15 min to allow transformation of the acetolactate to acetoin (chemical decarboxylation). The amount of the acetoin produced was quantified by adding 0.5% (w/v) creatine (final concentration 0.17%) and 5 % (w/v) 1-naphthol in 4 N NaOH (final concentration 1.7%). The mixture was incubated at 60°C for 15 min and then at room temperature for another 15 min with frequent mixing followed by centrifugation for 2 min at 10,000 ×g. The enzyme activity was determined by measuring the absorbance at 525 nm using a Genesys 10 UV-Vis spectrophotometer (Thermo Scientific, MA, USA). One unit of activity was defined as the formation of 1 μmol of acetolactate per min under these conditions.

4.3.11 PDC activity assay (of AHAS)

The pyruvate decarboxylase activity (PDC) was assayed by measuring the rate of the production of acetaldehyde from pyruvate. In principle, the acetaldehyde produced during the enzymatic reaction (**Figure 4-6**, step A) was derivatized with a freshly prepared acidic solution of 2, 4-dinitrophenylhydrazine (DNPH) also known as Brady's reagent (**Figure 4-6**, step B). Reaction of the reagent with aldehyde groups creates a yellow-reddish color resulting from formation of the corresponding hydrazone derivative. Subsequent to liquid-liquid phase extraction with a solvent (**Figure 4-6**, step C), the acetaldehyde-DNPH complex was quantified by reverse-phase high performance liquid chromatography (RP-HPLC). The general procedures and main steps involved in the assay are presented in **Figure 4-6**.

The enzyme assays were carried out in duplicates, in stoppered 8 ml vials under anaerobic conditions at 80°C, unless otherwise specified. The assay mixture (1 ml final volume) containing 100 mM sodium phosphate buffer (pH7.0), 200 mM sodium chloride, 10 mM MgCl₂, 2.5 mM thiamine pyrophosphate (TPP), 50 mM sodium pyruvate, and 10 μM FAD was pre-heated by incubation in an 80°C water bath for 4 min. When specified, sodium pyruvate was replaced with 50 mM of 2-ketoisovalerate. The reaction was started by adding the enzyme (or enzyme-containing fraction). As with AHAS activity assay, tests were done to make sure that there is a linear correlation between the activity and the amount of protein in the assay. After the enzymatic reaction time (30 min), the reaction was stopped by placing the assay vials on ice and adding 3 ml of freshly prepared saturated DNPH solution in 2 N HCl (stirred at room temperature in the dark for 1 h). The vials were then incubated overnight at room temperature with shaking (150-200 rpm) to allow derivatization of acetaldehyde with the DNPH. The resulting hydrazone (acetaldehyde-

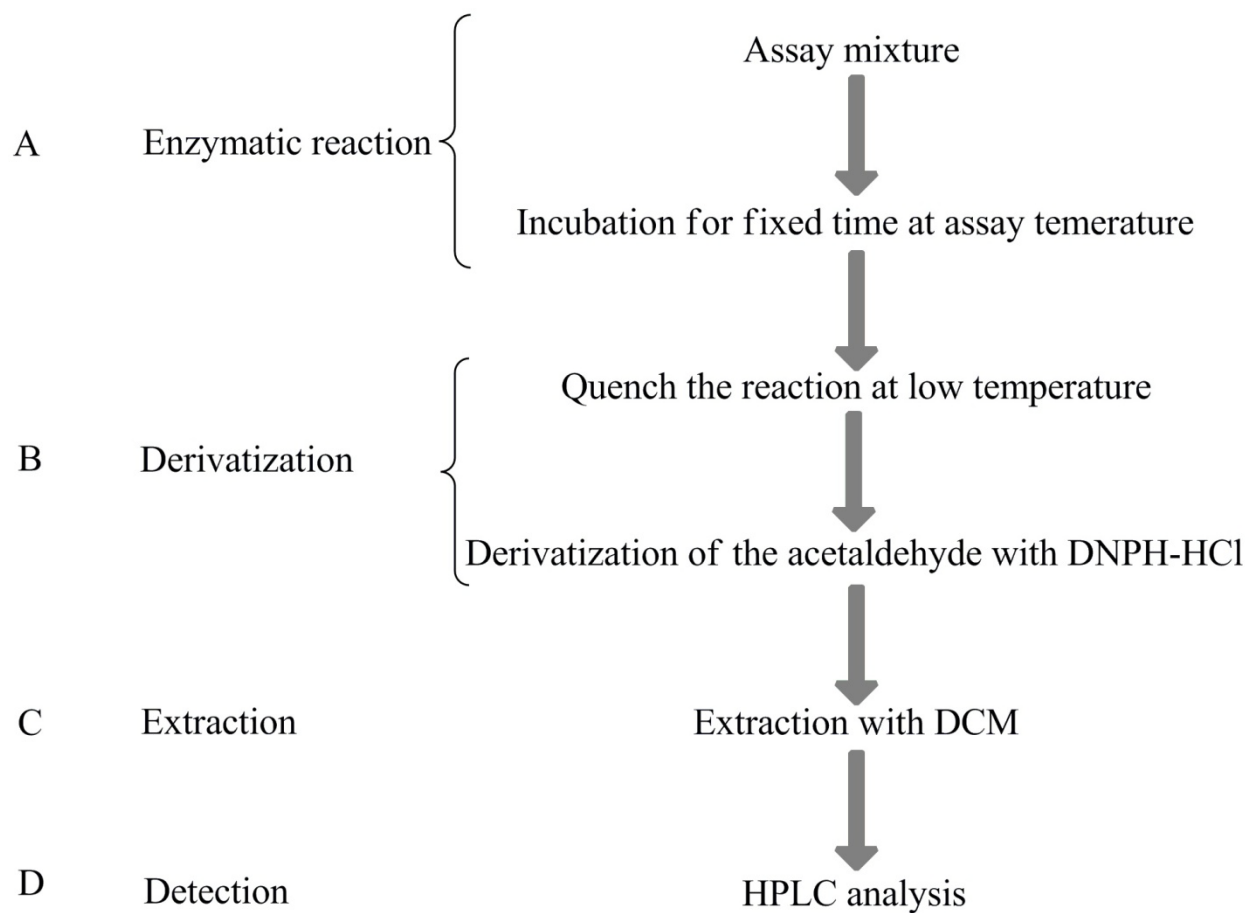


Figure 4-6. General steps of PDC activity assay for the AHAS

DNPH-HCl, hydrochloridric acid solution saturated with dinitrophenylhydrazine; DCM, Di chloromethane; HPLC, high performance liquid chromatography. Unless otherwise mentioned all assays were carried out at 80°C and under anaerobic conditions, the buffer routinely used for the assays were sodium phosphate (100 mM, pH 7.0).

DNPH) derivative was then extracted twice, each time with 1 ml of dichloromethane (DCM) by vigorous shaking at room temperature for 15 min. The organic (lower) phase was then transferred to a new clean vial covered with a piece of Parafilm M[®] membrane with few holes in it. The assay vials were placed in a vacuum desiccator covered with aluminum foil (to protect them from the light) connected to a water pump to evaporate the DCM in a fume hood. After evaporation of DCM (about 3-4 h), the resulting yellowish-red powder was dissolved in 4 ml of pure (HPLC grade) acetonitrile by incubation at 4°C overnight.

An aliquot of the assay product was filtered through a 0.2 µm nylon syringe filter (National Scientific, Rockwood, TN, USA), and the filtered sample was then analyzed by a Perkin-Elmer LC Series4 HPLC system (Norwalk, CT, USA) fitted with a reversed-phase Allure C18 column (150×4.6 mm, 5µm, 60 Å). Isocratic elution conditions with a mobile phase composition of acetonitrile/water (80:20 v/v) were used at a flow rate of 1 mlmin⁻¹. A micrometrics model 788 dual variable wavelength detector (Norcross, GA, USA) was used and operated at 365 nm. The sample was applied using a Rheodyne Model 7125 injection valve (Rheodyne Inc., CA, USA) with a 20 µl sample loop. The HPLC system was operated at room temperature. The final concentration of acetaldehyde and isobutyraldehyde were determined using a calibration curve prepared by linear regression plotting of known concentrations of each product processed under the same assay conditions.

4.3.12 Anaerobic techniques

All of the buffers and reagents were degassed in containers sealed with red rubber sleeved stoppers. The stoppers were punctured with needles to allow the alternate exposure to vacuum and nitrogen (N₂) using a manifold. The nitrogen gas (Praxair, ON, Canada) was deoxygenated by passing through a heated column containing a BASF catalyst (BASF, NJ, USA). Assay and purification buffers were degassed in magnetically stirred flasks for 30 min, then three cycles of flushing/evacuation (3 min each) were applied. Then a second needle was inserted to flush out more N₂ to ensure oxygen-free head space in the container (even if there is residual O₂ contamination in the manifold system). The containers were kept under nitrogen pressure.

4.3.13 Native molecular mass estimation

The apparent molecular masses of the purified large and small subunits were estimated by loading the concentrated individual proteins on a size exclusion chromatography column (2.6×60 cm) of HiLoad Superdex-200 (GE healthcare, QC, Canada) pre-equilibrated with buffer C (50 mM Tris, 5% glycerol, 100 mM KCl, pH 7.8) at the flow rate of 2 mlmin⁻¹. The following standards from Pharmacia protein standard kit (Pharmacia, NJ, USA) were applied to the column: blue dextran (2,000,000 Da),

thyroglobulin (669,000 Da), ferritin (440,000 Da), catalase (232,000 Da), aldolase (158,000, Da), bovine serum albumin (67,000, Da), ovalbumin (43,000), chymotrypsinogen A (25,000) and ribonuclease A (13,700).

4.3.14 Biochemical and biophysical characterization

To investigate the pH dependency of both AHAS and PDC activities, enzyme assays were carried out at different pH values ranging from 4.0 to 11.0. The pH values expressed throughout this manuscript were adjusted and measured at room temperature unless specified differently. In each case, assays were carried out at 80°C, under anaerobic conditions using 100 mM buffers degassed as described previously (section 4.3.12). For pH values between 4 and 5.6, sodium acetate buffer (pKa= 4.76, $\Delta pK_a/^\circ C=0.0002$) was used. Sodium phosphate buffer (pKa 7.20, $\Delta pK_a/^\circ C=-0.0028$) was used for pH values 6.0, 7.0, and 7.5. HEPES buffer (pKa 7.39, $\Delta pK_a/^\circ C=-0.014$) covered pH values 7.5, 8.0, 8.5 and 9.0 and glycine buffer (pKa 9.55, $\Delta pK_a/^\circ C=-0.0025$) was used for the pH values 9.0, 9.5, 10.0, and 10.5. Finally for the pH points of 10.0, 10.5, and 11.0 the CAPS buffer (pKa 10.40, $\Delta pK_a/^\circ C= -0.009$) was used.

To determine the steady-state kinetic parameters (K_m and V_{max}), enzyme assays were performed at optimum pH. All assays were carried out at 80°C and under strictly anaerobic conditions. The kinetic parameters were established for pyruvate (5 to 125 mM), TPP (0.05-4 mM), and FAD (0.05-40 μM) by applying various concentrations of each component and keeping the concentration of other assay components constant. All of the assays were repeated in duplicate or triplicate. The activity then was assayed for various concentrations and the kinetic parameters were calculated from the best fit of the results to the Michaelis-Menten equation by non-linear regression using SigmaPlot® software (SYSTAT Software Inc., CA, USA).

The oxygen sensitivity of each activity was established by exposing an enzyme aliquot to ambient atmosphere at 4°C by gentle stirring and comparing the synthase and decarboxylase activities at different time courses with the control preparation kept under anaerobic conditions. Both of the enzyme samples were protected from light through the experiments.

The temperature dependence of the enzyme was determined by measuring the enzyme activity at different temperatures ranging from 30°C to 95°C under anaerobic conditions and in 50 mM EPPS buffer, pH 8.4 containing 10 mM MgCl₂. Thermal stability of the enzyme was determined by incubation of an anaerobic enzyme preparation and determining the residual activity at different time points compared to unheated control.

4.3.15 Reconstitution of TmAHAS

The purified large and small subunits of the recombinant TmAHAS were combined in various molar ratios, incubated both at low temperature (ice bath) or heat treated (80°C) for various lengths of time and then were loaded on a size-exclusion chromatography column (2.6×60 cm) of HiLoad Superdex-200 (GE healthcare, QC, Canada) pre-equilibrated with buffer C (50 mM Tris, 5% glycerol, 100 mM KCl, pH 7.8) at a flow rate of 2 mlmin⁻¹. The activities of the reconstituted TmAHAS holoenzyme were determined using the AHAS and PDC enzyme assay procedures as described previously in sections 4.3.10 and 4.3.11.

4.4 Results

4.4.1 The *ilv* operon in hyperthermophiles: genome sequence analysis (*in silico* study)

The accessible genome sequences of various Thermotogales and Thermococcales were explored in search of genes encoding the enzymes involved in the biosynthesis of BCAAs. The results of searches for AHAS-encoding genes and the operon containing the other genes involved in the BCAA biosynthesis are presented in **Table 4-5**. To determine the phylogenetic relatedness of the putative proteins, phylogenetic trees were constructed based on the amino acid sequence of the some mesophilic and hyper/thermophilic catalytic (**Figure 4-7**) and regulatory subunits (**Figure 4-8**).

4.4.1.1 The *ilv* operon in Thermotogales

The catalytic and regulatory subunits of AHAS in bacteria are encoded by genes *ilvB* and *ilvN*, respectively. The survey of the genome sequences of Thermotogales demonstrated that all members of the genus *Thermotoga*, except for *T. lettingae*, had a complete set of coding sequences for the enzymes involved in the BCAA biosynthesis. Similarly, complete *ilv* operon is also present in the members of the closely related genus *Petrotoga*. However, other members of the order Thermotogales (with fully sequenced genomes) including *Thermosipho* and *Kosmotoga* did not have the genes of the *ilv* operon (**Table 4-5**).

In *T. maritima* (and most other *Thermotogae*), the first gene in the *ilv* operon is the gene encoding catalytic subunit (*ilvB*) of AHAS, followed immediately by the gene encoding small subunit (*ilvN*) and then other genes involved in the biosynthesis of the branched chain amino acids including ketol-acid reductoisomerase (*ilvC*), dihydroxy-acid dehydratase (*ilvD*), 2-isopropylmalate synthase (*leuA*), 3-isopropylmalate dehydratase large and small subunits (*leuC* and *leuD*), and 3-isopropylmalate dehydrogenase (*leuB*) (**Figure 4-9**).

The study of the gene organization of the *ilv* operon in Thermotogales indicates that the genes involved in the biosynthesis of the isoleucine and leucine have overlapping intercistronic regions, and the start

Table 4-5. Homologs of *ilv* operon in Thermotogales and Thermococcales^a

	Organism	AHAS catalytic subunit ^b (locus Tag)	AHAS regulatory subunit ^b (locus Tag)	Operon ^c
Thermococcales (Archaea)	<i>Palaeococcus ferrophilus</i>	-	-	-
	<i>Pyrococcus furiosus</i>	PF0935	PF0934	BCAA
	<i>Pyrococcus abyssi</i>	PAB0888	PAB0887	BCAA
	<i>Pyrococcus</i> sp. strain NA2	PNA2_1346	PNA2_1347	BCAA
	<i>Pyrococcus yayanosii</i>	-	-	-
	<i>Pyrococcus horikoshii</i>	-	-	-
	<i>Thermococcus sibiricus</i>	-	-	-
	<i>Thermococcus gammatolerance</i>	-	-	-
	<i>Thermococcus kodakaraensis</i>	-	-	-
	<i>Thermococcus barophilus</i>	-	-	-
	<i>Thermococcus</i> sp. strain 4557	-	-	-
	<i>Thermococcus</i> sp. strain AM4	-	-	-
	<i>Thermococcus zilligii</i>	-	-	-
	<i>Thermococcus litoralis</i>	-	-	-
	<i>Thermococcus</i> sp. strain PK	-	-	-
<i>Thermococcus onnurineus</i>	-	-	-	
Thermotogales (Bacteria)	<i>Thermotoga maritima</i>	TM0548	TM0549	BCAA
	<i>Thermotoga lettingae</i>	-	-	-
	<i>Thermotoga thermarum</i>	Theth_0200	Theth_0199	BCAA
	<i>Thermotoga neapolitana</i>	CTN_0120	CTN_0119	BCAA
	<i>Thermotoga naphthophila</i>	Tnap_0328	Tnap_0329	BCAA
	<i>Thermotoga petrophila</i>	Tpet_0372	Tpet_0371	BCAA
	<i>Thermotoga</i> sp. strain RQ2	TRQ2_0389	TRQ2_0388	BCAA
	Thermotogales bacterium MesG1.Ag.4.2 ^d	-	-	-
	<i>Thermosipho melanesiensis</i>	-	-	-
	<i>Thermosipho africanus</i>	-	-	-
	<i>Petrotoga mobilis</i>	Pmob_1592	Pmob_1591	BCAA
	<i>Petrotoga miotherma</i>	-	-	-
	<i>Fervidobacterium nodosum</i>	-	-	-
	<i>Fervidobacterium pennivorans</i>	-	-	-
	<i>Kosmotoga olearia</i>	-	-	-
<i>Marinitoga camini</i>	-	-	-	
<i>Marinitoga piezophila</i>	-	-	-	

^a The genome sequences were searched by annotation as well as by homology against the protein sequence of the closest known AHAS gene (*P. furiosus* in Thermococcales and *T. maritima* for Thermotogales)

^b Alphanumeric codes indicate the locus tag of the gene in the corresponding genome; -, not present

^c The presence of a complete set of *ilv* genes was checked

^d This strain was recently suggested to be named “Mesotoga prima” and to be the first member of a new sub-group of mesophilic Thermotogales (Ben Hania *et al.* 2011; Nesbø *et al.* 2012)

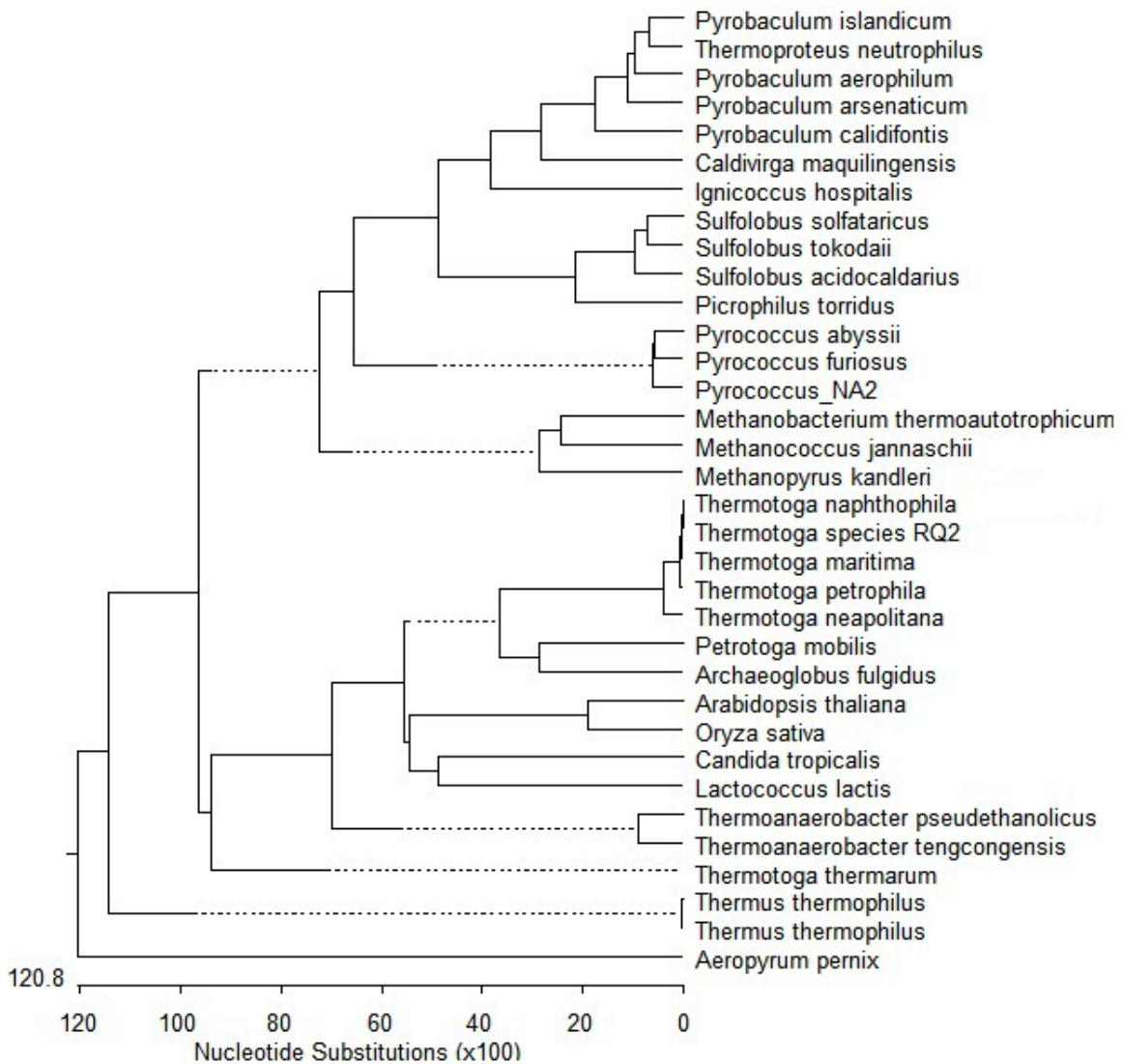


Figure 4-7. Relatedness of AHAS catalytic subunits

Genomes in the NCBI microbial genome database (http://www.ncbi.nlm.nih.gov/genomes/MICROBES/microbial_taxtree.html) were used to retrieve the amino acid and nucleotide sequences of AHASs from various thermophilic and mesophilic organisms. The amino acid sequence homology and the phylogenetic tree were prepared based on the ClustalW analysis using MegAlign software (Lasergene, DNASTar, Madison, USA).

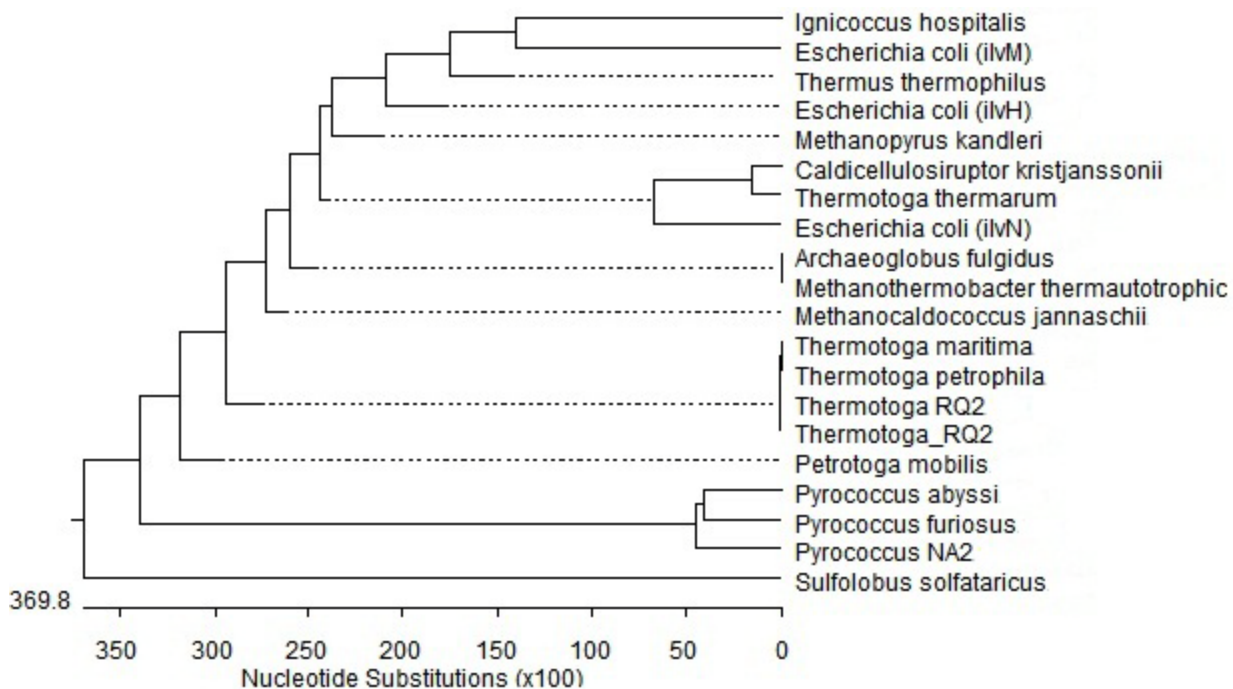


Figure 4-8. Relatedness of AHAS regulatory subunits

Genomes in the NCBI microbial genome database (http://www.ncbi.nlm.nih.gov/genomes/MICROBES/microbial_taxtree.html) were used to retrieve the amino acid and nucleotide sequences of AHASs from various thermophilic organisms. The numbers at the bottom of each tree indicate the number of the amino acid substitutions. A dotted line on the phenogram indicates a negative branch length, a common result of averaging. The amino acid sequences homology and the phylogenetic tree were prepared using MegAlign software (Lasergene, DNASTar, Madison, USA).

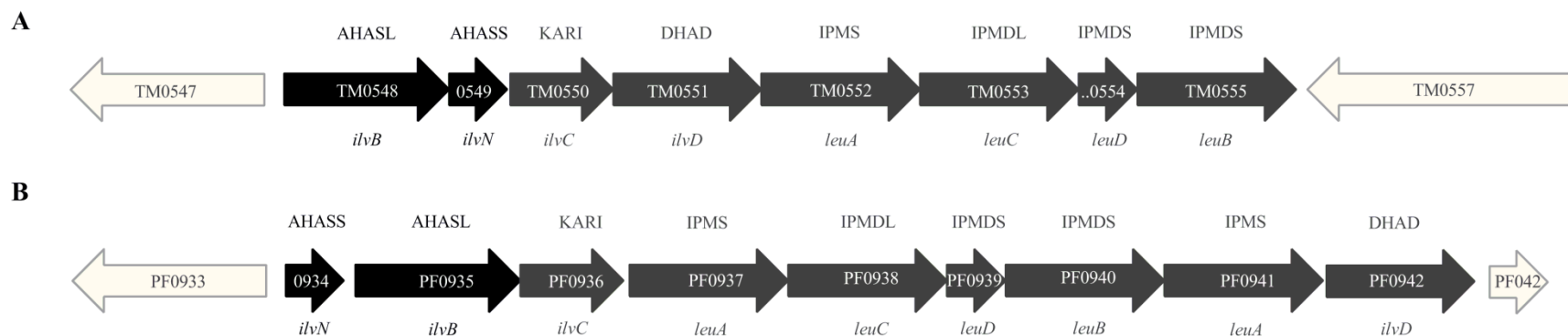


Figure 4-9. Gene organization of the *ilv* gene cluster in *T. maritima* (A) and *P. furiosus* (B)

The filled arrows indicate the genes encoding enzymes involved in BCAA biosynthesis in each scheme. The black arrows are the hypothetical genes encoding the catalytic and regulatory subunits of AHAS.

ilvB: catalytic subunit of acetohydroxyacid synthase (AHASL); *ilvN*, regulatory subunit of acetohydroxyacid synthase (AHASS); *ilvC*, ketol-acid reductoisomerase (KARI); *ilvD* ; dihydroxy-acid dehydratase (DHAD); *leuA*, 2-isopropylmalate synthase (IPMS); *leuC* 3-isopropylmalate dehydratase large subunit (IPMDL); and *leuD*, 3-isopropylmalate dehydratase small subunit (IPMDS).

codon of the adjacent gene is either overlapping or separated by few base pairs. This is the case with *ilvB-ilvN*, *ilvN-ilvC*, *ilvC-ilvD*, *leuA-leuC*, *leuC-leuD*, and *leuD-leuB*. In each of these pairs, a putative ribosome-binding site (RBS) for the downstream coding sequence was identifiable upstream of the start codon within the coding sequence of the upstream gene (**Figure 4-10**).

4.4.1.2 The *ilv* operon in Thermococcales

All of the available genome sequences of the genus *Thermococcus* (*T. gammatolerance*, *T. kodakaraensis*, *T. sibiricus*, *T. barophilus*, *T. onnurineus*, *Thermococcus* sp. strain AM4, *Thermococcus* sp. strain 4557, *Thermococcus* sp. strain PK) are lacking the the *ilv* operon (**Table 4-5**) or any AHAS-encoding genes. Within the members of the genus *Pyrococcus*, three members (namely *P. furiosus*, *P. abyssi*, and the recently sequenced hyperthermophilic archaeon *Pyrococcus* sp. strain NA2) have been found to contain the *ilv* operon. But, *P. yayanosii* and *P. horikoshii* lacked the operon (**Table 4-5**).

Surprisingly, the *ilv* operon lacked the gene encoding the regulatory subunit in the members of the genus *Pyrococcus*, and the operon starts with the gene encoding the catalytic (large) subunit followed by the genes for other BCAA biosynthesis pathway enzymes (ketol-acid reductoisomerase, 2-isopropylmalate synthase, 3-isopropylmalate dehydratase, 3-isopropylmalate dehydrogenase, 2-isopropylmalate synthase, and dihydroxy-acid dehydratase).

There was a gene encoding a hypothetical protein (PF0934 in *P. furiosus*) located just upstream of the gene encoding the catalytic subunit in the *ilv* operon of *P. furiosus*, *P. abyssi*, and *Pyrococcus* sp. strain NA2 (**Figure 4-9**). This gene may encode the regulatory subunit (*ilvN*) of PfAHAS and is annotated as “hypothetical protein”. However, the deduced amino acid sequences were very dissimilar from that produced by IlvN sequences from other hyperthermophiles. The amino acid sequences of this hypothetical protein showed about 15% amino acid identity to the regulatory subunit of Thermotogales and only about 16% identity to AHAS regulatory subunit of *E. coli* (IlvH). *Thermotogae* IlvH shows approximately 37% identity to its homolog in *E. coli*. In phylogenetic tree drawn based on the amino acid sequences of the regulatory subunits from different hyperthermophiles, the hypothetical genes of the *Pyrococcus ilv* operon showed divergence from the other sequences (**Figure 4-8**), while the catalytic subunit was clustered with other archaeal catalytic subunits (**Figure 4-7**).

4.4.2 FAD- and TPP-binding motif in hyperthermophilic AHASs

There was a highly conserved FAD-binding motif (RFDDR) in the catalytic (large) subunit of AHAS from different mesophilic organisms which was showed to be an indicator of the association with the FAD-requirement for its activity (Le 2005). Sequence alignments of AHASs indicated the presence of the FAD-binding motif in the catalytic subunits of the enzymes from extreme thermophiles and

AG <u>GAGAGG</u> TGATGAAAG ATGA	<i>ilvB-ilvN</i>
AGAAGGG <u>GAGGGA</u> TTCT GATG	<i>ilvN-ilvC</i>
AG <u>GAGAGG</u> AACGTCGATGAGGAG TGATG	<i>ilvC-ilvD</i>
AG <u>GAGGAGAT</u> GAGAAAC GATG AGGAGAATTAA	<i>leuA-leuC</i>
AC <u>GGAGGT</u> GCTGAGT GAGATG	<i>leuC-leuD</i>
GAAAGCTGT GAGGTGATG	<i>leuD-leuB</i>

Figure 4-10. Intercistronic sequences in the *ilv* operon of *T. maritima*

The translation initiation (start) codon of the distal genes are indicated in bold, the ribosome-binding site (RBS) of the distal gene is boxed, and the translation termination of the proximal genes are underlined

hyperthermophiles, including the Thermotogales and Thermococcales (**Figure 4-11A**). The motif is generally conserved as RFSDR in Thermotogales, but in and in Thermococcales (only in members of the genus *Pyrococcus* which have the gene cluster) the motif is RWSDR. The catalytic subunits of all anabolic and catabolic AHASs contained the typical TPP-binding motif (GDGX₂₄₋₂₆N) as indicated in **Figure 4-11B**. This highly conserved motif is a common feature of all TPP-dependent enzymes (Hawkins *et al.* 1989).

4.4.3 AHAS activity in cell-free extracts of hyperthermophiles

AHAS activities were determined in CFEs of three hyperthermophilic bacteria including *T. hypogea*, *T. maritima*, and *T. neapolitana* and three hyperthermophilic archaea belonging to the order Thermococcales, namely *T. guaymasensis*, *T. kodakaraensis* and *P. furiosus* at different pHs. The goal of the experiments was to determine the best pH range for the activity, and also to determine the nature of possible AHAS activities in the CFEs (**Table 4-6**). As expected, the organisms with the *ilv* gene cluster showed the highest levels of AHAS activity, but surprisingly, some levels of AHAS activity could be detected in the cell-free extracts of *T. kodakaraensis* and *T. neapolitana* which were known to have no *ilv* operon (**Table 4-5**). This was also the case for *T. guaymasensis* and *T. hypogea*, which are both expected not to contain any *ilv* gene cluster and then no AHAS activity (**Figure 4-12**).

4.4.4 Oxygen sensitivity of native AHAS activity

The effect of oxygen on the AHAS activities in the CFEs of *T. maritima* and *P. furiosus* was determined, and the half-life (the exposure time to air required for the enzyme to lose 50% of its activity) was estimated. A sample kept under anaerobic conditions (nitrogen pressure) served as a negative control in each case.

The AHAS activity in *T. maritima* was quite unstable. It was un-expected that both aerobic and anaerobic samples lost major portion of their activity at almost the same rate (**Figure 4-13A**), indicating that the decrease of the activity was likely caused by factors other than air exposure. The time for the exposed and unexposed CFEs of *T. maritima* to lose half of their AHAS activity was about 18 h. The air exposed CFE of *P. furiosus* lost about 50% of AHAS activity in approximately 48 h (**Figure 4-13B**). The oxygen sensitivity of AHAS (and its correlated PDC activity) was further studied using the purified recombinant enzyme from *T. maritima* (section 4.4.9).

Table 4-6. AHAS activity in cell-free extracts of different hyperthermophiles

Organism	pH^a	Buffer^b	Specific activity^c
<i>Pyrococcus furiosus</i>	6.0	Phosphate, pH 6.2	73±6m mUmg ⁻¹ (n=6)
<i>Thermococcus guaymasensis</i>	10.5	CAPS, pH 11.8	19±1.5 mUmg ⁻¹ (n=4)
<i>Thermococcus kodakaraensis</i>	10.5	CAPS, pH 11.8	12.5±4m mUmg ⁻¹ (n=4)
<i>Thermotoga maritima</i>	6.0	Phosphate, pH 6.2	100.2±9 Umg ⁻¹ (n=6)
<i>Thermotoga hypogea</i>	10.5	CAPS, pH 11.8	17.4±1.9 Umg ⁻¹ (n=4)
<i>Thermotoga neapolitana</i>	10.5	CAPS, pH 11.8	18.1±1.4 Umg ⁻¹ (n=4)

^a pH at 80°C

^b All buffers were used at 50 mM; the pH was adjusted at room temperature

^c The activity assays were all conducted at 80°C under anaerobic conditions with the assay compositions as described in Materials and Methods section; the value of “n” represents the number of independent repeats (each in duplicate) for each experiment

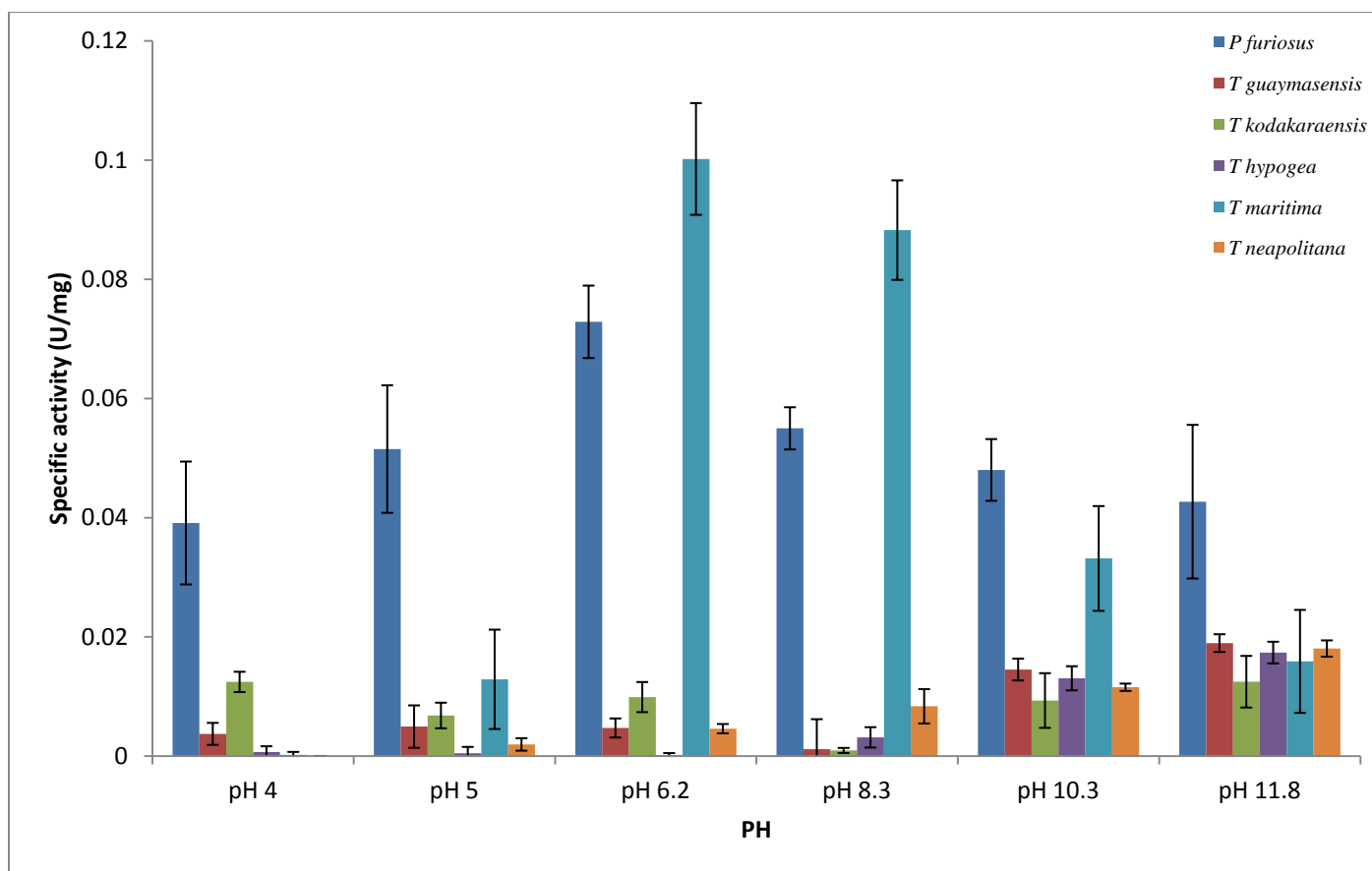


Figure 4-12. AHAS activity in CFEs of different hyperthermophilic bacteria and archaea

Buffers used for the experiment (all used at 50 mM concentration): pH 4.0 and pH 5.0, sodium acetate; pH 6.2, sodium phosphate; pH 8.4, EPPS; pH 10.3, glycine buffer, and pH 11.8, CAPS buffer. All of the pH values are at room temperature. The error bars indicate the standard error from mean. For the number of repeats (n) see **Table 4-6**.

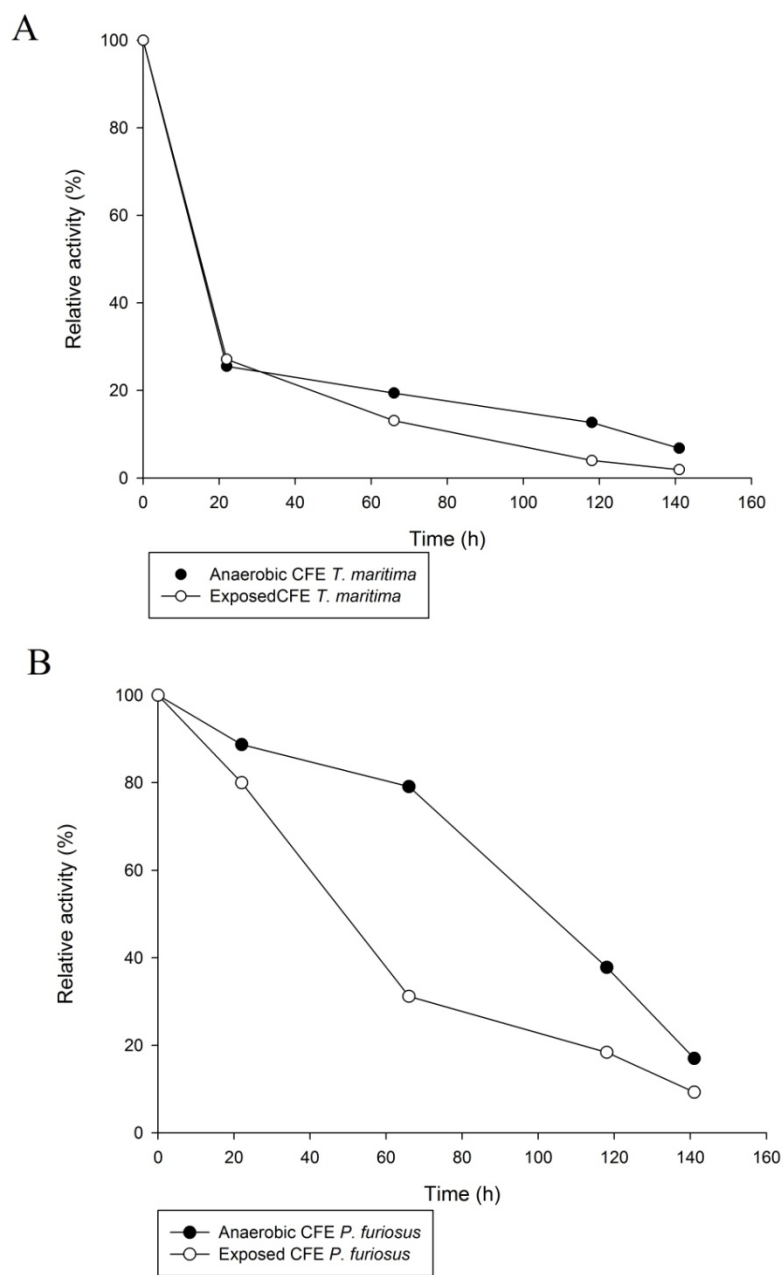


Figure 4-13. Oxygen sensitivity of AHAS activities in CFEs of *T. maritima* (A) and *P. furiosus* (B)

All assays were done in duplicates, at 80°C; the assay mixture contained EPPS buffer (50 mM), MgCl₂ (10 mM), TPP (0.5 mM), pyruvate (50 mM), and FAD (0.01 mM). All CFEs were kept on ice and magnetically stirred throughout the experiment.

4.4.5 Expression of recombinant AHAS

There is a significant difference between the codon usage of *E. coli* and hyperthermophiles. To solve the codon bias problem between the hyperthermophiles (*T. maritima* and *P. furiosus*) and the mesophilic expression hosts, *E. coli* strain Rosetta 2 BL21 (DE3) was used to supply tRNA for codons AUA, AGG, AGA, CUA, CCC, GGA, and CGG on a chloramphenicol-resistant plasmid. A total of five expression plasmids were constructed (**Figure 4-3** and **Figure 4-4**) for the following genes: the expression plasmids MI-pET30a, Ms-pET30a, and Mc-pET30a were constructed for the expression of catalytic (large) subunit, regulatory (small) subunits, and both the large and small subunits (simultaneously and in their native order) of TmAHAS-encoding genes, respectively (**Figure 4-14**) and the recombinant plasmid FI- and Fs-pET30a were constructed for the expression of the large subunit and the hypothetical small subunits of PfAHAS (**Table 4-5**).

Each construct encoded a fusion protein with six histidine-tags (hexa-histidine) at the N-terminal end for purification of the protein. After induction with IPTG, the recombinant strains produced bands with the expected sizes on SDS-PAGE for each corresponding protein (**Figure 4-15**). The expected sizes, the isoelectric points (PI) and net charges of the recombinant proteins at pH 7.0 were calculated from the deduced amino acid sequences resulted from the translation of gene sequence (**Table 4-7**).

The clone MI-pET30a produced reasonable amounts of soluble recombinant protein (**Figure 4-15**, lanes 1-3); addition of FAD, TPP, and the MgCl₂ both in the culture medium and in lysis buffer had no obvious effect on the expression levels or the solubility of the heterologously expressed catalytic subunit. In particular, the regulatory (small) subunit recombinant protein showed low solubility and mainly was aggregated in the insoluble fractions (**Figure 4-15**, lanes 4-6). In case of the clone Mc-pET30a the large subunit was expressed and present in the soluble fractions. The protein yield of the regulatory (small) subunit was very small as indicated by a weak protein band in SDS-PAGE of both soluble and insoluble fractions (**Figure 4-15**, lanes 7-9), suggesting the possible proteolysis or incomplete translation of the recombinant regulatory subunit.

Effect of different temperatures on the expression of TmAHAS clones was studied by incubation of the cultures at 18°C, 24°C, 30°C, and 37°C following growth at 37°C and induction. The expression levels were compared using SDS-PAGE (**Figure 4-16**) and enzyme activity assays (**Figure 4-17** and **Figure 4-18**). The highest yield of soluble recombinant proteins were expressed when the cultures were incubated at 30 or 37°C following induction.

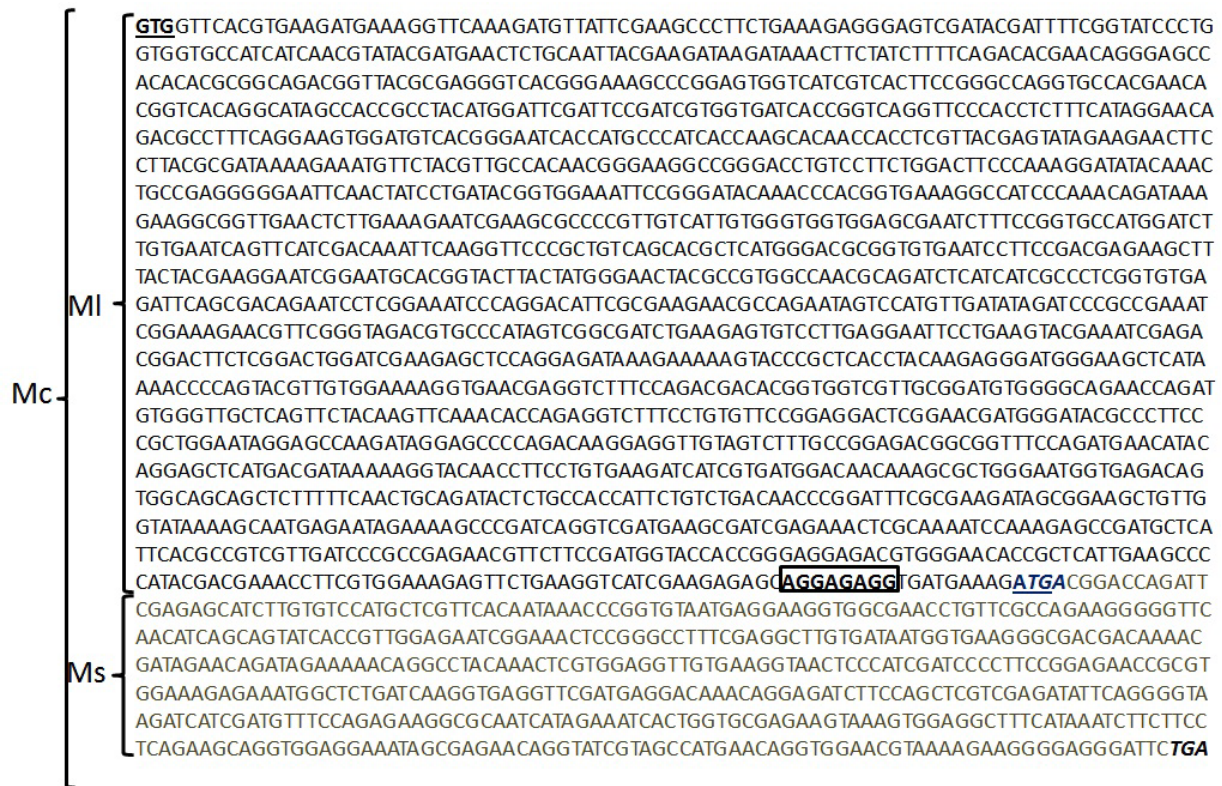


Figure 4-14. Coding sequences of catalytic and regulatory subunits of TmAHAS

The start codons for the large and small subunits are indicated in bold. Stop codon for the large subunit is italicized. Boxed sequence indicates the putative RBS for the small subunit; MI, the catalytic (large) subunit; Ms, regulatory (small) subunit; Mc, combined large and small subunits in their natural orders.

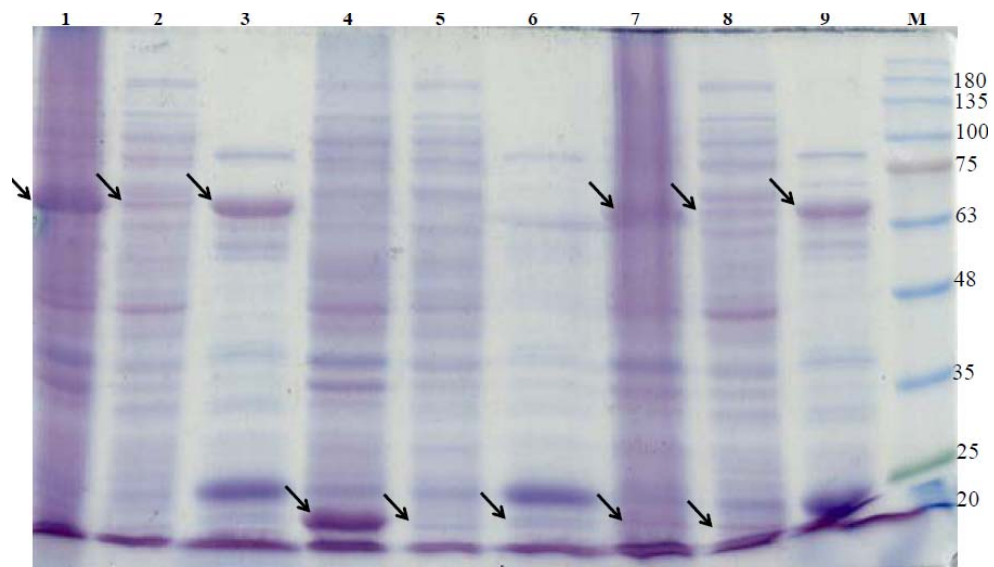


Figure 4-15. Analysis of over-expression of different clones at 37°C using SDS-PAGE (12.5%)

Lane 1, crude extract of MI-pET30a; lane 2, CFE of MI-pET30a; lane 3, heat-treated CFE of MI-pET30a; lane 4, crude extract of Ms-pET30a; lane 5, CFE of Ms-pET30a; lane 6, heat-treated CFE of Ms-pET30a; lane 7, crude extract of Mc-pET30a; lane 8, CFE of Mc-pET30a; lane 9, heat-treated CFE of Mc-pET30a; M: BLUeye pre-stained Protein Ladder (Froggibio, ON, Canada), the arrows indicate the position of the recombinant protein band; approximately 15 µg protein was loaded per lane.

Table 4-7. Properties of recombinant proteins as deduced from their primary structures^a

Clone	Description	Locus tag	Net charge at pH 7.0	P ₁	Molecular weight
MI-pET30a	Catalytic (large) subunit of TmAHAS	TM0548	-10	5.9	65.5
Ms-pET30a	Regulatory (small) subunit of TmAHAS	TM0549	+0.3	7.2	20.6
Fl-pET30a	Catalytic (large) subunit PfAHAS	PF0935	-4.6	6.4	64
Fs-pET30a	Regulatory (small) subunit PfAHAS	PF0934	+1.93	8.4	16.1

^a For plasmid Mc-pET30a (expressing the catalytic and regulatory subunits in their natural orders), the properties of the resulting recombinant protein is not included in the table as it was expected to produce two separate proteins of catalytic and regulatory subunits. The parameters were calculated using the EditSeq software (Lasergene, DNASTar, Madison, USA).

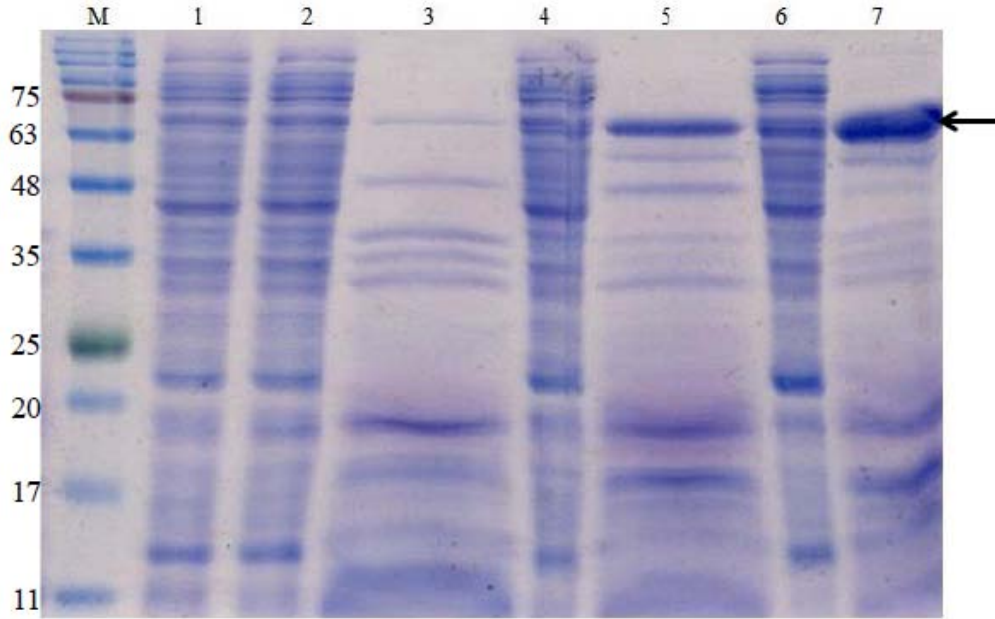


Figure 4-16. Analysis of the effect of temperatures on expression of MI-pET30a (recombinant catalytic subunit of TmAHAS) using SDS-PAGE (15%)

Lane 1, CFE, 18°C; lane 2, CFE 24°C; lane 3, heat-treated CFE, 24°C; lane 4, CFE 30°C; lane 5, heat-treated CFE, 30°C; lane 6, CFE, 37°C; heat-treated CFE 37°C; M: BLUeye pre-stained protein ladder (Froggibio, ON, Canada), the arrows indicate the position of the recombinant protein band (calculated molecular weight 65.5 kDa); 40 µg of the protein loaded per lane,

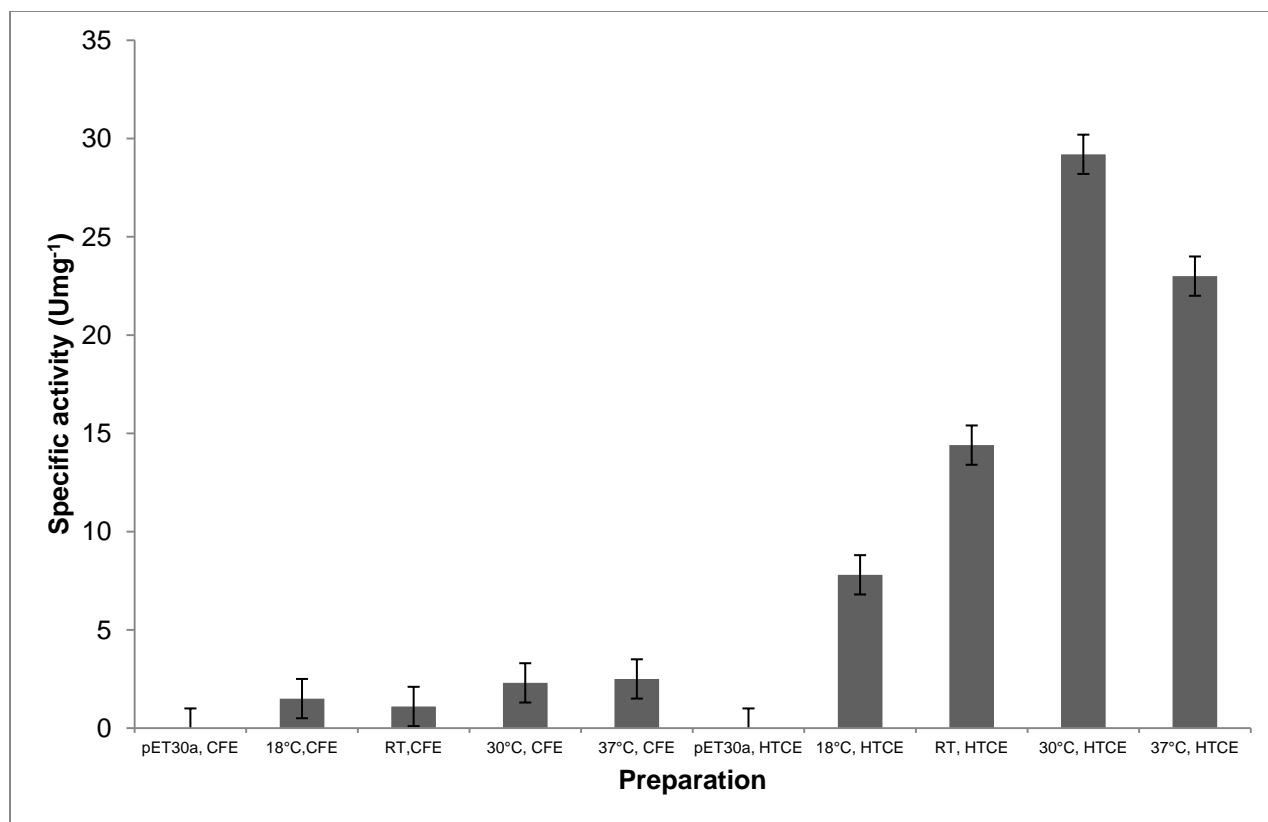


Figure 4-17. Effect of the expression temperature on AHAS activity of MI-pET30a

RT, room temperature (24°C); CE, crude extract; CFE, cell-free extract; HTCE, heat-treated (80°C, 1hr) crude extract. Assays were conducted in duplicates, at 80°C under anaerobic conditions; the assay mixture contained EPPS buffer (50 mM, pH 7.5), MgCl₂ (10 mM), TPP (0.5 mM), pyruvate (50 mM), and FAD (0.01 mM)

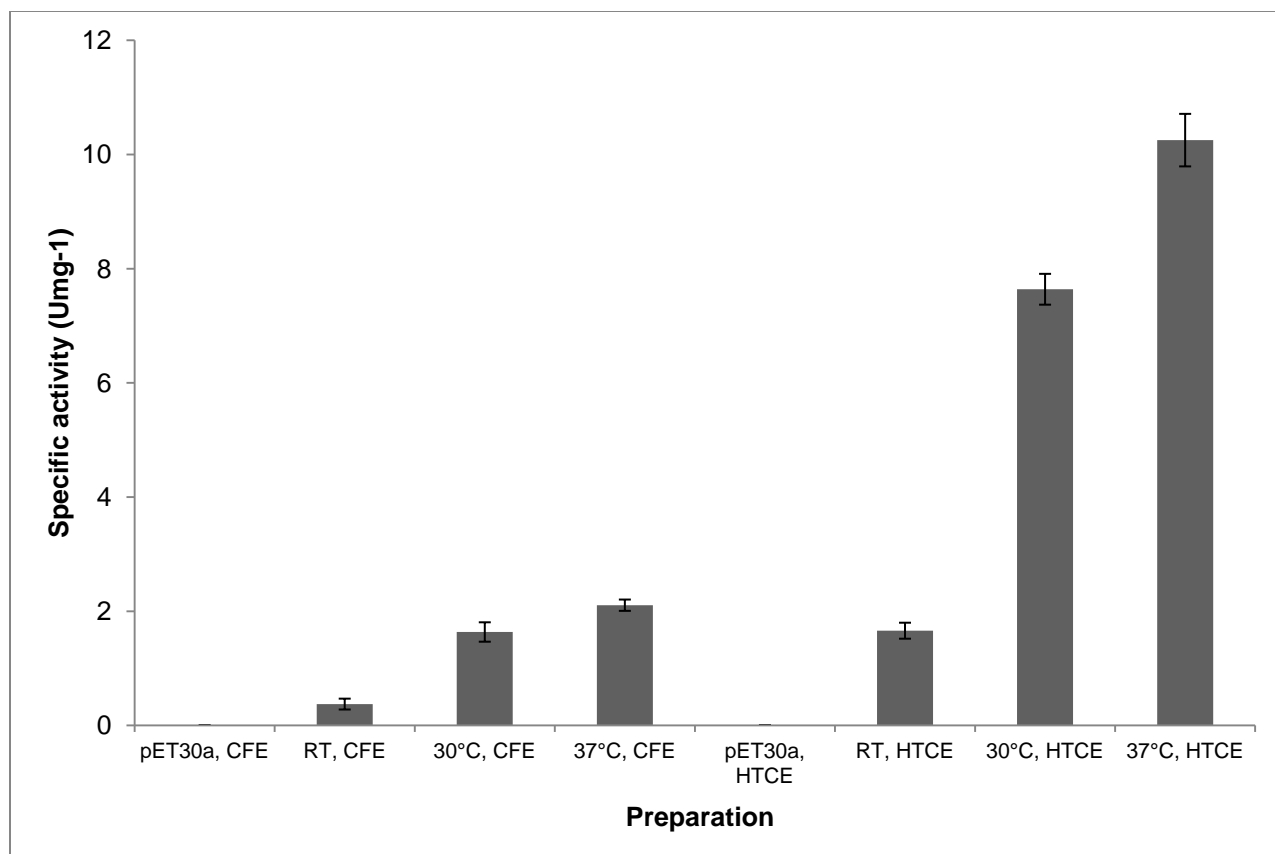


Figure 4-18. Effect of the expression temperature on AHAS activity of Mc-pET30a

RT, room temperature (24°C); CE, crude extract; CFE, cell-free extract; HTCE, heat-treated (80°C, 1 h) crude extract. Assays were conducted in duplicates, at 80°C under anaerobic conditions; the assay mixture contained EPPS buffer (50 mM, pH 7.5), MgCl₂ (10 mM), TPP (0.5 mM), pyruvate (50 mM), and FAD (0.01 mM).

No activity was detected in any of the crude extracts and CFEs from the *P. furiosus* clones despite checking the activity with different conditions including: the preparation with cofactors (1 μM) added to the lysis buffer, cell lysis in the presence of different detergent concentrations, different buffers and pHs, heat-treatment at different temperatures, and mixing the preparations from the large and small subunits with different ratios (1:5, 1:10, and 1:20).

4.4.6 Purification of recombinant TmAHAS subunits

The over-expressed catalytic and regulatory subunits of TmAHAS in *E. coli* were purified approximately 30-fold to a specific activity of 163 Umg^{-1} . The purification procedure is carried out in two major steps. First, heat-induced precipitation was exploited to simplify the recombinant protein purification. In the second step, DEAE and HAP column chromatography methods were used for the purification of the catalytic subunits, and immobilized metal affinity chromatography (IMAC) method was used for purification of the regulatory subunit.

Heat-induced precipitation (heat-treatment) is widely used for purification of the recombinantly expressed thermostable proteins. During the heat-treatment, majority of mesophilic host proteins are denatured and aggregated, rendering the recombinantly expressed thermostable protein in the soluble fraction. The optimal temperature for heat-induced precipitation was selected based on the examination of literatures on expression of various hyperthermophilic proteins in *E. coli*. The results of the survey indicated that the heat-precipitation step was mostly carried out successfully at the temperature close to the optimal growth temperature of the native organism (**Table 4-8**).

The effect of heating temperatures on the yield of the soluble protein and the corresponding enzyme activity of TmAHAS was studied on crude cell extracts incubated at 70°C and 80°C under anaerobic conditions. Samples that were taken at different time intervals were analyzed using SDS-PAGE and enzyme activity assays. The heat-treatment of TmAHAS (catalytic subunit) at 70°C and 80°C showed increased purity of the prepared protein over time (**Figure 4-19**). The highest AHAS activity was achieved after heat-treatment at 80°C for 60 min (**Figure 4-20**). Interestingly, the incubation of the cell crude extracts at any of the two temperatures (70 and 80°C) resulted in an increased AHAS activity with the highest activity found after 1hr of incubation at each temperature, but extended incubation caused enzyme inactivation (**Figure 4-20**) indicating its thermal stability.

Fractions containing the catalytic (large) subunit were eluted out from DEAE-sepharose column when a gradient of sodium chloride (from 275-370 mM) was applied. The protein was eluted from HAP column when a gradient of 180-230 mM of sodium phosphate was applied to the column.

Table 4-8. Survey of heat-precipitation temperatures for some recombinant hyperthermophilic proteins expressed in *E. coli*

The recombinant protein	Native organism	Heat-precipitation	T_{opt}^a	Reference
Glutaredoxin-like protein	<i>Pyrococcus furiosus</i>	65°C for 10min	100°C	Guagliardi <i>et al.</i> 1995
The HU protein	<i>Thermotoga maritima</i>	80°C for 20min	80°C	Esser <i>et al.</i> 1999
Phosphoglycerate kinase	<i>Thermotoga maritima</i>	60min at 80°C	80°C	Grättinger <i>et al.</i> 1998
ADP-dependent phosphofructokinase	<i>Pyrococcus furiosus</i>	30min at 80°C	100°C	Tuininga <i>et al.</i> 1999
Chemotaxis protein	<i>Thermotoga maritima</i>	80°C for 10min	80°C	Swanson <i>et al.</i> 1996
Maltose-binding protein	<i>Thermotoga maritima</i>	75°C for 30min	80°C	Wassenberg <i>et al.</i> 2000
Carboxylesterase	<i>Sulfolobus sulafataricus</i>	75°C for 30min	80°C	Morana <i>et al.</i> 2002
Glyceraldehyde-3-phosphate dehydrogenase	<i>Pyrococcus woesei</i>	90°C for 30min	100-103°C	Zwickl <i>et al.</i> 1990
Glyceraldehyde-3-phosphatdee hydrogenase	<i>Thermotoga maritima</i>	Inactive protein ^b	80°C	Tomschy <i>et al.</i> 1993
Xylose isomerase	<i>Thermotoga maritima</i>	90°C for 2.5h	80°C	Vieille <i>et al.</i> 1995
L-arabinose isomerase	<i>Thermotoga neapolitana</i>	85°C for 15min	80°C	Kim <i>et al.</i> 2002
Alcohol dehydrogenase (<i>adhC</i>)	<i>Pyrococcus furiosus</i>	80°C for 30min	100°C	Kube <i>et al.</i> 2006
<i>a</i> -L-arabinofuranosidase	<i>Thermotoga maritima</i>	80°C for 30min	80°C	Miyazaki 2005
6-phosphogluconate dehydrogenase	<i>Thermotoga maritima</i>	90°C for 30min	80°C	Wang and Zhang 2009

^a Optimum growth temperature of the native hyperthermophilic organism

^b The heat-treated purified recombinant protein was inactive

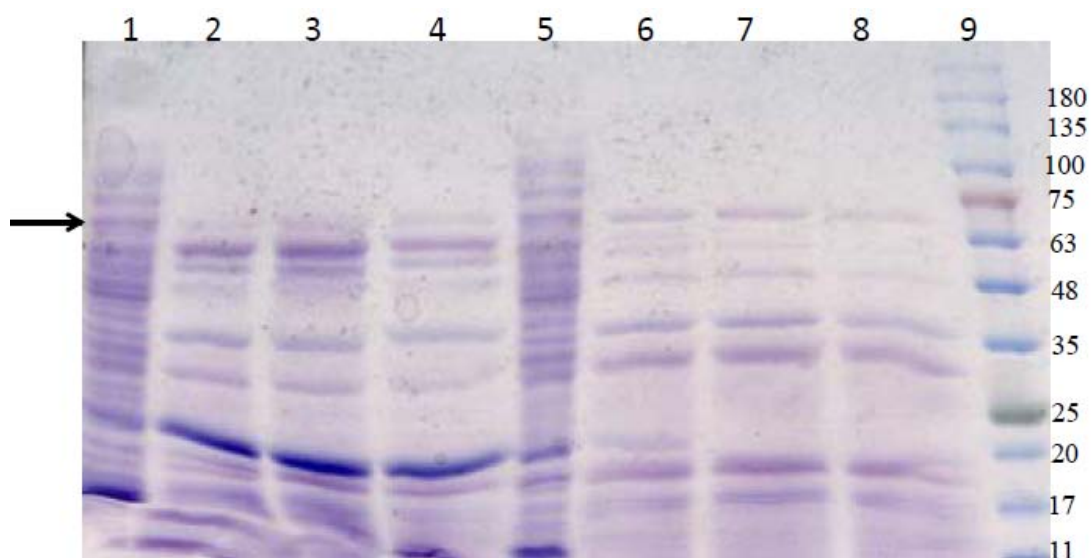


Figure 4-19. Analysis of the effect of heat-treatment on purification of MI-pET30a (recombinant catalytic subunit of TmAHAS) using SDS-PAGE (12.5%)

Lane 1, CFE with no heat-treatment; lane 2, CFE, 30 min at 70°C; lane 3, CFE, 60 min at 70°C; lane 4, CFE, 90 min at 70°C; lane 5, CFE with no heat-treatment; lane 6, CFE, 30 min at 80°C; lane 7, CFE, 60 min at 80°C; lane 8, CFE, 90 min at 80°C; M: BLUeye pre-stained protein ladder (Froggibio, ON, Canada), the black arrow indicate the position of the recombinant protein band (calculated molecular weight 65.5 KDa); approximately 30 µg of the protein loaded per lane

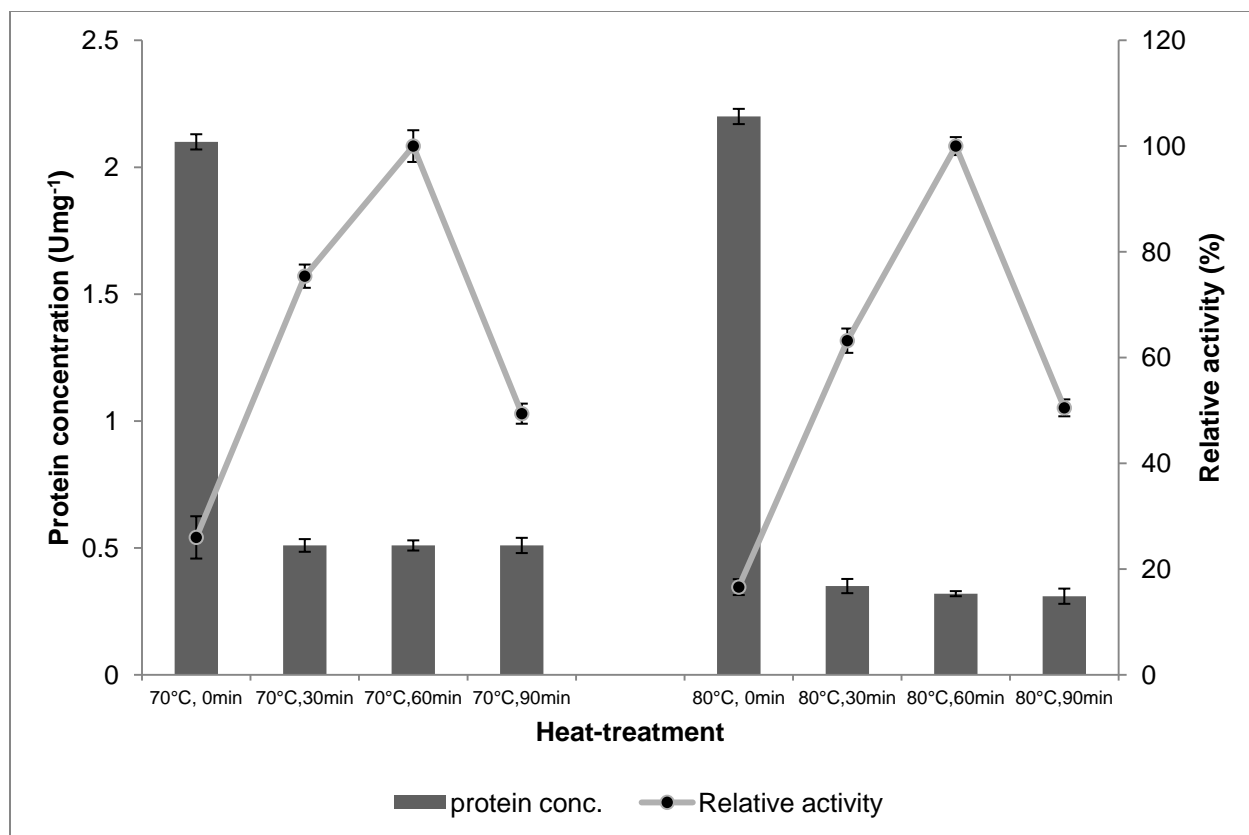


Figure 4-20. Effect of heat-treatment of crude extract on AHAS activity

The CFEs were heat-treated at 70°C and 80°C under anaerobic conditions and assayed for AHAS activity at different time points. The relative activities were calculated compared to the activity after 1 h at each temperature. Assays were carried out in duplicates, at each temperature under strictly anaerobic conditions; the assay mixture contained EPPS buffer (50 mM, pH 7.5), MgCl₂ (10 mM), TPP (0.5 mM), pyruvate (50 mM), and FAD (0.01 mM). A relative activity of 100% was considered as the highest specific activities measured at each temperature after 1h of heat-treatment (8.0 Umg⁻¹ and 8.7 Umg⁻¹, for 70 and 80°C, respectively).

After HAP column the TmAHAS catalytic subunit was judged to be pure by analysis on SDS-PAGE (**Figure 4-21**). A typical purification of the catalytic subunit is summarized in **Table 4-9**. Approximately 1mg purified recombinant protein was obtained from each gram (wet weight) of the *E. coli* biomass.

The small subunit was expressed partly as insoluble inclusion bodies as judged by SDS-PAGE analysis (**Figure 4-15**), which was expected based on a previous report pertaining to the expression of the same protein (Petkowski *et al.* 2007). Altering the expression conditions namely temperature and IPTG concentration (0.1-0.5 mM), growing the recombinant strain in the presence of different glycerol concentrations (0-40%), incorporation of TPP, FAD, and MgCl₂ (together or individually), as well as expression and cell lysis in the presence of different (Triton X-100) concentrations (0-0.5%), did not improve the solubility of the small subunit (although increasing the expression temperature from 18°C to 37°C increased expression of the recombinant protein). Hence, re-solubilization of the recombinant small subunit was carried out by its purification under denaturing conditions using hexa-histidine affinity chromatography and subsequent on-column refolding of the denatured protein which resulted in a soluble and highly pure protein (**Figure 4-22**). The solubility of the regulatory subunit was also highly dependent on the concentration of sodium chloride with the buffer of higher concentration (250-300 mM) resulting in better solubility of the protein.

4.4.7 Molecular weights of the recombinant proteins

The native molecular masses of catalytic and regulatory subunits were estimated by loading each protein separately on size-exclusion chromatography column. The recombinant catalytic subunit (calculated molecular mass was 65,497 Da and estimated molecular mass on SDS-PAGE was 66,398±7,700 Da) was eluted as a single peak and corresponded to molecular mass of 156,830±6,200 Da ($n=4$) indicating a dimeric structure. This is in agreement with previous finding of the minimal functional unit of TPP-dependent enzyme being a dimer to accommodate the active site of the enzyme in interface between subunits (Muller *et al.* 1993; Vyazmensky *et al.* 1996; Schellenberger 1998; Gedi and Yoon 2012) and also previous report on recombinantly expressed catalytic subunits from different organisms (Hill *et al.* 1997). The regulatory subunit of TmAHAS (calculated molecular mass was 20,508 Da and estimated molecular mass on SDS-PAGE gel 22,210±3,540 Da) had a native molecular mass of 37,700±413 Da ($n=4$) measured in size-exclusion chromatography, suggesting a dimeric structure for the small subunit. Increasing the salt concentration of the elution buffers from 50 to 300 mM had no effect on elution behavior of proteins.

Table 4-9. Purification of recombinant catalytic (large) subunit of TmAHAS^a

Step	Total protein ^b (mg)	Total activity ^c (Units)	Specific activity ^d (Umg ⁻¹)	Purification (fold)	Recovery (%)
Crude extract	1175	6345	5.4	1	100
Heat-treatment	138	4882	31.1	5.8	76.9
DEAE	53	3808	70.8	13.2	60.1
HAP	21	3302	163	30.2	52.1

^a CFE was prepared from 20 g (wet weight) of the recombinant *E. coli* strain MI-pET30a

^b As determined by Bradford assay using BSA as the standard protein as described in Materials and Methods (section 4.3.8)

^c AHAS activity assays were carried out using standard procedure as described in the Material and Methods (section 4.3.10)

^d Expressed as micromoles of acetolactate produced per min per milligram of the enzyme

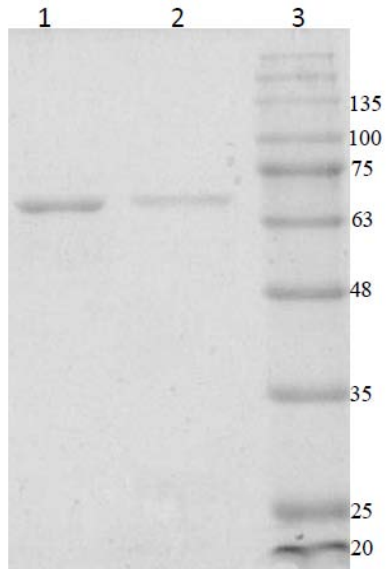


Figure 4-21. Analysis of purified catalytic subunit of TmAHAS (MI-pET30a) using SDS-PAGE (12.5%)

Lane 1, 4 µg of the purified protein; lane 2, 2 µg of the purified protein; lane 3, BLUeye pre-stained protein ladder (Froggibio, ON, Canada)

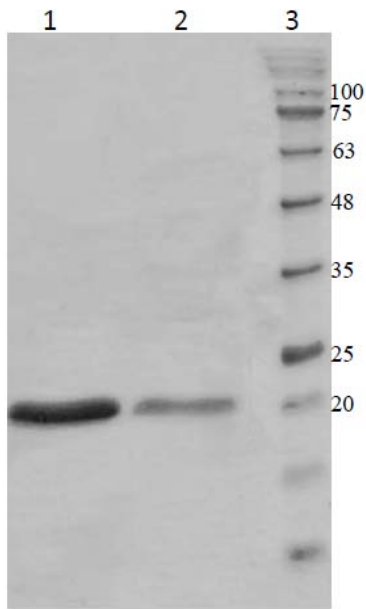


Figure 4-22. Analysis of purified recombinant regulatory subunit of TmAHAS (Ms-pET30a) using SDS-PAGE (15%)

Lane 1, 8 μ g of the purified protein; lane 2, 4 μ g of the purified protein; lane 3, BLUeye pre-stained protein ladder (Froggibio, ON, Canada)

4.4.8 PDC activity of recombinant AHAS

To determine if the recombinant AHAS would have pyruvate decarboxylase activity, different preparations of the recombinant clones were used. All CFEs, except that prepared from the clone expressing the regulatory (small) subunit showed PDC activity. The PDC activity of the recombinant TmAHAS was measured when FAD and TPP were added to the assay mixture. The CFE containing the catalytic subunit after heat-treatment showed a specific activity of approximately $0.7 \pm 0.18 \text{ Umg}^{-1}$ which increased to $16.7 \pm 3.4 \text{ Umg}^{-1}$ after purification. When FAD was not added to the assay buffers, the purified enzyme still showed about 45% of the full activity, suggesting presence of the cofactor (FAD) in the purified enzyme. However, omitting TPP from assay mixture resulted in decreased specific activity to approximately 10% of the full activity (1.6 Umg^{-1} versus 16.1 Umg^{-1}) indicating much less tight-binding of TPP incorporated to the the enzyme structure.

The ability of the catabolic AHAS (ALS) in catalyzing non-oxidative decarboxylation of 2-ketoisobutyrate (3-methyl-2-oxobutyrate) was reported previously (Atsumi *et al.* 2009). To investigate the ability of the recombinant anabolic TmAHAS for non-oxidative decarboxylation of other 2-keto acids, the decarboxylase activity assays were conducted with 2-ketoisovalerate instead of pyruvate. A standard curve was prepared with the product of decarboxylation reaction, isobutyraldehyde. Although with lower affinity, the recombinant TmAHAS was able to non-oxidatively decarboxylate the 2-ketoisovalerate to isobutyraldehyde with a rate about 10% of that when pyruvate was used.

4.4.9 Catalytic properties of synthase and decarboxylase reactions

To determine optimal pH for AHAS and PDC activities of TmAHAS, a set of 100 mM buffers were used under anaerobic conditions and at 80°C. The highest activities were measured for both AHAS and PDC reactions at pH 7.0 with phosphate buffer (**Figure 4-23**). The optimal pH of the AHAS was in agreement with the pH optima of the previously reported anabolic AHASs from various organisms (Grimminger and Umbarger 1979; Kalme *et al.* 2008).

The steady-state kinetic parameters were determined for each substrate (pyruvate, TPP, and FAD) at pH 7.0 and 80°C for both AHAS and PDC activities (**Table 4-10**). It seemed that the effect of the pyruvate concentration on velocity of the PDC reaction catalyzed by TmAHAS did not follow the simple Michaelis-Menten kinetics, but displays a sigmoid cooperative effect (**Figure 4-24**). Several repeats of the same experiment resulted in the similar curves shapes. The sigmoid effect did not seem to be the result of the change in the assay volume due to the addition of large pyruvate stock volumes; as the

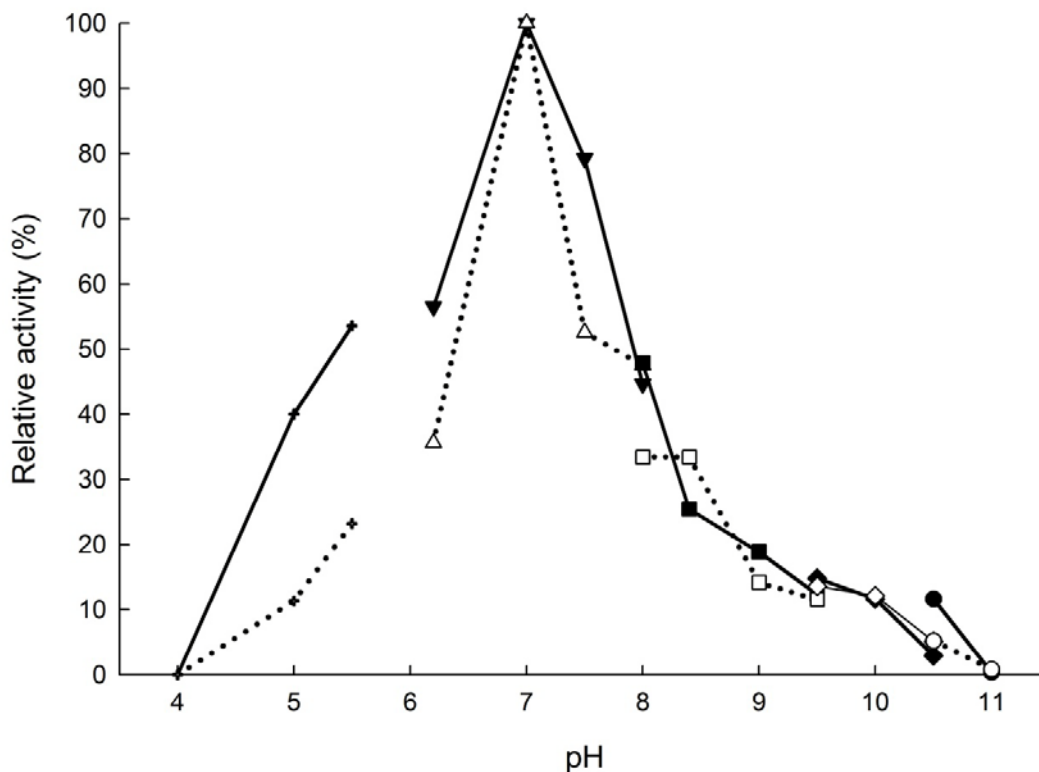


Figure 4-23. pH dependency of AHAS and PDC activities of recombinant TmAHAS

Both enzyme activities were measured as described previously (sections 4.3.10 and 4.3.11) under anaerobic conditions. The assay mixtures (1 ml total volume) contained corresponding buffers at 100 mM concentrations, 200 mM NaCl, 10 mM MgCl₂, 2.5 mM thiamine pyrophosphate (TPP), 50 mM sodium pyruvate, and 10 μM FAD. The relative activities of 100% equals to highest measured specific activity for both enzymes at 80°C and in sodium phosphate buffer, pH 7.0 (114 Umg⁻¹ for AHAS and 17.7 Umg⁻¹ for PDC activity).

The filled symbols represent the AHAS activity and the open symbols represent the PDC activity. The plus symbols represent the sodium acetate buffer (pH values 4.0, 5.0, and 5.5); the triangles and inverted triangles represent the sodium phosphate buffer (pH 6.2, 7.0, 7.5, and 8.0); the square symbols represent the EPPS buffer (pH 8.0, 8.4, 9.0, and 9.5); the triangles represent glycine buffer (pH 9.5 and 10); and circles represent the CAPS buffer (pH 10.5 and 11.0).

Table 4-10. Apparent kinetic parameters for AHAS and PDC activities of recombinant TmAHAS^a

Substrate	AHAS activity			PDC activity		
	Apparent K_m	Apparent V_{max} (Umg^{-1})	k_{cat} (S^{-1})	Apparent K_m	Apparent V_{max} (Umg^{-1})	k_{cat} (S^{-1})
Pyruvate	16.4±1.9 mM	246±7.4	98.5	ND	ND	ND
TPP ^b	57±6.0 μ M	242±3.8	96.9	35±0.6 μ M	25.9±0.6	7.6
FAD ^b	0.15±0.07 μ M	134±11	53.7	0.12±0.05 μ M	18.1±1.7	7.3

ND, not determined as the saturation curve is not following the Michaelis-Menten kinetics

^a The kinetics parameters were determined following the procedure explained in the Materials and Methods (section 4.3.14). The assays were all conducted at 80°C and under anaerobic conditions using the procedures described in sections 4.3.10 and 4.3.11 for AHAS and PDC activities, respectively. Various concentrations of each substrate were used for the determination of the kinetic parameters for the corresponding substrate while keeping the other concentrations constant.

^b The kinetic parameters for the TPP and CoA must be considered prudently, as even in the absence of these cofactors significant activity is present.

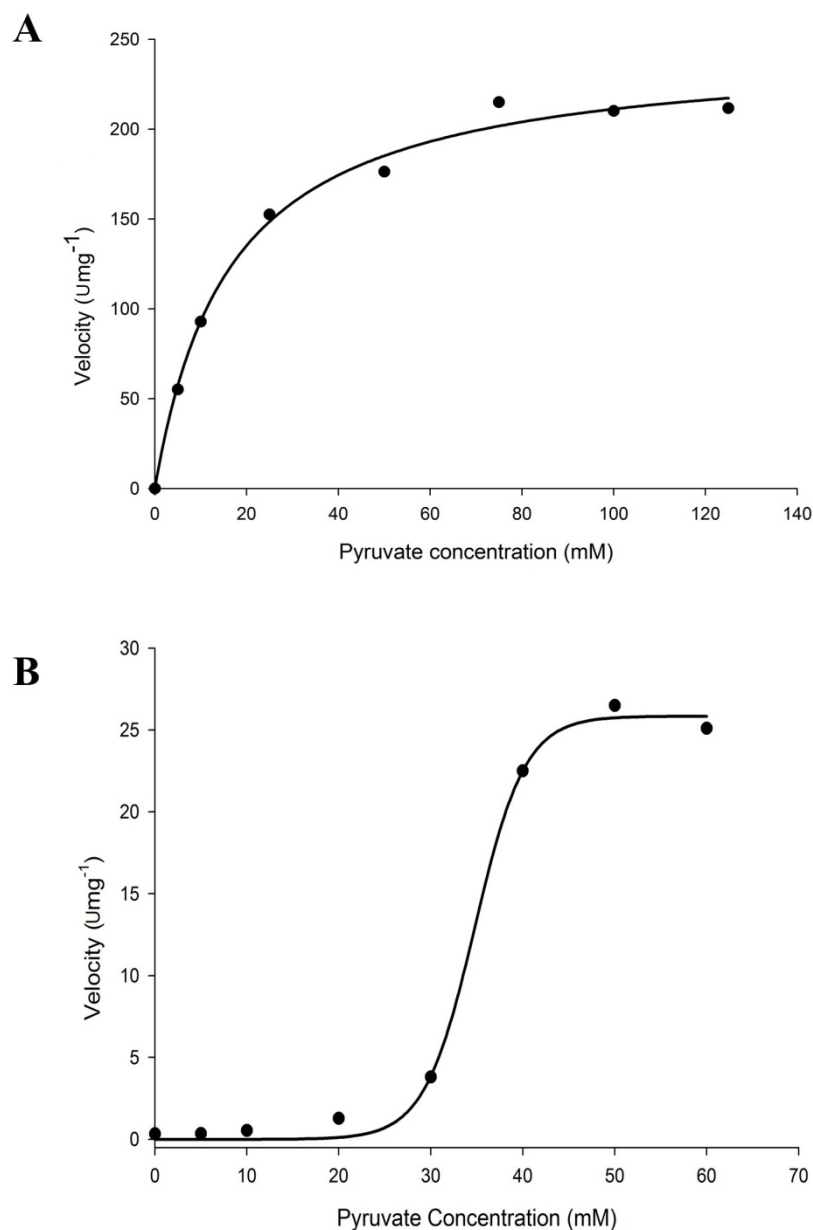


Figure 4-24. Dependence of AHAS (A) and PDC (B) activities on pyruvate concentration

The kinetics for pyruvate was determined for AHAS and PDC activities of TmAHAS. The assays were conducted as described in Material and Method (section 4.3.10 and 4.3.11) with the reaction mixtures (1 ml total volume) contained 100 mM sodium phosphate, 200 mM sodium chloride, 10 mM magnesium chloride, 2.5 mM thiamine pyrophosphate (TPP), 10 μM FAD and different concentrations of sodium pyruvate. The points are experimental values and repeated in duplicates (three independent repeats). The curves are the theoretical fit of data to the hyperbolic and sigmoid plot equations for AHAS and PDC activities, respectively.

reaction volumes were kept constant for different pyruvate concentrations. The non-Michaelis-Menten kinetics for the AHAS substrate pyruvate is a common phenomenon and the positive cooperativity was reported previously from the AHAS activities of *Lactococcus lactis* (Snoep *et al.* 1992), *Serratia marcescens* (Yang and Kim 1993), *Haemophilus influenza* (Choi *et al.* 2007; Gedi *et al.* 2011), *Mycobacterium tuberculosis* (Choi *et al.* 2005; Singh *et al.* 2011), and the mesophilic archaeon *Methanococcus aeolicus* (Xing and Whitman 1994).

When assayed in the cell-free extract or heat-treated cell-free extract, the activity of the enzyme was independent of FAD because the addition of FAD to the assay mixture showed no effect on the enzyme activities. However, FAD seems to be partially dissociated from the enzyme during chromatography steps. Omitting FAD from the assay mixture caused up to three times decrease in AHAS activity of the active DEAE sepharose fractions. Similarly, for the purified enzyme, the specific activity of the enzyme without adding the FAD into the assay mixture is almost four times lower compared to the assay mixture containing 10 μM FAD (43 Umg^{-1} without FAD *versus* 159 Umg^{-1} with FAD). The apparent K_m value of both activities are very close (0.15 μM and 0.12 μM for the synthase and decarboxylase activities, respectively) and much smaller than the K_m value for the other cofactor TPP. However, the K_m values for both TPP and FAD must be considered cautiously as there are some tightly bound cofactors present in the purified enzyme preparations. The presence of FAD in the enzyme structure was evident by the yellowish color of the purified enzyme preparation.

Both activities catalyzed by the recombinant TmAHAS were salt dependent and activities diminished considerably (approximately 80%) when the assays were conducted in buffer concentrations less than 100 mM. At concentrations higher than 100 mM the activity levels are quite similar (up to 500 mM salt was checked). This effect might be the results of the dissociation of the enzyme dimers. The gel-filtration of purified catalytic subunit at different salt concentrations (150-500 mM) showed no difference in elution profile. However, in each case, the salt content of the chromatography buffer was higher than 150 mM. Using a buffer with lower salt content was not recommended by the column manufacturer as it could cause an ionic interaction between the protein and the size-exclusion resin.

4.4.10 Oxygen sensitivity of TmAHAS

Both synthase and decarboxylase activities were highly susceptible toward exposure to air (protected from light, moderate stirring). The half-life ($t_{1/2}$) was about 30 min for each of the AHAS (**Figure 4-25**) and PDC (**Figure 4-26**). The unexposed samples were also extremely labile and had half life times ($t_{1/2}$) of approximately 85 min and 110 min for PDC and AHAS, respectively. Moreover, when the anaerobic sample was not stirred and kept under anaerobic conditions and at 4°C, the activities were quite stable and

lost only about 35-40% of their activity after 5 days (see control negatives in **Figure 4-27** A and B). Hence, it seemed that the physical factors rather than the oxidative damage affected the enzyme stability. There are few reports indicating the instability of the native and recombinant AHAS (Duggleby and Pang 2000).

4.4.11 Thermal stability of TmAHAS

When TmAHAS was incubated under anaerobic conditions the time needed to lose half of its activity ($t_{1/2}$) was about 25 h and 40h for AHAS and PDC activities, respectively (**Figure 4-27** A and B). When incubated at 4°C and under anaerobic conditions, both activities were highly stable and only about 40% of each activity lost after five days (**Figure 4-27** A and B). Both AHAS and PDC increased following raising the assay temperature to 85°C (**Figure 4-28**) which was the optimal temperature for the activities.

There are some reports on light sensitivity of the anabolic AHASs due to “FAD-mediated photo oxidation” (Hill *et al.* 1997; Duggleby and Pang 2000). The light sensitivity of the purified TmAHAS was tested. TmAHAS aliquots were incubated under anaerobic conditions with one of them exposed to light and the other vial protected from the light by aluminum foil. The AHAS enzyme assays were performed on both preparations and there was no difference in the specific activities of the preparation. Therefore, it seemed that light exposure had no negative effect of light on the activity of the TmAHAS.

4.4.12 Reconstitution of holoenzyme

In all of the anabolic AHASs studied so far, mixing the individually expressed catalytic and regulatory subunits resulted in reconstitution of the holoenzyme with full activity. The reconstitution process is usually a rapid and cooperative process and follows the hyperbolic saturation kinetics with a 1:1 stoichiometry (Duggleby and Pang 2000; Porat *et al.* 2004; Choi *et al.* 2005). The impact of the regulatory subunit on full activation of the enzyme is usually large but diverse, depending on the source of the enzyme. In case of the AHAS III from *E. coli* the catalytic subunit alone shows only about 5% of the activity of the holoenzyme (Vyazmensky *et al.* 1996). Reconstituted yeast AHAS has an increase of about 7-10-fold in the specific activity (Pang and Duggleby 1999). Reconstituted holoenzyme of *A. thaliana* showed least 2-3-folds increase over catalytic subunit alone. For all AHASs studied, the cofactor requirement and substrate specificity of the catalytic subunit is similar to the holoenzyme (Chipman *et al.* 1998; Duggleby and Pang 2000).

The purified catalytic and regulatory subunits were mixed under anaerobic conditions and with different molar ratios and the PDC and AHAS activities were determined. The reconstitution of the enzyme had evident impact on both AHAS and PDC activities. Both activities followed the same increment trend for most part, however, it appeared that when 1:5 ratio of catalytic and regulatory

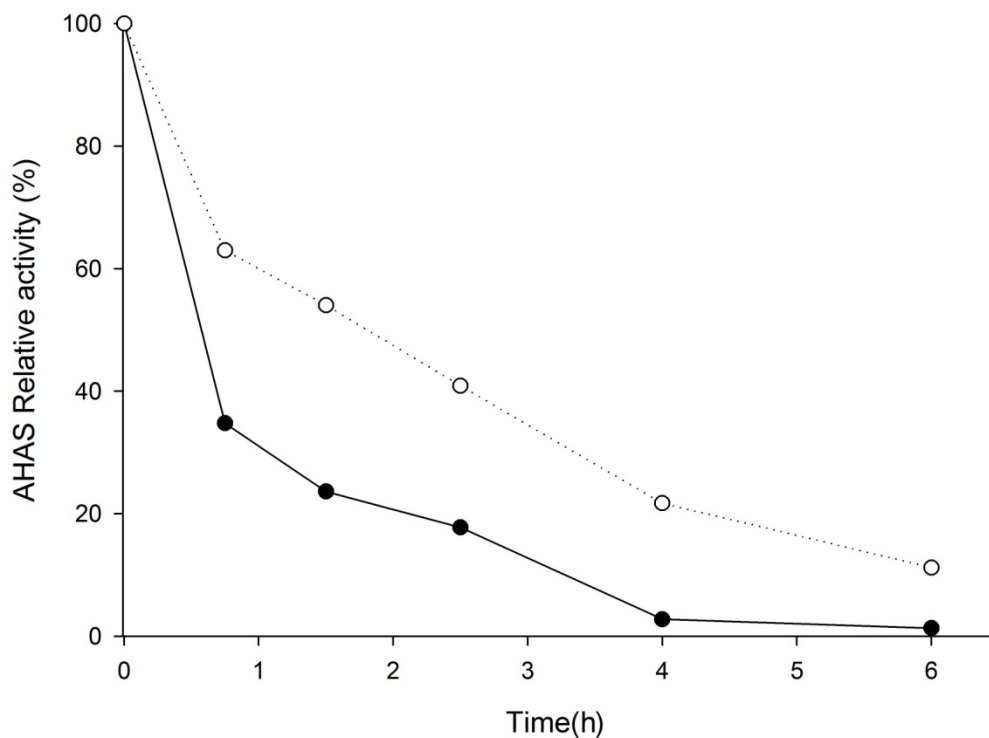


Figure 4-25. Oxygen sensitivity of recombinant TmAHAS when AHAS was measured

The enzyme assays were conducted as described previously in Materials and Methods (section 4.3.10) under anaerobic conditions. The assay mixtures (1 ml total volume) contained 100 mM sodium phosphate, 200 mM sodium chloride, 10 mM magnesium chloride, 50 mM sodium pyruvate, 2.5 mM thiamine pyrophosphate (TPP), and 10 μ M FAD. The relative activities of 100% equals to highest measured specific activity at time zero without exposure to air (166 U mg^{-1}). The filled circles indicate the exposed sample and open circles indicate the un-exposed sample.

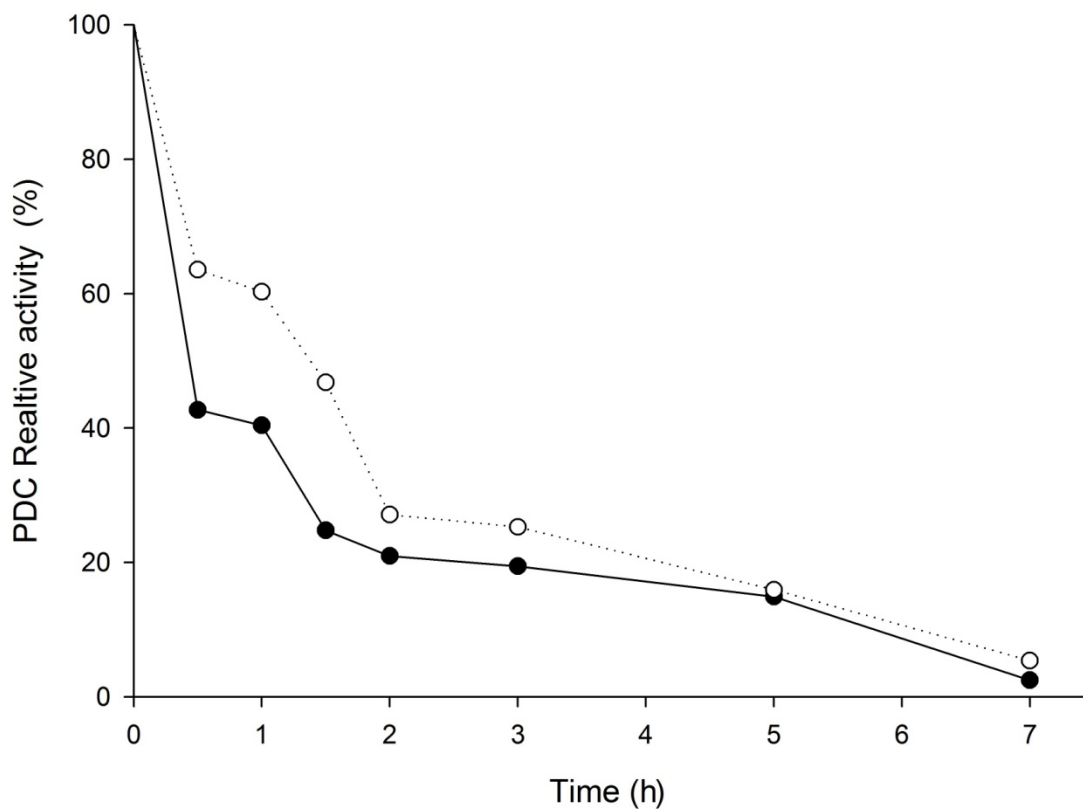


Figure 4-26. Oxygen sensitivity of recombinant TmAHAS when PDC was measured

Both enzyme activities were measured as described previously in Materials and Methods (section 4.3.11) under anaerobic conditions. The assay mixtures (1 ml total volume) contained 100 mM sodium phosphate, 200 mM sodium chloride, 10 mM magnesium chloride, 50 mM sodium pyruvate, 2.5 mM thiamine pyrophosphate (TPP), and 10 μ M FAD. The relative activities of 100% equals to highest measured specific activity at time zero without exposure to air (16.4 U mg^{-1}). The filled circles indicate the exposed sample and open circles indicate the un-exposed sample. The filled circles indicate the exposed sample and open circles indicate the un-exposed sample.

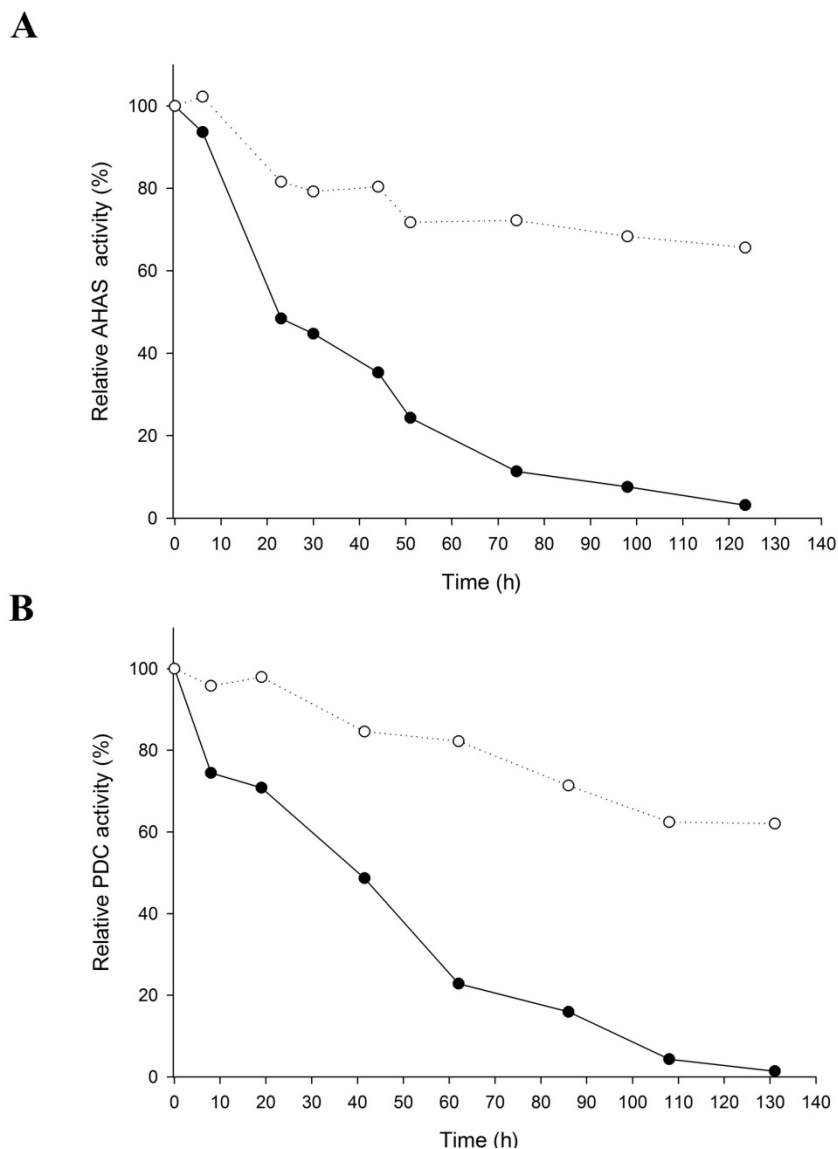


Figure 4-27. Thermal stability of synthase (A) and decarboxylase (B) activities

The thermal stabilities were determined for AHAS and PDC activities catalyzed by recombinant TmAHAS at 80°C and under anaerobic conditions. A similar aliquot of enzyme was incubated at 4°C as a control. At each time point the corresponding assay was conducted to assay the residual activity. All assays were carried out anaerobically and at 80°C. The reaction mixtures (1 ml total volume) contained 100 mM sodium phosphate, 200 mM sodium chloride, 10 mM magnesium chloride, 50 mM sodium pyruvate, 2.5 mM thiamine pyrophosphate (TPP), and 10 μM FAD. The relative activities of 100% equals to highest measured specific activity at time zero with no heat-treatment (195.0 U_{mg}⁻¹ for AHAS activity and 18.0 U_{mg}⁻¹ for PDC activity). Filled circles indicate the enzymes incubated at 80°C and the open circles indicate the enzymes stored at 4°C.

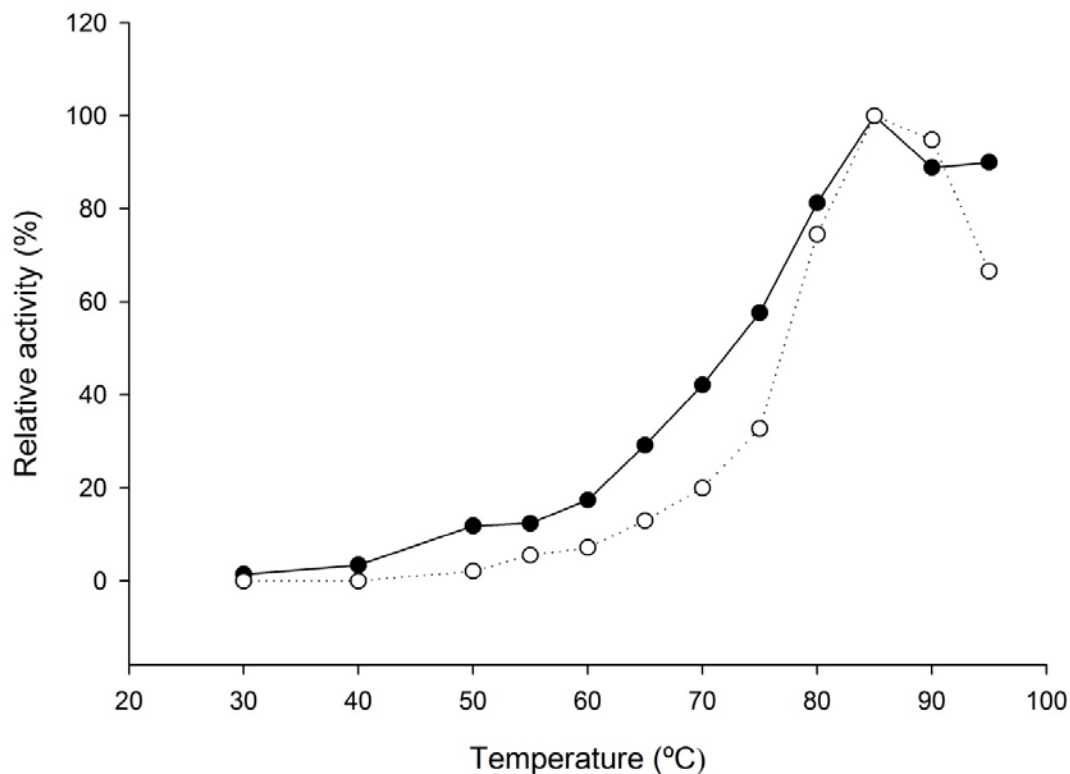


Figure 4-28. Determination of optimal temperatures of AHAS and PDC activities of recombinant TmAHAS

Both enzyme activities were measured as described previously (sections 4.3.10 and 4.3.11) under anaerobic conditions. The assay mixtures (1 ml final volume) contained 100 mM sodium phosphate, 200 mM sodium chloride, 10 mM magnesium chloride, 50 mM sodium pyruvate, 2.5 mM thiamine pyrophosphate (TPP), and 10 μ M FAD were equilibrated at each temperature for 4 min before adding the enzyme. The relative activities of 100% equals to highest measured specific activity for both enzymes at 85°C (235 Umg^{-1} for AHAS and 18.6 Umg^{-1} for PDC activity). The filled symbols indicate the AHAS and the open symbols indicate the PDC activity.

subunits were mixed, the stimulatory effect of the regulatory subunit became significant as there were a 3-fold increase in PDC activity only a slight increase in AHAS activity; But, no further increase of both activities were observed by mixing increasing ratios of catalytic to regulatory subunit up to 1:50 (**Figure 4-29**).

When the purified preparations were loaded on size-exclusion column individually each produced their corresponding bands (160 kDa and 50 kDa, respectively) at the expected elution volumes (**Figure 4-30 A** and **B**). When catalytic and regulatory subunits were mixed together in a molar ratio of 1:10 and pre-incubated at room temperature for 30 min before being loaded on size-exclusion column, the peak corresponding to large subunit was disappeared and a new peak with higher molecular mass appeared in a position equivalent to apparent molecular size of approximately 230 kDa (**Figure 4-30C**) which was suggestive of reconstitution of holoenzyme in higher oligomeric state as was expected. It seems then the holoenzyme is composed of two catalytic and two regulatory subunits ($\alpha_2\beta_2$). This is in accordance with findings on some mesophilic AHASs including AHAS III of *E. coli* (Vyazmensky *et al.* 1996).

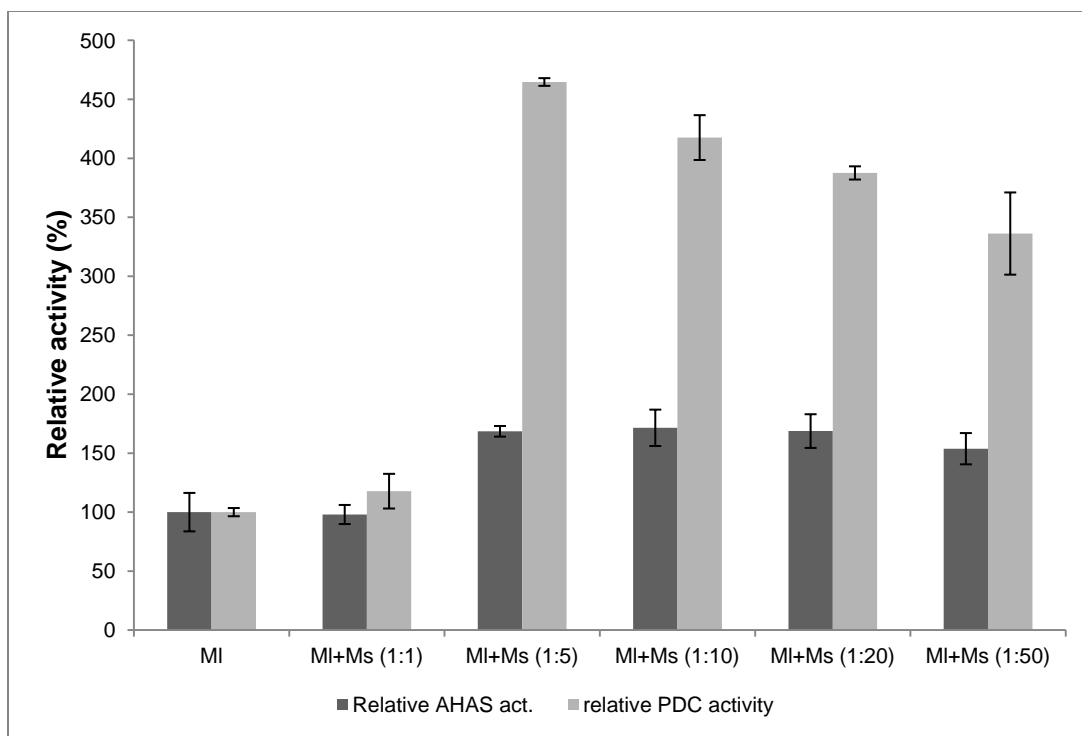


Figure 4-29. Effect of TmAHAS reconstitution on AHAS and PDC activities

MI, the purified catalytic subunit of TmAHAS; Ms, the purified regulatory subunit of TmAHAS

The effect of the enzyme reconstitution was studied on AHAS and PDC reactions catalyzed by recombinant TmAHAS. The purified catalytic subunit (50 pmol) was mixed with the purified regulatory subunit (50, 100, 250, and 500 pmol) in assay mixture. The AHAS and PDC activity assays (triplicates) were conducted as described previously (sections 4.3.10 and 4.3.11, respectively) using same batches of enzyme. In each case, the assay mixtures contained 100 mM sodium phosphate buffer (pH 7.0), 200 mM NaCl, 10 mM MgCl₂, 2.5 mM thiamine pyrophosphate (TPP), 50 mM sodium pyruvate, 10 μM FAD and when necessary various amounts of the regulatory subunit, was equilibrated at each temperature for 4 min before adding the enzyme. The specific activity of 100% was considered for AHAS and PDC activities of catalytic subunit alone and was corresponding to 145 Umg⁻¹ for AHAS and 9.5 Umg⁻¹ for PDC activity.

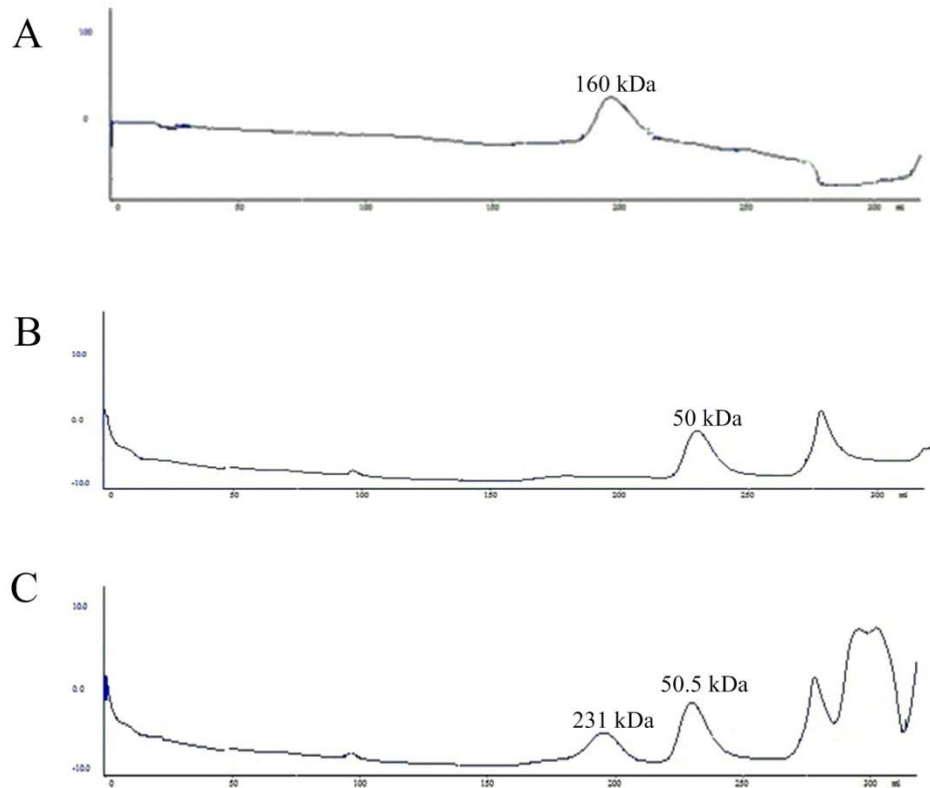


Figure 4-30. Gel-filtration chromatography of AHAS subunits

The catalytic subunit (**A**), regulatory subunit (**B**), and reconstituted holoenzyme (**C**) of AHAS were loaded on gel filtration column. The numbers indicate the apparent molecular masses of the proteins eluted in each peak. The column was eluted using buffer C as previously described (section 4.3.13). The peaks eluted after 250ml correspond to molecular weights of less than 5000 Da and are most likely resulted from the change in the buffer phase rather than elution of individual molecules. For reconstitution experiment a molar ratio of 1:10 of catalytic subunit to regulatory subunit were mixed together and incubated at room temperature for 1 h. The mixture then was loaded on the size-exclusion column to determine the oligomeric state.

4.5 Discussion

AHAS is a member of the decarboxylase family that catalyzes the reactions whose initial step is decarboxylation of 2-keto acids. The decarboxylase family is one of the five members of TPP-dependent enzymes superfamily (Duggleby 2006). AHAS shares a common ancestry with pyruvate decarboxylase (Kellermann *et al.* 1986; Neale *et al.* 1987; Green 1989) as is indeed apparent from its sequence homology to the PDCs from various organisms (**Table 4-1**) and pyruvate oxidase (POX) (Chang and Cronan 1988). Considering the catalytic mechanism of the enzyme, it is also believed that the enzyme is very close to pyruvate decarboxylase. Moreover, preliminary information on AHAS structure indicates high levels of similarity with PDCs.

The anabolic AHASs are relatively well studied in plants and a number of mesophilic bacterial pathogens (**Table 4-11**). The physiological substrate of AHASs are two molecules of keto acids, usually two molecules of pyruvate or one molecule of pyruvate and one molecule of 2-hydroxybutyrate. The first molecule of pyruvate is decarboxylated and the resulting hydroxyethyl moiety will be condensed with either another pyruvate or hydroxybutyrate (Barak *et al.* 1987; Gollop *et al.* 1989; Gollop *et al.* 1990). It seems that the first substrate binding site is very specific for pyruvate; however, the second substrate binding site seems to be less specific. AHAS I and II from *E. coli*, can also condense two molecules of 2-ketobutyrate, leading to 2-ethyl-2 hydroxy-3-oxopentanoate (Schloss *et al.* 1988; Gollop *et al.* 1989). The AHAS II and III from *E. coli* can accept 2-ketovalerate as a second substrate yielding 2-aceto-2-hydroxyvalerate (Gollop *et al.* 1989).

As a well known side reaction, AHASs are also capable of catalyzing the carboligation reactions and producing α -hydroxy ketones. During the reaction, decarboxylation of pyruvate generates a hydroxyethyl-TPP (HETDP), also known as “active acetaldehyde”, intermediate (Hübner *et al.* 1998) and the stereospecific condensation of this intermediate with aldehydes produces α -hydroxy ketones (Iding *et al.* 1998). The reaction has been extensively studied in pyruvate decarboxylases (Ward and Singh 2000), and there have been some studies demonstrating higher efficiency of AHASs than the pyruvate decarboxylases, presumably because the condensation reaction is an intrinsic property of the AHASs (Engel *et al.* 2003; Engel *et al.* 2005; Vyazmensky *et al.* 2011). Similar to PDC (Crout *et al.* 1991; Crout *et al.* 1994; Iding *et al.* 1998), AHAS I from *E. coli* was shown to be able to use a wide range of aldehydes as the second substrate, including benzaldehydes, heterocyclic, hetero-aromatic and non-aromatic aldehydes (Engel *et al.* 2004a). As another side reaction, it is reported that some AHASs can catalyze oxidative decarboxylation of pyruvate or 2-oxobutyrate, yielding peracetic acid or peroxypropionic acid, respectively. During this reaction, the enzyme bond hydroxyethyl-TPP

Table 4-11. Catalytic and structural properties of AHAS activity from different organisms^a

Organism	catalytic regulatory		Apparent K_m for				Specific activity (Umg^{-1}) ^b	Enzyme	Reference
	catalytic	regulatory	pyruvate (mM)	TPP (μ M)	Mg ²⁺ (μ M)	FAD (μ M)			
<i>Mycobacterium avium</i>	65.9	18.1	2±0.2	7.5±0.4	NR	0.1	4	R	Choi <i>et al.</i> 2005
<i>Haemophilus influenza</i>	63	NR	9.2	13.6	NR	NR	1.5	R	Gedi <i>et al.</i> 2011
<i>Shigella sonnei</i>	65	NR	8.1	0.01	180		0.12	R	Lim <i>et al.</i> 2011
<i>Mycobacterium tuberculosis</i>	NR	NR	1.56±0.39	1.40±0.3	NR	NR	4.6	R	Zohar <i>et al.</i> 2003
<i>Escherichia coli</i> Isozyme I	60.4	11.1	3.7	NR	NR	760	0.4	R	Barak <i>et al.</i> 1987; Weinstock <i>et al.</i> 1992
<i>Escherichia coli</i> Isozyme II	59.3	9.6	5.0±0.5 2.6	0.65±0.03 1.1	0.01±0.00 2 3.8	0.17±0.04 NR	20 52.7	R	Bar-Ilan <i>et al.</i> 2001 Hill <i>et al.</i> 1997
<i>Escherichia coli</i> Isozyme III	63.0	17.5	11.5±1.4	18±3	3300±800	2.2±0.5	2.6	R	Sella <i>et al.</i> 1993; Vyazmensky <i>et al.</i> 1996
<i>Saccharomyces cerevisiae</i>	~70	40	8.6±1.4	110	280	0.3	49±1.8	R	Pang and Duggleby 1999
<i>Arabidopsis thaliana</i> ^d	61	NR	11.7±0.6	25.3±1.4	198±19	1.46±0.22	7.9	R	Singh <i>et al.</i> 1991; Chang and Duggleby 1997
<i>Nicotiana tabacum</i> ^d	NR	NR	8.1-12.8	80-210	NR	1.4-2.6	2.8-3.4	R	Kil and Chang 1998
<i>Bacillus stearothermophilus</i> ^d	62.4	18.7	8.8±1.2	5.5±0.8	20±3	NR	9.2	R	Porat <i>et al.</i> 2004
<i>Corynebacterium glutamicum</i>	66.8	15.4	8.4	NR	NR	NR	0.37	N	Eggeling <i>et al.</i> 1987; Gollop <i>et al.</i> 1990
<i>Methanococcus aeolicus</i>	65	19	6.8	1.6	300	1.3	39.3	N ^c R	Xing and Whitman 1994; Bowen <i>et al.</i> 1997
<i>Haloferax volcanii</i>	50	NR	25.5±5	8.7±0.9	NR	NR	0.005	N	Vyazmensky <i>et al.</i> 2000
<i>Salmonella typhimurium</i>	59.3	9.7	10.6±0.7	1.5±0.2	22±4	0.8±0.1	25.3	R	Schloss <i>et al.</i> 1985
<i>Thermotoga maritima</i>	65.5	20	16.4±1.9	56.5±5.6	NR	0.15±0.07	134±30	R	this study

^a NR: not reported; R, recombinant; N, native enzyme

^b Expressed as micromoles of acetolactate produced per min per milligram of enzyme

^c The kinetic parameters are for the native

^d The kinetics parameters are only available for the catalytic subunit

(E-HETPP) reacts with the molecular oxygen, leading to the formation of hydroperoxide-HETPP, which is then decomposed to peracetic acid and TPP. The rate of this oxygen-consuming reaction is approximately 1% of the AHAS activity in case of AHAS II from *E. coli* (Tse and Schloss 1993; Abell and Schloss 2002). Within the members of the TPP-dependent enzymes, AHAS and pyruvate decarboxylases are the only enzymes that can catalyze this oxygenase side reaction (Chipman *et al.* 1998). The PDC activity that is being reported here is another “side reaction” of AHASs, though other possible side reactions of the enzyme were not tested.

All of the genes involved in the biosynthesis of leucine, valine and isoleucine appear to be transcribed in polycistronic compartments. For example, among the genes involved in the biosynthesis of isoleucine (*ilvB-ilvN-ilvC-ilvD*), the stop and start codons of every two adjacent genes are overlapping or are separated only by a few nucleotides (**Figure 4-10**). The same organization is found for genes involved in biosynthesis of leucine (*leuA-leuC-leuD-leuB*). The ribosome-binding sites (also known as Shine-Dalgarno (SD) sequence) of the genes except the first gene in the polycistronic complex, is located in coding sequence of the proximal (upstream) gene (**Figure 4-10**).

Similar polycistronic gene organization is reported for some bacterial and phage operons, for the tryptophan biosynthesis (*trp* operon) pathway in *E. coli*, which is the first and best studied (Nichols and Yanofsky 1979). This property may ensures the coupled translation of all genes involved in the same biological pathway by making sure that the translation of the distal gene is dependent on the translation of the proximal coding sequence (cistron) from a single messenger RNA (mRNA) transcript (Das and Yanofsky 1984; Schoner *et al.* 1984).

The *ilv* operon has been found to be present in most sequenced genomes of Thermotogales. Amongst ten fully sequenced genomes of *Thermotoga* genus, only *Thermotoga lettingae* had no recognizable *ilv* operon (**Table 4-5**), which was also in accordance with the auxotrophy of this organism for these three amino acids (leucine, valine, and isoleucine) (Balk *et al.* 2002). AHAS-encoding genes from different *Thermotogae* were highly conserved, showing more than 90% amino acid sequence identity. However, both catalytic and regulatory subunits of *Thermotoga thermarum* seem to be an exception, showing only 47% amino acid level sequence identity to that of other *Thermotogae* species (**Figure 4-7** and **Figure 4-8**). Considering differences in gene organization and its higher sequence identity (~70% identity) to those of the *Caldicellulosiruptor* genus, it can be speculated that the genes might have been acquired from another species.

The *ilv* operon was absent in most of the Thermococcales genomes studied and only a few could be found in genomes of *P. furiosus*, *P. abyssi*, and *Pyrococcus* sp. strain NA2. The gene organization and structure were different from those found in Thermotogales (**Figure 4-9**). Generally, the regulatory

subunits of AHASs are not easy to identify as they vary greatly, both in their sizes and sequences (Pang and Duggleby 1999; Gedi and Yoon 2012). Although located in the same operon as the catalytic subunit, sequence of the regulatory subunit, which was annotated as hypothetical protein (PF0934), showed very low similarity to other known genes annotated as regulatory subunit of AHAS (**Figure 4-8**). Interestingly, microarray study shows that transcription levels (and enzyme activity) increases approximately 6-fold for both PF0935 and its upstream hypothetical coding sequence (PF0934) during the early (1-2 h) and late (5 h) cold-shock (72°C) response (Weinberg *et al.* 2005). Other microarray studies only report the increase the transcription levels of the catalytic subunit. For example, transcription of the gene encoding the catalytic subunit AHAS (PF0935) increases approximately 7-fold by the addition of elemental sulfur (Schut *et al.* 2001a), 17-fold after growth on maltose based medium compared to the peptide based medium (Schut *et al.* 2003), and 9-fold when subjected to peroxide shock (Strand *et al.* 2010).

There is a 308 bp non-coding region between the gene encoding the hypothetical protein (PF0934) and the catalytic subunit of PFAHAS (PF0935) in *P. furiosus*. A putative ribosome-binding site (RBS) is recognized to be close to each of PF0934 and PF0935 genes, which may be suggestive of their translation from independent transcripts. The overlapping intercistronic sequences were not in the same order as they were in Thermotogales *ilv* operon. The genes encoding the catalytic subunit of AHAS and ketolacid reductoisomerase (*ilvB-ilvC*) displayed overlapping intercistronic sequences and same organization was observed for *leuA-leuC-leuD-leuB-leuA*, which are involved in the biosynthesis of leucine and valine (**Figure 4-9**). Interestingly, the *ilv* operon of *P. furiosus* and *P. abyssi* contains two different copies of genes encoding 2-isopropylmalate synthase (**Figure 4-9**) and the two genes PF0937 and PAB0890 are paralogs of PF0941 and PAB0894, respectively. The two genes showed approximately 32% amino acid sequence identity pair. Only a single copy of the isopropylmalate synthase (IPMS)-encoding gene was detectable in *Pyrococcus* sp. strain NA2 (PNA2_1340 that are the orthologues of PF0941 and PAB0894) that harbors an *ilv* operon. None of these genes were included in microarray studies of Pyrococcales (Schut *et al.* 2003; Weinberg *et al.* 2005; Williams *et al.* 2007; Strand *et al.* 2010) and it is not known whether presence of second copy has any physiological functions or whether it is only result of gene duplication or acquisition from two different ancestors.

The purified catalytic subunit of TmAHAS had much higher AHAS activity than any other AHAS activity characterized (**Table 4-11**), although some of these differences might be a result of various modifications of the assay systems. The regulatory subunit (Ms-pET30a) was often expressed partly as inclusion bodies (approximately 50%) in *E. coli* which is very similar to other reports (Engel *et al.* 2004b; Vinogradov *et al.* 2006; Petkowski *et al.* 2007). The inclusion bodies were purified under denaturing conditions followed by gentle renaturation steps.

The recombinant TmAHAS showed a much higher AHAS and PDC activities after heat-treatment for 30 min (**Figure 4-20**), indicating thermal activation of the expressed enzyme which was observed in many heterologously expressed hyperthermophilic proteins. A typical example of this phenomenon is the alcohol dehydrogenase (AdhC) from the hyperthermophilic archaeon *P. furiosus* expressed in *E. coli* (**Table 4-8**). The homotetrameric recombinant protein does not attain the correct configuration unless a heat-treatment step is applied to the enzyme (Kube *et al.* 2006). However, a monomeric short chain alcohol dehydrogenase expressed from the same organisms does not need this thermal activation step (Kube *et al.* 2006).

The optimal pH and temperature for both AHAS and PDC activities were 7.0 (**Figure 4-23**) and 85°C, respectively (**Figure 4-28**). The latter is the highest optimal temperature reported for AHASs. TmAHAS was highly thermostable when kept under anaerobic conditions without stirring (**Figure 4-27**). The exposure to light had no effect on either of the activities. Although there are reports of oxygen sensitivity of AHAS isolated from the mesophilic archaeon *Methanococcus aeolicus* (Xing and Whitman 1994; Bowen *et al.* 1997), TmAHAS was not oxygen sensitive, but other factors (*e.g.* stirring) inactivated the enzyme. Without stirring TmAHAS was fairly stable under anaerobic or aerobic conditions (**Figure 4-27**), however, it became extremely labile toward stirring under aerobic and anaerobic condition, though the air exposed samples lost the activity in a faster paces (**Figure 4-25** and **Figure 4-26**). Moreover, in *M. aeolicus*, the oxygen sensitivity of the enzyme cannot be explained (Bowen *et al.* 1997), but it might be related to the enzyme's high cysteine contents (12 cysteine residues compared to 3 residues in TmAHAS).

The FAD-dependence is a perplexing feature of the anabolic AHAS, since the enzyme is not catalyzing any redox reactions. In fact, the enzyme pyruvate oxidase (POX) is the only member in the TPP-dependent enzymes superfamily that catalyzes a redox reaction (Duggleby 2006). Based on experiments with FAD-analogue molecules (McCourt and Duggleby 2006), it has been suggested that the role of the FAD is merely structural (and not mechanistic). This may be further supported by the fact that the catabolic version of the enzyme (ALS) is completely FAD-independent, despite catalyzing the same reaction and have a very similar crystal structures (**Table 4-2**) (Tittmann *et al.* 2004; Duggleby *et al.* 2008). Other members present in the so called “non-redox flavoproteins” group including TPP-dependent enzymes pyruvate oxidase (EC 1.2.3.3) and glyoxylate carboligase (EC 4.1.1.47). The FAD-dependence in these enzymes is thought to be an evolutionary relic in this particular sub-family of TPP-dependent enzymes (Chang and Cronan 1988; Duggleby 2006).

A putative FAD-binding motif (RFDDR) was thought to be associated with FAD-dependence in anabolic AHASs. The motif is found to absent from amino acid sequences of catabolic AHASs (ALSs). The role of these highly conserved amino acid residues in incorporation of FAD into the enzyme structure

is confirmed by mutagenesis in the motif and measuring the FAD binding in the resulting mutants (Le 2005). The sequence alignments of the catalytic subunits of AHAS from various organisms, including hyper/thermophiles, (**Figure 4-11A**) also confirms the presence of FAD-binding motif (**Figure 4-11A**). Hence, it was expected that TmAHAS activity to be FAD-dependent. The addition of FAD to the assay mixtures had stimulatory effects on both AHAS (approximately 70% higher activity) and PDC activities (~55% higher activity). The difference in the FAD effect on each activity might be the result of using different enzyme preparations.

Even though the apparent K_m of FAD for TmAHAS (**Table 4-10**) was close to that of most other recombinant AHASs characterized (**Table 4-11**), it should be considered with caution as the purified enzyme still retained activity even without addition of FAD. The same observation is reported for other AHASs expressed from different organisms, suggesting a relatively tight-binding of FAD molecule to the protein.

Although the TPP-binding motif was detected in the sequences of TmAHAS and other hyperthermophiles (**Figure 4-11B**), the enzyme was not completely dependent on addition of TPP, but addition of TPP to assay mixture was stimulatory for both PDC and AHAS activities, resulting in more than 90% increase in both activities. It is predicted that TPP is bound to the enzyme non-covalently, which might result in dissociation of the cofactor from the enzyme during purification steps.

Anabolic AHASs have two subunits, large catalytically active subunit and smaller inactive regulatory subunit. Both subunits have been shown to be essential for the full activity and reconstitution of the holoenzyme; mixing the catalytic and regulatory subunits leads to a fully active enzyme. The two major functions of the regulatory subunit of anabolic AHAS are activation and allosteric feedback regulation of the catalytic subunit (Sella *et al.* 1993; Vyazmensky *et al.* 1996; Hill *et al.* 1997; Porat *et al.* 2004). Mixing the purified catalytic and regulatory subunits of TmAHAS resulted in the considerable and reproducible increase of both AHAS and PDC activities (**Figure 4-29**). Mixing the catalytic and regulatory subunits also resulted in higher oligomeric states for the holoenzyme, which is in accordance with findings in mesophilic AHASs such as *E. coli* AHAS III (Vyazmensky *et al.* 1996). Because of high propensity of the regulatory subunit for aggregation, it has been suggested that it is highly involved in the process of oligomerization and enzyme reconstitution (Choi *et al.* 2005).

The principal catalytic mechanism of AHAS, follows the activation step of the enzyme is similar to those of the other pyruvate utilizing TPP-dependent enzymes especially the classic example of this group, PDC (Bar-Ilan *et al.* 2001). Protonation of the N1 atom of pyrimidine ring by the highly conserved glutamine residue results in induction of a 1', 4'-iminotautomer. Due to the common "V-conformation" the 4-imino group is located in the proximity of the C₂ catalytic centre of the AHAS, which results in de-

protonation of the C₂ atom. The proton abstraction step gives rise to a highly reactive ylide (Kern *et al.* 1997; Lie *et al.* 2005; McCourt and Duggleby 2006). The nucleophilic attack of the ylide to the first molecule of pyruvate, results in production of 2-(2-lactyl)-TPP (also known as L-TPP or L-TDP). Later, decarboxylation of L-TPP gives the resonating carbanion/enamine forms of 2-(1-hydroxyethyl)-TPP (HETPP, also known as hydroxyethylidene-TPP), which acts as a central and highly reactive intermediate (Candy and Duggleby 1998; Tittmann *et al.* 2003; Kluger and Tittmann 2008).

During the normal course of the catalysis, HETPP intermediate reacts in an enantio-specific manner with the second molecule of 2-keto acid (usually pyruvate or 2-ketobutyrate), resulting in the release of the product. The ability of heterologously expressed TmAHAS to generate acetaldehyde is most likely the result of protonation of the HETDP/enamine intermediate in C₂ position. This step, results in the releases of acetaldehyde from active site of the enzyme. Unfortunately, with the available data on recombinant TmAHAS, it is not possible to deduce further mechanistic details of PDC activity of enzyme. Complete and accurate understanding of the mechanisms involved in acetaldehyde formation demands more in-depth study of the reaction intermediates and more importantly crystal structure of enzyme. Other than a preliminary X-ray crystal structure for catalytic subunit of *E. coli* AHAS II (Niu *et al.* 2011), so far, no crystal structure has been provided for any catalytic (large) subunit of AHAS (Gedi and Yoon 2012).

Catabolic AHAS (ALS) has been isolated and characterized mainly from enteric bacteria, including *Enterobacter*, certain *Klebsiella* and *Serratia* species, some lactic acid bacteria, and *Bacillus subtilis*. A typical ALS is composed of only one subunit of ~60 kDa (no regulatory subunit), generally located in the butanediol operon when it is present. It is FAD-independent. Despite catalyzing same reactions, anabolic and catabolic AHASs are very divergent, showing less than 30% amino acid sequence identity with each other (Chipman *et al.* 1998; Duggleby and Pang 2000; Gedi and Yoon 2012). Different factors can trigger activation of butanediol operon in bacteria, including low pH, presence of excess acetate and/or pyruvate, as well as growth during the stationary phase (Störmer 1968b; Störmer 1968c; Störmer 1968a; Tsau *et al.* 1992; Renna *et al.* 1993; Duggleby and Pang 2000). As an important development, it is shown that besides its synthase activity, the catabolic ALS of *B. subtilis* can also catalyze the non-oxidative decarboxylation of the 2-ketoisovalerate both *in vitro* and *in vivo* (Atsumi *et al.* 2009). Considering the major mechanistic similarities between the anabolic and catabolic AHAS, the involvement of the anabolic AHAS in the similar non-oxidative decarboxylation reaction is not very surprising.

Hyperthermophilic heterotrophic archaeon, *T. guaymasensis*, can produce acetoin (Ying and Ma 2011). A survey of database information confirmed that gene(s) encoding the AHAS are always clustered with other genes involved the branched chain amino acid biosynthesis (**Figure 4-9**). There is no report on detection of catabolic AHAS (ALS) and 2-acetolactate decarboxylase. Since no commonly-known

AHAS-encoding-gene(s) could be found in genomes of any species of the genus *Thermococcus* (**Table 4-5**), it is believed that besides the conventional AHAS present in some hyperthermophiles (many Thermotogales and few species of the genus *Pyrococcus*), there is an alternative, yet-to-be characterized enzyme, that catalyzes the production of acetoin in *T. guaymasensis* and *T. kodakaraensis* (**Table 4-6** and **Figure 4-12**). The same enzyme is presumably responsible for production of the acetoin detected in *T. guaymasensis* (Ying and Ma 2011).

There are two pathways that lead to production of acetoin: one is present in mesophilic organisms, like *Lactococcus lactis*, by which acetolactate can be converted to diacetyl spontaneously, particularly at low pH environments such as stationary growth phase (Goupil-Feuillerat *et al.* 1997). This spontaneous oxidative decarboxylation conversion seems to be even faster at high temperatures. The next step which is an irreversible conversion of diacetyl to acetoin is catalyzed by acetoin reductase/2, 3-butanediol dehydrogenase (Speckman and Collins 1982). An ADH with high acetoin reductase (EC 1.1.1.4) activity was detected in *T. guaymasensis* (Ying and Ma 2011).

There is yet another possible explanation for the origin of acetoin detected in spent culture of *T. guaymasensis*; by which 2-acetolactate can be directly decarboxylated to diacetyl by the enzyme 2-acetolactate decarboxylase. The enzyme 2-acetolactate decarboxylase is present in many mesophilic methanogenic archaea, including *Methanoplanus*, *Methanococcus*, *Methanoregula*, *Methanoculleus*, *Methanoseta*, but is absent from the studied genomes of hyperthermophilic archaea and bacteria (this study). However, there is no need for the presence of the acetolactate decarboxylase in hyperthermophiles. It is shown that high temperature and low pH can result in direct conversion (spontaneous conversion/degradation) of 2-acetolactate to acetoin (Ramos *et al.* 1994; Goupil-Feuillerat *et al.* 1997; Dulieu and Poncelet 1999).

The acetoin production pathway is likely present in hyperthermophiles and the resulting acetolactate can be further channeled to either branched-chain amino acids *via* BCAA biosynthesis pathway (**Figure 4-2**) or to acetoin and possibly to 2, 3-butanediol (**Figure 4-31**). Another possible pathway to explain the origin of acetoin (but not 2, 3-butanediol) is its production by pyruvate decarboxylase (Gocke *et al.* 2009b). It is shown that some bacterial and yeast PDCs can catalyze the carboligation of two molecules of acetaldehyde, yielding one molecule of acetoin. This reaction is reported for the PDCs from yeast (Chen and Jordan 1984; Bornemann *et al.* 1993; Neuser *et al.* 2000; Kurniadi *et al.* 2003), *Z. mobilis* PDC (Bornemann *et al.* 1993; Siegert *et al.* 2005) and *Zymobacter palmae* PDC (Rosche *et al.* 2003). However, to date there is no commonly-known PDC found in any hyperthermophilic microorganisms (this study). It is not known if the acetaldehyde-producing activity of AHAS can also catalyze such a condensation reaction with two molecules of acetaldehyde.

A more recently noticed aspect of the BCAA biosynthesis pathways in general and AHAS in particular is their potential application in the biosynthesis of modern biofuels, *via* non-fermentative pathways for biosynthesis of branched chain alcohols (C4-C5). The higher alcohols are preferred over traditional biofuels (such as ethanol) due to their higher energy density and octane number, lower volatility, and lower hygroscopicity. During these pathways, 2-keto acids are decarboxylated by specialized decarboxylases, and resulting aldehydes are converted to corresponding alcohols by ADHs (Atsumi *et al.* 2008; Cann and Liao 2010; Peralta-Yahya and Keasling 2010). However, none of these studies considered the possibility of ethanol- and acetaldehyde-production (classical biofuels) by using AHASs.

Although the presence of the *ilv* operon can be verified in organisms with available full genome sequences (**Table 4-5**), no enzymes of the *ilv* operon is purified and studied from hyper/thermophiles. Moreover, the data pertaining to amino acid requirements of hyperthermophiles are quite limited, and what is available comes from only a very few minimal media studies as well as the genome surveys of fully sequenced microorganisms (**Table 4-3**). The results of such studies are sometimes not conclusive and, in some cases, in disagreement or even contradictory to each other. For instance, there have been two studies on the minimal amino acid requirements of the relatively well-known hyperthermophilic archaeon *P. furiosus*. One suggested that the organism requires the BCAAs for growth (Hoaki *et al.* 1993; Hoaki *et al.* 1994) and the other reports that the growth is independent of BCAAs (Raven and Sharp 1997). As another example, *P. abyssi* was shown to contain the gene encoding for the BCAA biosynthesis operon (Cohen *et al.* 2003); another study indicated the organisms auxotrophy for BCAAs (Watrin *et al.* 1995). So verification of enzyme activity in the organisms seems to be critical to determining the presence of the enzymes and corresponding activities.

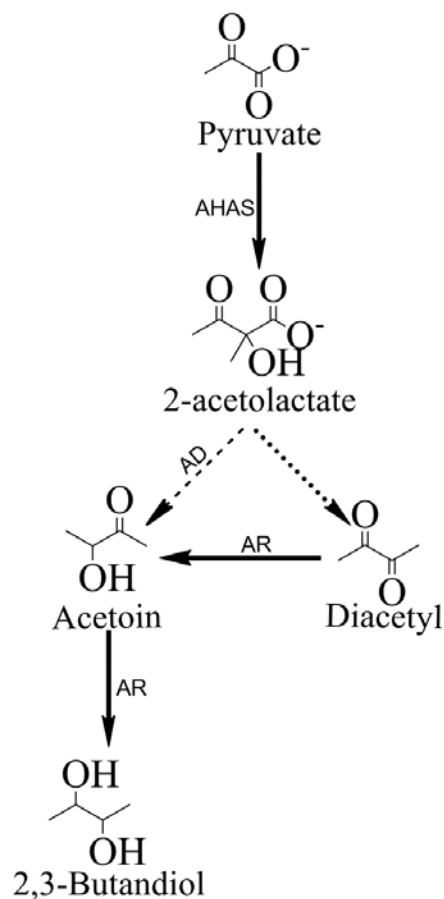


Figure 4-31. Proposed acetoin production pathway in hyperthermophiles

AD, acetolactate decarboxylase (EC 4.1.1.5); AR, acetoin reductase (EC 1.1.1.4).

The acetolactate produced by AHAS or the alternative AHAS can be converted to both acetoin and diacetyl at high temperature. The dashed arrows indicate the step that is generally catalyzed by the enzyme acetolactate decarboxylase, but at high temperature the reaction can occur spontaneously. The solid arrows indicate the enzymatic reactions that are known in hyperthermophiles. The dotted arrow indicates a spontaneous reaction in all the microorganisms that have a 2, 3-butanediol pathway.

Chapter 5 General conclusions

5.1 Commonly-known PDC and AcDH are not present in hyperthermophiles

Thermophilic and hyperthermophilic ADHs are studied extensively, however, very little is known about enzymes involved in acetaldehyde production in these organisms. PDC and AcDH are the commonly-known enzymes catalyzing the production of acetaldehyde from pyruvate. PDC catalyzes the direct conversion of pyruvate to acetaldehyde and AcDH catalyzes acetaldehyde formation by reducing acetyl-CoA produced from pyruvate by POR or PFL. The genes encoding CoA-dependent acetaldehyde dehydrogenase have previously been isolated and characterized from some mesophilic and thermophilic (but not hyper- or extremely thermophilic) bacteria, including members of the genera *Thermoanaerobacter* and *Geobacillus*, with optimal temperatures of approximately 55-60°C (Burdette and Zeikus 1994; Pei *et al.* 2010; Yao and Mikkelsen 2010a; Yao and Mikkelsen 2010b). However, such activities and the genes encoding such enzymes were absent from the hyperthermophilic bacteria and archaea studied here (Chapter 2).

5.2 POR/PDC and AHAS/PDC are novel enzymes catalyzing the production of acetaldehyde from pyruvate in hyperthermophiles

It is shown that pyruvate ferredoxin oxidoreductases, and most likely all 2-keto acid ferredoxin oxidoreductases (KORs), can catalyze the non-oxidative decarboxylation of keto acids to produce corresponding aldehydes (Ma *et al.* 1995; Ma *et al.* 1997). Hence, KORs can be regarded as regulating factors for conversion of keto acids to both acyl-CoA and corresponding aldehyde. For more than a decade, PfPOR has been considered to be the only acetaldehyde-producing enzyme known in hyperthermophiles, though; there was no systematic study to confirm either presence of the same bifunctionality in any other hyper/thermophilic counterparts or the occurrence of any other acetaldehyde-producing enzyme in hyperthermophiles. The present study confirms that POR/PDC bifunctionality is indeed a common trait of the enzyme from hyper/thermophilic bacteria and archaea (**Table 5-1**).

All of the bifunctional POR/PDCs characterized were strictly CoA- and TPP- dependent and highly thermostable. PDC activity was not affected by substitution of desulfo-CoA for CoA, suggesting a structural (rather catalytic) role of CoA. PDC activities were also highly sensitive to oxygen. All of

Table 5-1. POR/PDC and AHAS/PDC activities in hyperthermophiles

Category	Organism	POR or AHAS activity	PDC activity ^b	Ratio of PDC/POR (or AHAS)	References
POR/PDC	<i>T. maritima</i>	90.8±11 ^a	1.4±0.15	0.016	this study
	<i>T. hypogea</i>	96.7±15.1 ^a	1.82±0.44	0.018	this study
	<i>P. furiosus</i>	22.0±1 ^a	4.3±0.3	0.20	Ma <i>et al.</i> 1997 this study
	<i>T. guaymasensis</i>	20.2±1.8 ^a	3.8±0.22	0.19	this study
AHAS/PDC	<i>T. maritima</i>	134±3.0 ^c	16.7±3.4	0.13	this study

^a Expressed as micromoles of pyruvate oxidized per min per milligram of enzyme

^b Expressed as micromoles of acetaldehyde produced per min per milligram of enzyme

^c Expressed as micromoles of acetolactate produced per min per milligram of enzyme

the enzymes showed higher activity of POR compared to the PDC activity under the conditions examined (*in vitro*), suggesting that POR reaction would most likely dominate under physiological (*in vivo*) conditions. The bifunctional enzyme isolated from bacterial hyper/thermophiles had lower PDC to POR ratios when compared with their archaeal counterparts (**Table 5-1**). Bacterial hyper/thermophilic POR/PDC had similar pH optima for both activities, but archaeal hyperthermophilic POR/PDCs showed higher pH optima for PDC activity than POR activity. The potential physiological significance of such differences between bacterial and archaeal PORs/PDCs is not clear at this point. PDCs of Tg-, Tm-, and Th-POR/PDC had the highest temperature optima compared to commonly-known PDCs characterized from mesophilic bacteria *Z. mobilis* (Hoppner and Doelle 1983), *A. pasteurianus* (Raj *et al.* 2001; Raj *et al.* 2002), and *Z. palmae* (Raj *et al.* 2002), which are only moderately thermostable with a limit of up to 60°C for their activities.

AHASs were the second type of enzymes catalyzing the production of acetaldehyde from pyruvate in hyperthermophiles. For the first time, it was shown that AHAS was able to produce acetaldehyde beside its known catalytic reaction which is condensation of two molecules of 2-keto acids. Like the archaeal POR/PDC bifunctionality (and unlike the bacterial POR/PDC activity), the PDC to AHAS activity ratio was high (**Table 5-1**). The majority of Thermococcales lack the genes required for biosynthesis of amino acids and therefore rely on the uptake of the amino acids using the energy-dependent transport systems (Cohen *et al.* 2003; Lee *et al.* 2003). Even in the few Thermococcales able to perform BCAA biosynthesis such as *P. furiosus* (Raven and Sharp 1997), microarray data suggest that following growth on carbohydrates (maltose), the expression of genes involved in amino acid biosynthesis increases. This finding suggests that cells depend on amino acids imported into the cell to be used for the biosynthetic and physiological applications when growing on carbohydrates (Schut *et al.* 2003). Besides using the peptides as an energy source, amino acids are also needed for the biosynthesis of different components necessary for general housekeeping purposes. Therefore, the enzymes of amino acid catabolism (especially the 2-keto acid ferredoxin oxidoreductases) may not need to be highly active, especially considering the existence of four individual and specialized versions of these enzymes that act specifically on various keto acids resulting from transamination of different amino acids. Presumably, having the differentiated KORs is a mechanism to make sure that only the amino acids that are not required for cell survival are catabolized for energy conservation purposes.

Thermotogales are able to use both carbohydrates (simple and complex) and peptides as a source of carbon and energy (Connors *et al.* 2006), and many of them are capable of *de novo* synthesis of amino acids required for growth (Chapter 4). Presumably, the “extra” amino acids imported and/or synthesized inside the cells would be channeled to the energy conservation process, during which they are decarboxylated after a transamination step. Like Thermococcales, the reduced ferredoxin produced during the POR reaction can be used *via* different hydrogenase enzymes for energy conservation (Jenney and Adams 2008) and acetyl-CoA is used for both biosynthesis and energy conservation (Kelly and Adams 1994).

Both POR/PDC and AHAS/PDC were TPP-dependent and had the highly conserved canonical TPP-binding motifs in their primary structures. Although, the catalytic mechanisms of these two classes of enzymes are completely different, with the POR (and most likely PDC) using radical chemistry and the AHAS using non-radical mechanisms, there is not much information available on the catalytic mechanisms for the PDC activities. The bifunctionality does not seem to be a property of all TPP-dependent enzymes, as preliminary results showed that porcine PDH is unable to catalyze the production of acetaldehyde from pyruvate (Chapter 2).

It seems that the keto acids produced by catabolism of different amino acids and/or carbohydrates can be decarboxylated both oxidatively and non-oxidatively *via* either bifunctional POR/PDC or, when present, the bifunctional AHAS/PDC. The aldehydes resulting from the non-oxidative decarboxylation of keto acids can be further reduced to produce corresponding alcohols. This reduction is accompanied by the regeneration of oxidized NADP⁺.

5.3 Outlook

In this study, evidence supporting the involvement of bifunctional enzymes (POR/PDC or AHAS/PDC) in production of acetaldehyde from pyruvate in hyperthermophiles was presented. Although production of acetaldehyde was shown by POR/PDC and AHAS/PDC *in vitro*, and both enzymes are from ethanol-producers, it is still not known what factors favors one activity over another under physiological conditions. *In vivo* studies such as microarray and real-time PCR combined with enzyme activity studies may be exploited to determine the physiological conditions and substrates that regulate each of the activities. Also, detailed analysis of the end-products under each growth condition may further clarify potential roles of each enzyme activity. The elucidation of

the catalytic mechanism will be helpful in determining the amino acid residues that might be involved in non-oxidative pyruvate decarboxylation (PDC activity).

Since catalysis of the condensation reactions is an inherent feature of the anabolic AHASs, it is very likely that this enzyme can catalyze the condensation of two acetaldehyde molecules, which results in the production of acetoin. Considering the high volatility of the acetaldehyde, a specific assay method (most likely based on GC or HPLC) would need to be formulated to detect the products of the reaction. The results of such a study would be helpful in determining the metabolic pathway for the production of acetoin detected in hyperthermophiles (Ying and Ma 2011).

Biocatalysis using hyperthermophilic organisms and/or their thermostable enzymes are attracting increasing attention. Isolated hyperthermophilic POR/PDC and AHAS/PDC may have potential in the production of value-added commodities. Engineering the bifunctional enzymes to increase the activities is a promising approach, and even shifting the activity towards production of even the product that is unfavored under physiological conditions. This has previously been achieved for the commonly-known yeast PDC that is engineered to increase the unfavored carboligation reaction up to a 100-fold (Meyer *et al.* 2010).

Copyright Permissions

Copyright permission for Figure 1-1 (page 4)

SPRINGER LICENSE TERMS AND CONDITIONS

Sep 11, 2011

This is a License Agreement between Mohammad Eram ("You") and Springer ("Springer") provided by Copyright Clearance Center ("CCC"). The license consists of your order details, the terms and conditions provided by Springer, and the payment terms and conditions.

All payments must be made in full to CCC. For payment instructions, please see information listed at the bottom of this form.

License Number	2745730987068
License date	Sep 11, 2011
Licensed content publisher	Springer
Licensed content publication	Extremophiles
Licensed content title	History of discovery of the first hyperthermophiles
Licensed content author	Karl O. Stetter
Licensed content date	Oct 1, 2006
Volume number	10
Issue number	5
Type of Use	Thesis/Dissertation
Portion	Figures
Author of this Springer article	No
Order reference number	
Title of your thesis / dissertation	acetaldehyde producing enzymes from hyperthermophiles
Expected completion date	Jan 2012
Estimated size(pages)	200
Total	0.00 CAD
Terms and Conditions	

Copyright permission for Figure 1-4 (page 20)

 Copyright Clearance Center

 RightsLink[®]

[Home](#) [Account Info](#) [Help](#)

 ACS Publications
High quality. High impact.

Title: Thiamin Diphosphate Catalysis: Enzymic and Nonenzymic Covalent Intermediates

Author: Ronald Kluger et al.

Publication: Chemical Reviews

Publisher: American Chemical Society

Date: Jun 1, 2008

Logged in as: Mohammad Eram
Account #: 3000446349

[LOGOUT](#)

Copyright © 2008, American Chemical Society

PERMISSION/LICENSE IS GRANTED FOR YOUR ORDER AT NO CHARGE

This type of permission/license, instead of the standard Terms & Conditions, is sent to you because no fee is being charged for your order. Please note the following:

- Permission is granted for your request in both print and electronic formats.
- If figures and/or tables were requested, they may be adapted or used in part.
- Please print this page for your records and send a copy of it to your publisher/graduate school.
- Appropriate credit for the requested material should be given as follows: "Reprinted (adapted) with permission from (COMPLETE REFERENCE CITATION). Copyright (YEAR) American Chemical Society." Insert appropriate information in place of the capitalized words.
- One-time permission is granted only for the use specified in your request. No additional uses are granted (such as derivative works or other editions). For any other uses, please submit a new request.

Copyright permission for Figure 1-5 (page 28)



RightsLink[®]

[Home](#)

[Account Info](#)

[Help](#)



ACS Publications
High quality. High impact.

Title: Pyruvate Ferredoxin
Oxidoreductase and Its Radical
Intermediate†

Author: Stephen W. Ragsdale

Publication: Chemical Reviews

Publisher: American Chemical Society

Date: Jun 1, 2003

Copyright © 2003, American Chemical Society

Logged in as:
Mohammad Eram
Account #:
3000446349

[LOGOUT](#)

No charge permission and attribution

Permission for this particular request is granted for print and electronic formats at no charge. Figures and tables may be modified. Appropriate credit should be given. Please print this page for your records and provide a copy to your publisher. Requests for up to 4 figures require only this record. Five or more figures will generate a printout of additional terms and conditions. Appropriate credit should read: "Reprinted with permission from {COMPLETE REFERENCE CITATION}. Copyright {YEAR} American Chemical Society." Insert appropriate information in place of the capitalized words.

This permission does not apply to images that are credited to publications other than ACS journals. For images credited to non-ACS journal publications, you will need to obtain permission from the journal referenced in the Table/Figure/Micrograph legend or credit line before making any use of the image(s) or table(s).

Copyright permission for Figure 1-6 (page 29)

 Copyright Clearance Center

 RightsLink[®]

[Home](#) [Account Info](#) [Help](#)

 ACS Publications
High quality. High impact.

Title: The Roles of Coenzyme A in the Pyruvate:Ferredoxin Oxidoreductase Reaction Mechanism: Rate Enhancement of Electron Transfer from a Radical Intermediate to an Iron-Sulfur Cluster†

Author: Cristina Furdul et al.

Publication: Biochemistry

Publisher: American Chemical Society

Date: Aug 1, 2002

Copyright © 2002, American Chemical Society

Logged in as:
Mohammad Eram
Account #: 3000446349

[LOGOUT](#)

No charge permission and attribution

Permission for this particular request is granted for print and electronic formats at no charge. Figures and tables may be modified. Appropriate credit should be given. Please print this page for your records and provide a copy to your publisher. Requests for up to 4 figures require only this record. Five or more figures will generate a printout of additional terms and conditions. Appropriate credit should read: "Reprinted with permission from {COMPLETE REFERENCE CITATION}. Copyright {YEAR} American Chemical Society." Insert appropriate information in place of the capitalized words.

This permission does not apply to images that are credited to publications other than ACS journals. For images credited to non-ACS journal publications, you will need to obtain permission from the journal referenced in the Table/Figure/Micrograph legend or credit line before making any use of the image(s) or table(s).

Bibliography

- Abell, L. M. and J. V. Schloss (2002) Oxygenase side reactions of acetolactate synthase and other carbanion-forming enzymes. *Biochemistry*. **30**, 7883-7887.
- Adams, M. W. W. (1993) Enzymes and Proteins from Organisms that Grow Near and Above 100 degree C. *Annual Reviews in Microbiology*. **47**, 627-658.
- Adams, M. W. W. and A. Kletzin (1996) Oxidoreductase-type enzymes and redox proteins involved in fermentative metabolisms of hyperthermophilic archaea. *Advances in protein chemistry* **48**, 101-180.
- Adams, M. W. W., J. B. Park, S. Mukund, J. Blamey and R. M. Kelly (1992) Metabolic enzymes from sulfur-dependent, extremely thermophilic organisms. *Biocatalysis at extreme temperatures: enzyme systems near and above*. **100**, 4-22.
- Alain, K., V. T. Marteinsson, M. L. Miroshnichenko, E. A. Bonch-Osmolovskaya, D. Prieur and J. L. Birrien (2002) *Marinitoga piezophila* sp. nov., a rod-shaped, thermo-piezophilic bacterium isolated under high hydrostatic pressure from a deep-sea hydrothermal vent. *Int. J. Syst. Evol. Microbiol.* **52**, 1331-1339.
- Amend, J. P., D. A. R. Meyer-Dombard, S. N. Sheth, N. Zolotova and A. C. Amend (2003) *Palaeococcus helgesonii* sp. nov., a facultatively anaerobic, hyperthermophilic archaeon from a geothermal well on Vulcano Island, Italy. *Arch. Microbiol.* **179**, 394-401.
- Andrews, K. T. and B. K. C. Patel (1996) *Fervidobacterium gondwanense* sp. nov., a New Thermophilic Anaerobic Bacterium Isolated from Nonvolcanically Heated Geothermal Waters of the Great Artesian Basin of Australia. *Int. J. Syst. Bacteriol.* **46**, 265-269.
- Antoine, E., V. Cilia, J. R. Meunier, J. Guezennec, F. Lesongeur and G. Barbier (1997) *Thermosiphon melanesiensis* sp. nov., a new thermophilic anaerobic bacterium belonging to the order Thermotogales, isolated from deep-sea hydrothermal vents in the Southwestern Pacific Ocean. *Int. J. Syst. Bacteriol.* **47**, 1118-1123.
- Antoine, E., J.-L. Rolland, J.-P. Raffin and J. Dietrich (1999) Cloning and over-expression in *Escherichia coli* of the gene encoding NADPH group III alcohol dehydrogenase from *Thermococcus hydrothermalis*. *Eur. J. Biochem.* **264**, 880-889.
- Arab, H., H. Volker and M. Thomm (2000) *Thermococcus aegaeicus* sp. nov. and *Staphylothermus hellenicus* sp. nov., two novel hyperthermophilic archaea isolated from geothermally heated vents off Palaeochori Bay, Milos, Greece. *International journal of systematic and evolutionary microbiology*. **50**, 2101-2108.
- Arjunan, P., T. Umland, F. Dyda, S. Swaminathan, W. Furey, M. Sax, B. Farrenkopf, Y. Gao, D. Zhang and F. Jordan (1996) Crystal Structure of the Thiamin Diphosphate-dependent Enzyme Pyruvate Decarboxylase from the Yeast *Saccharomyces cerevisiae* at 2.3 Å Resolution. *J. Mol. Biol.* **256**, 590-600.
- Assary, R. and L. Broadbelt (2011) Computational screening of novel thiamine-catalyzed decarboxylation reactions of 2-keto acids. *Bioprocess Biosystems Eng.* **34**, 375-388.
- Atomi, H., T. Fukui, T. Kanai, M. Morikawa and T. Imanaka (2004) Description of *Thermococcus kodakaraensis* sp. nov., a well studied hyperthermophilic archaeon previously reported as *Pyrococcus* sp. KOD1. *Archaea*. **1**, 263-267.
- Atomi, H., T. Sato and T. Kanai (2011) Application of hyperthermophiles and their enzymes. *Curr. Opin. Biotechnol.* **22**, 618-626.
- Atsumi, S., T. Hanai and J. C. Liao (2008) Non-fermentative pathways for synthesis of branched-chain higher alcohols as biofuels. *Nature*. **451**, 86-89.
- Atsumi, S., Z. Li and J. C. Liao (2009) Acetolactate Synthase from *Bacillus subtilis* Serves as a 2-Ketoisovalerate Decarboxylase for Isobutanol Biosynthesis in *Escherichia coli*. *Appl. Environ. Microbiol.* **75**, 6306-6311.

- Bae, S.-S., Y.-J. Kim, S.-H. Yang, J.-K. Lim, J.-H. Jeon, H.-S. Lee, S.-G. Kang, S.-J. Kim and J.-H. Lee (2008) *Thermococcus onnurineus* sp. nov., a Hyperthermophilic Archaeon Isolated from a Deep-Sea Hydrothermal Vent Area at the PACMANUS Field, The Korean Society for Applied Microbiology and Biotechnology
- Bae, S., T. Kim, H. Lee, K. Kwon, Y. Kim, M.-S. Kim, J.-H. Lee and S. Kang (2012) H₂ production from CO, formate or starch using the hyperthermophilic archaeon, *Thermococcus onnurineus*. *Biotechnol. Lett.* **34**, 75-79.
- Balch, W. E., G. E. Fox, L. J. Magrum, C. R. Woese and R. S. Wolfe (1979) Methanogens: reevaluation of a unique biological group. *Microbiological reviews.* **43**, 260-93.
- Balk, M., J. Weijma and A. J. M. Stams (2002) *Thermotoga lettingae* sp. nov., a novel thermophilic, methanol-degrading bacterium isolated from a thermophilic anaerobic reactor. *Int. J. Syst. Evol. Microbiol.* **52**, 1361-1368.
- Bar-Ilan, A., V. Balan, K. Tittmann, R. Golbik, M. Vyazmensky, G. Hubner, Z. e. Barak and D. M. Chipman (2001) Binding and activation of thiamin diphosphate in acetohydroxyacid Synthase. *Biochemistry.* **40**, 11946-11954.
- Barak, Z., D. M. Chipman and N. Gollop (1987) Physiological implications of the specificity of acetohydroxy acid synthase isozymes of enteric bacteria. *J. Bacteriol.* **169**, 3750-3756.
- Barbier, G., A. Godfroy, J.-R. Meunier, J. Querellou, M.-A. Cambon, F. Lesongeur, P. A. D. Grimont and G. Ragueneas (1999) *Pyrococcus glycovorans* sp. nov., a hyperthermophilic archaeon isolated from the East Pacific Rise. *Int. J. Syst. Bacteriol.* **49**, 1829-1837.
- Barnard, D., A. Casanueva, M. Tuffin and D. Cowan (2010) Extremophiles in biofuel synthesis. *Environ. Technol.* **31**, 871-888.
- Bashir, Q., N. Rashid, F. Jamil, T. Imanaka and M. Akhtar (2009) Highly Thermostable L-Threonine Dehydrogenase from the Hyperthermophilic Archaeon *Thermococcus kodakaraensis*. *Journal of biochemistry.* **146**, 95-102.
- Baumgartner, M., A. Yapi, R. Gröbner-Ferreira and K. O. Stetter (2003) Cultivation and properties of *Echinamoeba thermarum* n. sp., an extremely thermophilic amoeba thriving in hot springs. *Extremophiles.* **7**, 267-274.
- Ben Hania, W., R. Ghodbane, A. Postec, C. Brochier-Armanet, M. Hamdi, M. L. Fardeau and B. Ollivier (2011) Cultivation of the first mesophilic representative (“mesotoga”) within the order Thermotogales. *Syst. Appl. Microbiol.*
- Birrien, J.-L., X. Zeng, M. Jebbar, M.-A. Cambon-Bonavita, J. Quérellou, P. Oger, N. Bienvenu, X. Xiao and D. Prieur (2011) *Pyrococcus yayanosii* sp. nov., the first obligate piezophilic hyperthermophilic archaeon isolated from a deep-sea hydrothermal vent. *Int. J. Syst. Evol. Microbiol.*
- Blamey, J. M. and M. W. Adams (1994) Characterization of an ancestral type of pyruvate ferredoxin oxidoreductase from the hyperthermophilic bacterium, *Thermotoga maritima*. *Biochemistry.* **33**, 1000-7.
- Blamey, J. M. and M. W. W. Adams (1993) Purification and characterization of pyruvate ferredoxin oxidoreductase from the hyperthermophilic archaeon *Pyrococcus furiosus*. *Biochimica et Biophysica Acta (BBA) - Protein Structure and Molecular Enzymology.* **1161**, 19-27.
- Bocchetta, M., S. Gribaldo, A. Sanangelantoni and P. Cammarano (2000) Phylogenetic Depth of the Bacterial Genera *Aquifex* and *Thermotoga* Inferred from Analysis of Ribosomal Protein, Elongation Factor, and RNA Polymerase Subunit Sequences. *J. Mol. Evol.* **50**, 366-380.
- Bock, A.-K., A. Prieger-Kraft and P. Schönheit (1994) Pyruvate a novel substrate for growth and methane formation in *Methanosarcina barkeri*. *Arch. Microbiol.* **161**, 33-46.

- Bock, A.-K., P. Schönheit and M. Teixeira (1997) The iron-sulfur centers of the pyruvate:ferredoxin oxidoreductase from *Methanosarcina barkeri* (Fusaro). *FEBS Lett.* **414**, 209-212.
- Bock, A. K., J. Kunow, J. Glasemacher and P. Schönheit (1996) Catalytic Properties, Molecular Composition and Sequence Alignments of Pyruvate: Ferredoxin Oxidoreductase from the Methanogenic Archaeon *Methanosarcina Barkeri* (Strain Fusaro). *Eur. J. Biochem.* **237**, 35-44.
- Bornemann, S., D. H. G. Crout, H. Dalton, D. W. Hutchinson, G. Dean, N. Thomson and M. M. Turner (1993) Stereochemistry of the formation of lactaldehyde and acetoin produced by the pyruvate decarboxylases of yeast (*Saccharomyces* sp.) and *Zymomonas mobilis*: different Boltzmann distributions between bound forms of the electrophile, acetaldehyde, in the two enzymatic reactions. *Journal of the Chemical Society, Perkin Transactions 1*, 309-311.
- Bothe, H., B. Falkenberg and U. Nolteernsting (1974) Properties and function of the pyruvate: Ferredoxin oxidoreductase from the blue-green alga *Anabaena cylindrica*. *Arch. Microbiol.* **96**, 291-304.
- Bowen, T. L., J. Union, D. L. Tumbula and W. B. Whitman (1997) Cloning and phylogenetic analysis of the genes encoding acetoxyacid synthase from the archaeon *Methanococcus aeolicus*. *Gene.* **188**, 77-84.
- Bowyer, A., H. Mikolajek, J. W. Stuart, S. P. Wood, F. Jamil, N. Rashid, M. Akhtar and J. B. Cooper (2009) Structure and function of the l-threonine dehydrogenase (TkTDH) from the hyperthermophilic archaeon *Thermococcus kodakaraensis*. *Journal of Structural Biology.* **168**, 294-304.
- Bradford, M. M. (1976) A rapid and sensitive method for the quantitation of microgram quantities of protein utilizing the principle of protein-dye binding. *Anal. Biochem.* **72**, 248-254.
- Brazelton, W. J., K. A. Ludwig, M. L. Sogin, E. N. Andreishcheva, D. S. Kelley, C.-C. Shen, R. L. Edwards and J. A. Baross (2010) Archaea and bacteria with surprising microdiversity show shifts in dominance over 1,000-year time scales in hydrothermal chimneys. *Proc. Natl. Acad. Sci. USA.* **107**, 1612-1617.
- Bredholt, S., J. Sonne-Hansen, P. Nielsen, I. M. Mathrani and B. K. Ahring (1999) *Caldicellulosiruptor kristjanssonii* sp. nov., a cellulolytic, extremely thermophilic, anaerobic bacterium. *Int. J. Syst. Bacteriol.* **49**, 991-996.
- Bringer-Meyer, S., K. L. Schimz and H. Sahm (1986) Pyruvate decarboxylase from *Zymomonas mobilis*. Isolation and partial characterization. *Arch. Microbiol.* **146**, 105-110.
- Brochier-Armanet, C., B. Boussau, S. Gribaldo and P. Forterre (2008) Mesophilic crenarchaeota: proposal for a third archaeal phylum, the Thaumarchaeota. *Nature Reviews Microbiology.* **6**, 245-252.
- Brock, T. D., K. M. Brock, R. T. Belly and R. L. Weiss (1972) *Sulfolobus*: A new genus of sulfur-oxidizing bacteria living at low pH and high temperature. *Arch. Microbiol.* **84**, 54-68.
- Bronnenmeier, K., A. Kern, W. Liebl and W. L. Staudenbauer (1995) Purification of *Thermotoga maritima* enzymes for the degradation of cellulosic materials. *Appl. Environ. Microbiol.* **61**, 1399-1407.
- Brostedt, E. and S. Nordlund (1991) Purification and partial characterization of a pyruvate oxidoreductase from the photosynthetic bacterium *Rhodospirillum rubrum* grown under nitrogen-fixing conditions. *Biochem J.* **1**, 155-158.
- Brown, D. M., J. A. Upcroft, H. N. Dodd, N. Chen and P. Upcroft (1999) Alternative 2-keto acid oxidoreductase activities in *Trichomonas vaginalis*. *Mol. Biochem. Parasitol.* **98**, 203-214.

- Bruchhaus, I. and E. Tannich (1994) Purification and molecular characterization of the NAD(+)-dependent acetaldehyde/alcohol dehydrogenase from *Entamoeba histolytica*. *Biochem. J.* **303**, 743-748.
- Buchholz, S. E., M. M. Dooley and D. E. Eveleigh (1987) *Zymomonas* -- an alcoholic enigma. *Trends Biotechnol.* **5**, 199-204.
- Buckel, W. and B. T. Golding (2006) Radical Enzymes in Anaerobes. *Annu. Rev. Microbiol.* **60**, 27-49.
- Burdette, D. and J. G. Zeikus (1994) Purification of acetaldehyde dehydrogenase and alcohol dehydrogenases from *Thermoanaerobacter ethanolicus* 39E and characterization of the secondary-alcohol dehydrogenase (2 degrees Adh) as a bifunctional alcohol dehydrogenase--acetyl-CoA reductive thioesterase. *The Biochemical journal.* **302**, 163-0.
- Bustard, M. T., J. G. Burgess, V. Meeyoo and P. C. Wright (2000) Novel opportunities for marine hyperthermophiles in emerging biotechnology and engineering industries. *J. Chem. Technol. Biotechnol.* **75**, 1095-1109.
- Cai, J., Y. Wang, D. Liu, Y. Zeng, Y. Xue, Y. Ma and Y. Feng (2007) *Fervidobacterium changbaicum* sp. nov., a novel thermophilic anaerobic bacterium isolated from a hot spring of the Changbai Mountains, China. *Int. J. Syst. Evol. Microbiol.* **57**, 2333-2336.
- Cambon-Bonavita, M.-A., F. Lesongeur, P. Pignet, N. Wery, C. Lambert, A. Godfroy, J. Querellou and G. Barbier (2003) Extremophiles, Thermophily section, species description *Thermococcus atlanticus* sp. nov., a hyperthermophilic Archaeon isolated from a deep-sea hydrothermal vent in the Mid-Atlantic Ridge. *Extremophiles.* **7**, 101-109.
- Cammack, R., L. Kerscher and D. Oesterhelt (1980) A stable free radical intermediate in the reaction of 2-oxoacid:ferredoxin oxidoreductases of *Halobacterium halobium*. *FEBS Lett.* **118**, 271-273.
- Canale-Parola, E. (1970) Biology of the sugar-fermenting *Sarcinae*. *Microbiol. Mol. Biol. Rev.* **34**, 82-97.
- Candy, J. M. and R. G. Duggleby (1998) Structure and properties of pyruvate decarboxylase and site-directed mutagenesis of the *Zymomonas mobilis* enzyme. *Biochimica et Biophysica Acta (BBA) - Protein Structure and Molecular Enzymology.* **1385**, 323-338.
- Canganella, F., W. Jones, A. Gambacorta and G. Antranikian (1998) *Thermococcus guaymasensis* sp. nov. and *Thermococcus aggregans* sp. nov., two novel thermophilic archaea isolated from the Guaymas Basin hydrothermal vent site. *Int. J. Syst. Bacteriol.* **48**, 1181-1185.
- Cann, A. and J. Liao (2010) Pentanol isomer synthesis in engineered microorganisms. *Appl. Microbiol. Biotechnol.* **85**, 893-899.
- Cavicchioli, R. (2002) Extremophiles and the Search for Extraterrestrial Life. *Astrobiology.* **2**, 281-292.
- Cavicchioli, R. (2011) Archaea- timeline of the third domain. *Nature Reviews Microbiology.* **9**, 51-61.
- Chabrière, E., M.-H. Charon, A. Volbeda, L. Pieulle, E. C. Hatchikian and J.-C. Fontecilla-Camps (1999) Crystal structures of the key anaerobic enzyme pyruvate:ferredoxin oxidoreductase, free and in complex with pyruvate. *Nat. Struct. Mol. Biol.* **6**, 182-190.
- Chabriere, E., X. Vernede, B. Guigliarelli, M.-H. Charon, E. C. Hatchikian and J. C. Fontecilla-Camps (2001) Crystal Structure of the Free Radical Intermediate of Pyruvate:Ferredoxin Oxidoreductase. *Science.* **294**, 2559-2563.
- Chang, A. K. and R. G. Duggleby (1997) Expression, purification and characterization of *Arabidopsis thaliana* acetohydroxyacid synthase. *Biochem J.* **327**, 161-169.

- Chang, Y. Y. and J. E. Cronan, Jr. (1988) Common ancestry of *Escherichia coli* pyruvate oxidase and the acetohydroxy acid synthases of the branched-chain amino acid biosynthetic pathway. *J. Bacteriol.* **170**, 3937-3945.
- Charon, M.-H., A. Volbeda, E. Chabriere, L. Pieulle and J. C. Fontecilla-Camps (1999) Structure and electron transfer mechanism of pyruvate:ferredoxin oxidoreductase. *Curr. Opin. Struct. Biol.* **9**, 663-669.
- Chen, G. C. and F. Jordan (1984) Brewers' yeast pyruvate decarboxylase produces acetoin from acetaldehyde: a novel tool to study the mechanism of steps subsequent to carbon dioxide loss. *Biochemistry.* **23**, 3576-3582.
- Chhabra, S. R., K. R. Shockley, S. B. Connors, K. L. Scott, R. D. Wolfinger and R. M. Kelly (2003) Carbohydrate-induced differential gene expression patterns in the hyperthermophilic bacterium *Thermotoga maritima*. *J. Biol. Chem.* **278**, 7540-7552.
- Chipman, D., Z. e. Barak and J. V. Schloss (1998) Biosynthesis of 2-aceto-2-hydroxy acids: acetolactate synthases and acetohydroxyacid synthases. *Biochimica et Biophysica Acta (BBA) - Protein Structure and Molecular Enzymology.* **1385**, 401-419.
- Chipman, D. M., R. G. Duggleby and K. Tittmann (2005) Mechanisms of acetohydroxyacid synthases. *Curr. Opin. Chem. Biol.* **9**, 475-481.
- Choi, K.-J., K. M. Noh, D.-E. Kim, B. H. Ha, E. E. Kim and M.-Y. Yoon (2007) Identification of the catalytic subunit of acetohydroxyacid synthase in *Haemophilus influenzae* and its potent inhibitors. *Archives of Biochemistry and Biophysics.* **466**, 24-30.
- Choi, K.-J., Y. G. Yu, H. G. Hahn, J.-D. Choi and M.-Y. Yoon (2005) Characterization of acetohydroxyacid synthase from *Mycobacterium tuberculosis* and the identification of its new inhibitor from the screening of a chemical library. *FEBS Lett.* **579**, 4903-4910.
- Chou, C.-J., F. E. Jenney Jr, M. W. W. Adams and R. M. Kelly (2008) Hydrogenesis in hyperthermophilic microorganisms: Implications for biofuels. *Metab. Eng.* **10**, 394-404.
- Cohen, G. N., V. Barbe, D. Flament, M. Galperin, R. Heilig, O. Lecompte, O. Poch, D. Prieur, J. Querellou, R. Ripp, J.-C. Thierry, J. Van der Oost, J. Weissenbach, Y. Zivanovic and P. Forterre (2003) An integrated analysis of the genome of the hyperthermophilic archaeon *Pyrococcus abyssi*. *Mol. Microbiol.* **47**, 1495-1512.
- Connors, S. B., E. F. Mongodin, M. R. Johnson, C. I. Montero, K. E. Nelson and R. M. Kelly (2006) Microbial biochemistry, physiology, and biotechnology of hyperthermophilic *Thermotoga* species. *FEMS Microbiol. Rev.* **30**, 872-905.
- Connors, S. B., C. I. Montero, D. A. Comfort, K. R. Shockley, M. R. Johnson, S. R. Chhabra and R. M. Kelly (2005) An Expression-Driven Approach to the Prediction of Carbohydrate Transport and Utilization Regulons in the Hyperthermophilic Bacterium *Thermotoga maritima*. *J. Bacteriol.* **187**, 7267-7282.
- Constantopoulos, G. and J. A. Barranger (1984) Nonenzymatic decarboxylation of pyruvate. *Anal. Biochem.* **139**, 353-358.
- Costelloe, S., J. Ward and P. Dalby (2008) Evolutionary Analysis of the TPP-Dependent Enzyme Family. *J. Mol. Evol.* **66**, 36-49.
- Cripps, R. E., K. Eley, D. J. Leak, B. Rudd, M. Taylor, M. Todd, S. Boakes, S. Martin and T. Atkinson (2009) Metabolic engineering of *Geobacillus thermoglucosidasius* for high yield ethanol production. *Metab. Eng.* **11**, 398-408.
- Crout, D. H. G., H. Dalton, D. W. Hutchinson and M. Miyagoshi (1991) Studies on pyruvate decarboxylase: acyloin formation from aliphatic, aromatic and heterocyclic aldehydes. *J. Chem. Soc. Lond. Chem. Commun.*, 1329-1334.

- Crout, D. H. G., S. Davies, R. J. Heath, C. O. Miles, D. R. Rathbone, B. E. P. Swoboda and M. B. Gravestock (1994) Applications of Hydrolytic and Decarboxylating Enzymes in Biotransformations. *Biocatalysis Biotransformation*. **9**, 1-30.
- Das, A. and C. Yanofsky (1984) A ribosome binding site sequence is necessary for efficient expression of the distal gene of a translationally-coupled gene pair. *Nucleic Acids Res.* **12**, 4757-4768.
- de Vrije, T., R. Bakker, M. Budde, M. Lai, A. Mars and P. Claassen (2009) Efficient hydrogen production from the lignocellulosic energy crop *Miscanthus* by the extreme thermophilic bacteria *Caldicellulosiruptor saccharolyticus* and *Thermotoga neapolitana*. *Biotechnology for Biofuels*. **2**, 12.
- Demain, A. L., M. Newcomb and J. H. D. Wu (2005) Cellulase, Clostridia, and Ethanol. *Microbiol. Mol. Biol. Rev.* **69**, 124-154.
- Dien, B. S., M. A. Cotta and T. W. Jeffries (2003) Bacteria engineered for fuel ethanol production: current status. *Appl. Microbiol. Biotechnol.* **63**, 258-266.
- DiPippo, J. L., C. L. Nesbo, H. Dahle, W. F. Doolittle, N.-K. Birkland and K. M. Noll (2009) *Kosmotoga olearia* gen. nov., sp. nov., a thermophilic, anaerobic heterotroph isolated from an oil production fluid. *Int. J. Syst. Evol. Microbiol.* **59**, 2991-3000.
- Dirmeier, R., M. Keller, D. Hafenbradl, F.-J. Braun, R. Rachel, S. Burggraf and K. O. Stetter (1998) *Thermococcus acidaminovorans* sp. nov., a new hyperthermophilic alkalophilic archaeon growing on amino acids. *Extremophiles*. **2**, 109-114.
- Dobritzsch, D., S. Konig, G. Schneider and G. Lu (1998) High Resolution Crystal Structure of Pyruvate Decarboxylase from *Zymomonas mobilis*. Implications for Substrate Activation in Pyruvate Decarboxylases. *J. Biol. Chem.* **273**, 20196-20204.
- Drake, H. L., S. I. Hu and H. G. Wood (1981) Purification of five components from *Clostridium thermoaceticum* which catalyze synthesis of acetate from pyruvate and methyltetrahydrofolate-properties of phosphotransacetylase. *J. Biol. Chem.* **256**, 1137-1144.
- Duffaud, G. D., O. B. d'Hennezel, A. S. Peek, A. L. Reysenbach and R. M. Kelly (1998) Isolation and characterization of *Thermococcus barossii*, sp. nov., a hyperthermophilic archaeon isolated from a hydrothermal vent flange formation. *Syst. Appl. Microbiol.* **21**, 40-49
- Duggleby, R. G. (2006) Domain Relationships in Thiamine Diphosphate-Dependent Enzymes. *Acc. Chem. Res.* **39**, 550-557.
- Duggleby, R. G., J. A. McCourt and L. W. Guddat (2008) Structure and mechanism of inhibition of plant acetohydroxyacid synthase. *Plant Physiol. Biochem.* **46**, 309-324.
- Duggleby, R. G. and S. S. Pang (2000) Acetohydroxyacid Synthase. *Journal of Biochemistry and Molecular Biology*. **33**, 1-36.
- Dulieu, C. and D. Poncelet (1999) Spectrophotometric assay of α -acetolactate decarboxylase. *Enzyme Microb. Technol.* **25**, 537-542.
- Dworkin, M., S. Falkow, E. Rosenberg, K.-H. Schleifer, E. Stackebrandt, C. Bertoldo and G. Antranikian (2006a) The Order Thermococcales. *The Prokaryotes*, pp 69-81, Springer New York
- Dworkin, M., S. Falkow, E. Rosenberg, K.-H. Schleifer, E. Stackebrandt, R. Huber and M. Hannig (2006b) Thermotogales. *The Prokaryotes*, pp 899-922, Springer New York
- Eggeling, I., C. Cordes, L. Eggeling and H. Sahm (1987) Regulation of acetohydroxy acid synthase in *Corynebacterium glutamicum* during fermentation of α -ketobutyrate to l-isoleucine. *Appl. Microbiol. Biotechnol.* **25**, 346-351.

- Egorova, K. and G. Antranikian (2005) Industrial relevance of thermophilic Archaea. *Curr. Opin. Microbiol.* **8**, 649-655.
- Elkins, J. G., M. Podar, D. E. Graham, K. S. Makarova, Y. Wolf, L. Randau, B. P. Hedlund, C. I. Brochier-Armanet, V. Kunin, I. Anderson, A. Lapidus, E. Goltsman, K. Barry, E. V. Koonin, P. Hugenholtz, N. Kyrpides, G. Wanner, P. Richardson, M. Keller and K. O. Stetter (2008) A korarchaeal genome reveals insights into the evolution of the Archaea. *Proc. Natl. Acad. Sci. USA.* **105**, 8102-8107.
- Emelyanov, V. V. and A. V. Goldberg (2011) Fermentation enzymes of *Giardia intestinalis*, pyruvate:ferredoxin oxidoreductase and hydrogenase, do not localize to its mitosomes. *Microbiology.* **157**, 1602-1611.
- Engel, S., M. Vyazmensky, D. Berkovich, Z. e. Barak and D. M. Chipman (2004a) Substrate range of acetohydroxy acid synthase I from *Escherichia coli* in the stereoselective synthesis of α -hydroxy ketones. *Biotechnol. Bioeng.* **88**, 825-831.
- Engel, S., M. Vyazmensky, D. Berkovich, Z. e. Barak, J. Merchuk and D. M. Chipman (2005) Column flow reactor using acetohydroxyacid synthase I from *Escherichia coli* as catalyst in continuous synthesis of *R*-phenylacetyl carbinol. *Biotechnol. Bioeng.* **89**, 733-740.
- Engel, S., M. Vyazmensky, S. Geresh, Z. e. Barak and D. Chipman, M. (2003) Acetohydroxyacid synthase: A new enzyme for chiral synthesis of *R*-phenylacetylcarbinol. *Biotechnol. Bioeng.* **83**, 833-840.
- Engel, S., M. Vyazmensky, M. Vinogradov, D. Berkovich, A. Bar-Ilan, U. Qimron, Y. Rosiansky, Z. e. Barak and D. M. Chipman (2004b) Role of a Conserved Arginine in the Mechanism of Acetohydroxyacid Synthase. *J. Biol. Chem.* **279**, 24803-24812.
- Erauso, G., A.-L. Reysenbach, A. Godfroy, J.-R. Meunier, B. Crump, F. Partensky, J. Baross, V. Marteinson, G. Barbier, N. Pace and D. Prieur (1993) *Pyrococcus abyssi* sp. nov., a new hyperthermophilic archaeon isolated from a deep-sea hydrothermal vent. *Arch. Microbiol.* **160**, 338-349.
- Esser, D., R. Rudolph, R. Jaenicke and G. Böhm (1999) The HU protein from *Thermotoga maritima*: recombinant expression, purification and physicochemical characterization of an extremely hyperthermophilic DNA-binding protein. *J. Mol. Biol.* **291**, 1135-1146.
- Fardeau, M. L., B. Ollivier, B. K. C. Patel, M. Magot, P. Thomas, A. Rimbault, F. Rocchiccioli and J. L. Garcia (1997) *Thermotoga hypogea* sp. nov., a Xylanolytic, Thermophilic Bacterium from an Oil-Producing Well. *Int. J. Syst. Bacteriol.* **47**, 1013-1019.
- Feng, Y., L. Cheng, X. Zhang, X. Li, Y. Deng and H. Zhang (2010) *Thermococcoides shengliensis* gen. nov., sp. nov., a new member of the order *Thermotogales* isolated from oil-production fluid. *Int. J. Syst. Evol. Microbiol.* **60**, 932-937.
- Fiala, G. and K. O. Stetter (1986) *Pyrococcus furiosus* sp. nov. represents a novel genus of marine heterotrophic archaeobacteria growing optimally at 100°C. *Arch. Microbiol.* **145**, 56-61.
- Forterre, P. (2002) A hot story from comparative genomics: reverse gyrase is the only hyperthermophile-specific protein. *Trends Genet.* **18**, 236-237.
- Friedrich, A. B. and G. Antranikian (1996) Keratin Degradation by *Fervidobacterium pennavorans*, a Novel Thermophilic Anaerobic Species of the Order *Thermotogales*. *Appl. Environ. Microbiol.* **62**, 2875-2882.
- Frock, A. D., S. R. Gray and R. M. Kelly (2012) Hyperthermophilic *Thermotoga* species differ with respect to specific carbohydrate transporters and glycoside hydrolases. *Appl. Environ. Microbiol.* **78**, 1978-1986.

- Fukui, T., H. Atomi, T. Kanai, R. Matsumi, S. Fujiwara and T. Imanaka (2005) Complete genome sequence of the hyperthermophilic archaeon *Thermococcus kodakaraensis* KOD1 and comparison with Pyrococcus genomes. *Genome Res.* **15**, 352-363.
- Furdui, C. and S. W. Ragsdale (2002) The Roles of Coenzyme A in the Pyruvate:Ferredoxin Oxidoreductase Reaction Mechanism: Rate Enhancement of Electron Transfer from a Radical Intermediate to an Iron-Sulfur Cluster. *Biochemistry.* **41**, 9921-9937.
- Garczarek, F., M. Dong, D. Typke, H. E. Witkowska, T. C. Hazen, E. Nogales, M. D. Biggin and R. M. Glaeser (2007) Octomeric pyruvate-ferredoxin oxidoreductase from *Desulfovibrio vulgaris*. *Journal of Structural Biology.* **159**, 9-18.
- Gedi, V., J.-Y. Moon, W.-M. Lim, M.-Y. Lee, S.-C. Lee, B.-S. Koo, S. Govindwar and M.-Y. Yoon (2011) Identification and characterization of inhibitors of *Haemophilus influenzae* acetohydroxyacid synthase. *Enzyme Microb. Technol.* **49**, 1-5.
- Gedi, V. and M.-Y. Yoon (2012) Bacterial acetohydroxyacid synthase and its inhibitors – a summary of their structure, biological activity and current status. *FEBS J.* **279**, 946-963.
- Glansdorff, N., Y. Xu and B. Labedan (2008) The Last Universal Common Ancestor: emergence, constitution and genetic legacy of an elusive forerunner. *Biology Direct.* **3**, 29.
- Gocke, D., T. Graf, H. Brosi, I. Frindi-Wosch, L. Walter, M. Müller and M. Pohl (2009a) Comparative characterisation of thiamin diphosphate-dependent decarboxylases. *Journal of Molecular Catalysis B: Enzymatic.* **61**, 30-35.
- Gocke, D., T. Graf, H. Brosi, I. Frindi-Wosch, L. Walter, M. Müller and M. Pohl (2009b) Comparative characterisation of thiamin diphosphate-dependent decarboxylases. *Journal of Molecular Catalysis B: Enzymatic.* **61**, 30-35.
- Godfroy, A., F. Lesongeur, G. Ragueneas, J. Querellou, E. Antoine, J.-R. Meunier, J. Guezennec and G. Barbier (1997) *Thermococcus hydrothermalis* sp. nov., a new hyperthermophilic archaeon Isolated from a deep-sea hydrothermal vent. *Int. J. Syst. Bacteriol.* **47**, 622-626.
- Godfroy, A., J.-R. Meunier, J. Guezennec, F. Lesongeur, G. Ragueneas, A. Rimbault and G. Barbier (1996) *Thermococcus fumicolans* sp. nov., a New Hyperthermophilic Archaeon Isolated from a Deep-Sea Hydrothermal Vent in the North Fiji Basin. *Int. J. Syst. Bacteriol.* **46**, 1113-1119.
- Goetz, G., P. Iwan, B. Hauer, M. Breuer and M. Pohl (2001) Continuous production of (*R*)-phenylacetylcarbinol in an enzyme-membrane reactor using a potent mutant of pyruvate decarboxylase from *Zymomonas mobilis*. *Biotechnol. Bioeng.* **74**, 317-325.
- Gollop, N., B. Damri, Z. e. Barak and D. M. Chipman (1989) Kinetics and mechanism of acetohydroxy acid synthase isozyme III from *Escherichia coli*. *Biochemistry.* **28**, 6310-6317.
- Gollop, N., B. Damri, D. M. Chipman and Z. Barak (1990) Physiological implications of the substrate specificities of acetohydroxy acid synthases from varied organisms. *J. Bacteriol.* **172**, 3444-3449.
- González, J. M., C. Kato and K. Horikoshi (1995) *Thermococcus peptonophilus* sp. nov., a fast-growing, extremely thermophilic archaeobacterium isolated from deep-sea hydrothermal vents. *Arch. Microbiol.* **164**, 159-164.
- González, J. M., Y. Masuchi, F. T. Robb, J. W. Ammerman, D. L. Maeder, M. Yanagibayashi, J. Tamaoka and C. Kato (1998) *Pyrococcus horikoshii* sp. nov., a hyperthermophilic archaeon isolated from a hydrothermal vent at the Okinawa Trough. *Extremophiles.* **2**, 123-130.
- González, J. M., D. Sheckells, M. Viebahn, D. Krupatkina, K. M. Borges and F. T. Robb (1999) *Thermococcus waiotapuensis* sp. nov., an extremely thermophilic archaeon isolated from a freshwater hot spring. *Arch. Microbiol.* **172**, 95-101.

- Goupil-Feuillerat, N., M. Coccain-Bousquet, J. J. Godon, S. D. Ehrlich and P. Renault (1997) Dual role of alpha-acetolactate decarboxylase in *Lactococcus lactis* subsp. *lactis*. *J. Bacteriol.* **179**, 6285-6293.
- Grandoni, J. A., P. T. Marta and J. V. Schloss (1998) Inhibitors of branched-chain amino acid biosynthesis as potential antituberculosis agents. *J. Antimicrob. Chemother.* **42**, 475-482.
- Grättinger, M., A. Dankesreiter, H. Schurig and R. Jaenicke (1998) Recombinant phosphoglycerate kinase from the hyperthermophilic bacterium *Thermotoga maritima*: catalytic, spectral and thermodynamic properties. *J. Mol. Biol.* **280**, 525-533.
- Green, J. B. A. (1989) Pyruvate decarboxylase is like acetolactate synthase (ILV2) and not like the pyruvate dehydrogenase E1 subunit. *FEBS Lett.* **246**, 1-5.
- Gribaldo, S., A. M. Poole, V. Daubin, P. Forterre and C. Brochier-Armanet (2010) The origin of eukaryotes and their relationship with the Archaea: are we at a phylogenomic impasse? *Nature Reviews Microbiology.* **8**, 743-752.
- Grimminger, H. and H. E. Umbarger (1979) Acetohydroxy acid synthase I of *Escherichia coli*: purification and properties. *J. Bacteriol.* **137**, 846-853.
- Grote, R., L. Li, J. Tamaoka, C. Kato, K. Horikoshi and G. Antranikian (1999) *Thermococcus siculi* sp. nov., a novel hyperthermophilic archaeon isolated from a deep-sea hydrothermal vent at the Mid-Okinawa Trough. *Extremophiles.* **3**, 55-62.
- Guagliardi, A., D. de Pascale, R. Cannio, V. Nobile, S. Bartolucci and M. Rossi (1995) The Purification, Cloning, and High Level Expression of a Glutaredoxin-like Protein from the Hyperthermophilic Archaeon *Pyrococcus furiosus*. *J. Biol. Chem.* **270**, 5748-5755.
- Guy, J. E., M. N. Isupov and J. A. Littlechild (2003) The Structure of an Alcohol Dehydrogenase from the Hyperthermophilic Archaeon *Aeropyrum pernix*. *J. Mol. Biol.* **331**, 1041-1051.
- Haki, G. D. and S. K. Rakshit (2003) Developments in industrially important thermostable enzymes: a review. *Bioresour. Technol.* **89**, 17-34.
- Hawkins, C. F., A. Borges and R. N. Perham (1989) A common structural motif in thiamin pyrophosphate-binding enzymes. *FEBS Lett.* **255**, 77-82.
- Heider, J., X. Mai and M. Adams (1996) Characterization of 2-ketoisovalerate ferredoxin oxidoreductase, a new and reversible coenzyme A-dependent enzyme involved in peptide fermentation by hyperthermophilic archaea. *J. Bacteriol.* **178**, 780-787.
- Hill, C. M., S. S. Pang and R. G. Duggleby (1997) Purification of *Escherichia coli* acetohydroxyacid synthase isoenzyme II and reconstitution of active enzyme from its individual pure subunits. *The Biochemical journal.* **327**, 891-898.
- Hirakawa, H., N. Kamiya, Y. Kawarabayashi and T. Nagamune (2004) Properties of an alcohol dehydrogenase from the hyperthermophilic archaeon *Aeropyrum pernix* K1. *J. Biosci. Bioeng.* **97**, 202-206.
- Hoaki, T., M. Nishijima, M. Kato, K. Adachi, S. Mizobuchi, N. Hanzawa and T. Maruyama (1994) Growth requirements of hyperthermophilic sulfur-dependent heterotrophic archaea isolated from a shallow submarine geothermal system with reference to their essential amino acids. *Appl. Environ. Microbiol.* **60**, 2898-2904.
- Hoaki, T., C. O. Wirsén, S. Hanzawa, T. Maruyama and H. W. Jannasch (1993) Amino Acid Requirements of Two Hyperthermophilic Archaeal Isolates from Deep-Sea Vents, *Desulfurococcus* Strain SY and *Pyrococcus* Strain GB-D. *Appl. Environ. Microbiol.* **59**, 610-613.
- Holden, J. F. and J. A. Baross (1993) Enhanced thermotolerance and temperature-induced changes in protein composition in the hyperthermophilic archaeon ES4. *J. Bacteriol.* **175**, 2839-2843.

- Hoppner, T. C. and H. W. Doelle (1983) Purification and kinetic characteristics of pyruvate decarboxylase and ethanol dehydrogenase from *Zymomonas mobilis* in relation to ethanol production. *Appl. Microbiol. Biotechnol.* **17**, 152-157.
- Horner, D. S., R. P. Hirt and T. M. Embley (1999) A single eubacterial origin of eukaryotic pyruvate:ferredoxin oxidoreductase genes: Implications for the evolution of anaerobic eukaryotes. *Mol. Biol. Evol.* **16**, 1280-1291.
- Huang, C.-Y., B. K. Patel, R. A. Mah and L. Baresi (1998) *Caldicellulosiruptor owensensis* sp. nov., an anaerobic, extremely thermophilic, xylanolytic bacterium. *Int. J. Syst. Bacteriol.* **48**, 91-97.
- Huber, H., M. J. Hohn, R. Rachel, T. Fuchs, V. C. Wimmer and K. O. Stetter (2002) A new phylum of Archaea represented by a nanosized hyperthermophilic symbiont. *Nature.* **417**, 63-67.
- Huber, H. and K. O. Stetter (1998) Hyperthermophiles and their possible potential in biotechnology. *J. Biotechnol.* **64**, 39-52.
- Huber, R. and M. Hanning (2006) Thermotogales. *The Prokaryotes*. Dworkin, M., Falkow, S., Rosenberg, E., Schleifer, K.-H. and Stackebrandt, E. (eds.), pp 899-922, Springer Science+Business Media, LLC New York
- Huber, R., T. A. Langworthy, H. König, M. Thomm, C. R. Woese, U. B. Sleytr and K. O. Stetter (1986) *Thermotoga maritima* sp. nov. represents a new genus of unique extremely thermophilic eubacteria growing up to 90°C. *Arch. Microbiol.* **144**, 324-333.
- Huber, R., J. Stöhr, S. Hohenhaus, R. Rachel, S. Burggraf, H. Jannasch and K. Stetter (1995) *Thermococcus chitonophagus* sp. nov., a novel, chitin-degrading, hyperthermophilic archaeum from a deep-sea hydrothermal vent environment. *Arch. Microbiol.* **164**, 255-264.
- Huber, R., C. R. Woese, T. A. Langworthy, J. K. Kristjansson and K. O. Stetter (1990) *Fervidobacterium islandicum* sp. nov., a new extremely thermophilic eubacterium belonging to the *Thermotogales*. *Arch. Microbiol.* **154**, 105-111.
- Huberts, D. H. E. W. and I. J. van der Klei (2010) Moonlighting proteins: An intriguing mode of multitasking. *Biochimica et Biophysica Acta (BBA) - Molecular Cell Research.* **1803**, 520-525.
- Hübner, G., K. Tittmann, M. Killenberg-Jabs, J. Schäffner, M. Spinka, H. Neef, D. Kern, G. Kern, G. Schneider, C. Wikner and S. Ghisla (1998) Activation of thiamin diphosphate in enzymes. *Biochimica et Biophysica Acta (BBA) - Protein Structure and Molecular Enzymology.* **1385**, 221-228.
- Hughes, N., P. Chalk, C. Clayton and D. Kelly (1995) Identification of carboxylation enzymes and characterization of a novel four-subunit pyruvate:ferredoxin oxidoreductase from *Helicobacter pylori*. *J. Bacteriol.* **177**, 3953-3959.
- Iding, H., P. Siegert, K. Mesch and M. Pohl (1998) Application of alpha-keto acid decarboxylases in biotransformations. *Biochimica et Biophysica Acta (BBA) - Protein Structure and Molecular Enzymology.* **1385**, 307-322.
- Ikeda, T., T. Ochiai, S. Morita, A. Nishiyama, E. Yamada, H. Arai, M. Ishii and Y. Igarashi (2006) Anabolic five subunit-type pyruvate:ferredoxin oxidoreductase from *Hydrogenobacter thermophilus* TK-6. *Biochem. Biophys. Res. Commun.* **340**, 76-82.
- Ikeda, T., M. Yamamoto, H. Arai, D. Ohmori, M. Ishii and Y. Igarashi (2009) Enzymatic and electron paramagnetic resonance studies of anabolic pyruvate synthesis by pyruvate:ferredoxin oxidoreductase from *Hydrogenobacter thermophilus*. *FEBS J.* **277**, 501-510.

- Ikeda, T., M. Yamamoto, H. Arai, D. Ohmori, M. Ishii and Y. Igarashi (2010) Enzymatic and electron paramagnetic resonance studies of anabolic pyruvate synthesis by pyruvate: ferredoxin oxidoreductase from *Hydrogenobacter thermophilus*. *FEBS J.* **277**, 501-510.
- Imlay, A. J. (2006) Iron-sulphur clusters and the problem with oxygen. *Mol. Microbiol.* **59**, 1073-1082.
- Iwasaki, T., T. Wakagi and T. Oshima (1995) Ferredoxin-dependent Redox System of a Thermoacidophilic Archaeon, *Sulfolobus* sp. Strain 7. *J. Biol. Chem.* **270**, 17878-17883.
- Jeanthon, C., A.-L. Reysenbach, S. L'Haridon, A. Gambacorta, N. Pace, P. Glénat and D. Prieur (1995a) *Thermotoga subterranea* sp. nov., a new thermophilic bacterium isolated from a continental oil reservoir. *Arch. Microbiol.* **164**, 91-97.
- Jeanthon, C., A.-L. Reysenbach, S. L'Haridon, A. Gambacorta, N. R. Pace, P. Glénat and D. Prieur (1995b) *Thermotoga subterranea* sp. nov., a new thermophilic bacterium isolated from a continental oil reservoir. *Arch. Microbiol.* **164**, 91-97.
- Jeffery, C. J. (1999) Moonlighting proteins. *Trends Biochem. Sci.* **24**, 8-11.
- Jeffery, C. J. (2003) Moonlighting proteins: old proteins learning new tricks. *Trends Genet.* **19**, 415-417.
- Jenney, F. E. and M. W. W. Adams (2008) Hydrogenases of the Model Hyperthermophiles. *Ann. N. Y. Acad. Sci.* **1125**, 252-266.
- Joe Shaw, A., F. E. Jenney Jr, M. W. W. Adams and L. R. Lynd (2008) End-product pathways in the xylose fermenting bacterium, *Thermoanaerobacterium saccharolyticum*. *Enzyme Microb. Technol.* **42**, 453-458.
- Jolivet, E., E. Corre, S. L'Haridon, P. Forterre and D. Prieur (2004) *Thermococcus marinus* sp. nov. and *Thermococcus radiotolerans* sp. nov., two hyperthermophilic archaea from deep-sea hydrothermal vents that resist ionizing radiation. *Extremophiles.* **8**, 219-227.
- Jolivet, E., S. L'Haridon, E. Corre, P. Forterre and D. Prieur (2003) *Thermococcus gammatolerans* sp. nov., a hyperthermophilic archaeon from a deep-sea hydrothermal vent that resists ionizing radiation. *Int. J. Syst. Evol. Microbiol.* **53**, 847-851.
- Jordan, F. (2003) Current mechanistic understanding of thiamin diphosphate-dependent enzymatic reactions. *Natural Product Reports.* **20**, 184-201.
- Kalme, S., C. N. Pham, V. Gedi, D. T. Le, J.-D. Choi, S.-K. Kim and M.-Y. Yoon (2008) Inhibitors of *Bacillus anthracis* acetohydroxyacid synthase. *Enzyme Microb. Technol.* **43**, 270-275.
- Karakashev, D., A. Thomsen and I. Angelidaki (2007) Anaerobic biotechnological approaches for production of liquid energy carriers from biomass. *Biotechnol. Lett.* **29**, 1005-1012.
- Keilhauer, C., L. Eggeling and H. Sahm (1993) Isoleucine synthesis in *Corynebacterium glutamicum*: molecular analysis of the *ilvB-ilvN-ilvC* operon. *J. Bacteriol.* **175**, 5595-5603.
- Keller, M., F.-J. Braun, R. Dirmeier, D. Hafenbradl, S. Burggraf, R. Rachel and K. O. Stetter (1995) *Thermococcus alcaliphilus* sp. nov., a new hyperthermophilic archaeum growing on polysulfide at alkaline pH. *Arch. Microbiol.* **164**, 390-395.
- Kellermann, E., P. G. Seeboth and C. P. Hollenberg (1986) Analysis of the primary structure and promoter function of a pyruvate decarboxylase gene (PDCI) from *Saccharomyces cerevisiae*. *Nucleic Acids Res.* **14**, 8963-8977.
- Kelly, R. M. and M. W. W. Adams (1994) Metabolism in hyperthermophilic microorganisms. *Antonie Van Leeuwenhoek.* **66**, 247-270.
- Kengen, S., F. de Bok, N. van Loo, C. Dijkema, A. Stams and W. de Vos (1994) Evidence for the operation of a novel Embden-Meyerhof pathway that involves ADP-dependent kinases during sugar fermentation by *Pyrococcus furiosus*. *J. Biol. Chem.* **269**, 17537-17541.

- Kern, D., G. Kern, H. Neef, K. Tittmann, M. Killenberg-Jabs, C. Wikner, G. Schneider and G. Hübner (1997) How Thiamin Diphosphate Is Activated in Enzymes. *Science*. **275**, 67-70.
- Kerscher, L. and D. Oesterhelt (1981a) The catalytic mechanism of 2-oxoacid:ferredoxin oxidoreductases from *Halobacterium halobium*. One-electron transfer at two distinct steps of the catalytic cycle. *Eur. J. Biochem.* **116**, 595.
- Kerscher, L. and D. Oesterhelt (1981b) Purification and Properties of Two 2-Oxoacid:ferredoxin Oxidoreductases from *Halobacterium halobium*. *Eur. J. Biochem.* **116**, 587-594.
- Kerscher, L. and D. Oesterhelt (1982) Pyruvate : ferredoxin oxidoreductase -- new findings on an ancient enzyme. *Trends Biochem. Sci.* **7**, 371-374.
- Kil, M. W. and S. I. Chang (1998) Expression in *Escherichia coli* , Purification , and Characterization of the Tobacco Sulfonylurea Herbicide - Resistant Recombinant Acetolactate Synthase and Its Interaction with the Triazolopyrimidine Herbicides. *Biochem.Mol. Biol. rep.* **31**, 287-297.
- Kim, B.-C., Y.-H. Lee, H.-S. Lee, D.-W. Lee, E.-A. Choe and Y.-R. Pyun (2002) Cloning, expression and characterization of l-arabinose isomerase from *Thermotoga neapolitana*: bioconversion of d-galactose to d-tagatose using the enzyme. *FEMS Microbiol. Lett.* **212**, 121-126.
- Klapatch, T. R., D. A. L. Hogsett, S. Baskaran, S. Pal and L. R. Lynd (1994) Organism development and characterization for ethanol production using thermophilic bacteria. *Appl. Biochem. Biotechnol.* **45-46**, 209-223.
- Kletzin, A. and M. Adams (1996) Molecular and phylogenetic characterization of pyruvate and 2-ketoisovalerate ferredoxin oxidoreductases from *Pyrococcus furiosus* and pyruvate ferredoxin oxidoreductase from *Thermotoga maritima*. *J. Bacteriol.* **178**, 248-257.
- Kluger, R. (1987) Thiamin diphosphate: a mechanistic update on enzymic and nonenzymic catalysis of decarboxylation. *Chemical reviews.* **87**, 863-876.
- Kluger, R. and K. Tittmann (2008) Thiamin diphosphate catalysis: enzymic and nonenzymic covalent intermediates. *Chemical reviews.* **108**, 1797-1833.
- Kluszens, L. D., G. J. van Alebeek, A. G. Voragen, W. M. de Vos and J. van der Oost (2003) Molecular and biochemical characterization of the thermoactive family 1 pectate lyase from the hyperthermophilic bacterium *Thermotoga maritima*. *The Biochemical journal.* **370**, 651-659.
- Kobayashi, T., Y. S. Kwak, T. Akiba, T. Kudo and K. Horikoshi (1994) *Thermococcus profundus* sp. nov., a new hyperthermophilic archaeon isolated from a deep-sea hydrothermal vent. *Syst. Appl. Microbiol.* **17**, 232-236.
- Konig, S. (1998) Subunit structure, function and organisation of pyruvate decarboxylases from various organisms. *Biochimica et Biophysica Acta (BBA) - Protein Structure and Molecular Enzymology.* **1385**, 271-286.
- Korkhin, Y., A. J. Kalb, M. Peretz, O. Bogin, Y. Burstein and F. Frolow (1998) NADP-dependent bacterial alcohol dehydrogenases: crystal structure, cofactor-binding and cofactor specificity of the ADHs of *Clostridium beijerinckii* and *Thermoanaerobacter brockii*. *J. Mol. Biol.* **278**, 967-981.
- Krampitz, L. O. (1969) Catalytic Functions of Thiamin Diphosphate. *Annu. Rev. Biochem.* **38**, 213-240.
- Kube, J., C. Brokamp, R. Machielsen, J. van der Oost and H. Märkl (2006) Influence of temperature on the production of an archaeal thermoactive alcohol dehydrogenase from *Pyrococcus furiosus* with recombinant *Escherichia coli*. *Extremophiles.* **10**, 221-227.

- Kulkarni, R. R., V. R. Parreira, S. Sharif and J. F. Prescott (2007) Immunization of Broiler Chickens against *Clostridium perfringens*-Induced Necrotic Enteritis. *Clinical and Vaccine Immunology*. **14**, 1070-1077.
- Kulkarni, R. R., V. R. Parreira, S. Sharif and J. F. Prescott (2008) Oral immunization of broiler chickens against necrotic enteritis with an attenuated Salmonella vaccine vector expressing *Clostridium perfringens* antigens. *Vaccine*. **26**, 4194-4203.
- Kunow, J., D. Linder and R. K. Thauer (1995) Pyruvate: ferredoxin oxidoreductase from the sulfate-reducing *Archaeoglobus fulgidus*: molecular composition, catalytic properties, and sequence alignments. *Arch. Microbiol.* **V163**, 21-28.
- Kurniadi, T., R. Bel Rhlid, L. B. Fay, M. A. Juillerat and R. G. Berger (2003) Chemoenzymatic synthesis of aroma active 5,6-dihydro- and tetrahydropyrazines from aliphatic acyloins produced by baker's yeast. *J. Agric. Food Chem.* **51**, 3103-3107.
- Kuwabara, T., A. Kawasaki, I. Uda and A. Sugai (2011) *Thermosipho globiformans* sp. nov., an anaerobic thermophilic bacterium that transforms into multicellular spheroids with a defect in peptidoglycan formation. *Int. J. Syst. Evol. Microbiol.* **61**, 1622-1627.
- Kuwabara, T., M. Minaba, Y. Iwayama, I. Inouye, M. Nakashima, K. Marumo, A. Maruyama, A. Sugai, T. Itoh, J.-i. Ishibashi, T. Urabe and M. Kamekura (2005) *Thermococcus coalescens* sp. nov., a cell-fusing hyperthermophilic archaeon from Suiyo Seamount. *Int. J. Syst. Evol. Microbiol.* **55**, 2507-2514.
- Kuwabara, T., M. Minaba, N. Ogi and M. Kamekura (2007) *Thermococcus celericrescens* sp. nov., a fast-growing and cell-fusing hyperthermophilic archaeon from a deep-sea hydrothermal vent. *Int. J. Syst. Evol. Microbiol.* **57**, 437-443.
- L'Haridon, S., M. L. Miroshnichenko, H. Hippe, M. L. Fardeau, E. Bonch-Osmolovskaya, E. Stackebrandt and C. Jeanthon (2001) *Thermosipho geolei* sp. nov., a thermophilic bacterium isolated from a continental petroleum reservoir in Western Siberia. *Int. J. Syst. Evol. Microbiol.* **51**, 1327-1334.
- L'Haridon, S., M. L. Miroshnichenko, H. Hippe, M. L. Fardeau, E. A. Bonch-Osmolovskaya, E. Stackebrandt and C. Jeanthon (2002) *Petrotoga olearia* sp. nov. and *Petrotoga sibirica* sp. nov., two thermophilic bacteria isolated from a continental petroleum reservoir in Western Siberia. *Int. J. Syst. Evol. Microbiol.* **52**, 1715-1722.
- Laemmli, U. K. (1970) Cleavage of Structural Proteins during the Assembly of the Head of Bacteriophage T4. *Nature*. **227**, 680-685.
- Lamed, R. and J. G. Zeikus (1980) Ethanol Production by Thermophilic Bacteria: Relationship Between Fermentation Product Yields of and Catabolic Enzyme Activities in *Clostridium thermocellum* and *Thermoanaerobium brockii*. *J. Bacteriol.* **144**, 569-578.
- Le, D. T., Choi, J.D. (2005) FAD-independent and herbicide-resistant mutants of tobacco acetohydroxy acid synthase. *Bulletin Korean Chemical Society*. **26**, 916-920
- Leach, C. K. and N. G. Carr (1971) Pyruvate: Ferredoxin oxidoreductase and its activation by ATP in the blue-green alga *Anabaena variabilis*. *Biochimica et Biophysica Acta (BBA) - Bioenergetics*. **245**, 165-174.
- Lebedinsky, A., N. Chernyh and E. Bonch-Osmolovskaya (2007) Phylogenetic systematics of microorganisms inhabiting thermal environments. *Biochemistry (Moscow)*. **72**, 1299-1312.
- Lee, H. S., S. G. Kang, S. S. Bae, J. K. Lim, Y. Cho, Y. J. Kim, J. H. Jeon, S.-S. Cha, K. K. Kwon, H.-T. Kim, C.-J. Park, H.-W. Lee, S. I. Kim, J. Chun, R. R. Colwell, S.-J. Kim and J.-H. Lee (2008) The Complete Genome Sequence of *Thermococcus onnurineus* NA1 Reveals a Mixed Heterotrophic and Carboxydrotrophic Metabolism. *J. Bacteriol.* **190**, 7491-7499.

- Lee, K., H. S. Lillehoj, G. Li, M.-S. Park, S. I. Jang, W. Jeong, H.-Y. Jeoung, D.-J. An and E. P. Lillehoj (2011) Identification and cloning of two immunogenic *Clostridium perfringens* proteins, elongation factor Tu (EF-Tu) and pyruvate:ferredoxin oxidoreductase (PFO) of *C. perfringens*. *Res. Vet. Sci.* **91**, e80-e86.
- Lee, S.-J., A. Engelmann, R. Horlacher, Q. Qu, G. Vierke, C. Hebbeln, M. Thomm and W. Boos (2003) TrmB, a Sugar-specific Transcriptional Regulator of the Trehalose/Maltose ABC Transporter from the Hyperthermophilic Archaeon *Thermococcus litoralis*. *J. Biol. Chem.* **278**, 983-990.
- Lee, T. C. and P. J. Langston-Unkefer (1985) Pyruvate Decarboxylase from *Zea mays* L. : I. Purification and Partial Characterization from Mature Kernels and Anaerobically Treated Roots. *Plant Physiol.* **79**, 242-247.
- Li, D. and K. J. Stevenson (1997) Purification and sequence analysis of a novel NADP(H)-dependent type III alcohol dehydrogenase from *Thermococcus* strain AN1. *J. Bacteriol.* **179**, 4433-7.
- Lie, M. A., L. Celik, K. A. Jorgensen and B. Schiott (2005) Cofactor Activation and Substrate Binding in Pyruvate Decarboxylase. Insights into the Reaction Mechanism from Molecular Dynamics Simulations. *Biochemistry*. **44**, 14792-14806.
- Lien, T., M. Madsen, F. A. Rainey and N.-K. Birkeland (1998) *Petrotoga mobilis* sp. nov., from a North Sea oil-production well. *Int. J. Syst. Bacteriol.* **48**, 1007-1013.
- Lim, W.-M., I. J. Baig, I. J. La, J.-D. Choi, D.-E. Kim, S.-k. Kim, J.-W. Hyun, G. Kim, C.-H. Kang, Y. J. Kim and M.-Y. Yoon (2011) Cloning, characterization and evaluation of potent inhibitors of *Shigella sonnei* acetohydroxyacid synthase catalytic subunit. *Biochimica et Biophysica Acta (BBA) - Proteins & Proteomics*. **1814**, 1825-1831.
- Lin, W. and W. Whitman (2004) The importance of porE and porF in the anabolic pyruvate oxidoreductase of *Methanococcus maripaludis*. *Arch. Microbiol.* **V181**, 68-73.
- Lin, W. C., Y.-L. Yang and W. B. Whitman (2003) The anabolic pyruvate oxidoreductase from *Methanococcus maripaludis*. *Arch. Microbiol.* **V179**, 444-456.
- Littlechild, J. A., J. E. Guy and M. N. Isupov (2004) Hyperthermophilic dehydrogenase enzymes. *Biochem. Soc. Trans.* **32**, 255-258.
- Liu, M., E. A. Sergienko, F. Guo, J. Wang, K. Tittmann, G. Hubner, W. Furey and F. Jordan (2001a) Catalytic Acid-Base Groups in Yeast Pyruvate Decarboxylase. 1. Site-Directed Mutagenesis and Steady-State Kinetic Studies on the Enzyme with the D28A, H114F, H115F, and E477Q Substitutions. *Biochemistry*. **40**, 7355-7368.
- Liu, M., E. A. Sergienko, F. Guo, J. Wang, K. Tittmann, G. Hubner, W. Furey and F. Jordan (2001b) Catalytic Acid-Base Groups in Yeast Pyruvate Decarboxylase. 1. Site-Directed Mutagenesis and Steady-State Kinetic Studies on the Enzyme with the D28A, H114F, H115F, and E477Q Substitutions. *Biochemistry*. **40**, 7355-7368.
- Lowe, S. E. and J. G. Zeikus (1992) Purification and characterization of pyruvate decarboxylase from *Sarcina ventriculi*. *Journal of General Microbiology*. **138**, 803-807.
- Lurz, R., F. Mayer and G. Gottschalk (1979) Electron microscopic study on the quaternary structure of the isolated particulate alcohol-acetaldehyde dehydrogenase complex and on its identity with the polygonal bodies of *Clostridium kluyveri*. *Arch. Microbiol.* **120**, 255-262.
- Lyashenko, A. V., E. Y. Bezsudnova, V. M. Gumerov, A. A. Lashkov, A. V. Mardanov, A. M. Mikhailov, K. M. Polyakov, V. O. Popov, N. V. Ravin, K. G. Skryabin, V. K. Zabolotniy, T. N. Stekhanova and M. V. Kovalchuk (2010) Expression, purification and crystallization of a thermostable short-chain alcohol dehydrogenase from the archaeon *Thermococcus sibiricus*. *Acta Crystallographica Section F*. **66**, 655-657.

- Lynd, L. R., C. E. Wyman and T. U. Gerngross (1999) Biocommodity Engineering. *Biotechnol. Prog.* **15**, 777-793.
- Ma, K. and M. W. W. Adams (1999) An Unusual Oxygen-Sensitive, Iron- and Zinc-Containing Alcohol Dehydrogenase from the Hyperthermophilic Archaeon *Pyrococcus furiosus*. *J. Bacteriol.* **181**, 1163-1170.
- Ma, K., A. Hutchins, S.-J. S. Sung and M. W. W. Adams (1997) Pyruvate ferredoxin oxidoreductase from the hyperthermophilic archaeon, *Pyrococcus furiosus*, functions as a CoA-dependent pyruvate decarboxylase. *Proc. Natl. Acad. Sci. USA.* **94**, 9608-9613.
- Ma, K., H. Loessner, J. Heider, M. Johnson and M. Adams (1995) Effects of elemental sulfur on the metabolism of the deep-sea hyperthermophilic archaeon *Thermococcus* strain ES-1: characterization of a sulfur-regulated, non-heme iron alcohol dehydrogenase. *J. Bacteriol.* **177**, 4748-4756.
- Ma, K., F. T. Robb and M. W. Adams (1994) Purification and characterization of NADP-specific alcohol dehydrogenase and glutamate dehydrogenase from the hyperthermophilic archaeon *Thermococcus litoralis*. *Appl. Environ. Microbiol.* **60**, 562-568.
- Ma, K., R. Weiss and M. W. W. Adams (2000) Characterization of Hydrogenase II from the Hyperthermophilic Archaeon *Pyrococcus furiosus* and Assessment of Its Role in Sulfur Reduction. *J. Bacteriol.* **182**, 1864-1871.
- Mabee, W. E. and J. N. Saddler (2010) Bioethanol from lignocellulosics: Status and perspectives in Canada. *Bioresour. Technol.* **101**, 4806-4813.
- Machielsen, R., A. R. Uria, S. W. M. Kengen and J. van der Oost (2006) Production and Characterization of a Thermostable Alcohol Dehydrogenase That Belongs to the Aldo-Keto Reductase Superfamily. *Appl. Environ. Microbiol.* **72**, 233-238.
- Maeder, D. L., R. B. Weiss, D. M. Dunn, J. L. Cherry, J. M. Gonzalez, J. DiRuggiero and F. T. Robb (1999) Divergence of the Hyperthermophilic Archaea *Pyrococcus furiosus* and *P. horikoshii* Inferred From Complete Genomic Sequences. *Genetics.* **152**, 1299-1305.
- Maheshwari, R., G. Bharadwaj and M. K. Bhat (2000) Thermophilic Fungi: Their Physiology and Enzymes. *Microbiol. Mol. Biol. Rev.* **64**, 461-488.
- Mai, X. and M. W. Adams (1994) Indolepyruvate ferredoxin oxidoreductase from the hyperthermophilic archaeon *Pyrococcus furiosus*. A new enzyme involved in peptide fermentation. *J. Biol. Chem.* **269**, 16726-16732.
- Mai, X. and M. W. Adams (1996a) Characterization of a fourth type of 2-keto acid-oxidizing enzyme from a hyperthermophilic archaeon: 2-ketoglutarate ferredoxin oxidoreductase from *Thermococcus litoralis*. *J. Bacteriol.* **178**, 5890-6.
- Mai, X. and M. W. Adams (1996b) Purification and characterization of two reversible and ADP-dependent acetyl coenzyme A synthetases from the hyperthermophilic archaeon *Pyrococcus furiosus*. *J. Bacteriol.* **178**, 5897-903.
- Marteinsson, V. T., J.-L. Birrien, A.-L. Reysenbach, M. Vernet, D. Marie, A. Gambacorta, P. Messner, U. B. Sleytr and D. Prieur (1999) *Thermococcus barophilus* sp. nov., a new barophilic and hyperthermophilic archaeon isolated under high hydrostatic pressure from a deep-sea hydrothermal vent. *Int. J. Syst. Bacteriol.* **49**, 351-359.
- McCourt, J. A. and R. G. Duggleby (2006) Acetohydroxyacid synthase and its role in the biosynthetic pathway for branched-chain amino acids. *Amino Acids.* **31**, 173-210.
- Meinecke, B., J. Bertram and G. Gottschalk (1989) Purification and characterization of the pyruvate-ferredoxin oxidoreductase from *Clostridium acetobutylicum*. *Arch. Microbiol.* **152**, 244-250.

- Menon, A. L., H. Hendrix, A. Hutchins, M. F. Verhagen and M. W. Adams (1998) The delta-subunit of pyruvate ferredoxin oxidoreductase from *Pyrococcus furiosus* is a redox-active, iron-sulfur protein: evidence for an ancestral relationship with 8Fe-type ferredoxins. *Biochemistry*. **37**, 12838-46.
- Menon, S. and S. W. Ragsdale (1996) Unleashing Hydrogenase Activity in Carbon Monoxide Dehydrogenase/Acetyl-CoA Synthase and Pyruvate:Ferredoxin Oxidoreductase. *Biochemistry*. **35**, 15814-15821.
- Menon, S. and S. W. Ragsdale (1997) Mechanism of the *Clostridium thermoaceticum* Pyruvate:Ferredoxin Oxidoreductase: Evidence for the Common Catalytic Intermediacy of the Hydroxyethylthiamine Pyropyrrophosphate Radical. *Biochemistry*. **36**, 8484.
- Mesbah, N. M., D. B. Hedrick, A. D. Peacock, M. Rohde and J. Wiegel (2007) *Natranaerobius thermophilus* gen. nov., sp. nov., a halophilic, alkalithermophilic bacterium from soda lakes of the Wadi An Natrun, Egypt, and proposal of *Natranaerobiaceae* fam. nov. and *Natranaerobiales* ord. nov. *Int. J. Syst. Evol. Microbiol.* **57**, 2507-2512.
- Meyer, D., L. Walter, G. Kolter, M. Pohl, M. Müller and K. Tittmann (2010) Conversion of Pyruvate Decarboxylase into an Enantioselective Carboligase with Biosynthetic Potential. *J. Am. Chem. Soc.* **133**, 3609-3616.
- Meza-Cervantez, P., A. González-Robles, R. E. Cárdenas-Guerra, J. Ortega-López, E. Saavedra, E. Pineda and R. Arroyo (2011) Pyruvate: Ferredoxin oxidoreductase (PFO) is a surface-associated cell-binding protein in *Trichomonas vaginalis* and is involved in trichomonal adherence to host cells. *Microbiology*. **157**, 3469-3482.
- Miranda-Tello, E., M.-L. Fardeau, C. Joulain, M. Magot, P. Thomas, J.-L. Tholozan and B. Ollivier (2007) *Petrotoga halophila* sp. nov., a thermophilic, moderately halophilic, fermentative bacterium isolated from an offshore oil well in Congo. *Int. J. Syst. Evol. Microbiol.* **57**, 40-44.
- Miroshnichenko, M., H. Hippe, E. Stackebrandt, N. Kostrikina, N. Chernyh, C. Jeanthon, T. Nazina, S. Belyaev and E. Bonch-Osmolovskaya (2001) Isolation and characterization of *Thermococcus sibiricus* sp. nov. from a Western Siberia high-temperature oil reservoir. *Extremophiles*. **5**, 85-91.
- Miroshnichenko, M. L., E. A. Bonch-Osmolovskaya, A. Neuner, N. A. Kostrikina, N. A. Chernych and V. A. Alekseev (1989) *Thermococcus stetteri* sp. nov., a new extremely thermophilic marine sulfur-metabolizing archaeobacterium. *Systematic and Applied Microbiology*. **12**, 257-262
- Miroshnichenko, M. L., G. M. Gongadze, F. A. Rainey, A. S. Kostyukova, A. M. Lysenko, N. A. Chernyh and E. A. Bonch-Osmolovskaya (1998) *Thermococcus gorgonarius* sp. nov. and *Thermococcus pacificus* sp. nov.: heterotrophic extremely thermophilic archaea from New Zealand submarine hot vents. *Int. J. Syst. Bacteriol.* **48**, 23-29.
- Miyazaki, K. (2005) Hyperthermophilic α -L-arabinofuranosidase from *Thermotoga maritima* MSB8: molecular cloning, gene expression, and characterization of the recombinant protein. *Extremophiles*. **9**, 399-406.
- Mizuhara, S. and P. Handler (1954) Mechanism of Thiamine-catalyzed Reactions1. *J. Am. Chem. Soc.* **76**, 571-573.
- Moon, Y.-J., J. Kwon, S.-H. Yun, H. L. Lim, M.-S. Kim, S. G. Kang, J.-H. Lee, J.-S. Choi, S. I. Kim and Y.-H. Chung (2012) Proteome analyses of hydrogen-producing hyperthermophilic archaeon *Thermococcus onnurineus* NA1 in different one-carbon substrate culture conditions. *Molecular & Cellular Proteomics*.

- Morana, A., N. Di Prizito, V. Aurilia, M. Rossi and R. Cannio (2002) A carboxylesterase from the hyperthermophilic archaeon *Sulfolobus solfataricus*: cloning of the gene, characterization of the protein. *Gene*. **283**, 107-115.
- Morikawa, M., Y. Izawa, N. Rashid, T. Hoaki and T. Imanaka (1994) Purification and characterization of a thermostable thiol protease from a newly isolated hyperthermophilic *Pyrococcus* sp. *Appl. Environ. Microbiol.* **60**, 4559-4566.
- Morozkina, E., E. Slutskaya, T. Fedorova, T. Tugay, L. Golubeva and O. Koroleva (2010) Extremophilic microorganisms: Biochemical adaptation and biotechnological application (review). *Appl. Biochem. Microbiol.* **46**, 1-14.
- Muller, F., T. Brissac, N. Le Bris, H. Felbeck and O. Gros (2010) First description of giant Archaea (Thaumarchaeota) associated with putative bacterial ectosymbionts in a sulfidic marine habitat. *Environ. Microbiol.* **12**, 2371-2383.
- Muller, Y. A., Y. Lindqvist, W. Furey, G. E. Schulz, F. Jordan and G. Schneider (1993) A thiamin diphosphate binding fold revealed by comparison of the crystal structures of transketolase, pyruvate oxidase and pyruvate decarboxylase. *Structure*. **1**, 95-103.
- Nair, R. V., G. N. Bennett and E. T. Papoutsakis (1994) Molecular characterization of an aldehyde/alcohol dehydrogenase gene from *Clostridium acetobutylicum* ATCC 824. *J. Bacteriol.* **176**, 871-85.
- Neale, A. D., R. K. Scopes, R. E. H. Wettenhall and N. J. Hoogenraad (1987) Nucleotide sequence of the pyruvate decarboxylase gene from *Zymomonas mobilis*. *Nucleic Acids Res.* **15**, 1753-1761.
- Nelson, K. E., R. A. Clayton, S. R. Gill, M. L. Gwinn, R. J. Dodson, D. H. Haft, E. K. Hickey, J. D. Peterson, W. C. Nelson, K. A. Ketchum, L. McDonald, T. R. Utterback, J. A. Malek, K. D. Linher, M. M. Garrett, A. M. Stewart, M. D. Cotton, M. S. Pratt, C. A. Phillips, D. Richardson, J. Heidelberg, G. G. Sutton, R. D. Fleischmann, J. A. Eisen, O. White, S. L. Salzberg, H. O. Smith, J. C. Venter and C. M. Fraser (1999) Evidence for lateral gene transfer between Archaea and Bacteria from genome sequence of *Thermotoga maritima*. *Nature*. **399**, 323-329.
- Nesbø, C. L., D. M. Bradnan, A. Adebussuyi, M. Dlutek, A. K. Petrus, J. Foght, W. F. Doolittle and K. M. Noll (2012) *Mesotoga prima* gen. nov., sp. nov., the first described mesophilic species of the Thermotogales. *Extremophiles*, 1-7.
- Nesbø, C. L., M. Dlutek, O. Zhaxybayeva and W. F. Doolittle (2006) Evidence for Existence of "Mesotogas," Members of the Order Thermotogales Adapted to Low-Temperature Environments. *Appl. Environ. Microbiol.* **72**, 5061-5068.
- Neuer, G. and H. Bothe (1982) The pyruvate: Ferredoxin oxidoreductase in heterocysts of the cyanobacterium *Anabaena cylindrica*. *Biochimica et Biophysica Acta (BBA) - General Subjects*. **716**, 358-365.
- Neuner, A., H. W. Jannasch, S. Belkin and K. O. Stetter (1990) *Thermococcus litoralis* sp. nov.: A new species of extremely thermophilic marine archaeobacteria. *Arch. Microbiol.* **153**, 205-207.
- Neuser, F., H. Zorn and R. G. Berger (2000) Generation of odorous acylolins by yeast pyruvate decarboxylases and their occurrence in sherry and soy sauce. *J. Agric. Food Chem.* **48**, 6191-6195.
- Nichols, B. P. and C. Yanofsky (1979) Nucleotide sequences of *trpA* of *Salmonella typhimurium* and *Escherichia coli*: an evolutionary comparison. *Proceedings of the National Academy of Sciences*. **76**, 5244-5248.

- Niu, X., X. Liu, Y. Zhou, C. Niu, Z. Xi and X.-D. Su (2011) Preliminary X-ray crystallographic studies of the catalytic subunit of *Escherichia coli* AHAS II with its cofactors. *Acta Crystallographica Section F*. **67**, 659-661.
- Nunoura, T., M. Hirai, H. Imachi, M. Miyazaki, H. Makita, H. Hirayama, Y. Furushima, H. Yamamoto and K. Takai (2010) *Kosmotoga arenicorallina* sp. nov. a thermophilic and obligately anaerobic heterotroph isolated from a shallow hydrothermal system occurring within a coral reef, southern part of the Yaeyama Archipelago, Japan, reclassification of *Thermococcoides shengliensis* as *Kosmotoga shengliensis* comb. nov., and emended description of the genus *Kosmotoga*. *Arch. Microbiol.* **192**, 811-819.
- Nunoura, T., H. Oida, M. Miyazaki, Y. Suzuki, K. Takai and K. Horikoshi (2007) *Marinitoga okinawensis* sp. nov., a novel thermophilic and anaerobic heterotroph isolated from a deep-sea hydrothermal field, Southern Okinawa Trough. *Int. J. Syst. Evol. Microbiol.* **57**, 467-471.
- Oelgeschläger, E. and M. Rother (2008) Carbon monoxide-dependent energy metabolism in anaerobic bacteria and archaea. *Arch. Microbiol.* **190**, 257-269.
- Oger, P., T. G. Sokolova, D. A. Kozhevnikova, N. A. Chernyh, D. H. Bartlett, E. A. Bonch-Osmolovskaya and A. V. Lebedinsky (2011) Complete Genome Sequence of the Hyperthermophilic Archaeon *Thermococcus* sp. Strain AM4, Capable of Organotrophic Growth and Growth at the Expense of Hydrogenogenic or Sulfidogenic Oxidation of Carbon Monoxide. *J. Bacteriol.* **193**, 7019-7020.
- Ozawa, Y., T. Nakamura, N. Kamata, D. Yasujima, A. Urushiyama, F. Yamakura, D. Ohmori and T. Imai (2005) *Thermococcus profundus* 2-Ketoisovalerate Ferredoxin Oxidoreductase, a Key Enzyme in the Archaeal Energy-Producing Amino Acid Metabolic Pathway. *J. Biochem., Tokyo.* **137**, 101-107.
- Pace, N. R. (2009) Mapping the Tree of Life: Progress and Prospects. *Microbiol. Mol. Biol. Rev.* **73**, 565-576.
- Pang, S. S. and R. G. Duggleby (1999) Expression, Purification, Characterization, and Reconstitution of the Large and Small Subunits of Yeast Acetohydroxyacid Synthase. *Biochemistry.* **38**, 5222-5231.
- Pang, S. S., R. G. Duggleby, R. L. Schowen and L. W. Guddat (2004) The Crystal Structures of *Klebsiella pneumoniae* Acetolactate Synthase with Enzyme-bound Cofactor and with an Unusual Intermediate. *J. Biol. Chem.* **279**, 2242-2253.
- Patel, B. K. C., H. W. Morgan and R. M. Daniel (1985) *Fervidobacterium nodosum* gen. nov. and spec. nov., a new chemoorganotrophic, caldoactive, anaerobic bacterium. *Arch. Microbiol.* **141**, 63-69.
- Pei, J., Q. Zhou, Y. Jiang, Y. Le, H. Li, W. Shao and J. Wiegel (2010) *Thermoanaerobacter* spp. control ethanol pathway via transcriptional regulation and versatility of key enzymes. *Metab. Eng.* **12**, 420-428.
- Peng, H.-L., P.-Y. Wang, C.-M. Wu, D.-C. Hwang and H.-Y. Chang (1992) Cloning, sequencing and heterologous expression of a *Klebsiella pneumoniae* gene encoding an FAD-independent acetolactate synthase. *Gene.* **117**, 125-130.
- Peng, H., G. Wu and W. Shao (2008) The aldehyde/alcohol dehydrogenase (AdhE) in relation to the ethanol formation in *Thermoanaerobacter ethanolicus* JW200. *Anaerobe.* **14**, 125-127.
- Pennacchio, A., A. Giordano, B. Pucci, M. Rossi and C. Raia (2010) Biochemical characterization of a recombinant short-chain NAD(H)-dependent dehydrogenase/reductase from *Sulfolobus acidocaldarius*. *Extremophiles.* **14**, 193-204.

- Peralta-Yahya, P. P. and J. D. Keasling (2010) Advanced biofuel production in microbes. *Biotechnology Journal*. **5**, 147-162.
- Petkowski, J. J., M. Chruszcz, M. D. Zimmerman, H. Zheng, T. Skarina, O. Onopriyenko, M. T. Cymborowski, K. D. Koclega, A. Savchenko, A. Edwards and W. Minor (2007) Crystal structures of TM0549 and NE1324—two orthologs of *E. coli* AHAS isozyme III small regulatory subunit. *Protein Sci.* **16**, 1360-1367.
- Piatigorsky, J., W. E. O'Brien, B. L. Norman, K. Kalumuck, G. J. Wistow, T. Borrás, J. M. Nickerson and E. F. Wawrousek (1988) Gene sharing by δ -crystallin and argininosuccinate lyase. *Proceedings of the National Academy of Sciences of the United States of America*. **85**, 3479-3483.
- Pieulle, L., E. Chabriere, C. Hatchikian, J. C. Fontecilla-Camps and M.-H. Charon (1999a) Crystallization and preliminary crystallographic analysis of the pyruvate-ferredoxin oxidoreductase from *Desulfovibrio africanus*. *Acta Crystallographica Section D*. **55**, 329-331.
- Pieulle, L., M.-H. Charon, P. Bianco, J. Bonicel, Y. Petillot and E. C. Hatchikian (1999b) Structural and kinetic studies of the pyruvate-ferredoxin oxidoreductase/ferredoxin complex from *Desulfovibrio africanus*. *Eur. J. Biochem.* **264**, 500-508.
- Pieulle, L., B. Guigliarelli, M. Asso, F. Dole, A. Bernadac and E. C. Hatchikian (1995) Isolation and characterization of the pyruvate-ferredoxin oxidoreductase from the sulfate-reducing bacterium *Desulfovibrio africanus*. *Biochimica et Biophysica Acta (BBA) - Protein Structure and Molecular Enzymology*. **1250**, 49-59.
- Pieulle, L., V. Magro and E. Hatchikian (1997) Isolation and analysis of the gene encoding the pyruvate-ferredoxin oxidoreductase of *Desulfovibrio africanus*, production of the recombinant enzyme in *Escherichia coli*, and effect of carboxy-terminal deletions on its stability. *J. Bacteriol.* **179**, 5684-5692.
- Pieulle, L., P. Stocker, M. Vinay, M. Nouailler, N. Vita, G. I. Brasseur, E. Garcin, C. Sebban-Kreuzer and A. Dolla (2011) Study of the Thiol/Disulfide Redox Systems of the Anaerobe *Desulfovibrio vulgaris* Points Out Pyruvate:ferredoxin Oxidoreductase as a New Target for Thioredoxin 1. *J. Biol. Chem.* **286**, 7812-7821.
- Pikuta, E. V., D. Marsic, T. Itoh, A. K. Bej, J. Tang, W. B. Whitman, J. D. Ng, O. K. Garriott and R. B. Hoover (2007) *Thermococcus thioeducens* sp. nov., a novel hyperthermophilic, obligately sulfur-reducing archaeon from a deep-sea hydrothermal vent. *Int. J. Syst. Evol. Microbiol.* **57**, 1612-1618.
- Pineda, E., R. Encalada, J. S. Rodríguez-Zavala, A. Olivos-García, R. Moreno-Sánchez and E. Saavedra (2010) Pyruvate:ferredoxin oxidoreductase and bifunctional aldehyde-alcohol dehydrogenase are essential for energy metabolism under oxidative stress in *Entamoeba histolytica*. *FEBS J.* **277**, 3382-3395.
- Plaga, W., F. Lottspeich and D. Oesterhelt (1992) Improved purification, crystallization and primary structure of pyruvate:ferredoxin oxidoreductase from *Halobacterium halobium*. *Eur. J. Biochem.* **205**, 391-397.
- Podosokorskaya, O. A., I. V. Kublanov, A. L. Reysenbach, T. V. Kolganova and E. A. Bonch-Osmolovskaya (2010) *Thermosipho affectus* sp. nov., a thermophilic, anaerobic, cellulolytic bacterium isolated from a Mid-Atlantic Ridge hydrothermal vent. *Int. J. Syst. Evol. Microbiol.* **61**, 1160-1164.
- Podosokorskaya, O. A., I. V. Kublanov, A. L. Reysenbach, T. V. Kolganova and E. A. Bonch-Osmolovskaya (2011) *Thermosipho affectus* sp. nov., a thermophilic, anaerobic, cellulolytic

- bacterium isolated from a Mid-Atlantic Ridge hydrothermal vent. *Int. J. Syst. Evol. Microbiol.* **61**, 1160-1164.
- Pohl, M. (1997) Protein design on pyruvate decarboxylase (PDC) by site-directed mutagenesis. *Advances in biochemical engineering/biotechnology.* **58**, 15-43.
- Pohl, M., B. Lingen and M. Müller (2002) Thiamin-Diphosphate-Dependent Enzymes: New Aspects of Asymmetric C-bond;C Bond Formation. *Chemistry - A European Journal.* **8**, 5288-5295.
- Pohl, M., P. Siegert K. Mesch H. Bruhn J. Grötzinger (1998) Active site mutants of pyruvate decarboxylase from *Zymomonas mobilis*. *Eur. J. Biochem.* **257**, 538-546.
- Pomel, S., F. C. Y. Luk and C. J. M. Beckers (2008) Host Cell Egress and Invasion Induce Marked Relocations of Glycolytic Enzymes in *Toxoplasma gondii* Tachyzoites. *PLoS Pathog.* **4**, e1000188.
- Porat, I., M. Vinogradov, M. Vyazmensky, C.-D. Lu, D. M. Chipman, A. T. Abdelal and Z. e. Barak (2004) Cloning and Characterization of Acetohydroxyacid Synthase from *Bacillus stearothermophilus*. *J. Bacteriol.* **186**, 570-574.
- Postec, A., C. L. Breton, M.-L. Fardeau, F. Lesongeur, P. Pignet, J. Querellou, B. Ollivier and A. Godfroy (2005) *Marinitoga hydrogenitolerans* sp. nov., a novel member of the order Thermotogales isolated from a black smoker chimney on the Mid-Atlantic Ridge. *Int. J. Syst. Evol. Microbiol.* **55**, 1217-1221.
- Postec, A., M. Ciobanu, J.-L. Birrien, N. g. Bienvenu, D. Prieur and M. Le Romancer (2010) *Marinitoga litoralis* sp. nov., a thermophilic, heterotrophic bacterium isolated from a coastal thermal spring on Ile Saint-Paul, Southern Indian Ocean. *Int. J. Syst. Evol. Microbiol.* **60**, 1778-1782.
- Postec, A., P. Pignet, V. Cueff-Gauchard, A. Schmitt, J. Querellou and A. Godfroy (2004) Optimisation of growth conditions for continuous culture of the hyperthermophilic archaeon *Thermococcus hydrothermalis* and development of sulphur-free defined and minimal media. *Res. Microbiol.* **156**, 82-87.
- Rabinowitz, J. C. (1975) Pyruvate-ferredoxin oxidoreductase from *Clostridium acidi-urici*. *Methods Enzymol.* **41**, 334-337.
- Radhakrishanan, A. N. and E. E. Snell (1960) Biosynthesis of valine and isoleucine. II. Formation of α -acetolactate and α -aceto-alpha-hydroxybutyrate in *Neurospora crassa* and *Escherichia coli*. *The Journal of biological chemistry.* **235**, 2316-21.
- Radianingtyas, H. and P. C. Wright (2003) Alcohol dehydrogenases from thermophilic and hyperthermophilic archaea and bacteria. *FEMS Microbiol. Rev.* **27**, 593-616.
- Raeburn, S. and J. C. Rabinowitz (1971) Pyruvate: ferredoxin oxidoreductase. I. The pyruvate-CO₂ exchange reaction. *Arch Biochem Biophys.* **146**, 9-20.
- Ragsdale, S. W. (2003) Pyruvate Ferredoxin Oxidoreductase and Its Radical Intermediate. *Chemical reviews.* **103**, 2333-2346.
- Ragsdale, S. W. and E. Pierce (2008) Acetogenesis and the Wood-Ljungdahl pathway of CO₂ fixation. *Biochimica et Biophysica Acta (BBA) - Proteins & Proteomics.* **1784**, 1873-1898.
- Raj, K. C., L. O. Ingram and J. A. Maupin-Furlow (2001) Pyruvate decarboxylase: a key enzyme for the oxidative metabolism of lactic acid by *Acetobacter pasteurianus*. *Arch. Microbiol.* **V176**, 443-451.
- Raj, K. C., L. A. Talarico, L. O. Ingram and J. A. Maupin-Furlow (2002) Cloning and Characterization of the *Zymobacter palmae* Pyruvate Decarboxylase Gene (*pdc*) and Comparison to Bacterial Homologues. *Appl. Environ. Microbiol.* **68**, 2869-2876.

- Ramos, A., K. N. Jordan, T. M. Cogan and H. Santos (1994) ^{13}C Nuclear Magnetic Resonance Studies of Citrate and Glucose Cometabolism by *Lactococcus lactis*. *Appl. Environ. Microbiol.* **60**, 1739-1748.
- Raven, N., D. H. and R. Sharp, J. (1997) Development of defined and minimal media for the growth of the hyperthermophilic archaeon *Pyrococcus furiosus* Vc1. *FEMS Microbiol. Lett.* **146**, 135-141.
- Ravot, G., M. Magot, M. L. Fardeau, B. K. C. Patel, G. Prensier, A. Egan, J. L. Garcia and B. Ollivier (1995) *Thermotoga elfii* sp. nov., a Novel Thermophilic Bacterium from an African Oil-Producing Well. *Int. J. Syst. Bacteriol.* **45**, 308-314.
- Ravot, G., B. Ollivier, B. K. C. Patel, M. Magot and J.-L. Garcia (1996) Emended Description of *Thermosipho africanus* as a Carbohydrate-Fermenting Species Using Thiosulfate as an Electron Acceptor. *Int. J. Syst. Bacteriol.* **46**, 321-323.
- Reed, G. H., S. W. Ragsdale and S. O. Mansoorabadi (2011) Radical reactions of thiamin pyrophosphate in 2-oxoacid oxidoreductases. *Biochimica et Biophysica Acta (BBA) - Proteins & Proteomics*.
- Reid, M. F. and C. A. Fewson (1994) Molecular Characterization of Microbial Alcohol Dehydrogenases. *Crit. Rev. Microbiol.* **20**, 13-56.
- Renna, M. C., N. Najimudin, L. R. Winik and S. A. Zahler (1993) Regulation of the *Bacillus subtilis* *alsS*, *alsD*, and *alsR* genes involved in post-exponential-phase production of acetoin. *J. Bacteriol.* **175**, 3863-3875.
- Rinker, K. D. and R. M. Kelly (2000) Effect of carbon and nitrogen sources on growth dynamics and exopolysaccharide production for the hyperthermophilic archaeon *Thermococcus litoralis* and bacterium *Thermotoga maritima*. *Biotechnol. Bioeng.* **69**, 537-547.
- Robertson, C. E., J. K. Harris, J. R. Spear and N. R. Pace (2005) Phylogenetic diversity and ecology of environmental Archaea. *Curr. Opin. Microbiol.* **8**, 638-642.
- Ronimus, R. S., A. L. Reysenbach, D. R. Musgrave and H. W. Morgan (1997) The phylogenetic position of the *Thermococcus* isolate AN1 based on 16S rRNA gene sequence analysis: a proposal that AN1 represents a new species, *Thermococcus zilligii* sp. nov. *Arch. Microbiol.* **168**, 245-248.
- Rosche, B., M. Breuer, B. Hauer and P. L. Rogers (2003) Screening of yeasts for cell-free production of *R*-phenylacetylcarbinol. *Biotechnol. Lett.* **25**, 841-845.
- Rudolph, F. B., D. L. Purich and H. J. Fromm (1968) Coenzyme A-linked Aldehyde Dehydrogenase from *Escherichia coli*. *J. Biol. Chem.* **243**, 5539-5545.
- Sakuraba, H. G., S., Ohshima, T. (2004) Unique sugar metabolism and novel enzymes of hyperthermophilic archaea. *The Chemical Record.* **3**, 281-287.
- Sambrook, J. and D. W. Russell (2001) *Molecular cloning: a laboratory manual*, 3rd ed., Cold Spring Harbor Laboratory Press, Cold Spring
- Sánchez, L. B. (1998) Aldehyde Dehydrogenase (CoA-Acetylating) and the Mechanism of Ethanol Formation in the Amitochondriate Protist, *Giardia lamblia*. *Archives of Biochemistry and Biophysics.* **354**, 57-64.
- Schäfer, T., M. Selig and P. Schönheit (1993) Acetyl-CoA synthetase (ADP forming) in archaea, a novel enzyme involved in acetate formation and ATP synthesis. *Arch. Microbiol.* **159**, 72-83.
- Schellenberger, A. (1998) Sixty years of thiamin diphosphate biochemistry. *Biochimica et Biophysica Acta (BBA) - Protein Structure and Molecular Enzymology.* **1385**, 177-186.
- Schiraldi, C. and M. De Rosa (2002) The production of biocatalysts and biomolecules from extremophiles. *Trends Biotechnol.* **20**, 515-521.

- Schloss, J. V., D. E. Van Dyk and J. R. S. Robert A. Harris (1988) Acetolactate synthase isozyme II from *Salmonella typhimurium*. *Methods in Enzymology*, pp 445-454, Academic Press
- Schloss, J. V., D. E. Van Dyk, J. F. Vasta and R. M. Kutny (1985) Purification and properties of *Salmonella typhimurium* acetolactate synthase isozyme II from *Escherichia coli* HB101/pDU9. *Biochemistry*. **24**, 4952-4959.
- Schoner, B. E., H. M. Hsiung, R. M. Belagaje, N. G. Mayne and R. G. Schoner (1984) Role of mRNA translational efficiency in bovine growth hormone expression in *Escherichia coli*. *Proceedings of the National Academy of Sciences*. **81**, 5403-5407.
- Schönheit, P. and T. Schafer (1995) Metabolism of hyperthermophiles. *World Journal of Microbiology and Biotechnology*. **V11**, 26-57.
- Schröder, C., M. Selig and P. Schönheit (1994) Glucose fermentation to acetate, CO₂ and H₂ in the anaerobic hyperthermophilic eubacterium *Thermotoga maritima*: involvement of the Embden-Meyerhof pathway. *Arch. Microbiol.* **161**, 460-470.
- Schut, G. J. and M. W. W. Adams (2009) The Iron-Hydrogenase of *Thermotoga maritima* Utilizes Ferredoxin and NADH Synergistically: a New Perspective on Anaerobic Hydrogen Production. *J. Bacteriol.* **191**, 4451-4457.
- Schut, G. J., S. D. Brehm, S. Datta and M. W. W. Adams (2003) Whole-Genome DNA Microarray Analysis of a Hyperthermophile and an Archaeon: *Pyrococcus furiosus* Grown on Carbohydrates or Peptides. *J. Bacteriol.* **185**, 3935-3947.
- Schut, G. J., A. L. Menon and M. W. W. Adams (2001a) 2-Keto Acid Oxidoreductases from *Pyrococcus furiosus* and *Thermococcus litoralis*. *Methods in Enzymology*. Adams, M. W. W. (ed.), pp 144-157, Academic press New York
- Schut, G. J., J. Zhou and M. W. W. Adams (2001b) DNA Microarray Analysis of the Hyperthermophilic Archaeon *Pyrococcus furiosus*: Evidence for a New Type of Sulfur-Reducing Enzyme Complex. *J. Bacteriol.* **183**, 7027-7036.
- Selig, M., K. B. Xavier and H. Santos (1997) Comparative analysis of Embden-Meyerhof and Entner-Doudoroff glycolytic pathways in hyperthermophilic archaea and the bacterium *Thermotoga*. *Arch. Microbiol.* **167**, 217-232.
- Sella, C., O. Weinstock, Z. Barak and D. M. Chipman (1993) Subunit association in acetohydroxy acid synthase isozyme III. *J. Bacteriol.* **175**, 5339-5343.
- Shah, V. K., G. Stacey and W. J. Brill (1983) Electron transport to nitrogenase. Purification and characterization of pyruvate:flavodoxin oxidoreductase. The *nifJ* gene product. *J. Biol. Chem.* **258**, 12064-12068.
- Shaw, A. J., K. K. Podkaminer, S. G. Desai, J. S. Bardsley, S. R. Rogers, P. G. Thorne, D. A. Hogsett and L. R. Lynd (2008) Metabolic engineering of a thermophilic bacterium to produce ethanol at high yield. *Proceedings of the National Academy of Sciences*. **105**, 13769-13774.
- Shiba, H., T. Kawasumi, Y. Igarashi, T. Kodama and Y. Minoda (1985) The CO₂ assimilation via the reductive tricarboxylic acid cycle in an obligately autotrophic, aerobic hydrogen-oxidizing bacterium, *Hydrogenobacter thermophilus*. *Arch. Microbiol.* **141**, 198-203.
- Siebers, B. and P. Schönheit (2005) Unusual pathways and enzymes of central carbohydrate metabolism in Archaea. *Curr. Opin. Microbiol.* **8**, 695-705.
- Siegert, P., M. J. McLeish, M. Baumann, H. Iding, M. M. Kneen, G. L. Kenyon and M. Pohl (2005) Exchanging the substrate specificities of pyruvate decarboxylase from *Zymomonas mobilis* and benzoylformate decarboxylase from *Pseudomonas putida*. *Protein Engineering, Design and Selection*. **18**, 345-357.

- Singh, B., G. Schmitt, M. Lillis, J. M. Hand and R. Misra (1991) Overexpression of Acetohydroxyacid Synthase from Arabidopsis as an Inducible Fusion Protein in *Escherichia coli*: Production of Polyclonal Antibodies, and Immunological Characterization of the Enzyme. *Plant Physiol. Biochem.* **97**, 657-662.
- Singh, B. K., M. A. Stidham and D. L. Shaner (1988) Assay of acetohydroxyacid synthase. *Anal. Biochem.* **171**, 173-179.
- Singh, V., D. Chandra, B. S. Srivastava and R. Srivastava (2011) Biochemical and transcription analysis of acetohydroxyacid synthase isoforms in *Mycobacterium tuberculosis* identifies these enzymes as potential targets for drug development. *Microbiology.* **157**, 29-37.
- Smith, E. T., J. M. Blamey and M. W. Adams (1994) Pyruvate ferredoxin oxidoreductases of the hyperthermophilic archaeon, *Pyrococcus furiosus*, and the hyperthermophilic bacterium, *Thermotoga maritima*, have different catalytic mechanisms. *Biochemistry.* **33**, 1008-16.
- Snoep, J. L., M. J. Teixeira de Mattos, M. J. Starrenburg and J. Hugenholtz (1992) Isolation, characterization, and physiological role of the pyruvate dehydrogenase complex and alpha-acetolactate synthase of *Lactococcus lactis* subsp. *lactis* bv. diacetylactis. *J. Bacteriol.* **174**, 4838-4841.
- Sokolova, T. G., C. Jeanthon, N. A. Kostrikina, N. A. Chernyh, A. V. Lebedinsky, E. Stackebrandt and E. A. Bonch-Osmolovskaya (2004) The first evidence of anaerobic CO oxidation coupled with H₂ production by a hyperthermophilic archaeon isolated from a deep-sea hydrothermal vent. *Extremophiles.* **8**, 317-323.
- Sommer, P., T. Georgieva and B. K. Ahring (2004) Potential for using thermophilic anaerobic bacteria for bioethanol production from hemicellulose. *Biochem. Soc. Trans.* **32**, 283-9.
- Speckman, R. A. and E. B. Collins (1982) Specificity of the Westerfeld adaptation of the Voges-Proskauer test. *Appl. Environ. Microbiol.* **44**, 40-43.
- Sprenger, G. A. and M. Pohl (1999) Synthetic potential of thiamin diphosphate-dependent enzymes. *Journal of Molecular Catalysis B: Enzymatic.* **6**, 145-159.
- Stekhanova, T. N., A. V. Mardanov, E. Y. Bezudnova, V. M. Gumerov, N. V. Ravin, K. G. Skryabin and V. O. Popov (2010) Characterization of a Thermostable Short-Chain Alcohol Dehydrogenase from the Hyperthermophilic Archaeon *Thermococcus sibiricus*. *Appl. Environ. Microbiol.* **76**, 4096-4098.
- Stern, K. G. and J. L. Melnick (1939) On the Mechanism of Cocarboxylase Action. *J. Biol. Chem.* **131**, 597-613.
- Stern, K. G. and J. L. Melnick (1940) On the mechanism of Cocarboxylase Action. *J. Biol. Chem.* **J. Biol. Chem.** **1940**, **135**, **365**, 365-369.
- Stetter, K. (2006) History of discovery of the first hyperthermophiles. *Extremophiles.* **10**, 357-362.
- Stetter, K. O. (1996) Hyperthermophilic prokaryotes. *FEMS Microbiol. Rev.* **18**, 149-158.
- Stetter, K. O., G. Fiala, G. Huber, R. Huber and A. Segerer (1990) Hyperthermophilic microorganisms. *FEMS Microbiol. Lett.* **75**, 117-124.
- Störmer, F. C. (1968a) Evidence for induction of the 2,3-butanediol-forming enzymes in *Aerobacter aerogenes*. *FEBS Lett.* **2**, 36-38.
- Störmer, F. C. (1968b) The pH 6 Acetolactate-forming Enzyme from *Aerobacter aerogenes*. I. Kinetic studies. *J. Biol. Chem.* **243**, 3735-3739.
- Störmer, F. C. (1968c) The pH 6 Acetolactate-forming Enzyme from *Aerobacter aerogenes*. II. Evidence that it is Not a Flavoprotein. *J. Biol. Chem.* **243**, 3740-3741.

- Strand, K., C. Sun, T. Li, F. Jenney, G. Schut and M. Adams (2010) Oxidative stress protection and the repair response to hydrogen peroxide in the hyperthermophilic archaeon *Pyrococcus furiosus* and in related species. *Arch. Microbiol.* **192**, 447-459.
- Swanson, R. V., M. G. Sanna and M. I. Simon (1996) Thermostable chemotaxis proteins from the hyperthermophilic bacterium *Thermotoga maritima*. *J. Bacteriol.* **178**, 484-489.
- Takahata, Y., M. Nishijima, T. Hoaki and T. Maruyama (2001) *Thermotoga petrophila* sp. nov. and *Thermotoga naphthophila* sp. nov., two hyperthermophilic bacteria from the Kubiki oil reservoir in Niigata, Japan. *Int. J. Syst. Evol. Microbiol.* **51**, 1901-1909.
- Takai, K. and K. Horikoshi (2000) *Thermosipho japonicus* sp. nov., an extremely thermophilic bacterium isolated from a deep-sea hydrothermal vent in Japan. *Extremophiles.* **4**, 9-17.
- Takai, K., A. Sugai, T. Itoh and K. Horikoshi (2000) *Palaeococcus ferrophilus* gen. nov., sp. nov., a barophilic, hyperthermophilic archaeon from a deep-sea hydrothermal vent chimney. *Int. J. Syst. Evol. Microbiol.* **50 Pt 2** 489-500.
- Talarico, L. A., L. O. Ingram and J. A. Maupin-Furlow (2001) Production of the Gram-positive *Sarcina ventriculi* pyruvate decarboxylase in *Escherichia coli*. *Microbiology.* **147**, 2425-2435.
- Taylor, M. P., K. L. Eley, S. Martin, M. I. Tuffin, S. G. Burton and D. A. Cowan (2009) Thermophilic ethanologenes: future prospects for second-generation bioethanol production. *Trends Biotechnol.* **27**, 398-405.
- Tersteegen, A., L. R. K. Dietmar and R. H. Thauer (1997) Structures and Functions of Four Anabolic 2-Oxoacid Oxidoreductases in *Methanobacterium Thermoautotrophicum*. *Eur. J. Biochem.* **244**, 862-868.
- Thammapalerd, N., D. Kotimanusvanij, M. Duchêne, J. A. Upcroft, R. Mitchell, A. Healey, N. Samarawickrema, S. Tharavani, G. Wiedermann and P. Upcroft (1996) Pyruvate: ferredoxin oxidoreductase from *Entamoeba histolytica* recognized by a monoclonal antibody. *Southeast Asian J. Trop. Med. Public Health.* **27**, 63-70.
- Thompson, A., D. Studholme, E. Green and D. Leak (2008) Heterologous expression of pyruvate decarboxylase in *Geobacillus thermoglucosidasius*. *Biotechnol. Lett.* **30**, 1359-1365.
- Thompson, J. D., D. G. Higgins and T. J. Gibson (1994) CLUSTAL W: improving the sensitivity of progressive multiple sequence alignment through sequence weighting, position-specific gap penalties and weight matrix choice. *Nucleic Acids Res.* **22**, 4673-4680.
- Tittmann, K. (2009) Reaction mechanisms of thiamin diphosphate enzymes: redox reactions. *FEBS J.* **276**, 2454-2468.
- Tittmann, K., R. Golbik, K. Uhlemann, L. Khailova, G. Schneider, M. Patel, F. Jordan, D. M. Chipman, R. G. Duggleby and G. Hubner (2003) NMR Analysis of Covalent Intermediates in Thiamin Diphosphate Enzymes *Biochemistry.* **42**, 7885-7891.
- Tittmann, K., K. Schröder, R. Golbik, J. McCourt, A. Kaplun, R. G. Duggleby, Z. Barak, D. M. Chipman and G. Hübner (2004) Electron transfer in acetohydroxy acid synthase as a side reaction of catalysis. Implications for the reactivity and partitioning of the carbanion/enamine form of (alpha-hydroxyethyl)thiamin diphosphate in a "nonredox" flavoenzyme. *Biochemistry.* **43**, 8652-8661.
- Tomschy, A., R. Glockshuber and R. Jaenicke (1993) Functional expression of d-glyceraldehyde-3-phosphate dehydrogenase from the hyperthermophilic eubacterium *Thermotoga maritima* in *Escherichia coli*. *Eur. J. Biochem.* **214**, 43-50.
- Toth, J., A. A. Ismaiel and J.-S. Chen (1999) The *ald* Gene, Encoding a Coenzyme A-Acylating Aldehyde Dehydrogenase, Distinguishes *Clostridium beijerinckii* and Two Other Solvent-

- Producing Clostridia from *Clostridium acetobutylicum*. *Appl. Environ. Microbiol.* **65**, 4973-4980.
- Townson, S. M., J. A. Upcroft and P. Upcroft (1996) Characterisation and purification of pyruvate:ferredoxin oxidoreductase from *Giardia duodenalis*. *Mol. Biochem. Parasitol.* **79**, 183-193.
- Tsau, J.-L., A. A. Guffanti and T. J. Montville (1992) Conversion of Pyruvate to Acetoin Helps To Maintain pH Homeostasis in *Lactobacillus plantarum*. *Appl. Environ. Microbiol.* **58**, 891-894.
- Tse, J. M. T. and J. V. Schloss (1993) The oxygenase reaction of acetolactate synthase. *Biochemistry.* **32**, 10398-10403.
- Tuininga, J. E., C. H. Verhees, J. van der Oost, S. W. M. Kengen, A. J. M. Stams and W. M. de Vos (1999) Molecular and Biochemical Characterization of the ADP-dependent Phosphofruktokinase from the Hyperthermophilic Archaeon *Pyrococcus furiosus*. *J. Biol. Chem.* **274**, 21023-21028.
- Tung, H. C., N. E. Bramall and P. B. Price (2005) Microbial origin of excess methane in glacial ice and implications for life on Mars. *Proc. Natl. Acad. Sci. USA.* **102**, 18292-18296.
- Umbarger, H. E. and B. Brown (1958) Isoleucine and Valine Metabolism in *Escherichia coli*. *J. Biol. Chem.* **233**, 1156-1160.
- Upcroft, J. A. and P. Upcroft (1999) Keto-Acid Oxidoreductases in the Anaerobic Protozoa. *Journal of Eukaryotic Microbiology.* **46**, 447-449.
- Urios, L., V. Cuffe-Gauchard, P. Pignet, A. Postec, M.-L. Fardeau, B. Ollivier and G. Barbier (2004) *Thermosipho atlanticus* sp. nov., a novel member of the Thermotogales isolated from a Mid-Atlantic Ridge hydrothermal vent. *Int. J. Syst. Evol. Microbiol.* **54**, 1953-1957.
- Uyeda, K. and J. C. Rabinowitz (1971a) Pyruvate-ferredoxin oxidoreductase. III. Purification and properties of the enzyme. *J. Biol. Chem.* **246**, 3111-9.
- Uyeda, K. and J. C. Rabinowitz (1971b) Pyruvate-ferredoxin oxidoreductase. IV. Studies on the reaction mechanism. *J. Biol. Chem.* **246**, 3120-5.
- van den Burg, B. (2003) Extremophiles as a source for novel enzymes. *Curr. Opin. Microbiol.* **6**, 213-218.
- van der Oost, J., W. G. B. Voorhorst, S. W. M. Kengen, A. C. M. Geerling, V. Wittenhorst, Y. Gueguen and W. M. de Vos (2001) Genetic and biochemical characterization of a short-chain alcohol dehydrogenase from the hyperthermophilic archaeon *Pyrococcus furiosus*. *Eur. J. Biochem.* **268**, 3062-3068.
- van Niel, E. W. J., P. A. M. Claassen and A. J. M. Stams (2003) Substrate and product inhibition of hydrogen production by the extreme thermophile, *Caldicellulosiruptor saccharolyticus*. *Biotechnol. Bioeng.* **81**, 255-262.
- Verhagen, M. F. J. M., A. L. Menon, G. J. Schut and M. W. W. Adams (2001) *Pyrococcus furiosus*: Large-scale cultivation and enzyme purification. *Methods Enzymol.* **330**, 25-30.
- Verhees, C. H., S. W. M. Kengen, J. E. Tuininga, G. J. Schut, M. W. W. Adams, W. M. De Vos and J. Van Der Oost (2003) The unique features of glycolytic pathways in Archaea. *The Biochemical journal* **375**, 231-246.
- Vieille, C., J. M. Hess, R. M. Kelly and J. G. Zeikus (1995) *xylA* cloning and sequencing and biochemical characterization of xylose isomerase from *Thermotoga neapolitana*. *Appl. Environ. Microbiol.* **61**, 1867-1875.
- Vieille, C. and G. J. Zeikus (2001) Hyperthermophilic Enzymes: Sources, Uses, and Molecular Mechanisms for Thermostability. *Microbiol. Mol. Biol. Rev.* **65**, 1-43.

- Vinogradov, V., M. Vyazmensky, S. Engel, I. Belenky, A. Kaplun, O. Kryukov, Z. e. Barak and D. M. Chipman (2006) Acetohydroxyacid synthase isozyme I from *Escherichia coli* has unique catalytic and regulatory properties. *Biochimica et Biophysica Acta (BBA) - General Subjects*. **1760**, 356-363.
- Vita, N., E. C. Hatchikian, M. Nouailler, A. Dolla and L. Pieulle (2008) Disulfide Bond-Dependent Mechanism of Protection against Oxidative Stress in Pyruvate-Ferredoxin Oxidoreductase of Anaerobic *Desulfovibrio* Bacteria. *Biochemistry*. **47**, 957-964.
- Vyazmensky, M., Z. Barak, D. M. Chipman and J. Eichler (2000) Characterization of acetohydroxy acid synthase activity in the archaeon *Haloferax volcanii*. *Comparative Biochemistry and Physiology -- Part B: Biochemistry and Molecular Biology*. **125**, 205-210.
- Vyazmensky, M., C. Sella, Z. e. Barak and D. M. Chipman (1996) Isolation and Characterization of Subunits of Acetohydroxy Acid Synthase Isozyme III and Reconstitution of the Holoenzyme *Biochemistry*. **35**, 10339-10346.
- Vyazmensky, M., A. Steinmetz, D. Meyer, R. Golbik, Z. e. Barak, K. Tittmann and D. M. Chipman (2011) Significant Catalytic Roles for Glu47 and Gln 110 in All Four of the C-C Bond-Making and -Breaking Steps of the Reactions of Acetohydroxyacid Synthase II. *Biochemistry*. **50**, 3250-3260.
- Wagner, I. D. and J. Wiegel (2008) Diversity of Thermophilic Anaerobes. *Ann. N. Y. Acad. Sci.* **1125**, 1-43.
- Wahl, R. C. and W. H. Orme-Johnson (1987) Clostridial pyruvate oxidoreductase and the pyruvate-oxidizing enzyme specific to nitrogen fixation in *Klebsiella pneumoniae* are similar enzymes. *J. Biol. Chem.* **262**, 10489-10496.
- Wang, Q., P. He, D. Lu, A. Shen and N. Jiang (2004) Purification, Characterization, Cloning and Expression of Pyruvate Decarboxylase from *Torulopsis glabrata* IFO005. *J. Biochem., Tokyo*. **136**, 447-455.
- Wang, Y. and Y. H. P. Zhang (2009) Overexpression and simple purification of the *Thermotoga maritima* 6-phosphogluconate dehydrogenase in *Escherichia coli* and its application for NADPH regeneration. *Microbial Cell Factories*. **8**, 30.
- Ward, O. P. and A. Singh (2000) Enzymatic asymmetric synthesis by decarboxylases. *Curr. Opin. Biotechnol.* **11**, 520-526.
- Wassenberg, D., W. Liebl and R. Jaenicke (2000) Maltose-binding protein from the hyperthermophilic bacterium *Thermotoga maritima*: stability and binding properties. *J. Mol. Biol.* **295**, 279-288.
- Watrin, L., V. Martin-Jezequel and D. Prieur (1995) Minimal Amino Acid Requirements of the Hyperthermophilic Archaeon *Pyrococcus abyssi*, Isolated from Deep-Sea Hydrothermal Vents. *Appl. Environ. Microbiol.* **61**, 1138-1140.
- Weinberg, M. V., G. J. Schut, S. Brehm, S. Datta and M. W. W. Adams (2005) Cold Shock of a Hyperthermophilic Archaeon: *Pyrococcus furiosus* Exhibits Multiple Responses to a Suboptimal Growth Temperature with a Key Role for Membrane-Bound Glycoproteins. *J. Bacteriol.* **187**, 336-348.
- Weinstock, O., C. Sella, D. M. Chipman and Z. Barak (1992) Properties of subcloned subunits of bacterial acetohydroxy acid synthases. *J. Bacteriol.* **174**, 5560-5566.
- Wery, N., F. Lesongeur, P. Pignet, V. Derennes, M. A. Cambon-Bonavita, A. Godfroy and G. Barbier (2001) *Marinitoga camini* gen. nov., sp. nov., a rod-shaped bacterium belonging to the order *Thermotogales*, isolated from a deep-sea hydrothermal vent. *Int. J. Syst. Evol. Microbiol.* **51**, 495-504.

- Westerfeld, W. W. (1945) A Colorimetric Determination of Blood Acetoin. *The Journal of biological chemistry*. **161**, 495-502.
- Williams, E., T. Lowe, J. Savas and J. DiRuggiero (2007) Microarray analysis of the hyperthermophilic archaeon *Pyrococcus furiosus* exposed to gamma irradiation. *Extremophiles*. **11**, 19-29.
- Williams, K., P. N. Lowe and P. F. Leadlay (1987) Purification and characterization of pyruvate: ferredoxin oxidoreductase from the anaerobic protozoon *Trichomonas vaginalis*. *The Biochemical journal*. **246**, 529-0.
- Windberger, E., R. Huber, A. Trincone, H. Fricke and K. O. Stetter (1989) *Thermotoga thermarum* sp. nov. and *Thermotoga neapolitana* occurring in African continental solfataric springs. *Arch. Microbiol.* **151**, 506-512.
- Witzmann, S. and H. Bisswanger (1998) The pyruvate dehydrogenase complex from thermophilic organisms: thermal stability and re-association from the enzyme components. *Biochimica et Biophysica Acta (BBA) - Protein Structure and Molecular Enzymology*. **1385**, 341-352.
- Woese, C. (1998) The universal ancestor. *Proceedings of the National Academy of Sciences*. **95**, 6854-6859.
- Woese, C., O. Kandler and M. Wheelis (1990) Towards a Natural System of Organisms: Proposal for the Domains Archaea, Bacteria, and Eucarya. *Proc. Natl. Acad. Sci. USA*. **87**, 4576-4579.
- Woese, C. R. and G. E. Fox (1977) Phylogenetic structure of the prokaryotic domain: the primary kingdoms. *Proceedings of the National Academy of Sciences*. **74**, 5088-5090.
- Xing, R. and W. B. Whitman (1994) Purification and characterization of the oxygen-sensitive acetohydroxy acid synthase from the archaebacterium *Methanococcus aeolicus*. *J. Bacteriol.* **176**, 1207-1213.
- Yakunin, A. F. and P. C. Hallenbeck (1998) Purification and characterization of pyruvate oxidoreductase from the photosynthetic bacterium *Rhodobacter capsulatus*. *Biochimica et Biophysica Acta (BBA) - Bioenergetics*. **1409**, 39-49.
- Yamamoto, M., T. Ikeda, H. Arai, M. Ishii and Y. Igarashi (2010) Carboxylation reaction catalyzed by 2-oxoglutarate:ferredoxin oxidoreductases from *Hydrogenobacter thermophilus*. *Extremophiles*. **14**, 79-85.
- Yang, H., H. Ichinose, M. Yoshida, M. Nakajima, H. Kobayashi and S. Kaneko (2006) Characterization of a Thermostable Endo-beta-1,4-D-galactanase from the Hyperthermophile *Thermotoga maritima*. *Biosci., Biotechnol., Biochem.* **70**, 538-541.
- Yang, J. H. and S. S. Kim (1993) Purification and characterization of the valine sensitive acetolactate synthase from *Serratia marcescens* ATCC 25419. *Biochimica et Biophysica Acta (BBA) - General Subjects*. **1157**, 178-184.
- Yang, X. and K. Ma (2005) Purification and characterization of an NADH oxidase from extremely thermophilic anaerobic bacterium *Thermotoga hypogea*. *Arch. Microbiol.* **V183**, 331-337.
- Yang, X. and K. Ma (2010) Characterization of a Thioredoxin-Thioredoxin Reductase System from the Hyperthermophilic Bacterium *Thermotoga maritima*. *J. Bacteriol.* **192**, 1370-1376.
- Yao, S. and M. Mikkelsen (2010a) Metabolic engineering to improve ethanol production in *Thermoanaerobacter mathranii*. *Appl. Microbiol. Biotechnol.* **88**, 199-208.
- Yao, S. and M. J. Mikkelsen (2010b) Identification and Overexpression of a Bifunctional Aldehyde/Alcohol Dehydrogenase Responsible for Ethanol Production in *Thermoanaerobacter mathranii*. *J. Mol. Microbiol. Biotechnol.* **19**, 123-133.

- Ying, X., A. Grunden, L. Nie, M. Adams and K. Ma (2009) Molecular characterization of the recombinant iron-containing alcohol dehydrogenase from the hyperthermophilic Archaeon, *Thermococcus* strain ES1. *Extremophiles*. **13**, 299-311.
- Ying, X. and K. Ma (2011) Characterization of a zinc-containing alcohol dehydrogenase with stereoselectivity from the hyperthermophilic archaeon *Thermococcus guaymasensis*. *J. Bacteriol.* **193**, 3009-3019.
- Ying, X., Y. Wang, H. Badiei, V. Karanassios and K. Ma (2007) Purification and characterization of an iron-containing alcohol dehydrogenase in extremely thermophilic bacterium *Thermotoga hypogea*. *Arch. Microbiol.* **187**, 499-510.
- Yoon, K.-S., M. Ishii, T. Kodama and Y. Igarashi (1997) Purification and characterization of pyruvate:ferredoxin oxidoreductase from *Hydrogenobacter thermophilus* TK-6. *Arch. Microbiol.* **V167**, 275-279.
- Yoon, M.-Y., J.-H. Hwang, M.-K. Choi, D.-K. Baek, J. Kim, Y.-T. Kim and J.-D. Choi (2003) The active site and mechanism of action of recombinant acetoxy acid synthase from tobacco. *FEBS Lett.* **555**, 185-191.
- Yun, S. H., S. O. Kwon, G. W. Park, J. Y. Kim, S. G. Kang, J. H. Lee, Y. H. Chung, S. Kim, J. S. Choi and S. I. Kim (2011) Proteome analysis of *Thermococcus onnurineus* NA1 reveals the expression of hydrogen gene cluster under carboxydrotrophic growth. *Journal of Proteomics*. **74**, 1926-1933.
- Zaldivar, J., J. Nielsen and L. Olsson (2001) Fuel ethanol production from lignocellulose: a challenge for metabolic engineering and process integration. *Appl. Microbiol. Biotechnol.* **V56**, 17-34.
- Zedníková, V., N. C. Beltrán, J. Tachezy and I. Hrdý (2012) Alternative 2-keto acid oxidoreductases in *Trichomonas vaginalis*: Artifact of histochemical staining. *Mol. Biochem. Parasitol.* **181**, 57-59.
- Zhang, Q., T. Iwasaki, T. Wakagi and T. Oshima (1996) 2-Oxoacid: Ferredoxin Oxidoreductase from the Thermoacidophilic Archaeon, *Sulfolobus* sp. strain 7. *Journal of Biochemistry*. **120**, 587-599.
- Zillig, W., I. Holz, D. Janekovic, W. Schaefer and W. D. Reiter (1983) The archaeobacterium *Thermococcus celer* represents a novel genus within the thermophilic branch of the archaeobacteria. *Syst. Appl. Microbiol.* **4**, 88-94.
- Zillig, W., I. Holz, H.-P. Klenk, J. Trent, S. Wunderl, D. Janekovic, E. Imself and B. Haas (1987) *Pyrococcus woesei*, sp.nov., an ultra-thermophilic marine archaeobacterium, representing a novel order, *Thermococcales*. *Syst. Appl. Microbiol.* **9**, 62-70.
- Zivanovic, Y., J. Armengaud, A. Lagorce, C. Leplat, P. Guerin, M. Dutertre, V. Anthouard, P. Forterre, P. Wincker and F. Confalonieri (2009) Genome analysis and genome-wide proteomics of *Thermococcus gammatolerans*, the most radioresistant organism known amongst the Archaea. *Genome Biology*. **10**, R70.
- Zohar, Y., M. Einav, D. M. Chipman and Z. Barak (2003) Acetoxyacid synthase from *Mycobacterium avium* and its inhibition by sulfonylureas and imidazolinones. *Biochimica et Biophysica Acta (BBA) - Proteins & Proteomics*. **1649**, 97-105.
- Zwickl, P., S. Fabry, C. Bogedain, A. Haas and R. Hensel (1990) Glyceraldehyde-3-phosphate dehydrogenase from the hyperthermophilic archaeobacterium *Pyrococcus woesei*: characterization of the enzyme, cloning and sequencing of the gene, and expression in *Escherichia coli*. *J. Bacteriol.* **172**, 4329-4338.